BEHAVIOR OF SENSITIVE CLAY SUBJECTED TO STATIC AND CYCLIC LOADING

KHALID JAVED

A Thesis

In

THE DEPARTMENT OF BUILDING, CIVIL AND ENVIRONMENTAL ENGINEERING

Presented in Partial Fulfillment of the Requirements

For the Degree of Doctor of Philosophy

CONCORDIA UNIVERSITY

Montreal, Quebec, Canada

February 2011

Khalid Javed

CONCORDIA UNIVERSITY

SCHOOL OF GRADUATE STUDIES

This is to certify that the thesis prepared

By: Mr. Khalid Javed

Entitled: Behavior of Sensitive Clay Subjected to Static and Cyclic Loading

and submitted in partial fulfillment of the requirements for the degree of

Doctor of Philosophy

complies with the regulations of this University and meets the accepted standards with respect to originality and quality.

Signed by the final examining committee:

Dr. B. Jaumard	Chair
Dr. Hesham El Naggar	External Examiner
Dr. G. Vatistas	External to Program
Dr. A. Zsaki	Examiner
Dr. O. Pekau	Examiner
Dr. A.M. Hanna	Thesis Supervisor

Approved by

Dr. M.Elektorowicz

Chair of Department or Graduate Program Director

June, 2011

Dr. Robin Drew

Dean of Faculty

ABSTRACT

Sensitive clay is the type of clay, which loses its shear strength when it is subjected to cyclic loading. High-rise buildings, towers, bridges etc., founded on sensitive clays and subjected to overturning moment are usually suffer from a steady reduction of the bearing capacity of their foundations and accordingly the safety factor. Cyclic loading of foundation on sensitive clay during the undrained period may lead to quick clay condition and catastrophic failure of the structure.

In the literature, governing parameters are listed as: cyclic deviator stress, pore water pressure, axial strain, pre-consolidation pressure, confining stress, initial degree of saturation, water content, liquidity index and the number of cycles. The present study has introduced the governing parameters in two categories; namely physical and mechanical as a function of sensitivity number of the clay material. A well planned experimental investigation was conducted to examine the effect of these governing parameters during the undrained and the drained periods of sensitive clay subjected to static or cyclic loadings. The soil samples, known as "Champlain clay" were obtained from the city of Rigaud, Quebec (Canada). Consolidation tests, static and cyclic undrained and drained triaxial tests were performed on representative samples of this clay.

Tests were conducted to identify the role of the key parameters governing this complex behavior during the drained and the undrained periods. The study examined individually the effect of cyclic loading, deviator stress, frequency, pre-consolidation pressure/OCR, and the confining pressure during the drained and undrained conditions. Absence or presence of the matric suction in fully saturated or partially saturated clay, effect of sensitivity number and liquidity index were also examined.

Based on the results of the present experimental investigation, a hypothetical model was introduced to explain the process of shear strength reduction for the case of static and cyclic loading of sensitive clay subjected to cycling loading. The model was capable to define the term remolding agent or degree of remolding, the reduction in shear strength due to remolding. The increase in the water content is identified as the most critical or intrinsic shear strength for sensitive clay.

The present study used the "Modified Cam Clay Model" to predict the factor of safety for a foundation on sensitive clay subjected to cyclic loading as function of the physical and mechanical parameters. A design procedure is developed to determine the safe zone for the undrained and drained responses, within which a combination of the cyclic deviator stress and the number of cycles for a given soil/loading/site conditions can achieve a quasi-elastic resilient state without reaching failure. The proposed design procedure is applicable to all regions around the world, where sensitive clays can be found. Furthermore, this procedure can be adopted to examine the conditions of existing foundations built on sensitive clay at any time during its lifespan.

Acknowledgement

I owe my most sincere gratitude to Al-mighty Allah who has been the source of my entire initiative and accomplishment required to fulfill this stupendous task.

My most fervent thanks are due to my mother whose prayers enabled me to see this day.

I pray to Allah for my late father Abdul Shakur to grant him paradise and elevate his level in the life hereafter. He was a competent civil engineer and a man-of-peace. Whatever achievements I have in my life are the result of his training.

The entire credit of the accomplishment of this research goes to Prof. Dr. Adel Hanna, my thesis director, whose technical guidance, deep involvement, personal interest and untiring assistance enabled me to present this work today.

The financial support provided by the Natural Sciences and Engineering Council of Canada is acknowledged and highly appreciated.

I am also thankful to my wife and kids for unexhausted support and encouragement.

Contents

LIST OF TABLES

LIST OF FIGURES

LIST OF SYMBOLS

A and B	Skempton Pore Water Pressure Parameters
a	Attraction
a_1	Constant
a_2	Hyodo's Model Constant
b_1	Hyodo's Model Constant
b_2	Hyodo's Model Constant
C	Static Shear Strength of unsaturated sample
C_{uo}	Original Undrained Static Shear Strength of an undisturbed sample
C_{ur}	Original Undrained Static Shear Strength of a remolded sample
C_{ur}^*	Intrinsic Static Shear Strength of a reconstituted sample of Group - III
C_{fc}	Cyclic shear strength at final cycle
C_{mc}	Cyclic shear strength with matric suction for partially saturated sample
C_{fc}^*	Cyclic intrinsic shear strength at final cycle
c_L	Shear Strength at Liquid Limit
c_a	Allowable Shear Strength
c_p	Shear Strength at Plastic Limit
c_u'	Modified Undrained Static Shear Strength
c_u	Undrained Static Shear Strength
c_u	Undrained Undisturbed Shear Strength
c_{ur}	Undrained Remolded Shear Strength
c_v	Co-efficient of Consolidation
c’	Effective cohesion

e	Deviator Strain Tensor in Modified Cam Clay Model
e	Void Ratio
e_f	Final Void Ratio
e_o	Initial Void Ratio
F	Factor of Safety
F	Function of u and τ_c given in proposed Hypothetical Model
f	Frequency in Hz
G	Shear Modulus
G_s	Specific Gravity of Soil Particles
H	Length of Drainage
h	Hour
I_L	Liquidity Index
I_p	Plasticity Index
k	Constant for Describing Variation in Sensitivity
k	Fatigue Parameter
k	Material Constant
LL	Liquid Limit
M	Clay Parameter
m	Slope of the Pore Pressure Line
N	Number of Cycles
N_y	Number of Cycles to Yield
P	Effective Pressure
p	Material Constant

p'	Mean Effective Normal Stress
p_c	Consolidation Pressure (at the start of the test)
p_f	Final Effective Stress
PI	Plasticity Index
PL	Plastic Limit
p_o	Drained Virgin Pressure
p_u	Undrained Virgin Pressure
Q	Function of u and τ_c given in proposed Hypothetical Model
q	Deviator Stress
q_{cyc}	Cyclic Deviator Stress
q_s	Static Deviator Stress
q_f	Final Deviator Stress
R	Ratio between c_p and c_L
r	Degree of remolding
S	Degree of Saturation
s	deviator Stress Tensor in Cam Clay Model
S_t	Sensitivity
T	Dimensionless Time Factor ($T = T_{50}$)
T	Peak Cyclic Strength Ratio
T_{fc}	Strength at the End of Cyclic Loading
t	Time Corresponding to the Particular Degree of Consolidation
u	Pore Water Pressure
u_a	Pore Air Pressure

u_w	Pore Water Pressure
u	Pore Water Pressure
Δu	Change in Pore Water Pressure
u^+	Pore Water Pressure generated by Cyclic loading
u_p	Permanent pore Water Pressure
u_{st}	Static Pore Water Pressure
w	Natural Water Content
w.c	Natural Water Content
w_L	Liquid Limit
w_n	Natural Water Content
w_p	Plastic Limit
Δe	Change in Void Ratio
ΔH	Change in the Height of a Soil Sample during Consolidation Test
Δu	Change in Pore Pressure
ϑ	Lode Angle
Λ	Parameter of the Cam Clay Model
α	Parameter of the Modified Cam Clay Model
ε	Axial Strain
ε	Strain Tensor
ε_p	Peak Axial Strain
ε_c	Cyclic Axial Strain
ϕ	Angle of Friction
ϕ'	Angle of Frictional Resistance

γ	Maximum Single Amplitude Shear Strain
γ_{st}	Shear Strain due to Initial Static Shear Stress
γ_y	Maximum Single Amplitude Shear Strain at Failure
η	Stress Ratio
η^*	Relative Effective Stress Ratio
η_f	Final Effective Stress Ratio
η_p	Peak Effective Stress Ratio
η_s	Initial Effective Stress Ratio
κ	Gradient of Swelling Line
λ	Gradient of Virgin Consolidation Line
σ'	Effective Stress
σ'	Pre-consolidation Pressure
σ^*	Equivalent Vertical Effective Stress
σ_c'	Effective Confining Pressure
σ_d	Deviator Stress
σ_n	Normal Stress
σ'_{vc}	Vertical Effective Stress Pressure
σ_1, σ_2, σ_3	Principal Stresses
τ	Cyclic Shear strength
τ_c	Cyclic Shear Strength
τ_{cyc}	Cyclic Shear Stress
τ_f	Maximum Cyclic Shear Strength

τ_{st}	Static Shear Strength
τ_{tot}	Total Shear Strength
υ	Specific Volume
υ_1	Virgin Volume at Unit Pressure
υ_l	Virgin Line Volume
υ_s	Volume for a Specific Swelling Line
θ_w	Volumetric water content
θ_w	Residual Volumetric water content
θ_s	Saturated volumetric water content

Chapter 1

Introduction

Due to the increase in world population, geotechnical engineers are forced to deal with difficult soils such as sensitive clay. Sensitive clay subjected to cyclic loading may experience gradual loss of its shear strength, which may lead to extensive settlement of the foundation and significant loss of its bearing capacity or perhaps catastrophic failure of the structure. Sensitive clay displays a considerable decrease in its shear strength when it is remolded. This property of clays is called sensitivity.

Terzaghi (1944) was the first to provide the quantitative measure of the sensitivity as a ratio of peak undisturbed shear strength to remolded shear strength. The sensitivity for normal clays is between 1and 4. Clays with sensitivities between 4 and 8 are referred to as sensitive and those with sensitivities between 8 and 16 are defined as highly sensitive. Clays having sensitivities greater than 16 are called quick clays. Sensitive clays occur in many parts of the world such as eastern Canada, Norway, Sweden, the coastal region of India and south East Asia. It challenges geotechnical engineers with specific problems concerning stability, settlement, and the prediction of soil response behavior. High rise buildings, towers, bridges etc., founded on sensitive clays usually suffer from reduction of the safety factor during its life span. Cyclic loading produced by wind, waves, ice and snow accumulation, earthquakes and other live loads cause cyclic stresses on foundations may lead to quick clay conditions and catastrophic failure. Tall flexible structures such as chimneys and long-span bridges are usually subjected to dynamic oscillations under wind loading which amplify the static wind forces. Structures supporting traveling machinery such as radar antenna, cranes and large telescopes, etc. transmit significant cyclic loads to their

foundations. Storage facilities such as: silos and oil tanks transmit very high foundation stresses when full and much lower stresses when empty.

The loose framework and the high water content are the main properties of this type of clay. The clay when gets remoulded, it rapidly liquefies and loses its shear strength. More than 250 cases of quick conditions of sensitive clays of various sizes have been identified within a 60-kilometre radius of the City of Ottawa in Canada due to the presence of sensitive clay in various pockets and varying depth in this region. Eastern Canada has extensive deposits of sensitive marine clay in the Saint Lawrence River Lowlands of southern Quebec and south eastern Ontario, which contains 20% of the country's population, as well as vital transportation and communication corridors. Large retrogressive landslides occur in these clay deposits. These landslides, which are developed very quickly and without warning, often involve millions of cubic meters of debris. Saint Lawrence Lowlands in southern Quebec and north eastern Ontario, contains the deposits from the Champlain and La Flamme Seas (see Figure 1.1), that existed between 8000 to 12,000 years ago during the last glaciation. This area contains extensive and often very thick deposits of marine clay, much of which is highly sensitive. This region experiences landslides in the marine clays, including the frequent occurrence of large retrogressive flow slides. Observations about the distribution of the so-called "sensitive clays" indicate that they are mostly made of materials, which consist of rock flour eroded from metamorphic terrain for example, St. Jean Vianney, Grande Baleine and Matagami clays located in northwestern Quebec. Also, the St. Lawrence Lowlands, the Champlain Sea clays are found over a wide area. This basin is limited to the south by the Appalachian Mountains and to the north by the Laurentian Plateau. The rock flour, clay-sized particles of quartz and feldspar tend to be negatively charged and mutually repellent in fresh water, but in salt water the presence of dissolved salts provides swarms of positively

charged salt ions which allow aggregation, or flocculation, of fine particles to occur. The small platelets of material tend to align themselves by forming bonds between particle edges and opposing particle faces in a three-dimensional card-house structure. This open, low-density structure favors the retention of large amounts of pore water. As a result of this, the cohesive strength of the card-house structure is progressively reduced over time. Due load fluctuations the potentially unstable card house structure collapses because of shearing or shaking, the pore water is compressed and the 'quick' condition rapidly develops.

Structures subjected to cyclic loading, Figures 1.2 to 1.6, cause a remolding action that helps the available water in the soil to dissolve away the salts, which results in the change of soil structure, which further substantially lower its strength, causing foundation failure and landslides. These landslides can retrogress, with large volumes of soil losing strength and flowing as a viscous liquid. Such retrogressive flow slides are often very large, occur very quickly, and can have catastrophic results. Figure 1.7 shows micrograph of a horizontal cleavage surface in undisturbed, desiccated St. Vallier clay, see Figure 1.8.

The different factors which, may contribute to the increase or decrease the sensitivity in the clayey soils are; Metastable fabric, Cementation, Weathering, Thixotropic hardening, Leaching, ion exchange and change in monovalent / divalent caution ratio, Formation or addition of dispersing agents, Size and topography of catchment areas, Presence of organic soils and Groundwater gradient and height above present sea level.

In flocculation process of fine grained soil, the initial fabric after sedimentation opens and involves some amount of edge to edge and edge to face associations. During consolidation, this fabric can carry effective stress at a void ratio higher than it would be possible if particles and particle groups were arranged in efficient and parallel array. When

clay formed in this way is remolded, the fabric is disrupted, effective stresses are reduced because of the tendency for the volume to decrease and the strength is less. This Metastable particle arrangement results in increasing the level of sensitivity in clayey soils. High water content, low load increment ratio and low rate of loading tend to give higher water content for a given effective stress and therefore higher values of sensitivity.

The presence of free carbonates, iron oxide, alumina and other organic matter act as a cementing agent on precipitations for clays. When this mass of clay gets disturbed, the soil fabric cemented bonds are destroyed leading to a loss of shear strength.

The flocculation and de-flocculation tendencies of the soils are affected by the weathering processes. Weathering causes change in the types and relative proportion of ions in solution. Hence, strength and sensitivity number increased or decreased depending on the nature of the changes in ionic distributions.

Thixotropic is an isothermal, reversible time dependent process which occurs under conditions of constant composition and volume, whereby a material stiffens while at rest and softens or liquefies upon remolding. Sedimentation, remolding and compaction of soil produce a structure compatible with conditions at that time. Once the externally applied energy of remolding or compaction is removed the structure may no longer be equilibrium with the surroundings. If however, the inter particle forces balance in such a way that attraction is more than the repulsion, there will be a tendency towards flocculation of particles and aggregates and for a reorganization of the water ion structure to a lower energy state. Hence, thixotropic may increase or decrease the sensitivity, depending on the way the soil particles settles down after disturbance.

Reduction in salt content due to leaching has a great effect in increasing the sensitivity of clay. Leaching of salt resulted when a drop in sea level or rise in land level caused the clay to be filled from above sea level so that it becomes exposed to a freshwater environment. The presence of percolating freshwater in silt and sand is sufficient to cause removal of salt from clay by diffusion without the requirement that water flow through zones of intact clay. Although, leaching causes little change in fabric, however, the inter particle forces may be changed, resulting in a decrease in undisturbed strength of up to 50 percent, and such a large reduction in remolded strength can cause the creation of a quick clay.

The presence of organic substances causes dispersing of the clay particles leading to repulsion. Hence, increase in sensitivity. Some inorganic substances having excess phosphate can induce sensitivity even in insensitive clay.

The size and profile of the catchment area along with variation in groundwater table and flow also adds to the problem in the sensitive clay regions. Especially, groundwater flow tends to affect both the sensitivity and the likelihood of trigging a landslide.

The possible remedial actions could be taken as; to replace the foundation soil with crush stones, or to penetrate the foundations through it or to deal with it. Also, light fill materials like polystyrene could be used or vertical wick drains or groundwater cutoff walls could be used to retain the strength of the foundation soil. The choice of the method depends upon the importance of the project, site limitations and engineering judgment.

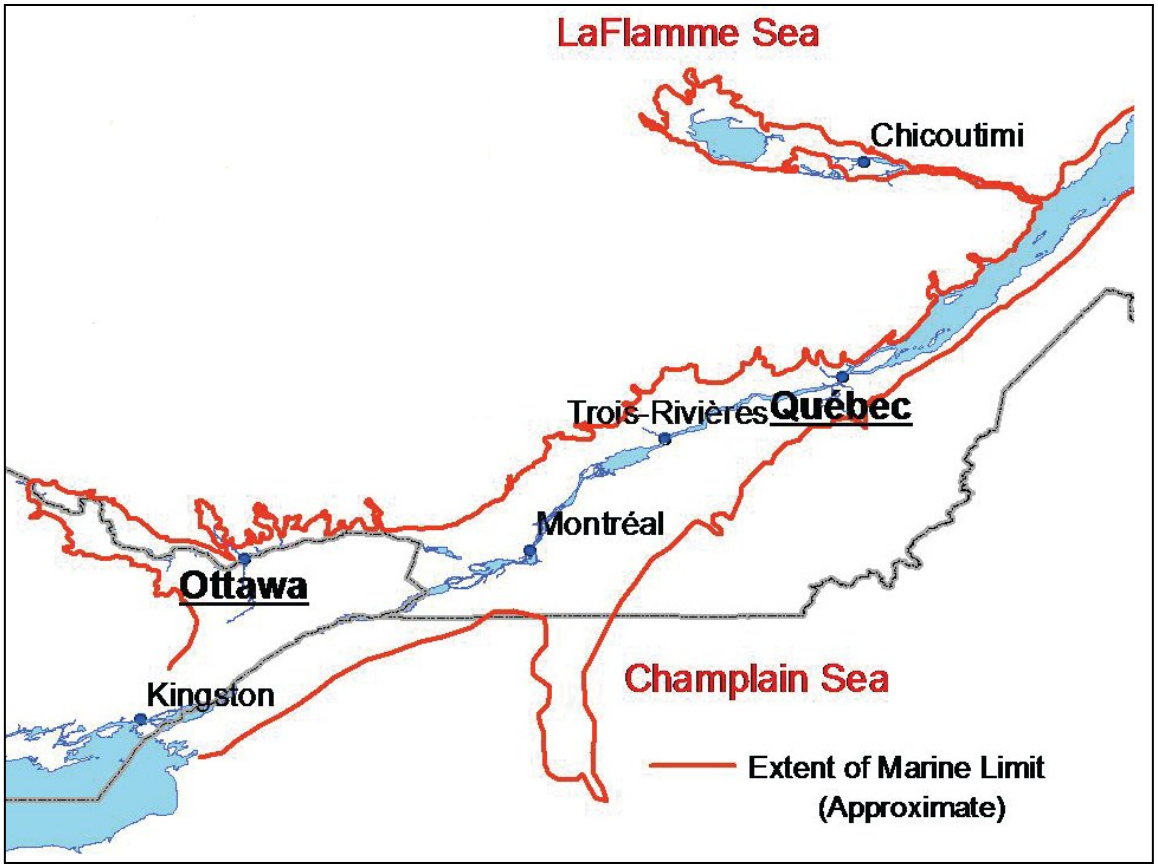

Figure 1.1: Approximate extent of sensitive clay deposition;

(After ESRI (2002) Satellite Imagery)

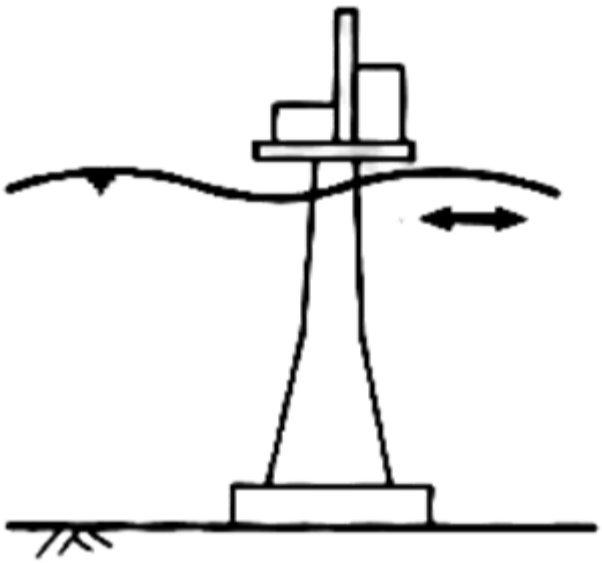

Figure 1.2: Cyclic loading due to offshore waves (After Reilly and Brown, 1991)

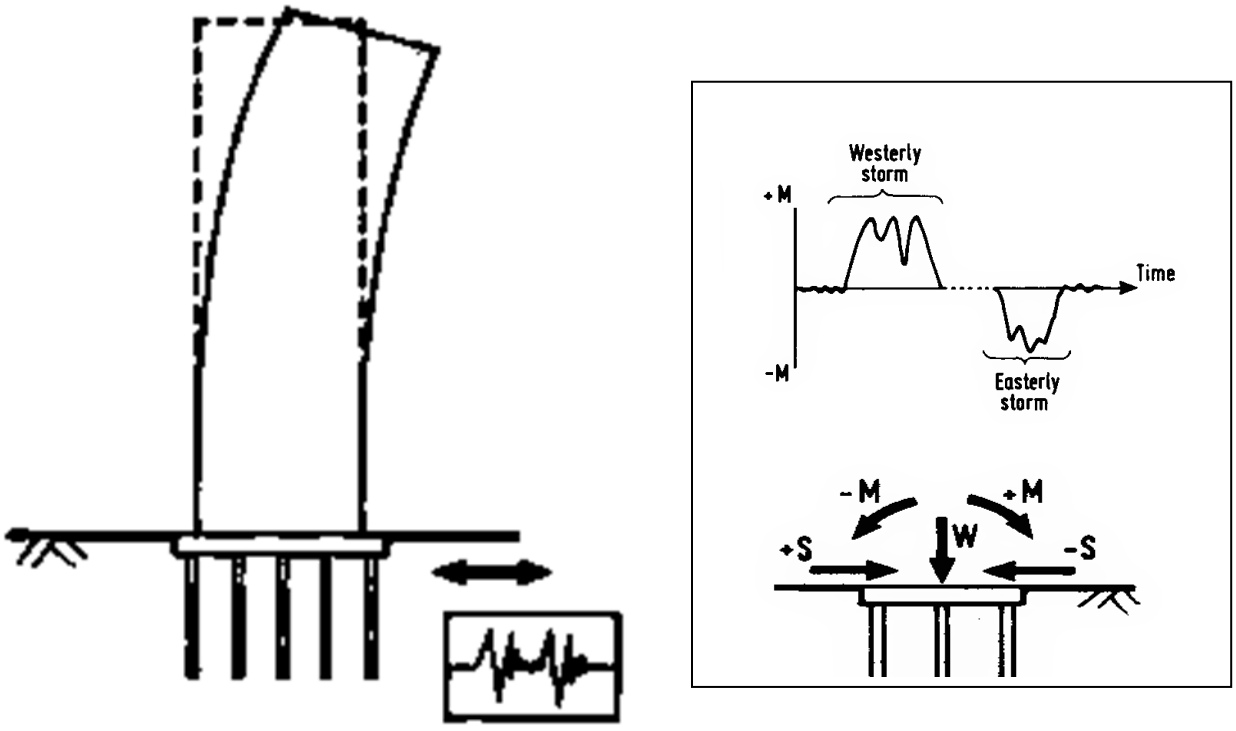

Figure 1.3: Cyclic loading due to wind (After Reilly and Brown, 1991)

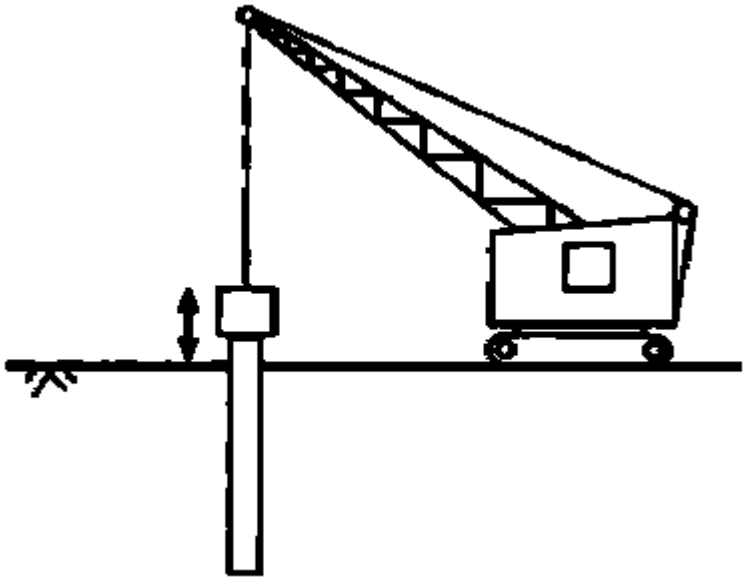

Figure 1.4: Cyclic loading due to construction (After Reilly and Brown, 1991)

Figure 1.5: Cyclic loading due to machines (After Reilly and Brown, 1991)

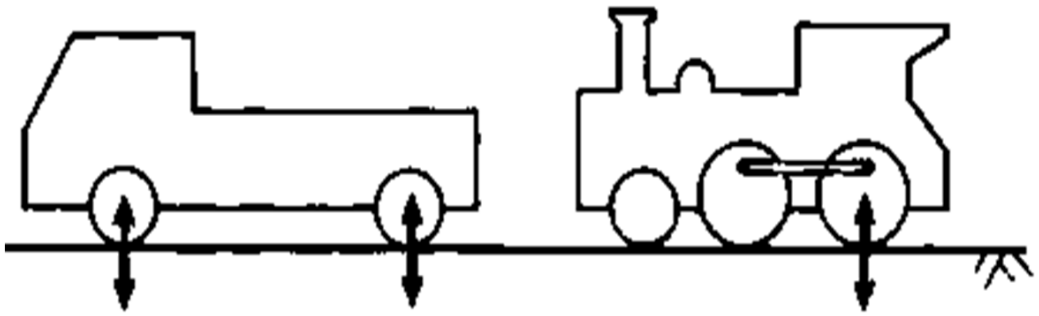

Figure 1.6: Cyclic loading due to traffic (After Reilly and Brown, 1991)

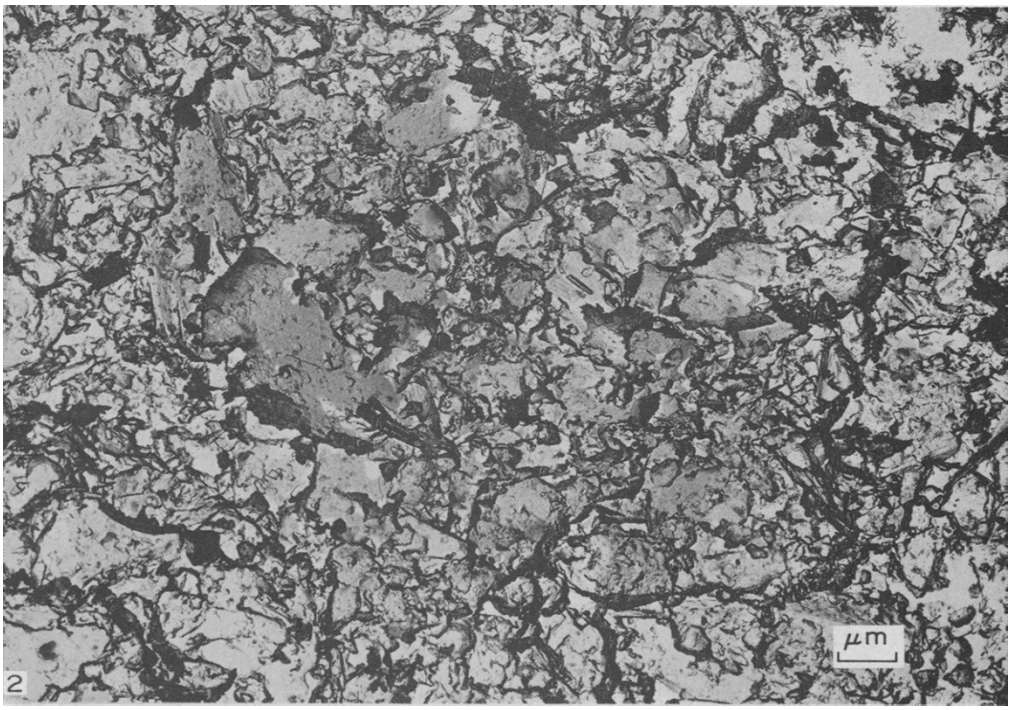

Figure 1.7: Micrograph of a horizontal cleavage surface in undisturbed and desiccated St. Vallier clay. (After McK et al. 1973)

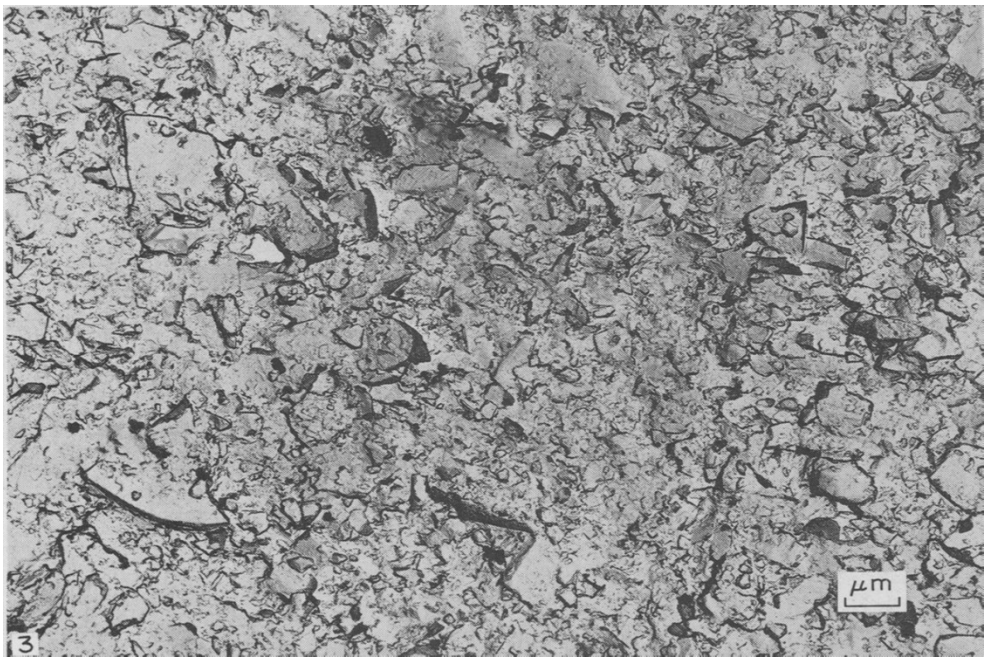

Figure 1.8: Micrograph of a horizontal cleavage surface in disturbed and desiccated St. Vallier clay. (After McK et al. 1973)

Chapter 2

Literature Review

In the literature, research on sensitive clays were focused on conducting experimental work on undisturbed and remolded clay for the purpose of developing relationship between cyclic stress-strain and pore water pressure (Seed and Chan 1966, Theirs and Seed (1968, 1969), Sangrey 1968, Sangrey et al 1969, Eden 1971, France and Sangrey 1977 and Sangrey et al 1978). They reported that cyclic loading increases the pore water pressure in the clay under undrained conditions up to a number of cycles, beyond which the failure will occur. Nevertheless the results are limited to the conditions of the experimental work, and accordingly, the validity of the empirical formulae developed is questionable. Mitchell and King (1977) have reported that the higher the initial confining stress and over-consolidation pressure, the higher the number of cycles needed to reach failure.

Eden (1971) studied the various techniques to obtain undisturbed samples of sensitive clays. He reported that block sampling is the best technique to obtain undisturbed samples for the sensitive clay.

Iwaski et al. (1978) conducted the cyclic torsional shear tests and showed that each load cycle is accompanied by a change in shear strain, some of which is partly recoverable. The magnitude of recoverable strain remains fairly constant during each cycle, while the irrecoverable or plastic strain developed during each successive cycle tends to reduce with an increase of the number of cycles. The study also established that the resilient stiffness of soil is stress level dependent on the magnitude of resilient shear strain.

Eekelen and Potts, (1978) performed static and cyclic triaxial compression tests on Drammen clay samples. They incorporated a single state parameter called 'fatigue' in Modified Cam Clay Model to give the reduction in shear strength at the end of cyclic loading.

Chagnon et al (1979) conducted field and laboratory investigations on the sensitive clays of eastern Canada. They suggested solutions for various engineering geological problems related to these clays in light of these field and laboratory investigations. Table 1 gives the summary of their investigations.

Houstan and Hermann (1980) conducted an experimental investigation on seven marine soils namely: Atlantic Calcareous Ooze, Reconstituted Atlantic Calcareous Ooze, Pacific Calcarreous Ooze, Pacific Hemi Pelagic, Atlantic Hemi Pelagic, Pacific Pelagic Clay and San Francisco Bay Mud. The objective of their study was to quantify the undrained response of seafloor soils to various combinations of static and cyclic loading. The average sensitivity (S_t) of all the clays tested was 3 or less except for San Francisco Bay Mud, which it was 8, the highest in all tested samples. Figure 2.1 shows the cyclic failure data of the Bay Mud for 0% static bias (percentage of initial deviator stress) and 40% static bias. In comparison to the other soils, the cyclic failure data of bay Mud shows highest resistance to cyclic loading. The results presented in Figure 2.1 were cross plotted to obtain cyclic strength contours shown in Figure 2.2. The width of the zone indicates the range of uncertainty associated with the cross-plotting operation. Three contours were established for this soil, the combination of static and cyclic stresses required to cause failure at 30 cycles, 3,000 cycles and 300,000 cycles of loading. Based on this cyclic strength contour analysis, Houstan and Hermann (1980) showed that cyclic strength of clays can be expressed as a function of plasticity index. Furthermore, the study confirms the quasi-elastic resilient state defined by

Iwaski et al (1978). The interesting part of the study is that it established a relationship between cyclic strength and plasticity index, and in Table 2 it is shown that the cyclic strength is a function of plasticity index. The close agreement of Pacific pelagic Clay and San Francisco Bay Mud reveals some important clues related to the present study. Although the Pacific Pelagic Clay may have slightly higher average plasticity index, the Bay Mud has the higher sensitivity (S_t =8) and has maximum static compressive strength at pure stress reversal. On the other hand sensitivity cannot be used instead of plasticity index. Literature review shows that in the case of Norwegian quick clays, the leaching process that is believed to make the clays quick (Chapter-1) also reduces the plasticity index (Bjerrum (1954))

Matsui et al. (1980) conducted experimental study on the shear characteristics of clays with respect to cyclic stress-strain history and its corresponding pore pressures. Senri clay was used in the study, having water content greater than the liquid limit. The results of the study clarified the effect of load frequency, effective confining pressure, cyclic stress level and over-consolidation ratio on the excess pore pressure during cyclic loading. The study also indicated that over-consolidated clay due to cyclic stress-strain history is similar in strength to an ordinary over-consolidation history.

Silvestri (1981) conducted triaxial tests on overconsolidated sensitive clay from Lachute (P.Q). The specimens of the undisturbed sensitive clay were tested in a triaxial chamber under K_0- (earth pressure at rest) conditions. The study showed that the response of the clay can be divided into three distinct phases of deformation. At low stress levels, the clay behaves as an elastic material. At intermediate stress levels, the clay behaves as a plastic material. At high stress levels, the clay becomes normally consolidated. Silvestri, (1981) used the experimental data to establish a model describing the mobilization of lateral stresses, and

showed that the *in situ* coefficient of earth pressure at rest could not be determined by laboratory testing.

Seed and Idris (1982) studied the effects of cyclic frequency. They concluded that the faster the rate of cycling the more the situation resembles the undrained conditions. Procter and Khaffaf (1984) studied the weakening behavior of undrained saturated remolded samples of Derwent Clay subjected to cyclic loading. They used the experimental data of Craig (1982) to compare the frequency response of cyclic shear stress ratio (τ/c_u) to frequency response of modified cyclic shear stress ratio ($\tau/\bar{c}_u$) causing 5% double amplitude strain. Figure 2.3 shows the ratio of static shear strengths ($\bar{c}_u/c_u$) versus strain rate from which the modified shear strength ($\bar{c}_u$) relevant to a given load controlled cyclic strain contour is determined on the basis of a mean strain rate equal to $2 * \varepsilon_{da} * f$, where ε_{da} is mean double amplitude axial strain "peak to peak" and "f" is the frequency of cyclic loading in hertz (Hz). Figures 2.4 and 1.6(b) show the frequency response of cyclic shear stress ratio (τ/c_u) and frequency response of modified cyclic stress ratio ($\tau/\bar{c}_u$) causing 5% double amplitude strain. Figure 2.4 shows that a frequency change from 1/120 Hz to 1 Hz causes approximately a 30% increase in cyclic stress ratio (τ/c_u) within the limit $10 \leq N \leq 5000$, where N = number of cycles.

Lefebyre and leBoeuf (1987) conducted a series of monotonic and cyclic triaxial tests to study the influence of the rate of strain and load cycles on the undrained shear strength of three undisturbed sensitive clays from Eastern Canada. Table 3.1 shows the general properties of these investigated soils. For each clay type, two distinct series of tests were carried out, one on naturally over-consolidated clays or undisturbed samples and the other on remolded specimens. The results showed that for structured clay, strain rate as high as 15% can be used for degree of pore pressure equalization of about 95% due to very low compressibility. On the

other hand, for the same degree of equalization, the calculated strain rate of remolded clay was about 1%/h. Figure 2.6 shows the undrained shear strength measured for the undisturbed and remolded specimens at different strain rates, normalized by the undrained shear strength measured at a strain rate of 1%/h and plotted against the log of the strain rate. Also figure 2.6 shows that there is a very narrow boundary, which indicates a linear relationship between the normalized shear strength ratio and the strain rate. Furthermore, the study indicated that the strain rate effect on undrained shear strength ratio appears to be the same for both undisturbed and remolded specimens. Based on test analyzes, the study concluded that for naturally consolidated clays, pore pressure generated at a given deviator stress are essentially independent of the strain rate, while the peak shear strength envelope is lowered as the strain rate was decreased. For normally consolidated clay, a lower strain rate results in an increase in pore pressure generation during shearing due to the tendency of the clay skeleton to creep, while the peak shear strength envelope remains the same. It should be noted that the clays tested in this study were highly sensitive, suggesting that there is no big difference in the shear stress ratio if these clays are tested at a consolidation pressure greater or less than the historical pre-consolidation pressure (see Table 3)

Ansal and Erken (1989) made an experimental investigation on the cyclic behavior of normally consolidated clays by using cyclic simple shear tests on one-dimensionally and isotropically consolidated kaolinite samples. As a result of their investigation, they developed an empirical model to estimate the response of a soil element subjected to cyclic shear stresses for a given number of cycles. Figure 2.7 shows the results of variation of cyclic shear stress ratio $(\tau/\tau_f)_y$ with respect to the number of cycles, N. The linear relationship between the cyclic shear stress ratio $(\tau/\tau_f)_y$ and the number of cycles (N) shown in Figure 2.7 is as follows:

$$\left[\frac{\tau}{\tau_f}\right]_y = a - b\log N \text{.....2.1}$$

Where; $(\tau/\tau_f)_y$ = cyclic shear strength ratio; N = the number of cycles; and a and b = material constants obtained from linear regression analysis. This figure also shows that, for any specified cyclic shear strain amplitude (2%) taken as the upper allowable limit for a specific design purpose, the same approach can be used. The results of the study also indicated that for normally consolidated clays there is a critical shear stress ratio level or a threshold cyclic shear stress ratio below which no pore pressure will develop, as shown in Figure 2.8. The study also defined the variation of the slope of the pore pressure lines with respect to the number of cycles. Figure 2.9 gives a relationship between the slope of pore water pressure lines and the number of cycles as follows:

$$u = \left[\frac{\tau}{\tau_f} - (S.R)_t\right] m \text{.....2.2}$$

$$m = k + p\log N \text{.....2.3}$$

Where; m = the slope of the pore pressure line $\Delta u/(\tau/\tau_f)$; N = the number of cycles; k and p = material constants obtained from the regression analysis; and $(S.R)_t$ is the threshold cyclic shear stress ratio. Based on their experimental study, Ansal and Erken (1989) also found that the influence of frequency can be neglected in problems such as offshore platforms where the number of cycles with respect to wave action will be large. The study also indicates that cyclic behavior of normally consolidated clay, as in the case of natural deposits, is similar to those for completely remolded clay samples. Tests show that remolded samples appear to be more resistant to cyclic shear stresses; cyclic shear strain amplitude developed in these tests (remolded samples) are smaller in comparison to cyclic shear strains measured in one-

dimensionally consolidated samples. However, the pore pressure is higher in the case of remolded samples. Figure 2.10 and 2.11 show the comparison of the shear strain and the pore water pressure behavior of one–dimensionally consolidated and remolded samples. Furthermore, based on their experimental results, Ansal and Erken (1989) give a three equation empirical model. Although the model seems to be simple and useful in predicting shear stress ratio corresponding to a specific strain, it is based on only a simple shear test and on only one type of one-dimensionally and isotropically consolidated kaolinite clay.

Wood (1990) analyzed the data collected by Skempton and Northey (1953) for studying the effect of liquidity index on the undrained shear strength of sensitive clays from various parts of the world. His study showed a clear trend of increasing sensitivity with increasing liquidity index (I_L) as shown in Figure 2.12. He used the relationship given by Bejerrum (1954) for the Norwegian clays as follows:

$$S_t = \exp(kI_L) \quad \text{.....2.4}$$

Where; k is a constant describing variation in sensitivity with liquidity. A value of k~2 provides a reasonable fit. This implies a sensitivity S_t~7.4 for a clay approximately at its liquid limit ($w = w_L$, $I_L = 1$). Based on his analysis, he established the relationship between the liquidity index and the undrained shear strength of the sensitive clays as shown in Figure 2.13. He assigned strengths of 2 kPa and 200 kPa for the shear strength of the soils at their liquid and plastic limits respectively, (see Figure 2.13) and gave a relationship between the remolded strength of the soils solely based on the liquidity index:

$$C_u = c_L R\exp\left[(k - \ln R)I_L\right] \quad \text{.....2.5}$$

Where C_u = undrained shear strength, c_L = shear strength at liquid limit, R= ratio between shear strength at plastic limit (c_P) and shear strength at liquid limit (c_L), I_L = liquidity index and k = constant describing the variation in sensitivity. Furthermore, he found that, in the case of undrained shear strength, the Mohr circle of effective stress at failure point F (Figure 2. 14) can be associated with an infinite number of possible stress circles (T_1,T_2,…….) displaced along the normal stress axis by an amount equal to the pore pressure. The pore pressure does not affect the differences of the stresses or shear stresses, so all stress circles must have the same size especially in case of clay soils, which are usually loaded fast to avoid the drainage of shear-induced pore pressures.

Wood (1990) proposed that it is more desirable to mention the maximum shear stress (τ_f) in terms of undrained shear strength (c_u), which is the radius of all the Mohr circles in Figure 2.14. Therefore, the maximum shear stress that a clay soil can withstand and the failure criterion for undrained conditions become:

$$\tau_f = \pm c_u \quad \text{.....2.6}$$

O' Reilly et al (1991) presented a soil model which takes into account the complexity of stress conditions in the soil beneath structures subjected to a combination of static and cyclic loads. Figure 2.15 shows the model's simplified stress conditions for some soil elements (1, 2, 3 and 4) along a potential failure surface. In the figure, W= weight of the platform, H_{cy} = horizontal shear stress, M_{cy} = stresses due to wind load or other cyclic loading., DSS = direct simple shear test, τ = shear stress, τ_{cy} = cyclic shear stress, τ_a = average shear stress, τ_o = initial shear stress prior to the installation of platform and $\Delta\tau_a$ = additional shear stress induced by the submerged weight of the platform. The model stated that these elements (1,2, 3 and 4) follow various stress paths which may be approximated to a triaxial or

a direct shear type of loading, and they are subjected to various combinations of average shear stresses (τ_a) and cyclic shear stresses (τ_{cy}). The average shear stress (τ_a) is composed of the initial shear stress (τ_o) and additional shear stress ($\Delta\tau_a$). The model shows that in the case of element 2, the weight of the platform gives a higher vertical than horizontal static normal stress hence, during cyclic loading, element 2 will tend to compress vertically. Element 4 is in the passive zone, and the weight of the platform causes a higher horizontal than vertical static normal stress, element 4 will, therefore, tend to compress horizontally and extend vertically during the application of cyclic loading. Consequently, element 2 is best represented by a triaxial compression test and element 4 by a triaxial extension test. The model also shows that for elements 1 and 3 the shear surface will be horizontal. Therefore, these elements are best represented by direct simple shear (DSS) tests, and these tests should be run to establish the shear strength on the horizontal plane, i.e., the horizontal shear stress at failure. Hence, the study emphasizes that since both the shear strength and the deformation properties of soils under cyclic loading are anisotropic, therefore, the triaxial compression, the triaxial extension and the DSS tests should be included in the laboratory test program for gravity structure of some importance. It should also be noted that the model depicts the importance of the actual conditions of stresses in the field, which are usually the combination of static and cyclic loading.

Liang and Ma (1992) developed a constitutive model for the stress strain-pore pressure behavior of fluid-saturated cohesive soils. The model adopts the joint invariant of the second order stress tensor and clay fabric tensor as a formalism to account for material anisotropy. The model includes three internal variables: the density hardening variable representing changes in void ratio; the rotational hardening variable depicting fabric ellipsoid changes; and

finally, the distortional hardening variable controlling the shape of the bounding surface. The concept of quasi-pre-consolidation pressure was used in formulating an internal variable for the isotropic density hardening. For evolutionary laws based on micro-mechanics and phenomenological observations, Liang and Ma (1992) constitutive model gives the relationships for isotropic density hardening and anisotropic or rotational hardening in drained conditions. The model considers two counterpart mechanisms for the evolution of distortional hardening (R). One mechanism is that the bounding surface will widen along with the clay fabric moving to preferred orientations, meaning that a smaller value of R permits lower pore water pressure response. The other one is that the bounding surface will flatten along with the loading involving the principal stress rotation, meaning a larger value for R causes a sharper pore water pressure response. For un-drained conditions the model assumes that both water and clay particles are compressible which means a zero volumetric strain. The predictive capability of the model is tested on a database created from the available literature. The results show that the model is quite capable of predicting the behavior of saturated clays subjected to undrained cyclic loading, such as degradation of undrained strength and stiffness, accumulation of permanent strain and pore pressure, influence of initial consolidation conditions, and the effect of rotation of principal stress direction.

Wathugala and Desai (1993) modified hierarchical single surface (HiSS) models into a modified series of models (termed as δ^*) which could capture the behavior of cohesive soils. These models consider monotonic loading as virgin loading and unloading and reloading as non-virgin loading. An associated (δ_o) model of the series was found to be sufficient for predicting the cyclic behavior of clays. The model defines a new hardening function based on that the normally consolidated (NC) clays that do not dilate; and instead they show a

contractive response under monotonic loading. The model considers the unloading phase as elastic and reloading similar to virgin loading with some modification like a plastic modulus for virgin loading is replaced by a plastic modulus of reloading and a unit normal tensor is replaced by a unit normal tensor for a reference surface (R) which passes through the current stress point in the stress space. The results show that the model is capable of capturing the undrained shear behavior of normally consolidated clay, slightly over-consolidated clay behavior and drained behavior during hydrostatic compression tests and stress-strain behavior during cyclic loadings.

Hyodo et al (1993) proposed a semi-empirical model for the evaluation of developing residual shear strain during cyclic loading. The model considers 10% peak axial strain as a failure criterion in both reversal and non-reversal regions and gives a relationship between the cyclic deviator stress ratio and the number of cycles required to cause failure for each initial static deviator stress (q_s). The unified cyclic shear strength is given by:

$$R_f = \left\{(q_{cyc} + q_s)/p_c\right\}_f = \kappa N^{\beta} \quad \text{.....2.7}$$

Where; R_f = cyclic strength ratio; q_{cyc} = cyclic deviator stress; q_s = initial deviator stress; p_c = constant mean principal stress; N = number of cycles; $\kappa = 1.0+1.5q_s/q_c$ and $\beta = -0.088$.

The peak axial strains ε_p from all tests were related using an effective stress ratio:

$$\varepsilon_p = \eta_p/(2.0 - \eta_p) \quad \text{.....2.8}$$

Where; η_p = peak deviator stress divided by mean effective principal stress of each peak to peak cyclic stress (q_s / p). In order to introduce the undrained cyclic behavior of clay, two parameters were introduced in the model. The first parameter defined is an index (R/R_f) showing the possibility of cyclic failure, which is the ratio of peak cyclic deviator stress ($R = q_s + q_{cyc}$) to cyclic shear strength (R_f) in a given number of cycles. R/R_f is termed as a cyclic

shear strength ratio and is equivalent to a reciprocal of the safety factor against cyclic failure. When the magnitude of R is constant, R/R_f increases with the increasing number of cycles and carries from zero at non-loading to unity at failure. The second parameter in the model is defined as:

$$\eta^* = (\eta_p - \eta_s)/(\eta_f - \eta_s) \quad \text{.....2.9}$$

Where; η_p is an effective stress ratio at the peak cyclic stress in each cycle, η_s is the effective stress ratio of initially consolidated condition, η_f = effective stress ratio at the failure, and η^* = the relative effective stress ratio between initial point and final point in p-q space. These parameters were originally introduced for sand by Hyodo et al (1991). By correlating the values of both parameters, the model establishes a simple but useful relationship between the accumulated peak axial strain and the effective stress ratio. The best fit curve for each relation is given by a unique curve formulated as the following equation in spite of the difference of initial static and subsequent cyclic deviator stresses:

$$\eta^* = R/R_f/\{a - (a - 1)R/R_f\} \quad \text{.....2.10}$$

Where; the value of "a" is given as 6.5 by the experiments of Hyodo and Suiyama (1993).

McManus and Kulhway (1993) studied the behavior of cyclic loading of drilled shafts in laboratory-made cohesive soil (Cornell Clay). The applied loading was designed to simulate realistic windstorm events (both one-way and two-way loading), which is an important source of cyclic loading for foundations. Results show that for one-way uplift loading, the upward displacement accumulated by a drilled shaft was not found to be affected by either the size or the geometry of the model-drilled shafts or by the soil deposit stress history. In case of two-way loading, the direction of loading reverses twice every cycle

causing minimal response at low load levels but a sudden degradation in displacement response at moderate load levels, with an associated substantial reduction in capacity.

Silvestri, (1994) studied the water content relationships of sensitive clay subjected to cycles of capillary pressures. The study presents the results of an experimental investigation carried out to determine the volume change response of sensitive clay subjected to cycles of air pressure in a pressure plate apparatus. Several clay samples of varying initial water content were used in the test program. He reported that at high air pressures, the initially soft clay specimens become less compressible than stiff clay specimens of comparable water content. Also, the study indicates that the clay became unsaturated at a water content varying between 25 and 30%.

Bardet (1995) extended the novel concept of scaled memory (SM) model to anisotropic behavior and presented a technique to calibrate the material constants from laboratory data. He showed that SM generalizes closed stress-strain loops and, therefore, avoids the artificial ratcheting predicted by bounding surface plasticity. The extended SM model generalizes Ramberg-Osgood and Hardin Drenvich models and is simpler than, but as capable as, multiple yield surface plasticity.

Puzrin et al (1995) showed the consistency of normalized simple shear behavior of soft clays with the Massing rules. The study reveals that the degradation of soil properties in undrained simple shear is considered to be the main reason for deviation of cyclic shear behavior of soft clays from the pattern described by the Massing rules. Using the mean effective stress as a single fatigue parameter, it was found possible to describe this degradation in terms of Iwan's series-parallel model which leads to the concept of a non-degrading, normalized backbone curve. The results of the study also prove that the set of slip

stresses degrade proportionally to the decrease in the mean effective stress, whereas the small strain shear modulus appears to be invariant to changes in this stress. The study also reveals that by using the mean effective stress as a single fatigue parameter, it would be possible to describe degradation in terms of the parameters of Iwan's series-parallel model, which leads to the concept of a non-degrading, normalized backbone curve.

Lefebvre and Pfendler (1996) studied the results of the cyclic constant volume direct simple shear (DSS) on intact specimens of sensitive clay obtained at the St. Alban site in the St. Lawrence valley, 80 km west of Quebec City, Canada. The results of their tests are summarized in Table 4. In this table, c_u = monotonic undrained shear strength; I_p = plasticity index; N = number of cycles; N_y = number of cycles at failure; S_t = sensitivity to remolding; w = water content; w_L = liquid limit; w_p = plastic limit; γ = maximum single amplitude shear strain; γ_{st} = shear strain due to initial static shear stress; γ_y = maximum single-amplitude shear strain at failure; σ'_p = pre-consolidation stress; σ'_{vc} = vertical consolidation stress; τ_c = cyclic shear stress; τ_{st} = initial static shear stress; and τ_{tot} = total shear stress. The study shows that the shear strength of intact sensitive clay degrades fairly rapidly with the number of cycles when there is no initial static shear stress. However, the shape of the τc/Cu versus N curves indicates a lesser degradation of the cyclic strength with the number of cycles when there is an initial static shear stress. The study indicates that at a strain rate equivalent to a 0.1-Hz cyclic loading, the sensitive clay tested in this study can mobilize an undrained shear strength, which is about 40% higher than that determined at a standard strain rate, which is equivalent to a 12% increase per log cycle of the strain rate. The study also proves that, in cyclic tests, the high-strain-rate effect partially compensates for shear strength degradation with the number of cycles in such a way that, at 12 cycles, the cyclic shear strength can be

taken as equal to the undrained shear strength determined in monotonic tests at standard rates. Thus, confirming the results of one of the previous studies using triaxial tests on sensitive clay (Lefebvre and LeBoeuf 1987).

Yu, H. S. (1997) presented a simple, unified critical state constitutive model for both clay and sand. The model, called CASM (Clay and Sand Model), was formulated in terms of the state parameter, defined as the vertical distance between current state (v, p') and the critical state line in v-$ln\ p'$ space. The paper shows that the standard Cam-clay models (i.e. the original and modified Cam-clay models) can be reformulated in terms of the state parameter.

Faker et al (1999) studied the behavior of soft clays, which usually have water content higher than their liquid limits. The study proposes that a rotary viscometer should be used to measure the yield stress of the super soft clays instead of using a conventional soil mechanics apparatus. By plotting the results of yield stress measurements of soft clays in terms of w/LL, it could be shown that the true liquid limit is 1.5 – 2 times that which is arbitrarily selected and measured by the established conventional methods. The results of the study also show the variation in shear stress with respect to the liquidity index (Figure 2.16). Furthermore, it is indicated that the logarithmic of the yield stress of soft clay normalized with respect to the equivalent effective vertical stress (σ*) on the intrinsic compression line (ICL) is linearly related to the ratio of water content to liquid limit (w/LL) for all clays in the study, and that the lines for each soil are parallel.

Miller et al (2000) studied the behavior of soft compacted clayey soil (used in railroad sub-grade) subjected to repeated loading under train traffic. Cyclic triaxial tests were conducted on tube samples at their natural water content (partially drained) and on samples subjected to back-pressure saturation (undrained). The study indicates that, for repeatedly

loaded soils, a critical cyclic stress or normalized cyclic shear strength exists above which the soil will exhibit shear failure. For the highly plastic clay tested, the normalized cyclic shear strength was sensitive to the initial degree of saturation in the relatively narrow range encountered, i.e., a degree of saturation (S) between 90 and 100%. For the samples at natural water content, the normalized cyclic shear strength decreased as the initial degree of saturation increased. An empirical relationship was defined to describe the variation of normalized cyclic strength as a function of the degree of saturation. In the case of tests conducted on back pressure saturated specimens or undrained conditions, the normalized cyclic shear strength fell between 0.50 and 0.79, whereas the normalized undrained shear strength from the static test at the same confining pressure was 0.89. The normalized undrained cyclic shear strength for the specimen with laboratory-induced over consolidation ratio (OCR) of 3 was greater than 0.79 for the same confining stress. The magnitude of the deviator stresses estimated from stress cell measurements under traffic in the Low Track Modulus (LTM) zone suggest that the cyclic shear strengths were frequently exceeded in the nearly saturated sub-grade zones along the test track. Measurement of track settlements and corresponding degrees of saturation appear to corroborate the relationship between cyclic shear strength and degree of saturation.

Zhou and Gong (2001) studied soil degradation from the point of view of cyclic axial strain through stress-controlled triaxial tests on Hangzhou normally consolidated clay. Different influence factors on strain, such as cyclic stress ratio, overconsolidation ratio, and frequency, were studied. Degradation index was redefined according to the tests. A mathematical model for strain degradation was presented and verified.

Javed (2002) categorized the parameters that are believed to govern the behavior of sensitive clay into two categories: physical and mechanical. The study proposed a procedure to design and/or examine the conditions regarding foundations on sensitive clay. The study also indicates how to use a part of Modified Cam Clay Model to cross check the reduction in strength before and after the application of cyclic loading. A relationship is proposed for the number of cycles, factor of safety, cyclic strength ratio with respect to sensitivity of clays.

Li and Meissner (2002) developed a two-surface model for predicting the undrained behavior of saturated cohesive soils under cyclic loads. They used kinematic hardening and the theory of critical state soil mechanics. The proposed model was verified with respect to the observed behavior of soil samples. The study shows that like other multi-surface model, this model can realistically describe some important responses of clays subjected to both monotonic and cyclic loading, while incorporating the memory of particular loading events.

Oka et al (2003) proposed a cyclic viscoelastic-visco-plastic constitutive model in order to estimate viscous effect of clay in the wide range of low to high level of strain. The model was used to analyze the seismic response against foreshocks, main shock as well as aftershocks of 1995 Hyogoken Nambu Earthquake. The study concludes that the proposed model gives a good description of the damping characteristics of clay layer during large earthquakes.

Min et al. (2004) studied, based on a series of cyclic triaxial tests, the effect of cyclic load frequency on the undrained behavior of undisturbed marine clay. The results showed that for a given dynamic stress ratio the accumulated pore water pressure and dynamic strain increased with the number of cycles. The study also indicates that, a threshold value exists for both the accumulated pore water pressure and dynamic strain, below which the effect of

cyclic frequency is very small, but above which the accumulated pore water pressure and dynamic strain increase intensely with the decrease of cyclic frequency for a given number of cycles. Furthermore, the dynamic strength increases with the increase of cyclic frequency, whereas the effect of cyclic frequency on it gradually diminishes to zero when the number of cycles is large enough, and the dynamic strengths at different frequencies tend to the same limiting minimum dynamic strength. The test results demonstrate that the reasons for the frequency effect on the undrained soil behaviors are both the creep effect induced by the loading rate and the decrease of sample effective confining pressure caused by the accumulated pore water pressure.

Kakoli (2004) studied the chemical aspects involved in increasing or decreasing the shear strength of sensitive clay subjected to cyclic loading. In addition to chemical parameters she also reviewed the effects of physical and mechanical parameters and came to the fact that no single model can precisely predict the behavior of sensitive clay under cyclic loading.

Thammathiwat and Chim-oye (2004) studied experimentally the behavior of cyclic strength and pore pressure characteristics of soft Bangkok clay. The experimental investigation was conducted by using the cyclic triaxial apparatus under stress controlled and undrained conditions. The undisturbed samples were collected at the depth of 7.50-8.00 meter at the Faculty of Engineering, Thammasa University. The physical property test results showed that subsoil was silty-clay with 78-95% of natural water content, LL in the range 75-99%, PL in the range of 30-42 % and specific gravity in the range of 2.57 -2.73 . The test results showed the axial strain and the excess pore water pressure both increased with increasing the number of loading cycles in all cases. But the shear modulus decreased with the increase in number of loading cycles. While, the damping ratio decreased lightly with

increasing the number of loading cycles. The effect of rate of loading on the cyclic properties was also investigated. The loading frequencies adopted for the test were 0.l, 0.5 and 1.0 Hz. It was found that the cyclic strength increased with increasing of loading frequencies for a given confining stress but excess pore water pressure decreased with the increasing of loading frequencies.

Vinod et al. (2005) conducted a significant number of stress-path triaxial tests with stress probes in various directions, to study the stress-path dependent behavior of an overconsolidated weathered crust of Champlain clay in Eastern Ontario. Both undrained and drained tests were conducted for samples isotropically consolidated to the in situ vertical stress and anisotropically consolidated to the in situ state of stress. The yield locus of the clay crust was defined. The study proved that the strength-deformation and yielding behavior of this weathered clay crust highly depends on the stress-path as well as on the in situ stress history.

Erken and Ulker 2006 studied the effect of cyclic loads on monotonic shear strength on torsional apparatus. Tests were conducted on both reconstituted and undisturbed fine-grained hollow soil specimens. The existence of a critical shear strain level, called yield shear strain, where softening starts, was determined from cyclic tests. The level of cyclic yield strain was ± 0.75% for the reconstituted soil specimens and ± 0.5% for the undisturbed soils. The study shows that if soil undergoes a cyclic shear strain level below the cyclic yield strain, reduction of monotonic strength of reconstituted and undisturbed specimens is limited, but when cyclic shear strain level is larger than yield strain monotonic strength decreases down to 40% of its initial strength.

Hanna and Javed (2008) defined the safe-zone, within which a combination of the cyclic deviator stress (q_{cyc}) and number of cycles (N) for a given soil condition, a quasi-elastic resilient state can be achieved during the undrained period without reaching failure. The schematic presentation of this safe zone is shown in Figure 2.17. In this figure, the failure line should be developed in the laboratory for the given soil condition (I_L, S_t and σ_p). For any number of cycles (N), the corresponding point on the failure line reveals the ultimate cyclic deviator stress. A reasonable factor of safety should be implemented for determination of the allowable cyclic deviator stress (q_{cyc}), depending on the size and nature of the project. A combination of the cyclic deviator stress (q_{cyc}) and the number of cycles (N) located on or above the failure line indicates that foundations built on this clay will eventually reach failure during the undrained period.

2.1 Discussion

Studies dealing with the sensitive clays are very limited and most of them are not directly linked with the sensitivity (S_t) or with the variation in sensitivity constant (k). Early investigations on sensitive clays were focused on conducting triaxial tests on undisturbed and remolded clay for the purpose of developing relationship between cyclic stress-strain and pore water pressure (Seed and Chan 1966, Theirs and Seed (1968, 1969), Sangrey 1968, Sangrey et al 1969, France and Sangrey 1977 and Sangrey et al 1978). Their study established the fact that cyclic loading increases the pore water pressure under undrained conditions up to a number of cycles, which defined as a critical level beyond which the failure will occur. Iwaski et al (1978) defined the quasi-elastic resilient state of soils subjected to regular drained cycling during stress-controlled loading between the two general stress states. Field and laboratory investigations conducted by

Changnon et al (1979) provide useful data base for studying the behavior of sensitive clays under varying conditions of index properties. An interesting study reported by Houstan and Hermann (1980) raised a question concerning the relative importance of plasticity and sensitivity and also the need of analysis based on the combination of static and cyclic loading in the case of sensitive clays. Matsui et al (1980) proved experimentally that an over-consolidation clay due to cyclic stress-strain history is similar to strength to one due to the ordinary over-consolidation history. He also established the fact that, inspite of the temporary loss in shear strength and deformation modulus immediately after cyclic loading, the dissipation of pore pressure leads to strength higher than the initial strength. Seed and Idris (1982) established the fact that in case of clay the faster the rate of cycling the more the situation resembles to undrained conditions. The experimental study of Procter and Khaffaf (1984) gives an idea that, if data from load controlled tests are reanalyzed to account for rate effects on shear strength, then a constant value independent of frequency is obtained. The Lefebyre and LeBoeuf (1987) experimental study on highly sensitive clays (S_t>100) indicates that the effect of the strain rate on undrained shear strength ratio appears to be the same for both naturally overconsolidated clays and normally consolidated clays. McManus and Kulhway (1993) indicated that for a drilled shaft in a cohesive soil foundation, a two-way moderate cyclic loading causes a sudden degradation in displacement with an associated substantial reduction in bearing capacity. The Lefebvre and Pfendler (1996) study shows that for a sensitive clay (St = 300) the shear strength of clay degrades fairly rapidly with the number of cycles when there is no initial static shear stress as compared to the case when there is an initial static shear stress component. Faker et al (1999) achieved the realistic results by using the rotary viscometer instead of a conventional soil mechanics apparatus to measure the shear strength of super soft clays. This approach can be used for quick clays as well.

Nevertheless, the results are limited to the conditions of the experimental work and do not include the combined effect of the parameters which govern the behavior of sensitive clay subjected to static or cyclic loading.

Eekelen and Potts (1978) introduced a fatigue parameter as a function of pore water pressure, in the Modified Cam Clay Model, which assisted in predicting reliable results for the shear strength of clays at the end of a given number of load cycles. Ansal and Erken (1989) proposed an empirical model based on their experimental results and defined critical level of cyclic deviatoric stress. Wood (1990) established a relationship among the sensitivity number, the sensitivity constant, k (given by Bejerrum 1954) and the liquidity index. He proposed that it is more desirable to mention maximum shear stress (τ_f) in terms of undrained shear strength (c_u), which is the radius of all the Mohr circles. The model proposed by O' Reilly et al. (1991) emphasizes that since both the shear strength and the deformation properties of soils under cyclic loading are anisotropic; therefore, triaxial compression, triaxial extension and direct simple shear (DSS) tests should be included in the laboratory test program for gravity structure of some importance. Liang and Ma (1992) constitutive model's results indicate that it is quite capable of predicting the behavior of saturated clays subjected to undrained cyclic loading, such as degradation of undrained strength and stiffness, accumulation of permanent strain and pore pressure, influence of initial consolidation conditions, and the effect of rotation of principal stress direction. The Wathugala and Desai (1993) modifications for hierarchical single surface (HiSS) model make it capable of capturing the undrained shear behavior of normally consolidated clay, slightly over-consolidated clay, drained behavior during hydrostatic compression tests and stress-strain behavior during cyclic loading. Hydo et al (1993) proposed a semi-empirical model by introducing two parameters: namely, the ratio of peak cyclic deviator

stress to cyclic shear strength for a given number of cycles and the relative effective stress ratio between initial and final point in p-q (deviator stress-mean effective stress) plane. Bardet (1995) extended the Scaled Memory Model (SM) to accommodate the anisotropic behavior of the clays. The study conducted by Puzrin et al. (1995) indicates that by using a mean effective stress as a single fatigue parameter, it would be possible to describe degradation in cohesive soils subjected to cyclic loading. Results of the Miller et al (2000) study confirms the studies of Sangrey et al (1969), Matsui et al (1980) and Ansal and Erken (1989) for the critical cyclic stress level and established an empirical relationship between cyclic shear strength ratio and the degree of saturation. All these model studies provide useful relationship among the different governing parameters. These models mainly deal with the normal nature of cohesive soils and extremely useful in predicting the behavior of foundation soil when subjected to static or cyclic loading. Nevertheless, none of the model truly addressed the complex behavior of sensitive clay. Most of these Model studies are mainly focused on the mathematical introduction or modification of a single physical or mechanical parameter in a proposed or an existing model to predict the behavior of soil under a special condition. The major short coming is that none of the model can be used as a reliable tool to design new or examine existing foundations by keeping in view the sensitivity of the clay and the influence of the combined effect of major physical and mechanical parameters on the complex behavior of the clay.

The schematic model for the “Safe Zone” given by Hanna and Javed (2008) was the first of its kind to deal with this complex material and to link the physical and mechanical parameters governing the behavior of sensitive clay. They introduced a useful guideline and theory to predict reliable safety factor for designing foundation in those regions of clay where a wide range of sensitivity number and extreme variations in physical and mechanical parameters exists.

Keeping in view the important relationships among shear stress, number of cycles, consolidation history, pore water pressure development and strain accumulations and so forth established by experimental investigation. The use of numerical and analytical models which explained and further enhanced the concepts of strain hardening, normal and over-consolidation behavior, total and effective stress paths both for static loadings and cyclic loadings.

It is therefore imperative to conduct such studies which, take into account the sensitivity of clayey soils as a deciding element to establish a reasonable factor of safety for designing foundations subjected to cyclic loading or combination of static and cyclic loading. The present investigation addresses the short coming in the experimental and model investigation given in the literature. This study redefines the useful tool of the "safe zone" (Hanna and Javed, 2008) based on detailed experimental investigation and analysis. The study also used a well-known existing model "Modified Cam Clay Model" to cross check the reduction in shear strength due to cyclic load application for a given sets of governing parameters. A relationship is proposed for the number of cycles, factor of safety, cyclic strength ratio with respect to sensitivity of clays. Based on this discussion, the objectives of the present study can be defined as follows:

2.2 Thesis objectives

Based on literature review described above the following are the objectives of this study:

- To identify and prioritize the relative importance of the governing mechanical and physical parameters under drained and undrained conditions.

- To model this complex behavior using the "Modified Cam Clay" to predict the shear strength in view of various parameters, which governs this complex nature of sensitive clay subjected to static or cyclic loading.
- To establish the safe zone and to redefine its critical limits based on the selection of the lowest shear strength ratio either from the experimental data or those predicted by using Modified Cam Clay Model.
- In order to achieve these objectives a comprehensive experimental investigation was planned to examine the behavior of sensitive clay under the undrained or drained conditions and subjected to static or cycling loading.
- To present the result of this investigation in the form of design theory and design procedure for practicing use.

Table 2.1: General Properties of Investigated Soils

(Lefebyre and leBoeuf 1987)

Location	Depth (m)	Natural water content w (%)	Liquid limit w_l	Plastic limit w_p	Plasticity Index I_p	Liquidity Index I_l	< 2μm	Sensitiviy S_t	Pre-consoli-dation pressure σ'_p
Dyke-12	-	54-65	33.5	21.8	11.7	2.84	59	>300	112
Dyke-39	-	35-52	27	20.0	7.0	2.85	45	500	190
Olga	4	90-93	68	28	40	1.55	90	-	78
B6	6.8	50	38	24	14	1.80	76	100	145
B6	10.1	48	32.5	22.3	10.1	2.47	75.7	450	175
St. Jean	-	42	36	20	16	1.38	50	100	940

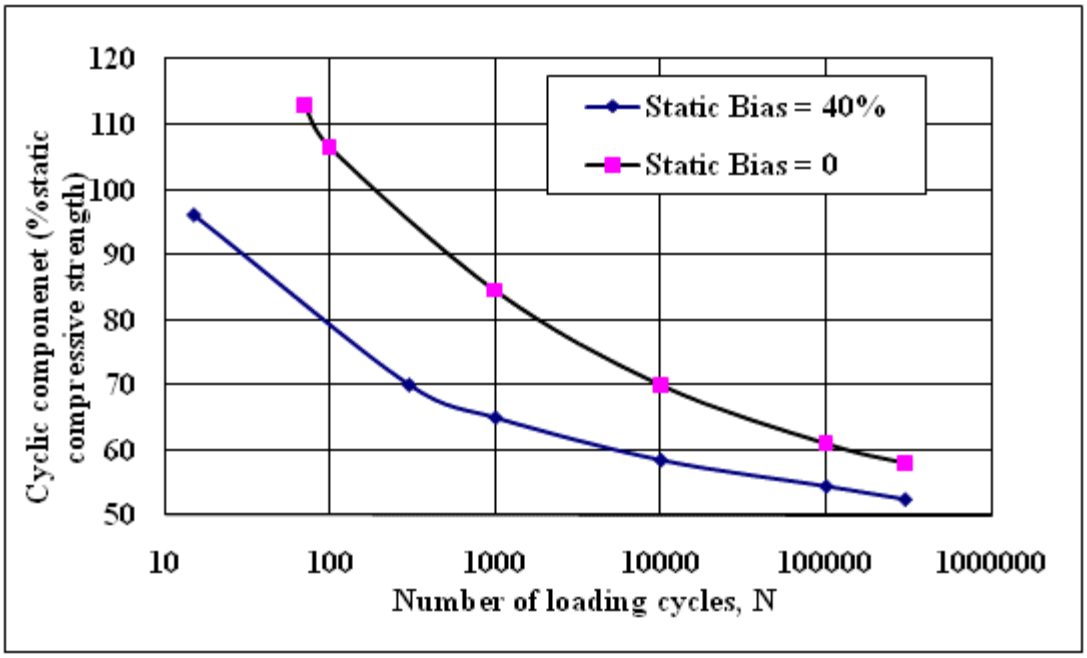

Figure 2.1: Cyclic failure data for San Francisco Bay Mud (Houstan and Hermann, 1979)

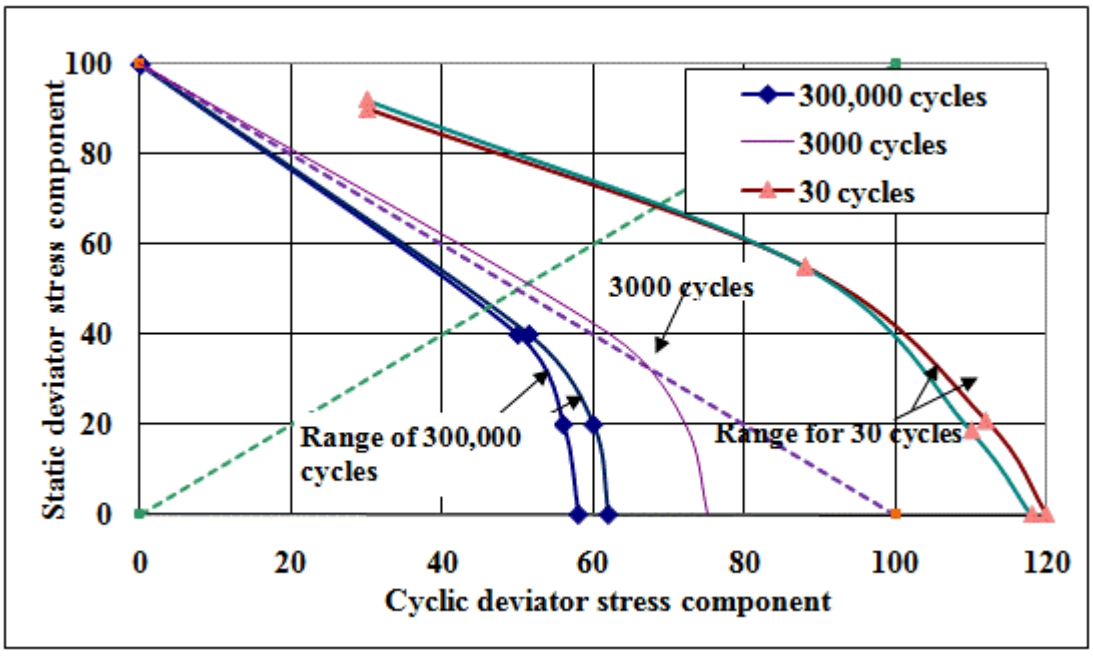

Figure 2.2: Cyclic strength contours for San Francisco Bay Mud

(Houstan & Hermann, 1979)

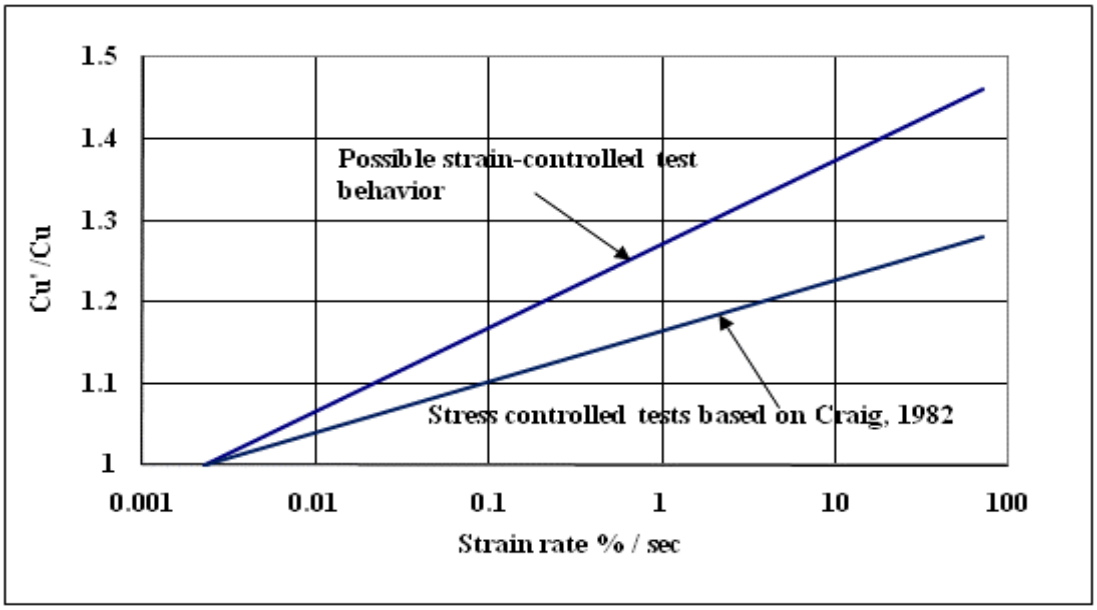

Figure 2.3: Ratio of modified to static shear strengths versus strain rate (Procter and Khaffaf, 1984)

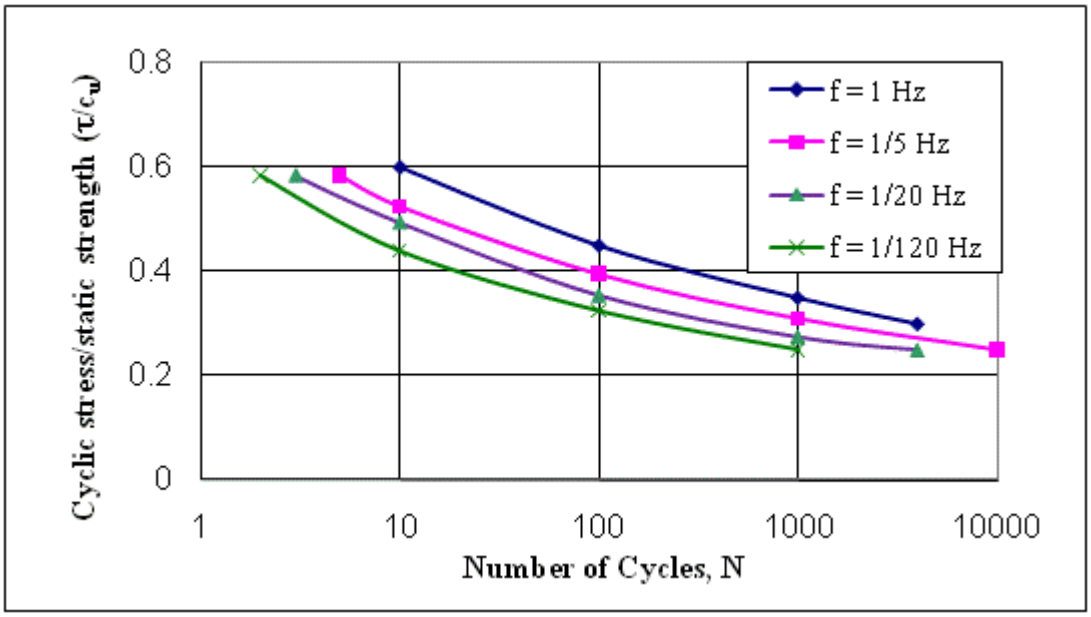

Figure 2.4: Frequency response of cyclic stress ratio (τ/c_u) (Procter and Khaffaf, 1984)

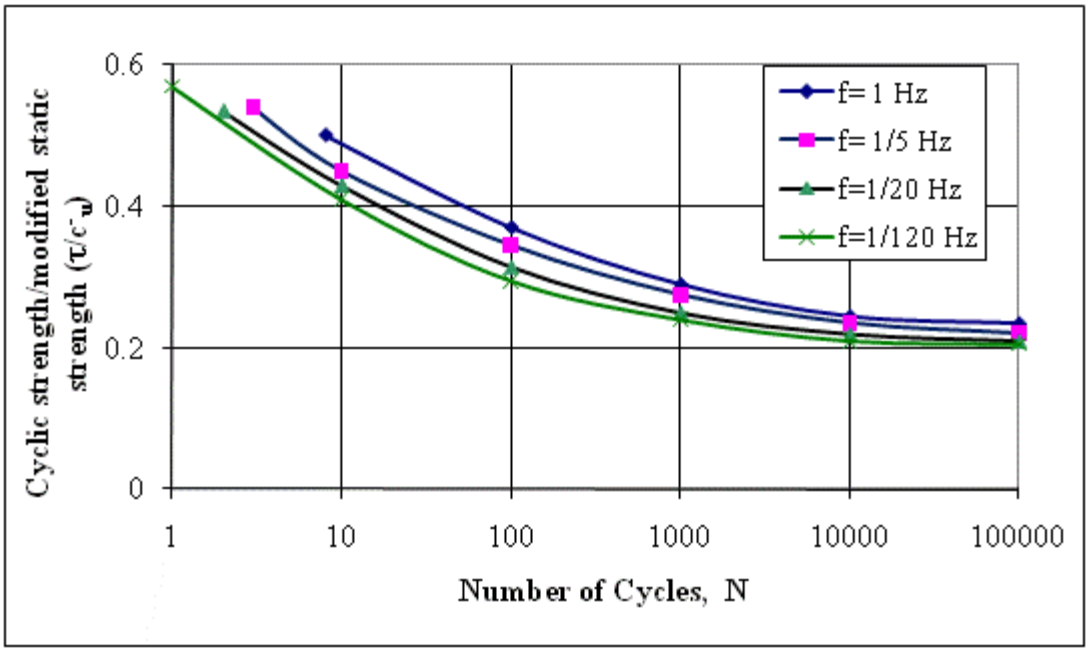

Figure 2.5: Frequency response of modified cyclic stress ratio (τ/c'_u)

(Procter and Khaffaf, 1984)

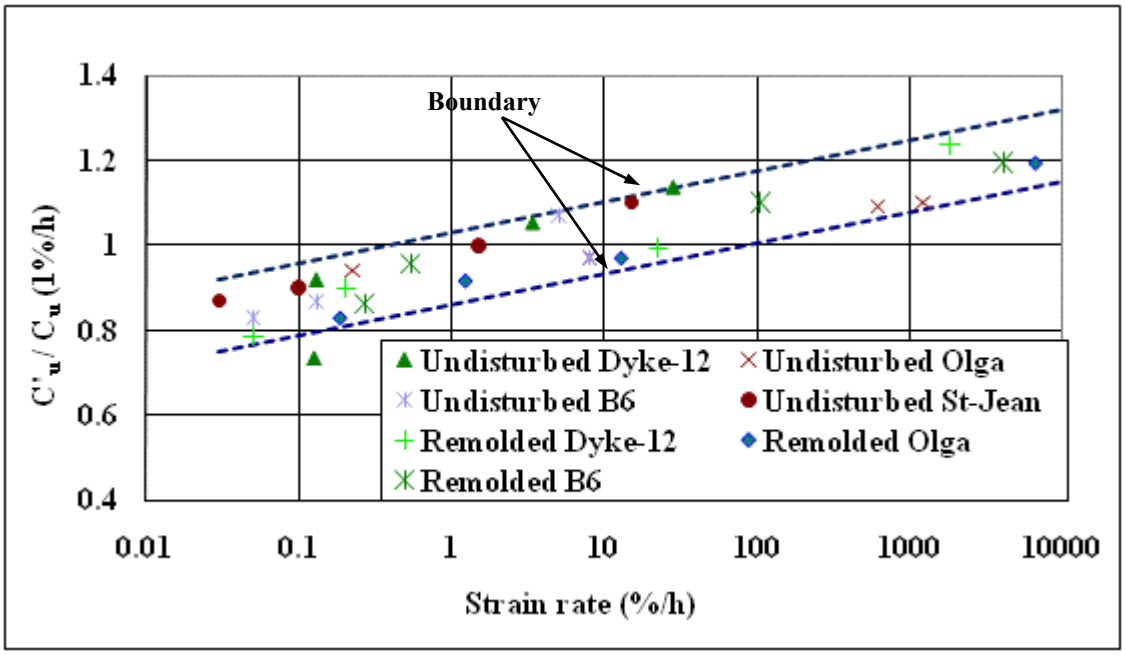

Figure 2.6: Change of undrained strength ratio, normalized to undrained strength ratio at strain rate for all investigated clays (Lefebyre and LeBoeuf, 1987)

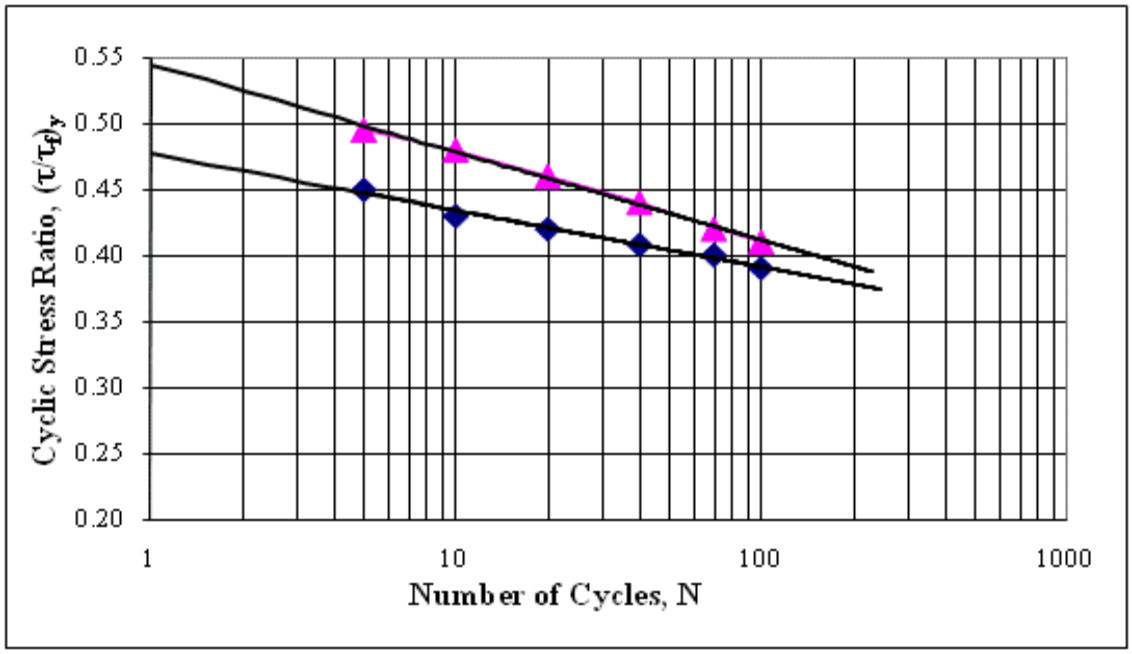

Figure 2.7: Cyclic yield strength versus number of cycles

(Ansal and Erken, 1989)

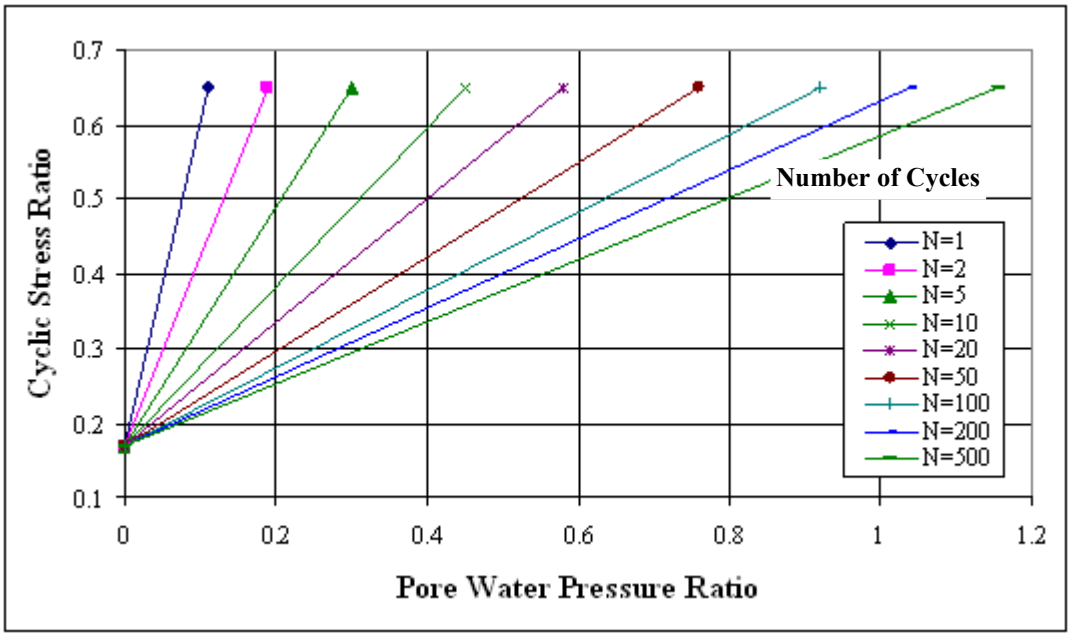

Figure 2.8: Cyclic stress ratio-pore pressure relationship for different numbers of cycles

(Ansal and Erken, 1989)

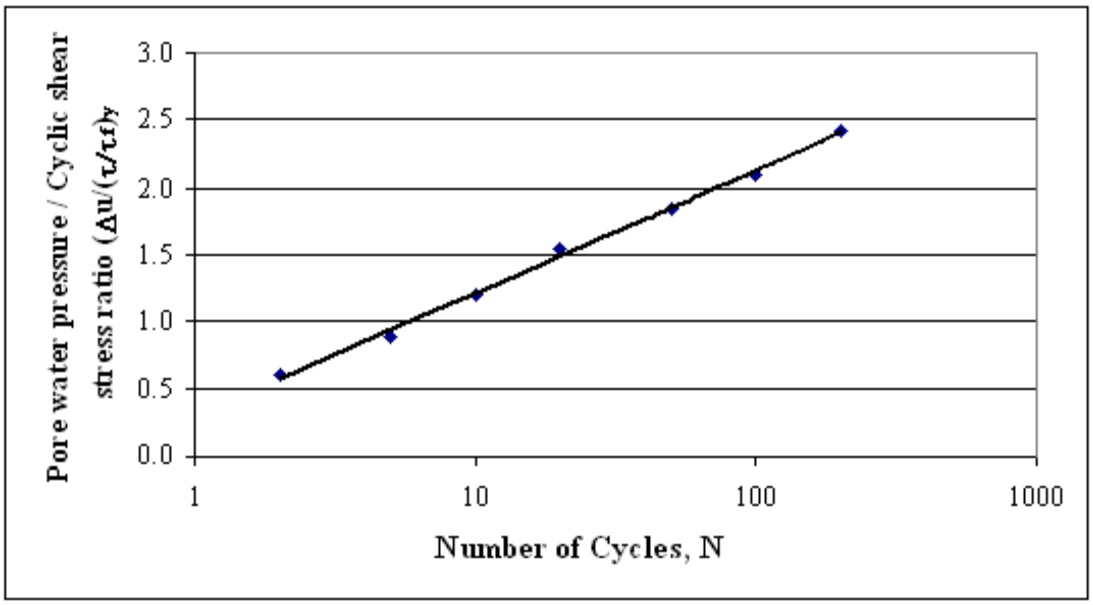

Figure 2.9: Slope of pore water pressure lines versus number of cycles (Ansal and Erken, 1989)

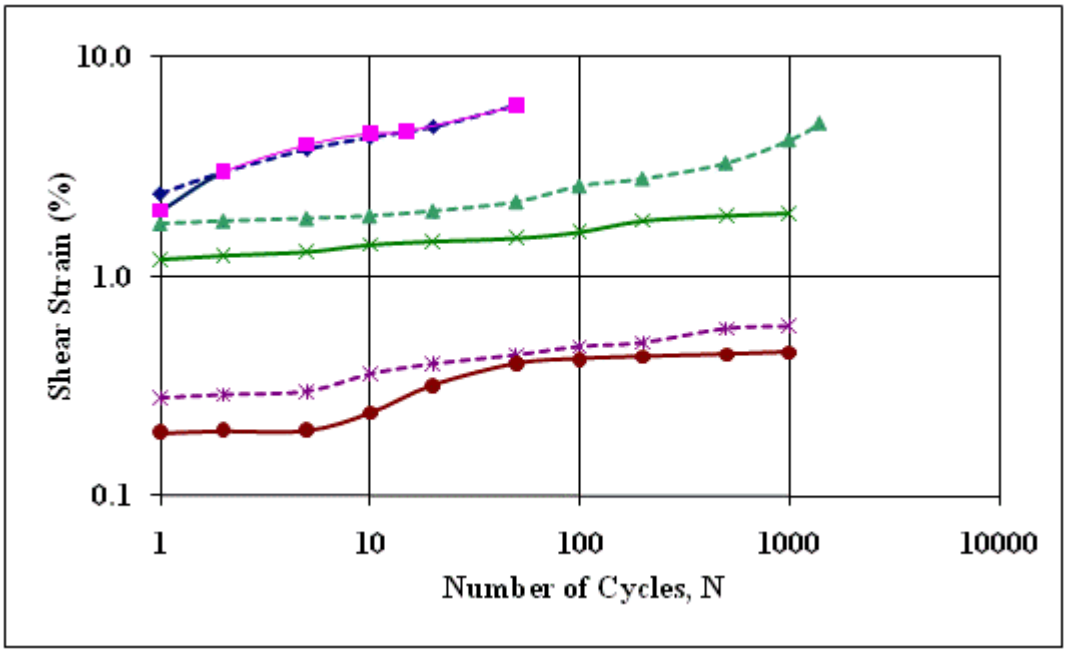

Figure 2.10: Comparison of shear strain of one-dimensionally consolidated and remolded samples (Ansal and Erken, 1989)

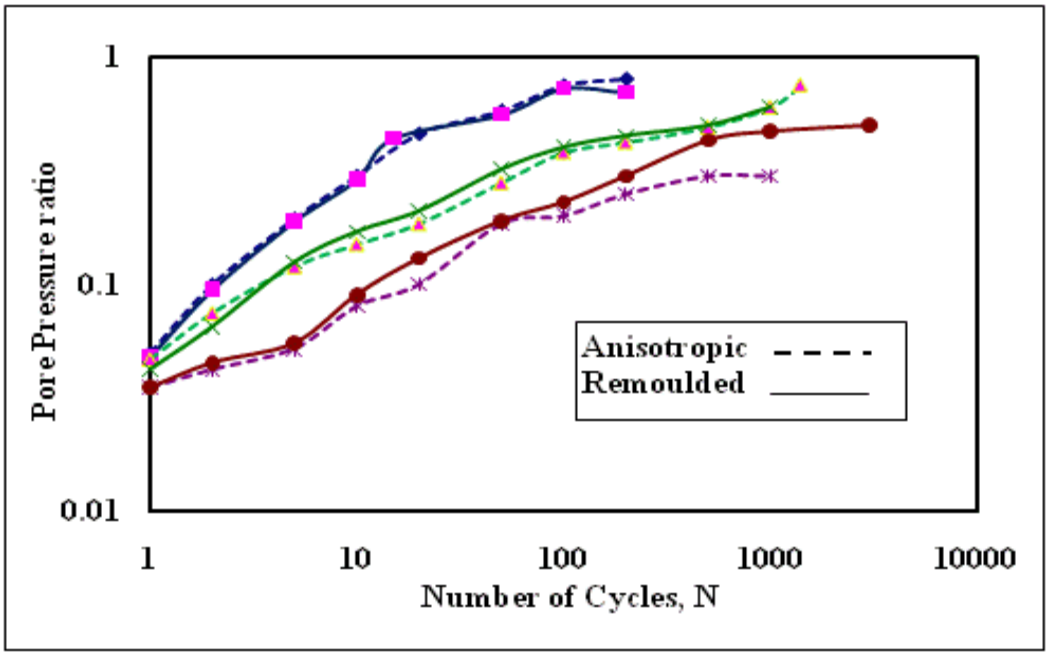

Figure 2.11: Comparison of pore water pressure of one-dimensionally consolidated and remolded samples (Ansal and Erken, 1989)

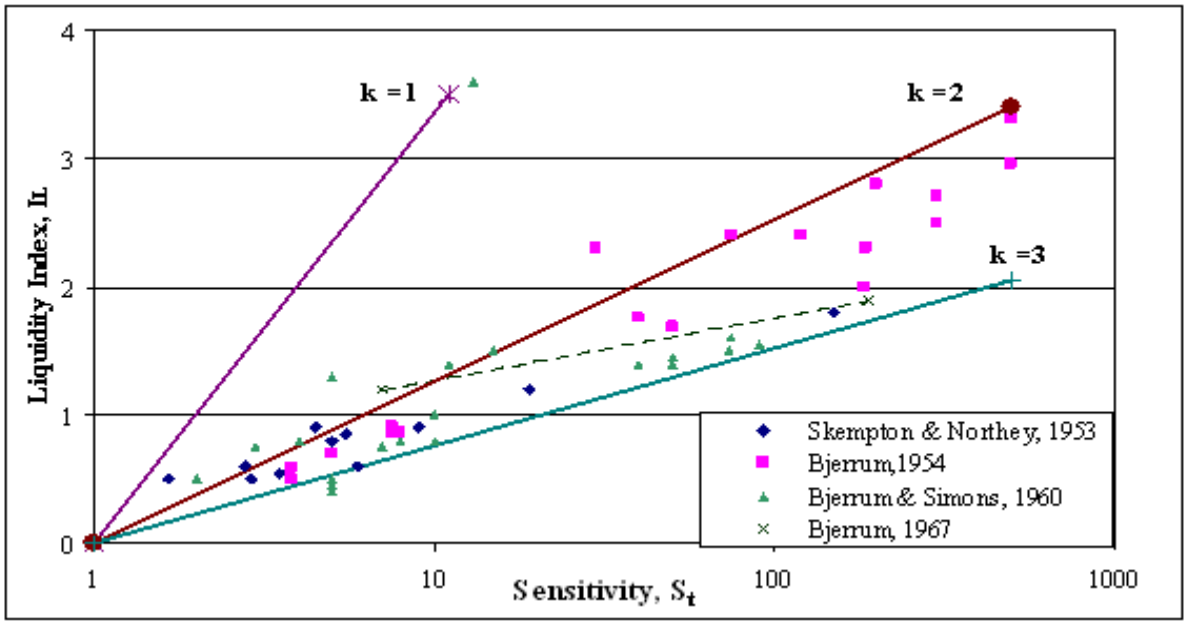

Figure 2.12: Interrelationship between sensitivity and liquidity index for natural clays (Wood, 1990)

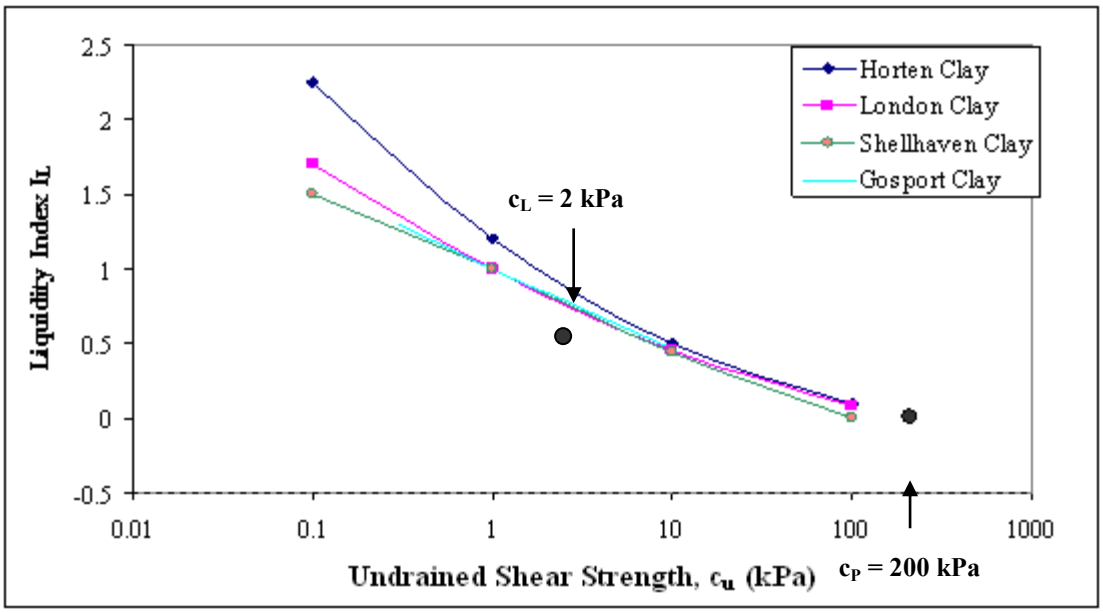

Figure 2.13: variation of remolded undrained strength c_u with Liquidity index, IL (Wood, 1990)

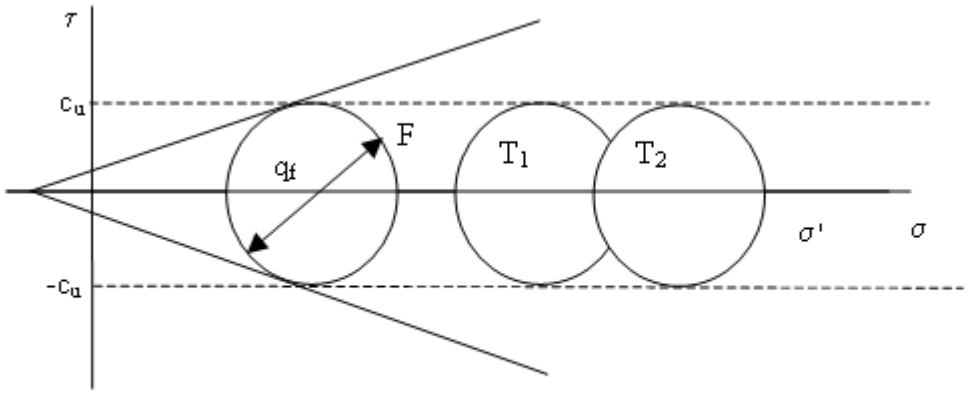

Figure 2.14: Mohr's circles of total stress and effective stress

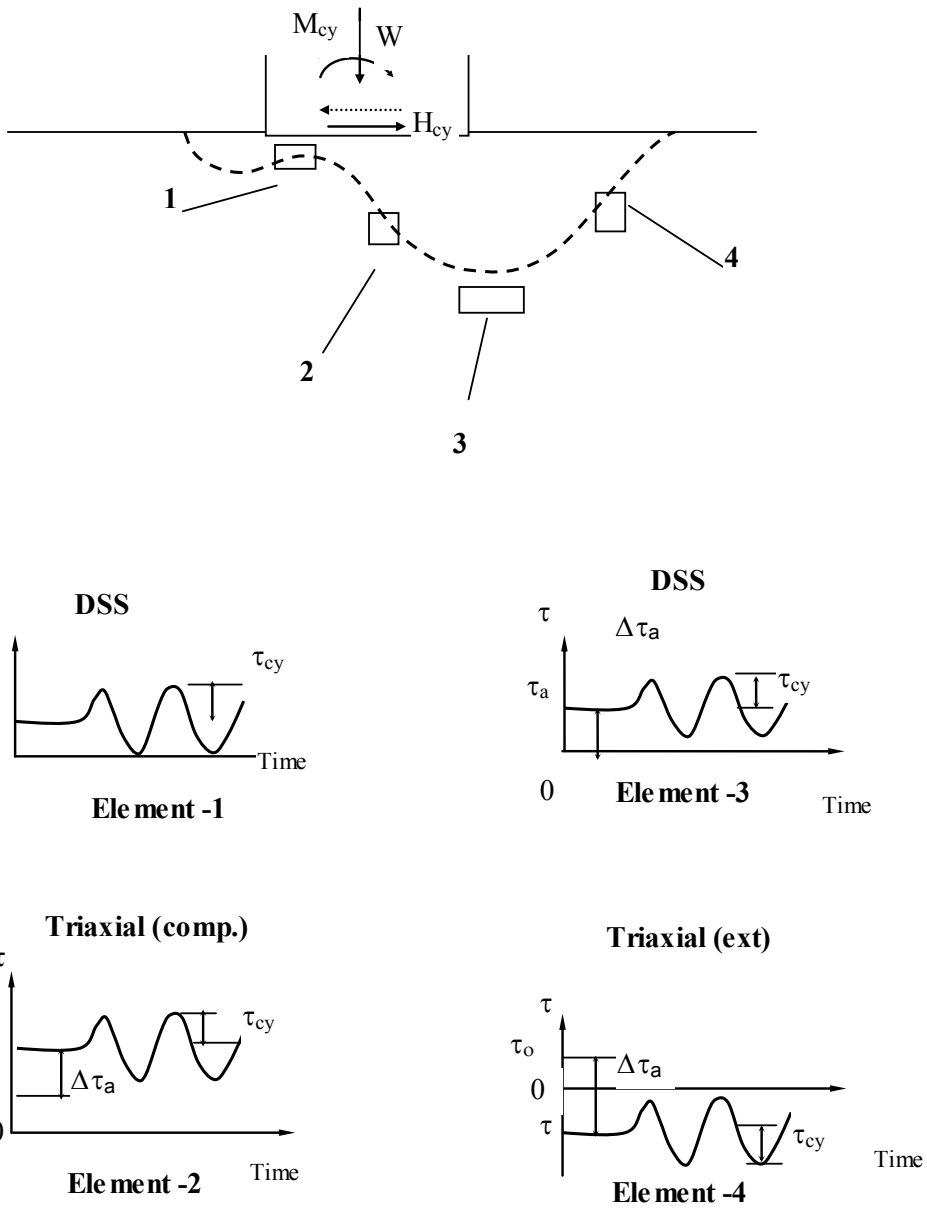

Figure 2.15: Simplified stress conditions for some elements along a potential failure surface (Reilly and Brown, 1991)

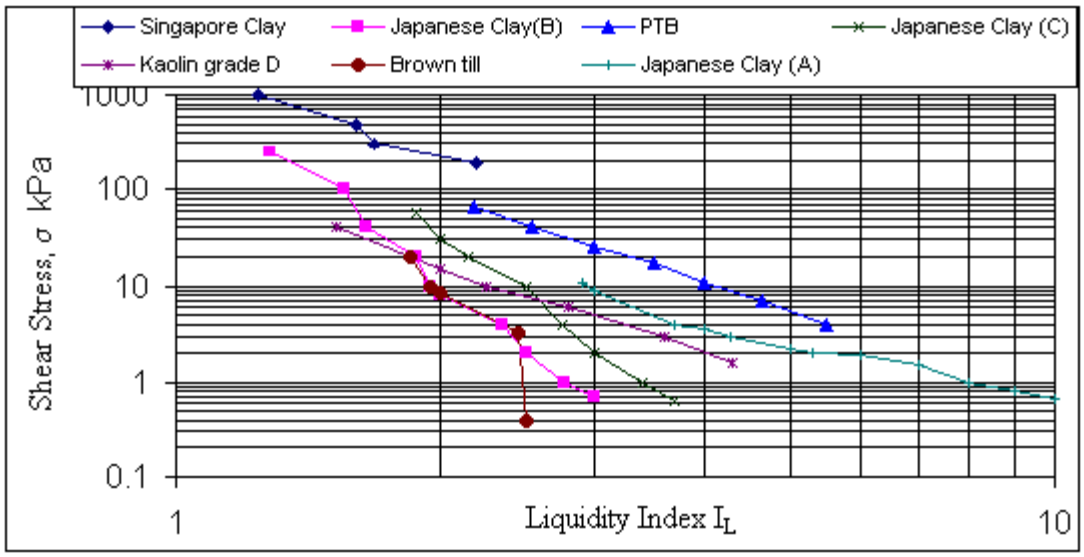

Figure 2.16: Variation in shear stress with respect to liquidity index (Faker et al, 1999)

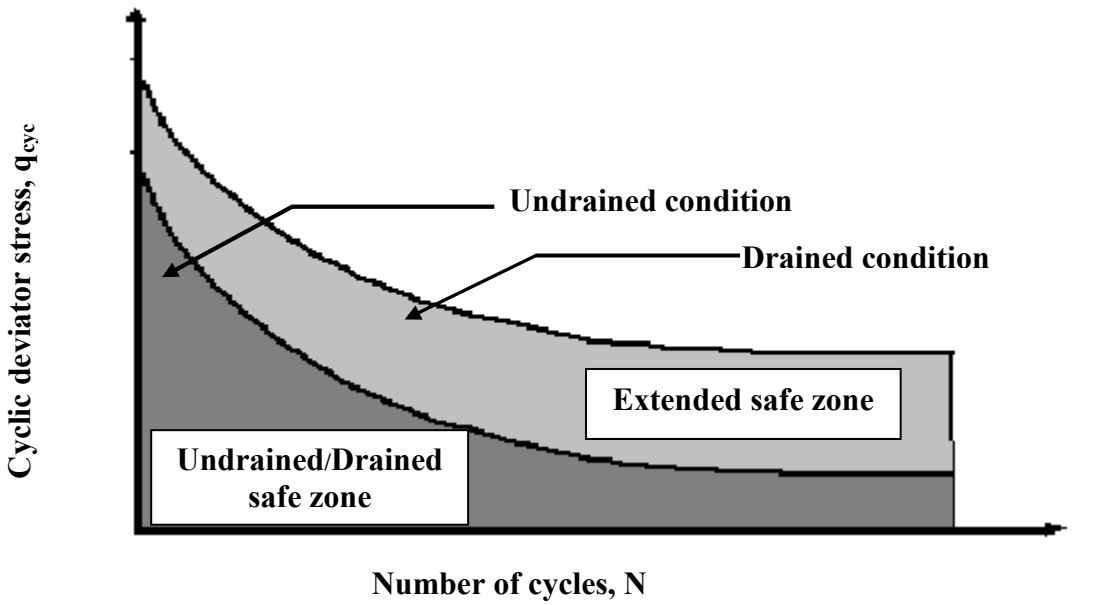

Figure 2.17: Safe Zone for foundation on sensitive clay (Hanna and Javed, 2008

Chapter 3

Experimental Investigation

To achieve the goals of the present study, it was necessarily to design a well-planned experimental framework, which is capable to answer the many outstanding questions concerning the role of major physical and mechanical parameters affecting the shear strength of sensitive clay under static or cyclic loading. This chapter describes the experimental set-up, samples source, techniques used to obtain undisturbed and remolded samples, grouping of samples, laboratory test conducted to determine the physical, mechanical, sensitivity number and index properties and test procedure for static and triaxial compression tests.

3.1 Sample Source

Considering the nature of the sensitive clay, tests were conducted on samples that cover reasonable variation of governing parameters. Moreover, samples are taken from sites, whose physical and mechanical properties covering a wide range in practice. These sites are the well-known sensitive clay regions of Eastern Canada. These sites (see Figure 3.1.1) have a well-established database and can be considered, representative of various conditions encountered to sensitive clay regions all over the world.

3.2 Methods of Acquiring Samples

Based on the information collected from the literature (Silvestri 1981), the block sampling method was used to obtain undisturbed samples from different parts of Eastern Canada. The

samples were taken from a depth ranging 4 to 10 meters deep. A geotechnical company named Queformat from Longueuil Quebec, has assisted in extracting these samples, where the soil was sufficiently stiff or cemented. If however, the soil was comparatively soft, Sherbrooke sampler was used, which give soil samples of comparable quality to that produced by block sampling.

The block sample was obtained by cutting a column of soil about 300mm cube, so that it would fit inside a box with a clearance of 10 to 20 mm from all sides. A box with a detachable lid and bottom was used for storage. With the lid and bottom removed, the sides of the box were slid over the prepared soil block, which was as yet attached to the bottom of the pit. After filling the space between the sides of the box and block with paraffin wax, and similarly sealing the top of the block, the lid was placed on the box. The block was then cut from the soil using a spade, and the base of the sample trimmed and sealed. In order to obtain samples from depth more than 3m and to avoid base heave, Sherbrooke sampler (Levebvre and Poulin, 1979) was used as shown in Figure 3.2.1.

For cylindrical samples, a borehole of about 400 mm diameter, which was best cleaned using a flat- bottomed auger, in order to reduce disturbance and minimize the amount of disturbed material left in the base of the hole before sampling. The hole was kept full of bentonite mud. The sampler was lowered to the base of the hole, and rotated, using a small electric motor, at about 5r.p.m. A cylinder of soil, about 250 mm in diameter, was carved out by three circumferential blades, spaced at 120°. These blades made a slot of about 50mm wide, and were fed by bentonite to help clear the cuttings. After carving out a cylinder about 350 mm high, the operator pulled a pin and the blades (which were spring-mounted) gradually rotated under the base of the sample, as rotation was continued. Closure of the blades

separated the sample from the underlying soil, and the sample was then lifted to the surface with a block and tackle. The sample was then coated with layers of paraffin wax and placed in a container packed with damp sawdust. The disturbed samples or the samples which were accidently disturbed used to determine most of the index properties.

3.3 Types of Selected Clays

Four types of clays with different sensitivity numbers were selected for the present research work. To avoid any confusion, samples were identified in site for the location and depth. The clays were named as; Type-A, Type-B, Type-C and Type-D.

The samples for the Clay Type-A were mostly taken from Petite-Patrie and Chambly areas of Eastern, Canada. For the clay Type-B, samples were taken from Grande Balene and St Nicolas. The samples for Type-C were taken from St. Huges and Terrebonne area. For the clay Type-D, the samples were mostly taken from Mont. St. Hilarie area.

3.4 Grouping of Samples and Type of Tests Conducted

The clay samples obtained were divided into five groups, each group contained all types of sensitive clays (A, B, C and D) used for the present study. Group-I consisted of virgin undisturbed samples directly from the field. The samples of Group-II were derived from Group-I which, were failed in triaxial static or cyclic test or got excessively disturbed while transportation. The samples of Group-II were remolded samples, at same water contents (w_c) as Group-I. Group-III samples were derived from Groups I & II, which were failed in triaxial static or cyclic test. The samples of Group-III were reconstituted at water content (w_c) ranged from 1 to 1.5 of LL. Therefore, Group-III represents those clay samples which, were influenced by intrinsic aspects (intrinsic shear strength). For Groups II & III, normally consolidated specimens were made by isotropic consolidation for 24 hours under three

effective confining pressures (150 kPa, 200 kPa & 250 kPa). Overconsolidated specimens were made by isotropic consolidation under an effective confining pressure of 200 kPa, followed by swelling for 24 hours to give an overconsolidation ratio between 1.5 and 4. Group-IV consisted of those samples of Group-I, which reached quasi elastic resilient state at N number of cycles in the initial cyclic triaxial test. Similarly, Group-V consisted of those samples of Group II & III, which reached quasi elastic resilient state at N number of cycles in the initial cyclic triaxial test. Group-IV and V samples were subjected to static undrained triaxial test to estimate the reduction in static shear strength after suffering N number of cycles and acquiring equilibrium state. Table 3.1 shows the grouping of these samples along with the type of tests conducted. As a result of this grouping and sampling, various physical and mechanical parameters were calculated and estimated, which influence in controlling the shear strength of sensitive clays especially, when subjected to cyclic loading.

3.5 Determination of Physical and Index Properties

Physical parameters of the clay samples to include; moisture content, liquid limit, plastic limit, degree of saturation etc. etc. were determined from the samples of Group-I or II (disturbed samples or remolded samples). Table 3.2 presents summary of test results of the index properties. The oven-dry- method, was used to determine the moisture content of the soil. In brief, a mass of an empty, clean, and dry moisture-can with its lid was determined followed by placing the moist soil in the moisture-can and securing the lid. The mass of the moisture-can (now containing the moist soil) with the lid was then determined. Then the moisture-can (containing the moist soil) was placed in the drying oven that was set at 105 °C

with its lid removed for 24 hours. After 24 hours, the moisture-can was removed cooled down at the room temperature with its lid on the top. The new mass was determined for the moisture can and lid (containing the dry soil). Similarly, the plastic limit was determined for the moisture content at which the thread of soil was rolled without breaking until it was only 3 mm in diameter. For determining the liquid limit, the conventional method of counting number of blows (droppings) to a cup containing soil sample was used. The sample was separated by a grooving tool along a distance of 12mm until the soil sample came in contact with the number of blows.

The samples of Clay Type-A, were taken from Petite-Patrie and Chambly, had the water content ranged from 71% to 42 %. The average water content for the clay Type-A was equal to 58%. The liquid limit determined for the clay Type-A ranged from 73% to 47%, and the plastic limit from 45% to a minimum of 26%. Similarly, the plasticity index ranged from 41 to 19 and the liquidity index ranged from 1 to a minimum of 0.7. Using the plasticity chart (Casagrande), on average the clay Type-A can be placed in the category of inorganic clays of high plasticity. In case of clay Type-B, the maximum water content ranged from 67% to 27 %. The average water content for the clay Type-B was equal to 50%. The liquid limit determined for the clay Type-B ranged from 70% to 24% and the plastic limit from 44% to a minimum of 19%. Similarly, the plasticity index ranged from 33 to 5 and the liquidity index ranges from 1.6 to a minimum of 0.6. Using the plasticity chart (Casagrande), on average the clay Type-B can be placed in the category of inorganic clays of medium plasticity. For the clay Type-C, the maximum water content ranged from 65% to 38 %. The average water content for all the samples of the clay Type-C was equal to 54%. The liquid limit for the clay Type-C ranged from 67% to 40% and the plastic limit from 29% to a minimum of 17%.

Similarly, the plasticity index ranged from 45 to 15 and the liquidity index ranged from 1 to a minimum of 0.7. Using the plasticity chart (Casagrande), on average the clay Type-C can be placed in the category of highly compressible clay with silt. For the clay Type-D, the samples were mostly taken from Mont. St. Hilarie area of Eastern, Canada. The maximum water content for this clay ranged from 70% to 43%. The average water content for all the samples of clay Type-D was equal to 43%. The liquid limit for the clay Type-D ranged from 75% to 41% and the plastic limit from 31% to a minimum of 21%. Similarly, the plasticity index ranged from 44 to 20 and the liquidity index ranged from 1.1 to a minimum of 0.9. Using the plasticity chart (Casagrande), on average the Type-D clay can be placed in the category of inorganic clays of high plasticity.

3.6 Conventional Consolidation Test

For this test, standard load increment duration of 24 hours was taken and at least two load increments, including one increment after the pre-consolidation pressure. The change in height of the sample was recorded with time intervals of approximately 0.1, 0.25, 0.5, 1, 2, 4, 8, 15 and 30 minutes; and 1, 2, 4, 8, and 24 hours. The coefficient of consolidation for each load increment was then computed by using the following equation:

$$c_v = \frac{TH^2}{t} \qquad 3.1$$

Where; T = the dimensionless time factor ($T=T_{50}=0.197$), t = time corresponding to the particular degree of consolidation ($t = t_{50}$) and, H= length of drainage path at 50% consolidation. For the double drainage H_{D50} was half the specimen height at the appropriate increment.

The results of these tests (in general are in accordance with ASTM standards) are summarized in Table 3.3. For the clay Type-A the compression index (C_c) ranges from 0.541 to 0.33. The pre-consolidation pressure (σ_p) ranges from 323 kPa to 64 kPa, and the co-efficient of consolidation (C_v) varies from 0.068 cm^2/sec to 0.015 cm^2/sec. In case of the clay Type-B, the compression index (C_c) ranges from 0.52 to 0.144. The pre-consolidation pressure (σ_p) ranges from 473 kPa to 56 kPa, and the co-efficient of consolidation (C_v) varies from 0.098 cm^2/sec to 0.019 cm^2/sec. For the clay Type-C, the compression index (C_c) ranges from 0.5 to 0.273. The pre-consolidation pressure (σ_p) ranges from 298 kPa to 117 kPa, and the co-efficient of consolidation (C_v) varies from 0.07 cm^2/sec to 0.04 cm^2/sec. For the clay Type-D, the compression index (C_c) ranges from 0.561 to 0.28. The pre-consolidation pressure (σ_p) ranges from 279 kPa to 127 kPa, and the co-efficient of consolidation (C_v) varies from 0.08 cm^2/sec to 0.013 cm^2/sec. Figure 3.6.1 shows the graph between time and deformation in mm for one of the tests done on the samples of the clay Type-A. The pre-consolidation stress was determined by using the Log-Time Method (due to Casagrande). A typical e-logσ curve is shown in Figure 3.6.2 for the clay sample ID # 13352-GE2.

3.7 Sensitivity Number

The sensitivity as defined earlier is the ratio of undisturbed to remolded un-drained strength of a clay soil. In order to determine the sensitivity of the tested samples the unconfined triaxial tests were conducted on both undisturbed and remolded samples.

The remolded clay samples were prepared by using the kneading technique followed by standard compaction. Firstly, the sample kneaded in an air tight jar for approximately 10 minutes to make sure that all the cemented bonds were broken down. Finally the sample was

compacted in three layers into the mould (50mm x 100mm) under a fix compacting effort (weight of hammer = 0.25kg, drop height = 30.5 mm). A uniform remolding procedure is adopted for all the remolded samples. Hence, the effect of remolding effort can be taken out from the complex equation of governing parameters.

Table 3.4 shows the summary of triaxial tests conducted to determine the sensitivity number, S_t. The clay Type-A bears the least sensitivity range among the four selected types. The sensitivity number (S_t) for this clay ranged from 4 to 6. The clay Type-B bears, the sensitivity number (S_t) ranging from 6 to 10. The clay Type-C bears the sensitivity number (S_t) ranging from 10 to 14. The clay Type-D bears the sensitivity number (S_t) greater than 14. Hence, the four selected types could be written as; Type-A ($4 \leq S_t \leq 6$), Type-B ($6 < S_t \leq 10$), Type-C ($10 < S_t \leq 14$) and Type-D ($14 < S_t$).

According to the classification given by Das (2001) in the book "Principles of Geotechnical Engineering" fifth edition Clay A comes under the heading of medium sensitive, Clay B as very sensitive, C as a slightly quick and D as a medium quick clay.

3.8 Triaxial Testing

Triaxial set-up was used to measure the shear strength of a soil under controlled drainage conditions. Both, static and cyclic compression tests were conducted in order to determine the behavior of sensitive clays under varying conditions of drainage, confining pressures, disturbed and undisturbed states, degree of saturation etc., etc. Hence, a careful plan for conducting these tests was prepared to handle the complexity of the experimental work.

3.8.1 Triaxial Test Principle and Program

In this series, a cylindrical a specimen of soil encased in a rubber membrane, was placed in the triaxial compression chamber, subjected to a confining fluid pressure and then loaded axially to failure. Connections at the ends of the specimen permit controlled drainage of pore water from the specimen. Prior to the shear, the three principal stresses are equal to the chamber fluid pressure. During the shear, the major principal stress, σ_1 is equal to the applied axial stress (P/A) plus the chamber pressure, σ_3. The applied axial stress, σ_1-σ_3 is termed the "principal stress difference" or the "deviator stress". The intermediate principal stress, σ_2 and the minor principal stress, σ_3 are identical in the test, and are equal to the confining or the chamber pressure referred to as σ_3. Figure 3.8.1 gives a schematic sketch of this triaxial test principle.

3.8.2 Setting up the Triaxial Apparatus for Static and Cyclic Triaxial Tests

The apparatus used in the present study is WF (Wykeham Farrance) 10056 Tritech Triaxial Load Frame 50 kN cap. Figure 3.8.2 shows the Tritech, Triaxial load frame available at the geotechnical lab of Concordia University. The load frame is flexible to be used as a part of computer-controlled triaxial system or as a stand-alone unit. The frame is also equipped with RS 232 interface, which help the triaxial setup to be connected to any computer-aided setup.

The triaxial apparatus was reassembled and calibrated properly to serve the purpose of this research. A careful study of different components of the triaxial apparatus (Tritech 50 kN) was done before reassembling the apparatus. Figure 3.8.3 shows the main components of the whole triaxial testing system and the way, they were finally reassembled. The air supply tubing and de-aired water supply, was connected to valve #1 and #2 respectively. To keep the

water in the air water cylinder air free, valve # 3 was connected to the base of an air bladder assembly. The water line from valve #4, was connected to the air water cylinder. The valves at the base of triaxial cell were connected accordingly, keeping in view, the specified valve for the pore pressure transducer. The connectors from the four transducers were connected to the four channels display electronic readout unit. The readout unit was further connected, to an Agilent Data Acquisition System, which in turn, connected to the computer. This Agilent Data Acquisition System could only communicate with other components of the triaxial system through specific software installed on the computer. The software in turn needed a program coded in Visual Basic (VB), to communicate among the different components of triaxial system especially, the sample within in the triaxial cell during static or cyclic test. A careful programming of Visual Basic was done to obtain a meaningful data output from the triaxial tests both in the form of numbers and step by step graphical presentation to elaborate the changes happening to the sample being tested.

3.9 Calibration of various Instruments and Transducers used in Triaxial Testing

All testing equipment and measuring devises, to include; load cell, linear variable differential transducers (LVDT) and pore water pressure transducers, etc were calibrated prior testing. These calibrations were repeated often during testing to assure good results. The average readings were taken for specific load intervals in case of load cell, lengths in case of LVDTs and pressures for pore water pressure transducer.

3.9.1 Calibrating Submersible Load Cell

A 5 kN WF 17104 submersible load cell fitted with a ram was used in the current experimental work. Before starting the triaxial test, the load cell was calibrated using a hydraulic load applying machine in mechanical lab. The load cell was connected with a transducer, which gave the readings in mV for the corresponding applied load. For calibration, the load cell was loaded to its maximum capacity of 5kN with small increments of load application by the hydraulic load applying machine. The corresponding readings in mili-volt (mV) were noted down for the each load increment. In the similar way, the readings were recorded during the unloading phase of the load cell. The procedure was repeated for three to five times. The three set of reading are graphed for a load versus mV readings. A straight-line equation is obtained and used in computer program for triaxial test. Table 3.5 and Figure 3.9.1 give the results of this calibration.

3.9.2 Calibrating LVDT

Two linear variable differential transducers (LVDT) were used, mounted to the loading piston, external to the triaxial cell, for measuring axial displacement. For calibrating these LVDTs metallic rings of 1.58 mm thickness were used. Both LVDT-1 and LVDT-II were fixed in metallic frame with their suppressible needles extended to the full length in such a way that they just touch the metallic frame base without being pressed. This was taken as zero for calibration purposes. After that, metallic rings were inserted one by one to make the needles deflection at equal intervals. The corresponding mV readings were noted down. These

readings were used to plot a linear relationship between length and milli-volt (mV) Table 3.6 and Figure 3.9.2 give the results of this calibration.

3.9.3 Calibrating Pore Pressure Transducer

The pore pressure transducer was calibrated by putting together all the assembly of triaxial test setup, including the submersible load cell. When the system became stable, the zero for pore pressure transducer was noted down. After that, the pressure was applied at an interval of 50 kPa till a maximum of 300 kPa. The corresponding readings in Volts were recorded as the mili-volt (mV) was shown out of range for the pore pressure transducer. Table 3.7 and Figure 3.9.3 give the results of this calibration.

3.10 Programming the Agilent Data Acquisition System

As mentioned above, the Agilent Software works in general with the visual basic coded program files having extension VEE. Before running the test, it was important to design an objective oriented program, which could communicate with the sample and various transducers before, during and at the end of a static or cyclic triaxial test. The program should be such that it could convey the changes happening to the sample inside the triaxial cell, and translate meaningfully these changes in form of numbers and graphical presentations. Hence, the goal was to write a well-designed program in such a way, which could help in controlling and displaying the output and the test results in particular fashion as required by the researcher.

To achieve the above mentioned goal, a visual basic program named Master-Vee was written to co-ordinate the triaxial testing system, soil sample, digital four channels display

electronic readout unit, Agilent Data Acquisition System and the computer. The channels were assigned as; Channel #1 for LVDT-I, Channel # 2 for LVDT-II, Channel #3 for pore water pressure and Channel # 4 for static or cyclic deviator stress. The straight line equations obtained from Figures 3.9.1, 3.9.2 and 3.9.3 were used in the (Master.vee) visual basic coded program. Master.vee gave the final output for all the channels according to their respective units in an Excel Spreadsheet along with the graphical presentation. The program was capable of taking readings minimum after 1 second to the maximum after one hour. Keeping in view the nature of sensitive clay, the program was designed in such a way that an observer could see stepwise variations in pore water pressure, stresses and strains. The gradual graphical buildup of the stress strain curves, the pore water pressure and the stress paths with each step recorded by the program and stored in excel spreadsheet. On top of this, one could easily identify the stage when the stress path hit the failure envelope or if a sample attained quasi elastic resilient state during a cyclic triaxial compression test. The subroutines of the programs were prepared in such way that the graphical variations were adjusted automatically to accommodate a lengthy, slow static or cyclic triaxial compression tests. The output from the program was saved in the Microsoft Excel file named according to the sample identification number and the type of the test run. Furthermore, a macro named Mohr's Circle was designed within the "Output Excel File" to compare the shear strength values with those determined by static triaxial compression tests. Figures 3.10.1, 3.10.2 and 3.10.3 show the different parts of master.vee program. Figure 3.10.1 shows the overall flow chart of the program. The Figure shows that how the different components of the program were integrated together to make the system run according to the desired output. Figure 3.10.2 shows the efforts involved in adjusting the programming codes. The sub-routines for Excel spreadsheet,

formatting codes, graphing tools and the specification of data output units were nicely embedded in the program. Figure 3.10.3 shows the part of Excel spreadsheet for the data output file.

3.11 Experimental Program

To achieve the goals of present study an efficient and well planned experimental framework was important to avoid the unusual and time-consuming efforts. The experimental work along with precautionary measures could easily nullify not all, but some of the main factors like chemical composition and environmental impacts. Hence, many chemical and environmental parameters could be easily balanced out from the complex equation of parameters involved in governing the behavior of sensitive clay under static or cyclic loading. Figure 3.11.1 gives a general layout of the experimental plan for each type of sensitive clay used in the present study. Figure 3.11.2 shows the complexity of the experimental work in the present study. In other words, the figure reveals the efforts involved to keep the control of various physical and mechanical parameters which governs the behavior of the sensitive clay. This control was maintained throughout the experimental work, in such a way, that the leading parameters causing increase or decrease of the shear strength of the sensitive clay subjected to static or cyclic loading could easily be identified and prioritized accordingly.

The experimental program was planned in such a way, that each type (A, B, C and D) of soil is tested for both static and cyclic triaxial compression tests. Table 3.8 gives the details, that how the samples from different groups (I, II, II, IV & V) were managed for this testing plan.

3.12 Static Triaxial Compression Test (Undrained)

A series of isotropically consolidated undrained static triaxial compression (CU) tests were done under different confining stresses for the clay types; A, B, C and D using 50mm diameter by 100 mm high rubber membrane encased samples. The undisturbed samples for Group-I were obtained from the wax coated block samples. All possible precautions while trimming, encasing with rubber membrane, pulling over "O-rings", placing inside the triaxial chamber till the start of the application of deviator stress were taken to keep the sample intact and undisturbed. Although, the samples belonging to Groups II, III, IV and V were remolded, reconstituted or survived samples from initial triaxal testing, every possible measure was taken to keep the integrity of those samples.

The complete list of static triaxial compression tests is given in Table 3.9. A maximum value of 121 kPa for the clay type A (St < 6) was obtained under the undrained conditions for a confining stress of 200 kPa, while a minimum value of 2 kPa was obtained for a remolded sample of clay type D (St > 16) under a confining stress of 150 kPa. The strain rates of 0.5 mm/min to 1.2 mm/min were used in these static triaxial compression tests. The overall test results show decreasing deviator stress with increase in sensitivity number (S_t). The samples which were reconstituted (Group-III) at water content = LL – 1.5 LL were weaker than the remolded samples with water content less than LL. The friction angle (ϕ') was determined with the help of consolidated undrained triaxial test. For the clay Type-A the maximum friction angle (ϕ') determined is about 29.75^o and the minimum about 24.20^o. Similarly, maximum friction (ϕ') angles are; 32^o, 30.60^o, 28.21^o and minimum; 25.35^o, 21.75^o and 23.43^o for the clay Types B, C and D respectively. The average friction angle (ϕ') value for these clay ranges from 27^o to 25^o. The values of static undrained shear strength obtained from

Groups IV & V gives an idea about reduction in static undrained shear strength of a sample after suffering N number of cycles for a given level of cyclic deviator stress.

3.13 Cyclic Triaxial Compression Test

A series of 112 cyclic compression triaxial tests were conducted under varying cyclic frequencies, drainage conditions, cyclic deviator stress and confining stress at the Concordia University Geo-technical Laboratory. Out of these, 48 were done on undisturbed samples i.e., Group-I of these clays (A, B, C & D) mostly under undrained conditions. The remaining 64 tests were conducted on samples in Groups II, III, IV and V.

As mentioned above, the undisturbed samples were handled with all possible precautions while trimming, encasing with rubber membrane, pulling over "O-rings", placing inside the triaxial chamber till the start of the application of cyclic deviator stress. The cell pressures, back pressures and pore water pressures were measured by pressure transducers with a precision of 0.25 kPa. The linear variable differential transformers (LVDT) used for axial strain measurements, the load cells used for vertical load measurements and volume gauges used for volume change measurements.

In case of undrained tests on back-pressure saturated specimens, water was used as the confining pressure fluid. For unsaturated or partially saturated samples (having matric suction component), air was used instead of water as the confining fluid to avoid the possibility of increasing moisture content due to water penetration across the membrane. For the remolded samples, an effective isotropic confining pressure was employed for the initial consolidation stage, by opening the drainage valve, the specimen was consolidated isotropically in order to allow the complete dissipation of the excessive pore-water pressures before starting the test. For the undrained tests, the valves were closed after the test started and vice versa for the

drained tests. Each cyclic test was conducted under a constant cyclic deviator stress ratio right from the beginning until the end of the test. Different cyclic deviator stress ratios (q_{cyc}/q_s = 70%, 60%, 50%, 40%, 30% and 25%) were used for the different confining stresses ranging from 100 kPa to 250 kPa for clay types; A, B, C and D. The cyclic stress (q_{cyc}) varied from 70% of the static deviator stress (q_s) for the least sensitive clay (Type –A) under undrained / darined contions to 20% of the static deviator stress (q_s) for the remolded samples of clay (types C and D). The Tritech Frame was allowed to increase the cyclic deviator stress till the desired percentage of cyclic stress ratio is achieved (q_{cyc}/q_s).

To check the effect of frequency, the selected samples from Group I, II and III were tested for frequencies ranging from 12 to 24 cycles per hour. Selection of comparatively slower rate of load application was keeping in view that pore water pressures should allowed to equilibrate throughout the specimen as compare to fast loading rate in which case it does not happen. Hence, the values of pore pressure are not likely the one induced on the potential plane of failure.

In all the tests, the deviator stress was reduced to zero or to the lower value of cyclic deviator stress (in case of load cycle between two ranges of cyclic deviator stress) and then reloaded to the required level of cyclic deviator stress. The cyclic tests were conducted only on the samples belonging to Group-I, Group-II and Group-III. A summary of these cyclic traxial test results is given in Table 3.10.

3.14 Discussion

In Group-I, samples were mostly used to get the undisturbed shear strength or maximum static deviator strength in case of static triaxial compression tests and maximum cyclic deviator strength in case of cyclic triaxial compression tests. Group-II samples (the failed samples of

Group-I) were the remolded samples at the same moisture content as their parent samples of Group-I. Extra precautions were taken in storing these samples so they would not lose or gain any extra moisture content other then they inherit from Group-I. Those samples were then reconsolidated close to the initial conditions prior to testing. The final sensitivity numbers for the clays (A, B, C & D) in the present study were obtained by the ratio of undisturbed unconfined shear strength (C_{uo}) of the samples of Group-I to the corresponding unconfined remolded shear strength of the samples of Group-II. The intrinsic shear strength (C_{ur}*) was obtained from Group-III reconstituted samples. These samples were reconstituted at a moisture content (w_c) equal to LL – 1.5 LL.

The first three tests shown in Table 3.8 were conducted on Group-I to check the undrained static shear strength for the sensitive clays selected in this research. Table 3.9 gives the results of those static triaxial tests. Based on the static shear strength the ratio for cyclic deviator stress was decided for the cyclic triaxial tests. Tests 4 to 11 in Table 3.8 were done on Group-I undisturbed samples for both drained and undrained conditions. The purpose for these tests was to determine the number of cycles required by a sample of a particular clay type and sensitivity number to get failed or reach a quasi-elastic resilient state under drained and undrained conditions. Similarly, the tests from 12 to 17 in the Table 3.8 were done for the remolded samples derived from Group-I but, at the same moisture content as their parent samples under drained and undarined conditions. These tests were done at a lower cyclic deviator stress ratio as compared to undisturbed sample tests (4-11), assuming, that a considerable decrease in shear strength on remolding. The comparison of test results for the disturbed and undisturbed samples gives an idea about reduction in cyclic shear strength due to remolding. In other words the comparison gives an idea that how much the level of cyclic

deviator stress is needed to reduce the strength of an undisturbed sample of clay of a particular sensitivity to its remolded shear strength for a given number cycles. In other words, number of cycles needed to reduce the undisturbed shear strength to remolded cyclic shear strength could be predicted. Such type of comparison could be helpful for the geotechnical engineers to take measures for reducing the cyclic stress ratio or number of cycles especially, in the initial stages of a construction project in the regions of sensitive clay. Similarly, the tests from 18 to 22 were done on samples of Group-III give idea about the increase or decrease in shear strength of sensitive clay due to matric suction (pore air pressure $(u_a) - (u_w)$ pore water pressure).

Only a few selected samples of the Group I, II and III were tested for variation in the loading frequencies and over-consolidation ratios (OCR). Static triaxial compression Tests 23 and 24 initiate the idea of a hypothetical model that under ideal conditions the ratio of undisturbed shear strength, C_u to disturbed or in other words remolded shear strength C_{ur} increases with the increase in number of cycles. Hence, a 100% undisturbed sample of sensitive clay start displaying its sensitivity number, C_u/C_{ur} when being disturbed by the cyclic loading.

Overall, by carrying out the experimental work based on framework given in Tables 3.1, 3.8 and Figures 3.11.1, 3.11.2 assisted in demonstrating the behavior of sensitive clays with different sensitivity in view of variations in physical and mechanical parameters. Therefore, effect of reduction in static shear strength due to cyclic loading, number of loading cycles, increase or decrease in deviator stress, frequency of cyclic loading, pre-consolidation pressure/OCR, confining pressure, degree of saturation other parameters could easily be analyzed keeping in view the objectives of this research. Furthermore, by adopting this

experimental work along with the precautionary measures helped in keeping constant most of the chemical and environmental parameters. Hence, the experimental work has resulted in focusing the analysis to those physical and mechanical parameters, which govern the behavior of sensitive clay under static or cyclic loading.

Table 3.1 Grouping, type of sample, test conducted & parameters obtained

Group No	Type of Sample	Type of Tests Conducted	Parameters determined
Groups I & II	Disturbed or remolded	Atterberg Limits	LL, PL, I_P, I_L & Activity
Group -I	Undisturbed	Static Odeometer Compression Test or Consolidation Test	Virgin comp. index (I_c), recomp. index (I_r) co-efficient of consld. (c_v)& preconsld. stress (σ_p)
Group -I	Undisturbed	Static Triaxial Compression Test	Axial Strain (ε), Pore water pressure (u) & Static shear stress (τ_f)
Group -I	Undisiturbed	Cyclic Triaxial Compression Test	Axial Strain (ε), Pore water pressure (u), cyclic shear stress (τ_c) & Number of cycles (N)
Group-II	Remolded at same water content as Group-I	Static Odeometer Compression Test or Consolidation Test	Virgin comp. index (I_c), recomp. index (I_r) co-efficient of consld. (c_v)& preconsld. stress (σ_p)
Group-II	Remolded at same water content as Group-I	Cyclic and Static Triaxial Compression Test	Axial Strain (ε), Pore water pressure (u), cyclic shear stress (τ_c) & Number of cycles (N)
Group -III	Reconstituted at w =LL-1.5LL (Intrinsic Shear Strength)	Static Odeometer Compression Test or Consolidation Test	Virgin comp. index (I_c), recomp. index (I_r) co-efficient of consld. (c_v)& preconsld. stress (σ_p)

Table 3.1(continued): Grouping, type of sample, test conducted & parameters obtained			
Group-III	Reconstituted at w =LL-1.5LL (Intrinsic Shear Strength)	Cyclic and Static Triaxial Compression Test	Intrinsic axial strain (ε_{INT}), Pore pressure (u) & Intrinsic Static (τ_{INT}) and cyclic shear stress (τ_{clNT})
Group -IV	Group-I Samples reached Quasi Elastic State	Static Compression Test	Axial Strain (ε), Pore pressure (u) & Reduction in static strength after N no. of cycles
Group -V	Group-II Samples reached Quasi Elastic State	Static Compression Test	Axial Strain (ε), Pore pressure (u) & Reduction in static strength after N no. of cycles

Table 3.2: Summary of index property test results

Clay Type		Depth m	w.c (%)	LL (%)	PL (%)	I_L	I_P	Location
A	**Avge.**	7	57.8	60.8	31.4	0.9	29	Petite-Patrie, & Chambly
	Max.	10	71	73	45	1	41	
	Min.	4	42	47	26	0.7	19	
B	**Avge.**	7	49.8	53.3	28.9	0.9	24	Grande Balene & St Nicolas
	Max.	10	67	70	44.8	1.6	33	
	Min.	4	27	24	19	0.6	5	
C	**Avge.**	7	54.7	57.9	25.7	0.9	32	St Huges & Terrebonne
	Max.	10	65	67	29	1	45	
	Min.	4	38	40	17	0.7	15	
D	**Avge.**	7	60.5	62.4	27.8	1	35	Mont. St Hilarie
	Max.	10	70	75	31	1.1	44	
	Min.	4	43	41	21	0.9	20	

Table 3.3: Summary of consolidation test

Clay Type		Virgin Comp. Index C_c	Preconsold. Pressure kPa	Initial Void Ratio e_o	Vert. Stress σ/σ_o	Co-eff of Consold. Cv cm^2/sec	OCR
A	**Avge.**	0.4416	163.037	1.551	0.06443		(1 – 4)
	Max.	0.54094	322.795	1.8094	0.07175	0.068	
	Min.	0.33011	63.3132	1.2611	0.05065	0.015	
B	**Avge.**	0.38079	154.107	1.3929	0.07749		(1 – 4)
	Max.	0.51661	473.404	1.7461	0.07732	0.098	
	Min.	0.14361	56.6084	0.7761	0.00302	0.019	
C	**Avge.**	0.41863	169.182	1.4913	0.06222		(1 – 4)
	Max.	0.49228	298.121	1.6828	0.06855	0.083	
	Min.	0.27335	117.048	1.1135	0.03898	0.028	
D	**Avge.**	0.45486	171.36	1.5855	0.0656		(1 – 4)
	Max.	0.55715	279.929	1.8515	0.07268	0.078	
	Min.	0.28146	126.836	1.1346	0.04096	0.013	

Table 3.4 Summary of unconfined triaxial tests

Group		Undiisturbed Unconfined Shear Strength C_u	Undiisturbed Unconfined Shear Strength C_{ur}	S_t No.
A	**Avge.**	25	4.4	5.69
	Max.	32	5.4	5.86
	Min.	19	3.5	5.43
B	**Avge.**	18	1.9	9.68
	Max.	21	2.1	9.74
	Min.	16	1.7	9.61
C	**Avge.**	17	1.4	12.5
	Max.	26	2	13
	Min.	8.5	0.8	11.3
D	**Avge.**	14	0.8	16.9
	Max.	17	1	17
	Min.	11	0.6	16.8

Table 3.5: Calibration of submersible load cell 5 kN

S. No.	kN	loading	unloading	loading	unloading	loading	unloading	Readings
		1	1	2	2	3	3	Average
1	0.56	0.0069	0.0071	0.0072	0.0074	0.0070	0.0073	0.0072
2	1.13	0.0308	0.0310	0.0308	0.0309	0.0310	0.0310	0.0309
3	2.15	0.0740	0.0743	0.0739	0.0741	0.0740	0.0742	0.0741
4	3.50	0.1259	0.1261	0.1258	0.1260	0.1258	0.1260	0.1259
5	3.88	0.1389	0.1391	0.1390	0.1392	0.1390	0.1391	0.1391
6	5.00	0.1828	0.1829	0.1827	0.1830	0.1828	0.1829	0.1829

Table 3.6 Calibration for LVDTs

S.No	Volts	Observed mm	m-Volts Readings	Observed mm	m-Volts Readings
		LVDT-I		LVDT-II	
1		1.58	2.345	1.57	255.64
2		3.16	5.964	3.14	265.53
3		4.74	9.86	4.71	273.46
4		6.32	13.51	6.28	281.62
5		7.90	17.387	7.85	287.63
6		9.48	21.145	-	-
7		11.06	24.849	-	-

Table 3.7: Calibration for pore water pressure transducer

S.No	Volts Readings	Observed kPa	m-Volts Readings
1	0.054	75.00	54
2	0.07626	100.00	76.26
3	0.12255	150.00	122.55
4	0.165	200.00	165
5	0.186	225.00	186
6	0.20965	250.00	209.65
7	0.231	275.00	231
8	0.252	300.00	252
9	0.2733	325.00	273.3
10	0.295	350.00	295
11	0.301	360.00	301

Table 3.8 Nature of tests conducted on each type of sensitive clay (A, B, C and D)

Test No.	Grp No.	Pre-con. Lab / Field	OCR	Drainage Condition	No. of Cycles	Freq. f_z cyc/h	Confining. Pressure (kPa)	Cycic deviator Stress (qcyc)(kPa)
1	I	L a b	1	Undrn. Static	-		$\geq\sigma_p$	
2	I I	L a b	1	Undrn. Static	-		$\geq\sigma_p$	
3	I I I	L a b	1	Undrn. Static	-		$\geq\sigma_p$	
4	I	L a b	1-4	Undrained	N	12-24 /hr	$\geq\sigma_p$	70- 60% qs
5	I	L a b	1-4	Undrained	N	12-24 /hr	$\geq\sigma_p$	60-50% qs
6	I	L a b	1-4	Undrained	N	12-24 /hr	$\geq\sigma_p$	50-40% qs
7	I	L a b	1-4	Undrained	N	12-24 /hr	$\geq\sigma_p$	40-30% qs
8	I	L a b	1-4	Drained	N	12-24 /hr	$\geq\sigma_p$	70- 60% qs
9	I	L a b	1-4	Drained	N	12-24 /hr	$\geq\sigma_p$	60-50% qs
1 0	I	L a b	1-4	Drained	N	12-24 /hr	$\geq\sigma_p$	50-40% qs
1 1	I	L a b	1-4	Drained	N	12-24 /hr	$\geq\sigma_p$	40-30% qs
1 2	I I	L a b	1-4	Undrained	N	12-24 /hr	$\geq\sigma_p$	50-40% qs
1 3	I I	L a b	1-4	Undrained	N	12-24 /hr	$\geq\sigma_p$	40-30% qs
1 4	I I	L a b	1-4	Undrained	N	12-24 /hr	$\geq\sigma_p$	30-20% qs
1 5	I I	L a b	1-4	Drained	N	12-24 /hr	$\geq\sigma_p$	60-50% qs
1 6	I I	L a b	1-4	Drained	N	12-24 /hr	$\geq\sigma_p$	50-40% qs
1 7	I I	L a b	1-4	Drained	N	12-24 /hr	$\geq\sigma_p$	40-30% qs
1 8	I I I	L a b	1-4	Undrained	N	12-24 /hr	$\geq\sigma_p$	3 0 % q s
1 9	I I I	L a b	1-4	Undrained	N	12-24 /hr	$\geq\sigma_p$	2 5 % q s
2 0	I I I	L a b	1-4	Undrained	N	12-24 /hr	$\geq\sigma_p$	2 0 % q s
2 1	I I I	L a b	1-4	Drained	N	12-24 /hr	$\geq\sigma_p$	3 0 % q s
2 2	I I I	L a b	1-4	Drained	N	12-24 /hr	$\geq\sigma_p$	2 0 % q s
2 3	I V	L a b	1-4	Static Comp.	-	-	$\geq\sigma_p$	6 0 % q s
2 4	V	L a b	1-4	Static Comp.	-	-	$\geq\sigma_p$	4 5 % q s

Table 3.9 Summary of static triaxial compression test

S. No.	Name of the Out Put File	Sample ID No.	Confining Pressure kPa	Static Dev. Stress	Peak Pore Pressure	Peak Axial strain	Strain Rate	Clay Type	Name of the site	Sensitivity range
			σ_3, kPa	σ_1-σ_3 kPa	Δu	ε_p	mm/min			
1	Drained_Static_S-13252_GE-2 FOS- TS06 4.80-4.9	S-13252_GE	200	80	check	check	check	A	Grande-Baleine	4 - 6
2	Rem-Static_13293-G(2) BH-02 - TS-04_3.5-3.6	13293-G(2)	150	n/a	n/a	n/a	n/a	A	Alexandria, Ont	4 - 6
3	Static_13227_E- FOI-TS-09_11.0-11.10	13227_E- F	150	47	90	11%	1.2	A	Saint-Hugues	4 - 6
4	Static_13293-G(2) BH-02 - TS-04_3.5-3.6	13293-G(2)	150	60	62	11%	1.2	A	Alexandria, Ont	4 - 6
5	Static_13293-G_3.5-3.60	13293-G_3.	200	58	101	19%	1.2	A	Alexandria, Ont	4 - 6
6	Static_13293-G_BH-02_TS-04_3.5-3.6	13293-G_BH	200	60	112	18%	1.2	A	Alexandria, Ont	4 - 6
7	Static_13352_GE2 FO2.TS-09 5.05-5.15 A	13352_GE2	300	63	303	10%	1.2	A	Petite-Patrie, QC	4 - 6
8	Static_13352_GE2 FO2.TS-09 10.30-10.40 D	13352_GE2	200	121.3	109	9%	1.2	A	Petite-Patrie, QC	4 - 6
9	Static_13352_GE2- FOI-TS-05_4.60-4.70	13352_GE2-	150	51	97	6%	1.2	A	Petite-Patrie, QC	4 - 6
10	Static_13352_GE F10.TS-05 4.20-4.30 D	13352_GE F	200	38	185	9%	1.2	A	Petite-Patrie, QC	4 - 6
11	Static_S12647-11G_FOITSS_12.4-12.5	S12647-11G	200	45	160	6%	1.2	A	Grande-Baleine	4 - 6
12	Static_S-13252_ZFI- PO-301-E 0.5-0.6	S-13252_ZF	200	48	158	11%	1.2	A	Grande-Baleine	4 - 6
13	Rem-Static_S-13252_ZFI- PO-301-E 0.25-0.5A	S-13252_ZF	100	32	check	check	check	B	Grande-Baleine	6 - 10
14	Rem-Static_13221-G_FOITS-08_4.50-4.60	13221-G_FO	150	18	126	19%	1.2	B	St-Nicolas	6 - 10
15	Static_13221-G_FOITS-08_4.50-4.60	13221-G_FO	250	27	57	6%	0.5	B	St-Nicolas	6 - 10
16	Rem-Static_13352_GE2 FO2.TS-09 10.30-10.40 D	13352_GE2	150	13	169	20%	0.2 / 0.5	C	Petite-Patrie, QC	10-14
17	Rem-Static_S-13252_GE-2 FOS- TS06 4.80-4.9	S-13252_GE	150	12	93	19%	1.2 / 5.2	C	Grande-Baleine	10-14
18	Rem-Static_13352_GE- F10-TS-05_3.90-4.00A	13352_GE-	100	10	36	20%	1.2	C	Petite-Patrie, QC	10-14
19	Static_13252_ZNA- DO-301.E-0.25-0.35A	13252_ZNA-	200	31	126	6%	1.2	C	Grande-Baleine	10-14
20	Static_13252_ZNA- PO-301.E-035-0.45	13252_ZNA-	250	29	210	10%	1.2	C	Grande-Baleine	10-14
21	Static_13252_ZNA- PO-301.F-3.50-3.60	13252_ZNA-	200	26	20	12%	1.2	C	Grande-Baleine	10-14
22	Static_S13048-G_BH-02_10.80-10.90	S13048-G_B	200	40.35	150	14%	1.2	C	Terrebonne, QC	10-14
23	Static_S13048-G_BH-02_13.70-13.80	S13048-G_B						C	Terrebonne, QC	10-14
24	Static_S12647-11G_FOITSS_11.5-11.6	S12647-11G	150	52	62	11%	1.2	C	Mont St-Hilarie, QC	10-14
25	Static_S-13252_CLT PO-301.G-0.2-0.3	S-13252_CL	200	17	185	10%	1.2	C	Grande-Baleine	10-14
26	Rem-Static_13252_CLT PO-301.J-0.2-0.35	13252_CLT	200	6	188	12%	1.2	D	Grande-Baleine	> 14
27	Rem-Static_13252_CLT PO-301.J-0.35-0.55	13252_CLT	150	2	106	20%	0.5	D	Grande-Baleine	> 14

Table 3.10 Summary of cyclic triaxial compression test

Name of the Output File / Nature of Test	Test ID	Confining pressure	Static Dev. Stress	Group No.	Pore Pres. u (taken)	Δu (%) at taken	Cyclic Dev. Stress	% qcyc/qs	Test Result	Number Cycles, N	Frequency cycles/hr
Cyclic_13213-G_FE1.s1-04_	A1	150	85	1	140.4254	11.59%	57	60%	failed	81	12
Cyclic_13213-G_FE1.s1-04_	A2	150	85	1	135.2054	15.45%	47.5	50%	failed	168	12
Cyclic_S-13252_RDX-PO-30	A3	200	67	1	109.6972	6.71%	37	55%	failed	163	12
Cyclic_13283-G_BH02TS-04	A4	200	60	1	181.0372	5.88%	30	65%	failed	94	12
Rem-Cyclic_13213-G_FE1.s1	A5	100	23	11	79.86361	4.33%	11.5	50%	failed	157	24
Rem-Cyclic_13283-G_BH02T	A6	100	20	11	89.95361	3.70%	9	45%	failed	182	24
Rem-Cyclic_13213-G_FE1.s1	A7	100	19	11	87.19361	3.50%	12.3	65%	failed	95	24
Rem-Cyclic_13293-G_BH-02_	A8	150	20	111	140.4654	2.38%	8	40%	failed	195	24
Rem-Cyclic_13213-G_FE1.s1	A9	150	23	111	141.7554	2.77%	10.3	45%	failed	177	24
Drained_Cyclic_S-13252_RD	A10	200	67	11	133.3872	6.71%	47	70%	failed	80	24
Drained_Cyclic_13352_GE2	B11	250	63	11	162.039	4.81%	30	60%	failed	73	24
Drained_Cyclic_13352_GE2	B12	200	63	11	132.3672	6.23%	30	60%	failed	112	24
Drained_Cyclic_13352_GE2	B13	150	63	11	79.77541	8.86%	34.5	55%	failed	102	24
Cyclic_S-13252_CIT FO-301	B14	200	67	1	173.3672	6.71%	33.5	50%	failed	145	12
Cyclic_S-13252_CIT FO-301	B15	200	67	1	188.3672	6.71%	30	45%	failed	142	12
Cyclic_S-13252_CIT FO-301	B16	200	67	1	172.5172	6.71%	27	40%	failed	174	12
Cyclic_S-13252_RDX-PO-30	C17	150	67	1	121.7754	9.59%	33.5	50%	failed	115	12
Drained_Cyclic_13352_GE-2	C18	200	63	11	138.0172	6.23%	41	65%	failed	43	24
Cyclic_13352_GE2FO2.TS-0	C19	200	63	1	182.7972	6.23%	38	60%	failed	107	12
Cyclic_13252_ZNA-PO-303.	C20	200	67	1	184.6972	6.71%	43.5	65%	failed	61	12
Cyclic_13352_GE2F10.TS-0	C21	200	63	1	181.0372	6.23%	34.5	55%	failed	78	12
Drained_Cyclic_13252_ZNA-	C22	200	67	11	125.0472	6.71%	30	45%	failed	61	24
Cyclic_13352_GE-2FO2.TS-	C23	200	63	1	185.1372	6.23%	38	60%	failed	95	12
Cyclic_13352_GE2FO9.TS-0	C24	200	63	1	182.3772	6.23%	25	40%	failed	175	12
Cyclic_13252_ZNA-PO-302.	C25	250	65	1	235.649	4.98%	29	45%	failed	151	20
Cyclic_13352_GE-FOI-TS-0	C26	250	63	1	236.939	4.81%	25	40%	failed	170	20
Cyclic_13048-C_BH0213.8-	C27	150	58	1	135.7954	7.99%	26	45%	failed	165	12
Cyclic_S13048-G_BH-02_13.	C28	150	52	1	136.8554	6.99%	21	40%	failed	160	12
Cyclic_13252_ZNA-PO-302	C29	200	45	1	182.3672	4.23%	20.3	45%	failed	112	12
Cyclic_13227_G-FOI-TS-06	C30	250	47	1	224.959	3.46%	26	55%	failed	89	20
Cyclic_S13048-G_BH-02-TS	C31	200	52	1	173.3672	4.98%	28.5	55%	failed	105	12
Rem-Drained_Cyclic_13352_	C32	100	15	11	93.18361	2.70%	8.8	65%	failed	75	24
Rem-Cyclic_13352_GE2FO2.	C33	100	16	11	77.33361	2.90%	5.6	35%	failed	171	24
Rem-Drained_Cyclic_13352_	C34	150	15	11	121.7754	1.75%	8	60%	failed	84	24
Rem-Cyclic_13252_ZNA-PO-	C35	100	12	11	92.83361	2.13%	4.8	40%	failed	143	24
Rem-Drained_Cyclic_13352_	C36	100	15	11	87.61361	2.70%	8.8	65%	failed	97	24
Rem-Cyclic_13352_GE-2FO7	C37	150	15	11	137.1054	1.75%	7.5	50%	failed	103	20
Rem-Cyclic_S13048-G_BH-02	C38	150	17	11	133.4454	2.00%	8.5	50%	failed	98	12
Rem-Cyclic_13252_ZNA-PO-	C39	150	12	11	127.4554	1.39%	6	50%	failed	120	24
Rem-Cyclic_13352_GE-2FO7	C40	150	15	11	137.5454	1.75%	5.3	35%	failed	155	20
Rem-Cyclic_13252_ZNA-PO-	C41	150	12	11	134.7854	1.39%	4.2	35%	failed	144	12
Rem-Cyclic_S13048-G_BH-02	C42	150	12	11	140.4654	1.39%	4.8	40%	failed	122	12

Table 3.10 (continued): Summary of cyclic triaxial compression test

Name of the Output File / Nature of Test	Test ID	Confining pressure	Static Dev. Stress	Group No.	Pore Pres. u (takn)	Δ_p (%) at taken	Cyclic Dev. Stress	% qcyc/qs	Test Result	Number Cycles, N	Frequency cycles/hr
Drained_Cyclic_S-13252_ZF	A55	250	90	[illegible]	176.609	2.20%	49.5	55%	equilibrm	78	24
Drained_Cyclic_S-13252_ZF	A56	150	90	[illegible]	76.20541	4.29%	45	50%	equilibrm	86	24
Drained_Cyclic_S-13252_ZF	A57	200	90	[illegible]	125.6972	2.23%	40.5	45%	equilibrm	97	24
Cyclic_13213-G_FE1.st-04_	A58	150	85	[illegible]	124.4454	4.63%	31.5	35%	equilibrm	111	12
Cyclic_13213-G_FE1.st-04_	A59	150	85	[illegible]	118.4554	4.63%	28.8	35%	equilibrm	174	12
Cyclic_S-13252_MIX- FO-39	A60	200	87	[illegible]	176.1372	2.01%	20	35%	equilibrm	195	12
Cyclic_13283-G_BH02 TS-04	A61	200	88	[illegible]	173.3772	1.76%	20	35%	equilibrm	123	12
Rem-Cyclic_1323G-G_FE1.st	A62	100	23	[illegible]	83.87361	6.50%	4.7	20%	equilibrm	212	24
Rem-Cyclic_13288-G_BH02 T	A63	100	20	[illegible]	85.16361	2.22%	5	25%	equilibrm	207	24
Rem-Cyclic_13288-G_BH-02_	A64	150	20	[illegible]	126.7954	1.43%	5	25%	equilibrm	197	24
Rem-Cyclic_13288-G_BH-02_	A65	200	20	[illegible]	175.4472	1.05%	4	20%	equilibrm	203	24
Drained_Cyclic_13252_GE2	B66	250	63	[illegible]	170.959	2.88%	31.2	50%	equilibrm	57	24
Cyclic_S-13252_CLT FO-391	B67	200	87	[illegible]	168.3672	4.02%	23.5	35%	equilibrm	123	12
Drained_Cyclic_13252_GE-2	B68	200	63	[illegible]	114.3672	3.74%	31.2	50%	equilibrm	72	24
Drained_Cyclic_13252_GE-2	B69	150	63	[illegible]	81.77541	5.32%	28.5	45%	equilibrm	81	24
Cyclic_13252_ZNA- FO-393	B70	200	87	[illegible]	163.5172	2.52%	22	33%	equilibrm	103	12
Cyclic_S-13252_CLT FO-391	B71	200	87	[illegible]	160.3672	2.01%	20	35%	equilibrm	125	12
Drained_Cyclic_13252_GE2	C72	200	63	[illegible]	90.01721	1.87%	28.5	45%	equilibrm	78	12
Cyclic_S-13252_MIX- FO-39	C73	150	87	[illegible]	126.2054	2.88%	17	25%	equilibrm	80	12
Cyclic_13252_ZNA- FO-393	C74	200	87	[illegible]	175.6972	2.01%	27	40%	equilibrm	71	12
Drained_Cyclic_13252_ZNA-	C75	200	87	[illegible]	97.03721	1.44%	22	33%	equilibrm	87	12
Cyclic_13252_GE-2 FO2.TS-	C76	200	63	[illegible]	166.0472	3.74%	22	35%	equilibrm	74	12
Cyclic_13252_ZNA- FO-393.	C77	200	87	[illegible]	176.1372	4.02%	20	30%	equilibrm	92	12
Drained_Cyclic_13252_ZNA-	C78	150	87	[illegible]	42.78541	2.88%	22	33%	equilibrm	89	12
Cyclic_13252_GE2 FO8.TS-8	C79	200	63	[illegible]	179.0572	3.74%	22	35%	equilibrm	91	12
Cyclic_13252_GE2- FO1-TS-	C80	200	63	[illegible]	180.3472	3.74%	21	33%	equilibrm	98	12
Cyclic_13252_GE-2 FO2.TS-	C81	200	63	[illegible]	174.3872	3.74%	21	33%	equilibrm	97	12
Cyclic_13252_GE2- FO1-TS-	C82	200	63	[illegible]	175.4472	3.74%	21	33%	equilibrm	114	12
Cyclic_13252_ZNA- FO-392.	C83	250	65	[illegible]	220.959	2.99%	23	35%	equilibrm	102	12
Cyclic_13227-G_FO1.TS-08	C84	200	47	[illegible]	108.3972	2.08%	18	40%	equilibrm	85	12
Cyclic_13252_ZNA- FO-392.	C85	250	65	[illegible]	211.959	2.99%	18.5	30%	equilibrm	91	12
Cyclic_S13848-G_BH-02_13.	C86	150	52	[illegible]	131.7754	4.19%	13	25%	equilibrm	105	12
Cyclic_13252_ZNA- FO-392.	C87	250	65	[illegible]	211.109	2.99%	18	25%	equilibrm	125	12
Cyclic_13252_ZNA- FO-392.	C87	250	65	[illegible]	207.959	2.99%	18	25%	equilibrm	120	12
Cyclic_13252_ZNA- FO-392	C88	200	45	[illegible]	179.0172	2.54%	15.8	35%	equilibrm	104	12
Cyclic_13252_ZNA- FO-392	C88	200	45	[illegible]	173.7972	2.54%	15.8	35%	equilibrm	101	12
Cyclic_13227_G- FO1-TS-08	C89	250	47	[illegible]	223.289	2.08%	18	40%	equilibrm	85	12
Rem-Drained _Cyclic_13252	C90	100	15	[illegible]	76.85361	1.62%	8	40%	equilibrm	76	24
Rem-Drained_Cyclic_13252_	C91	150	15	[illegible]	118.4554	1.05%	8	40%	equilibrm	83	24
Rem-Cyclic_13252_ZNA- FO-	C92	100	12	[illegible]	80.95361	1.28%	3	25%	equilibrm	119	24
Rem-Cyclic_13252_GE2 FO2.	C93	150	15	[illegible]	125.7854	1.05%	5.3	35%	equilibrm	95	24
Rem-Cyclic_13252_GE-2 FO2	C94	150	15	[illegible]	131.4654	1.05%	5	33%	equilibrm	107	24

Table 3.10 (continued): Summary of cyclic triaxial compression test

Name of the Output File / Nature of Test	Test ID	Confining pressure	Static Dev. Stress	Group No.	Pore Pres. u (takn)	$\forall_p$ (%) at taken	Cyclic Dev. Stress	% qcyc/qs	Test Result	Number Cycles, N
Rem-Cyclic_13352_GE2 FO2.	C95	150	15	II	132.7554	1.05%	4.5	30%	equilibrm	105
Rem-Cyclic_13252_ZNA- PO-	C96	150	12	II	126.7954	0.83%	3	25%	equilibrm	117
Rem-Cyclic_13252_ZNA- PO-	C97	150	12	II	127.8554	0.83%	2.4	20%	equilibrm	125
Rem-Cyclic_S13048-G_BH-02	C98	150	12	II	125.7754	0.83%	4	33%	equilibrm	113
Rem-Cyclic_13252_ZNA- PO-	C99	150	12	II	120.7754	0.83%	4	33%	equilibrm	109
Rem-Cyclic_13252_ZNA- PO-	C100	150	12	II	116.7754	0.83%	3	25%	equilibrm	129
Rem-Cyclic_S13048-G_BH-02	C101	150	12	II	131.7754	0.83%	4	33%	equilibrm	116
Rem-Cyclic_13352_GE2 FO2.	C102	200	15	II	163.5172	0.78%	4.5	30%	equilibrm	122
Rem-Drained_Cyclic_S13048	C103	150	10	III	112.7754	0.69%	3	30%	equilibrm	126
Rem-Cyclic_13252_ZNA- PO-	C104	150	12	II	131.4254	0.83%	4	33%	equilibrm	115
Rem-Cyclic_13252_ZNA- PO-	C105	150	12	II	126.2054	0.83%	4	33%	equilibrm	121
Cyclic_13252_CLT PO-301.J	D106	200	67	I	175.6972	4.14%	20	30%	equilibrm	76
Cyclic_13252_CLT PO-301.J	D107	200	67	I	190.3672	4.02%	17	25%	equilibrm	98
Cyclic_13252_CLT PO-301.J	D108	200	67	I	190.3672	4.02%	13.5	20%	equilibrm	86
Rem-Cyclic_13252_CLT PO-3	D109	200	12	III	190.3672	0.62%	3.6	30%	equilibrm	87
Rem-Cyclic_S12647-11G_FOI	D110	200	7	II	190.3672	0.36%	2.45	35%	equilibrm	67
Rem-Cyclic_S12647-11G_FOI	D111	150	7	II	142.7754	0.48%	2.3	33%	equilibrm	84
Rem-Cyclic_S12647-11G_FOI	D112	100	7	II	95.18361	0.73%	2.1	30%	equilibrm	93

Figure 3.1.1: Region of sensitive clay from where the samples are taken for the present study River Lowlands (Loacat, J., 1995)

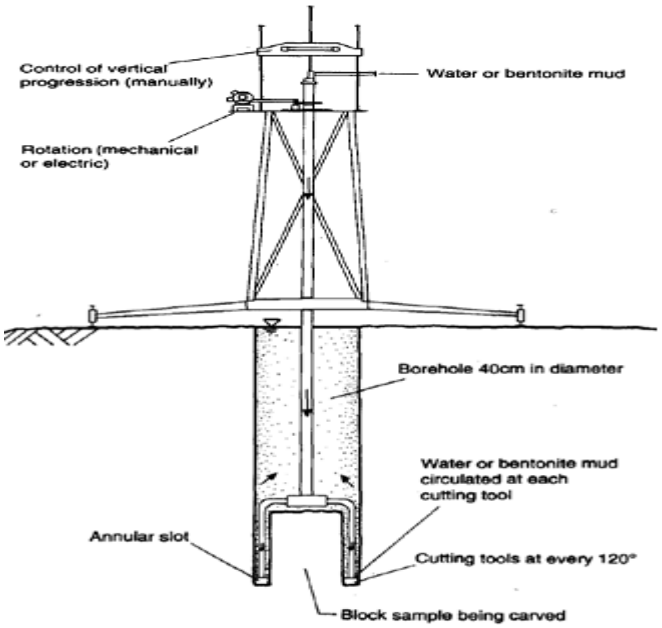

Figure 3.2.1: Schematic diagram of the Sherbrooke down-hole block sampler (Lefebvre and Poulin 1979).

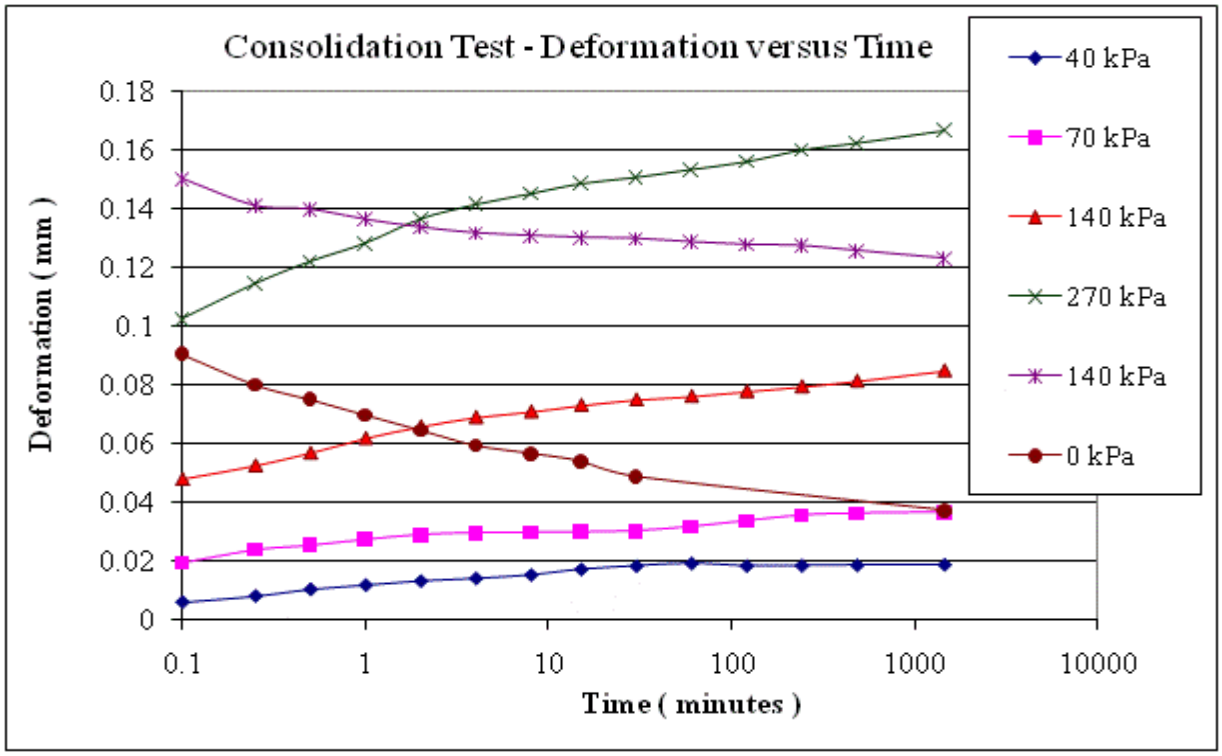

Figure 3.6.1: Consolidation Test–Deformation (mm) versus Time (min) Clay Type-A

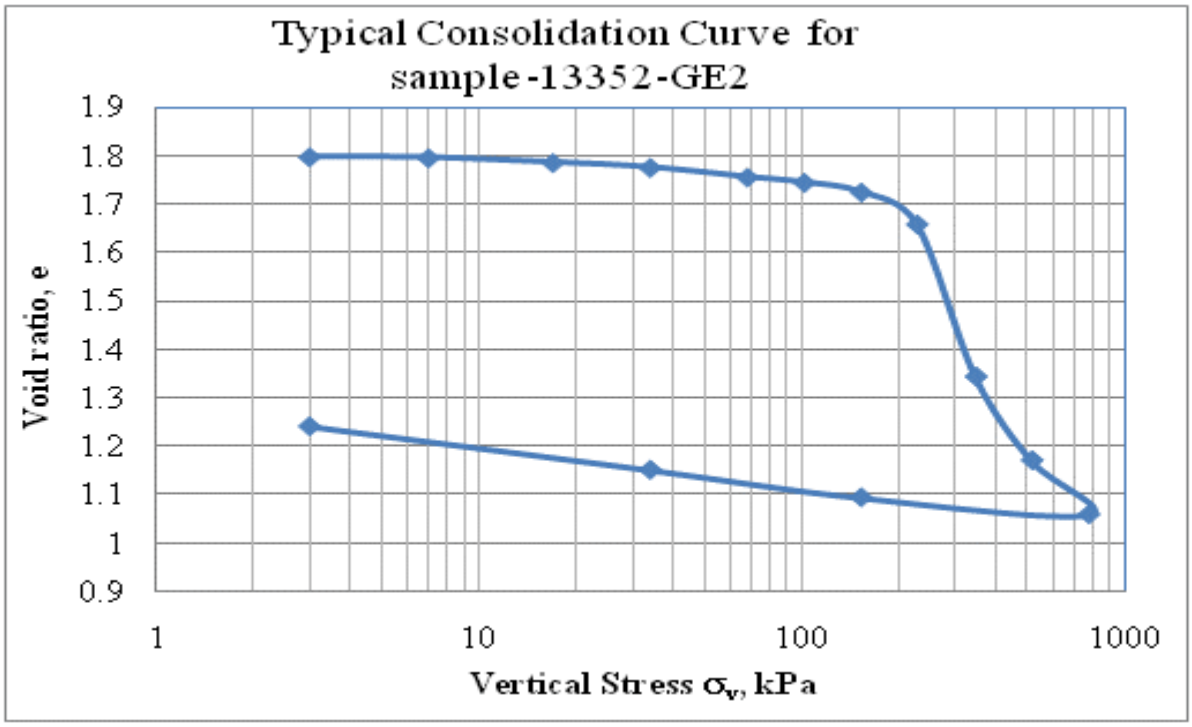

Figure 3.6.2: Typical consolidation curve (e-log σ_v) for sample 13352-GE2

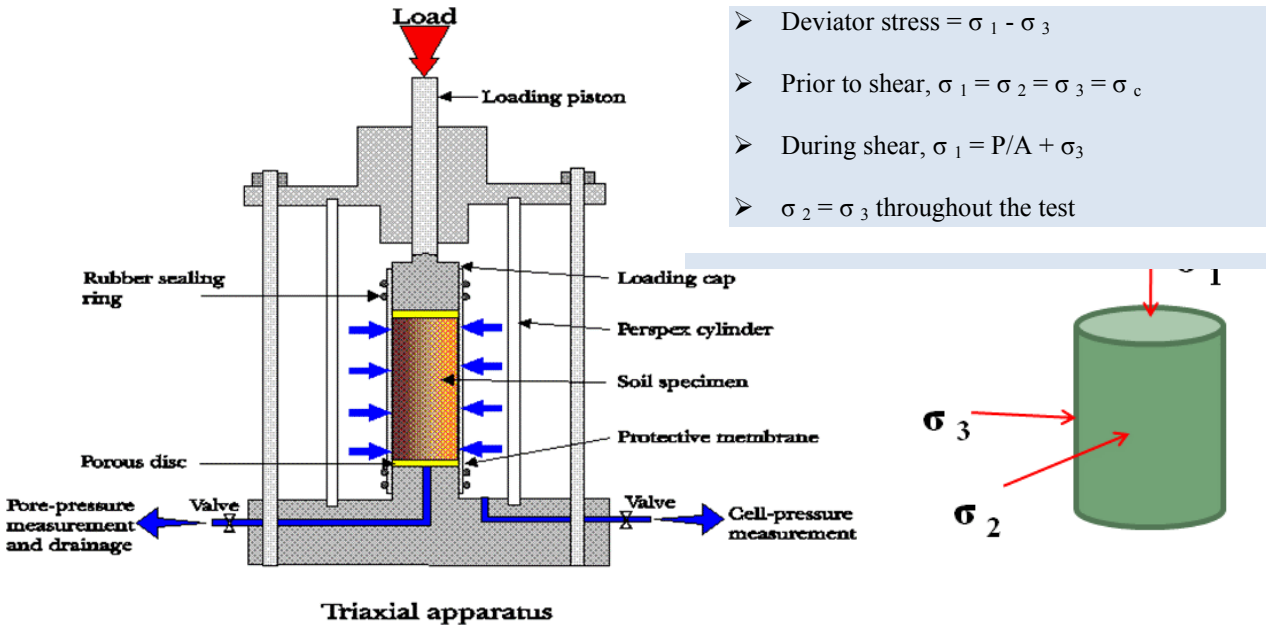

Figure 3.8.1: Schematic sketch of triaxial test principle

Figure 3.8.2:- Tritech, Triaxial Load Frame at Concordia University Geotechnical Laboratory

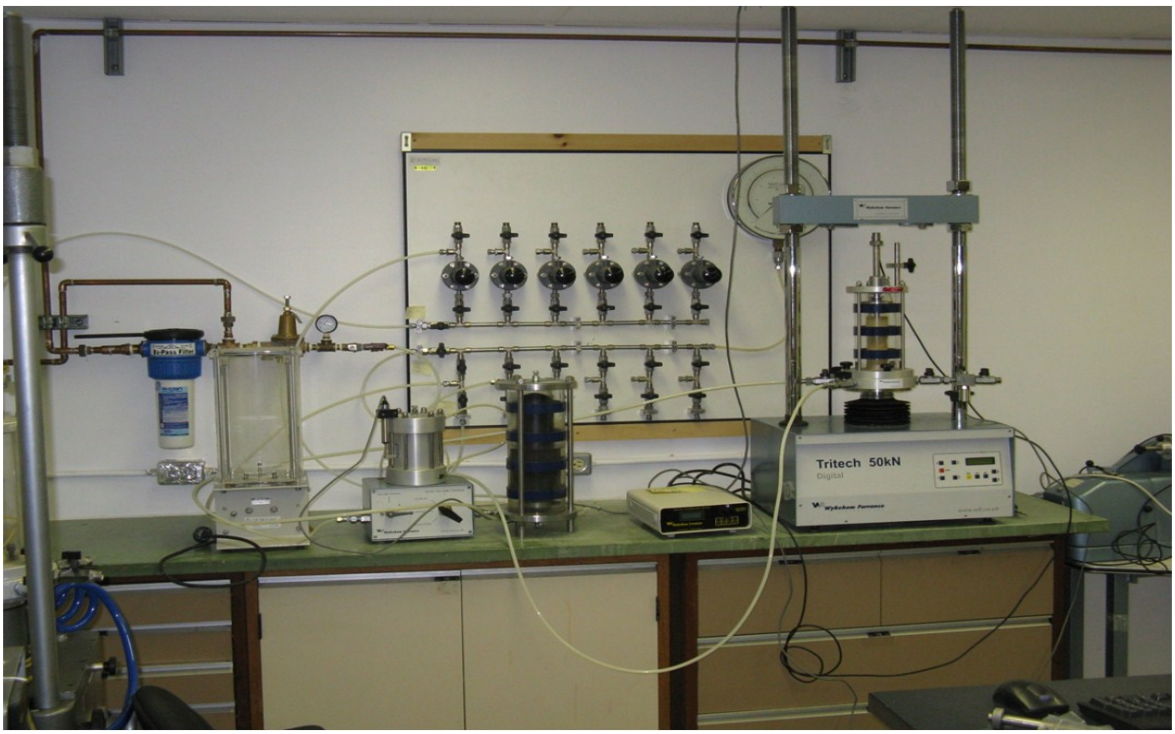

Figure 3.8.3: Main Components of the Triaxial System and the way they are connected.

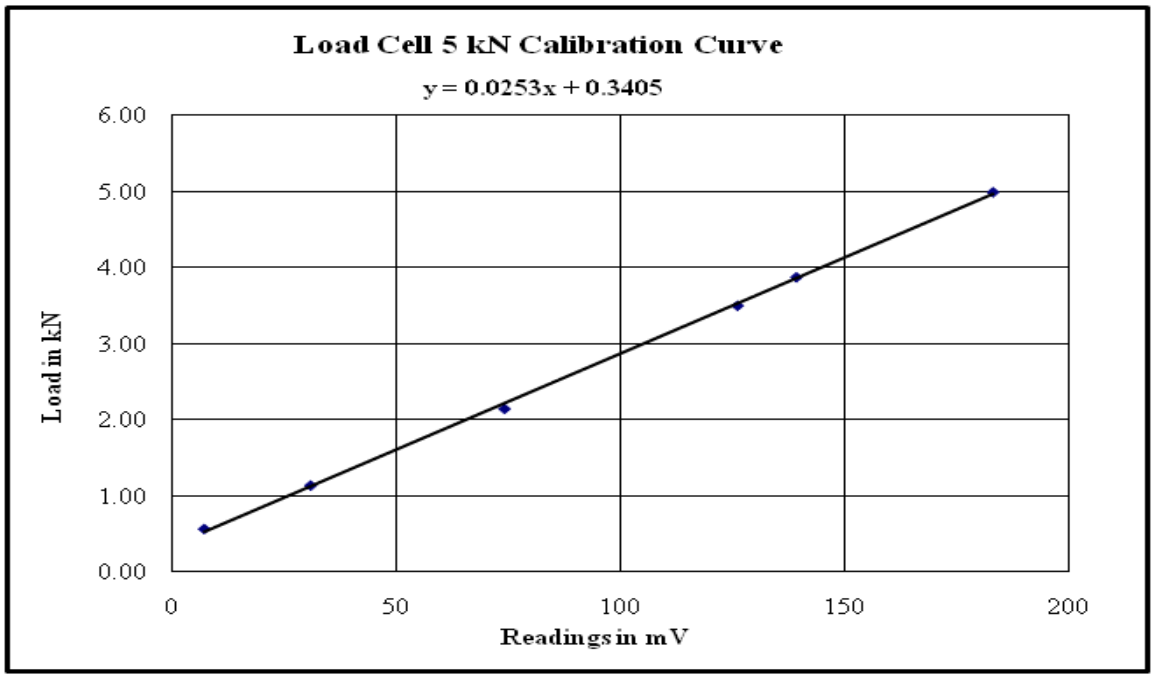

Figure 3.9.1:- Calibration – Submersible Load Cell 5 kN

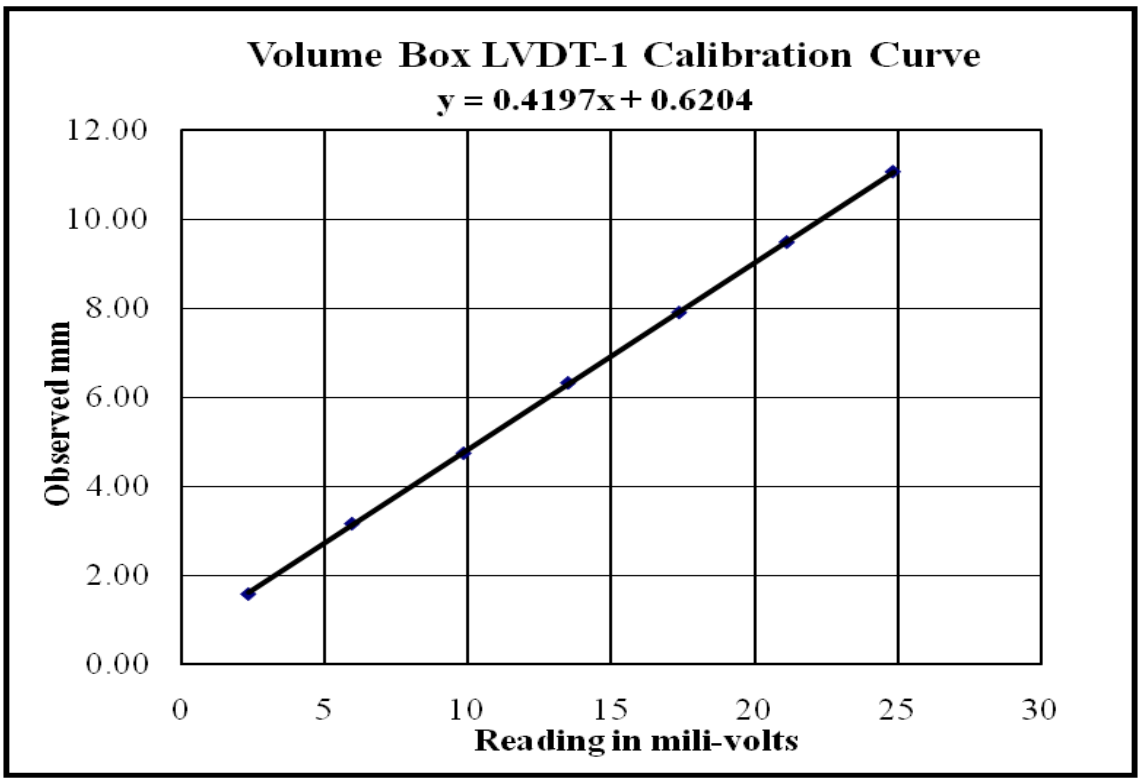

Figure 3.9.2: Calibration Curve for LVDT

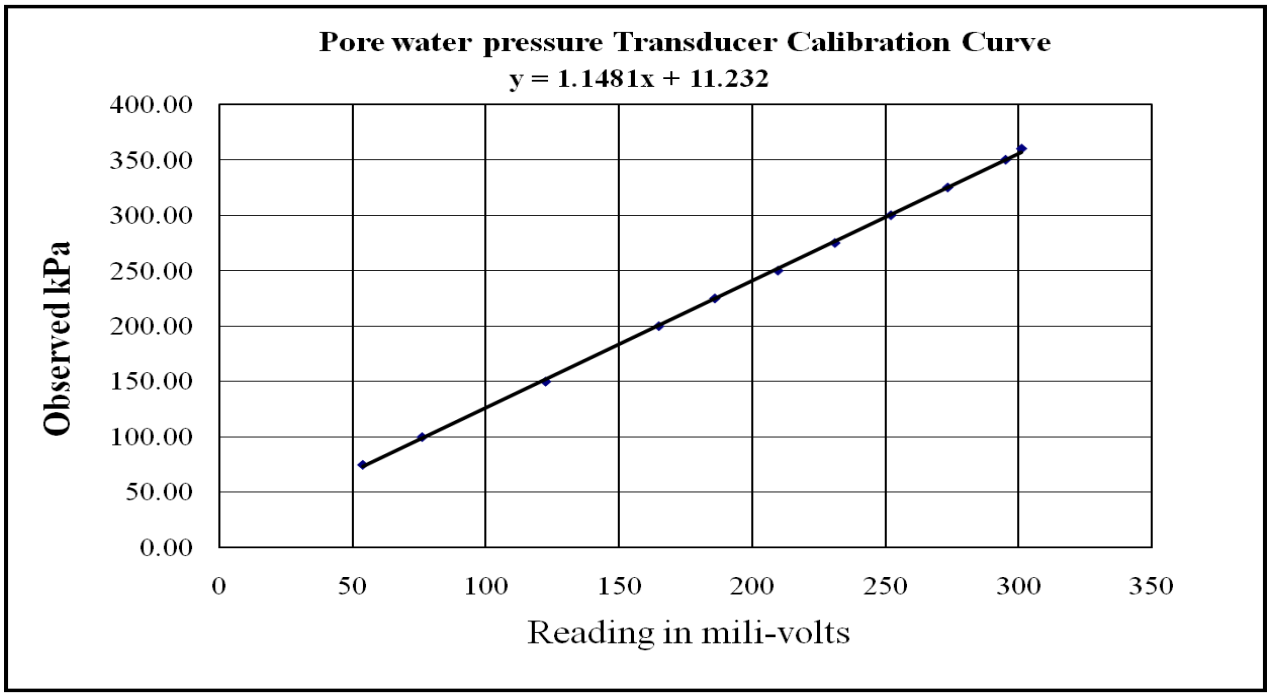

Figure 3.9.3: Calibration Curve for Pore Water Pressure Transducer

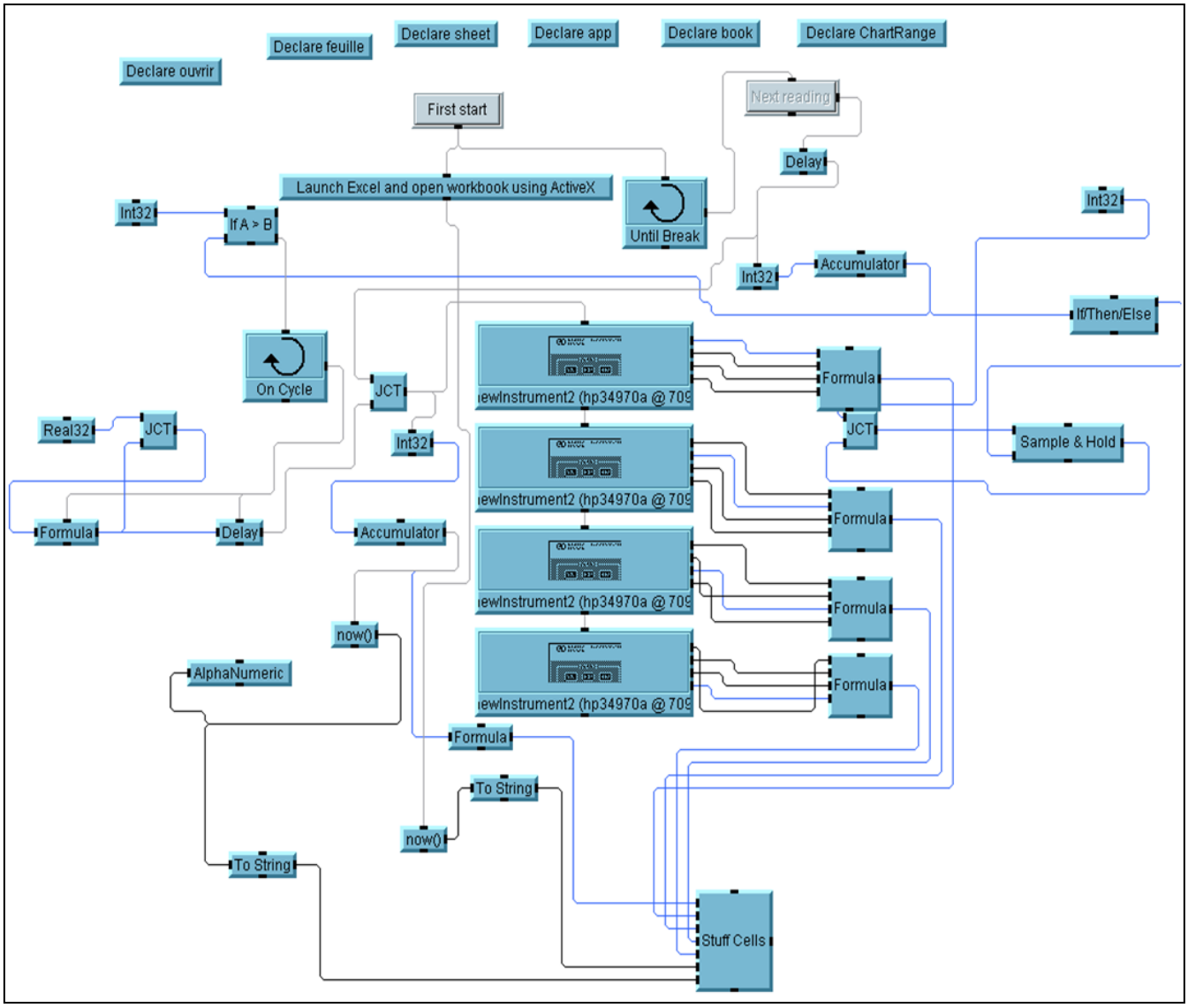

Figure 3.10.1 Overall Master.vee Visual Basic based program

Includes EXCEL File output Subroutine

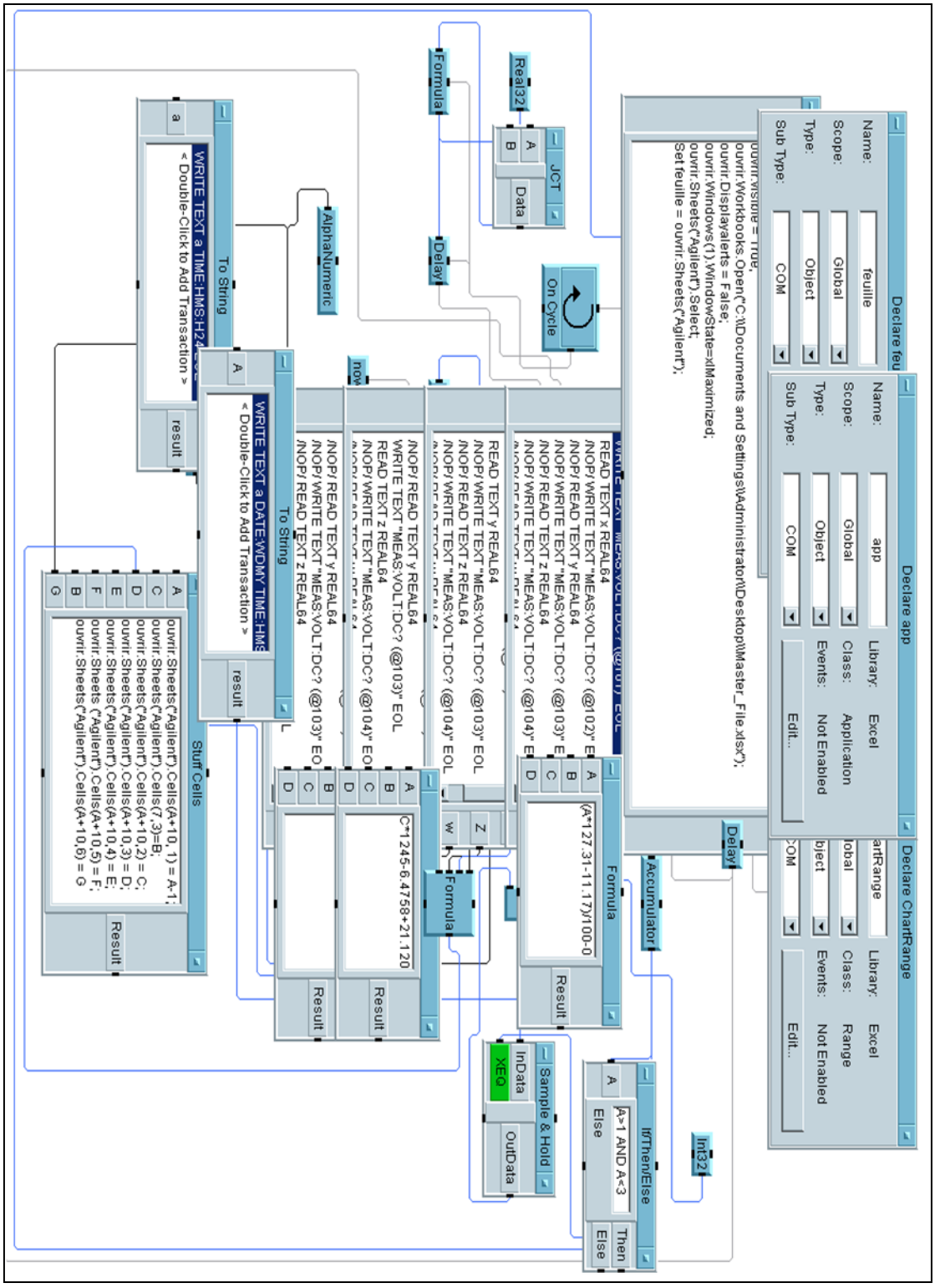

Figure 3.10.2 Overall Master.vee Visual Basic Coded Program – Showing Program Codes

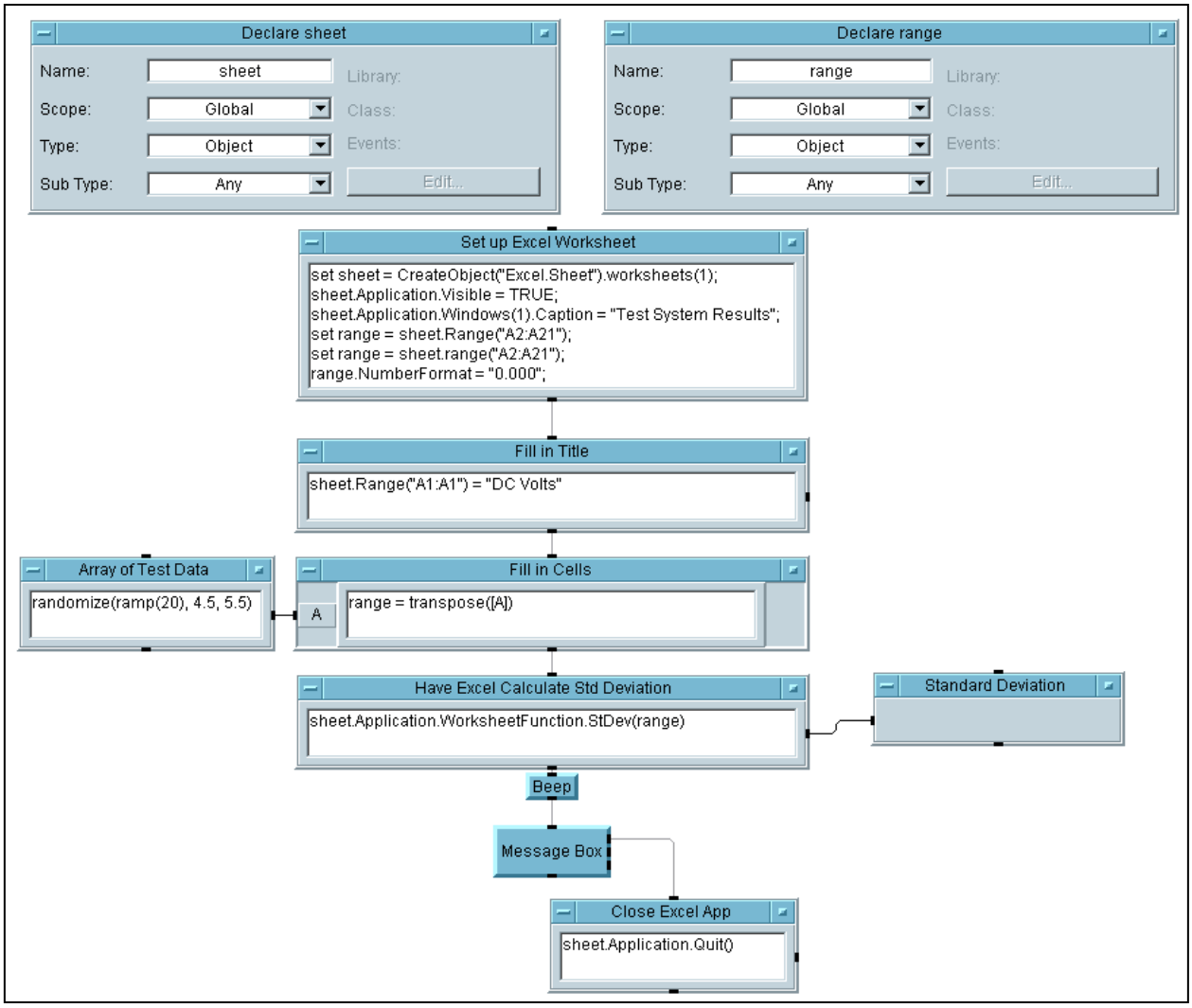

Figure 3.10.3: Master.vee - subroutine for setting up Excel Worksheet for data output

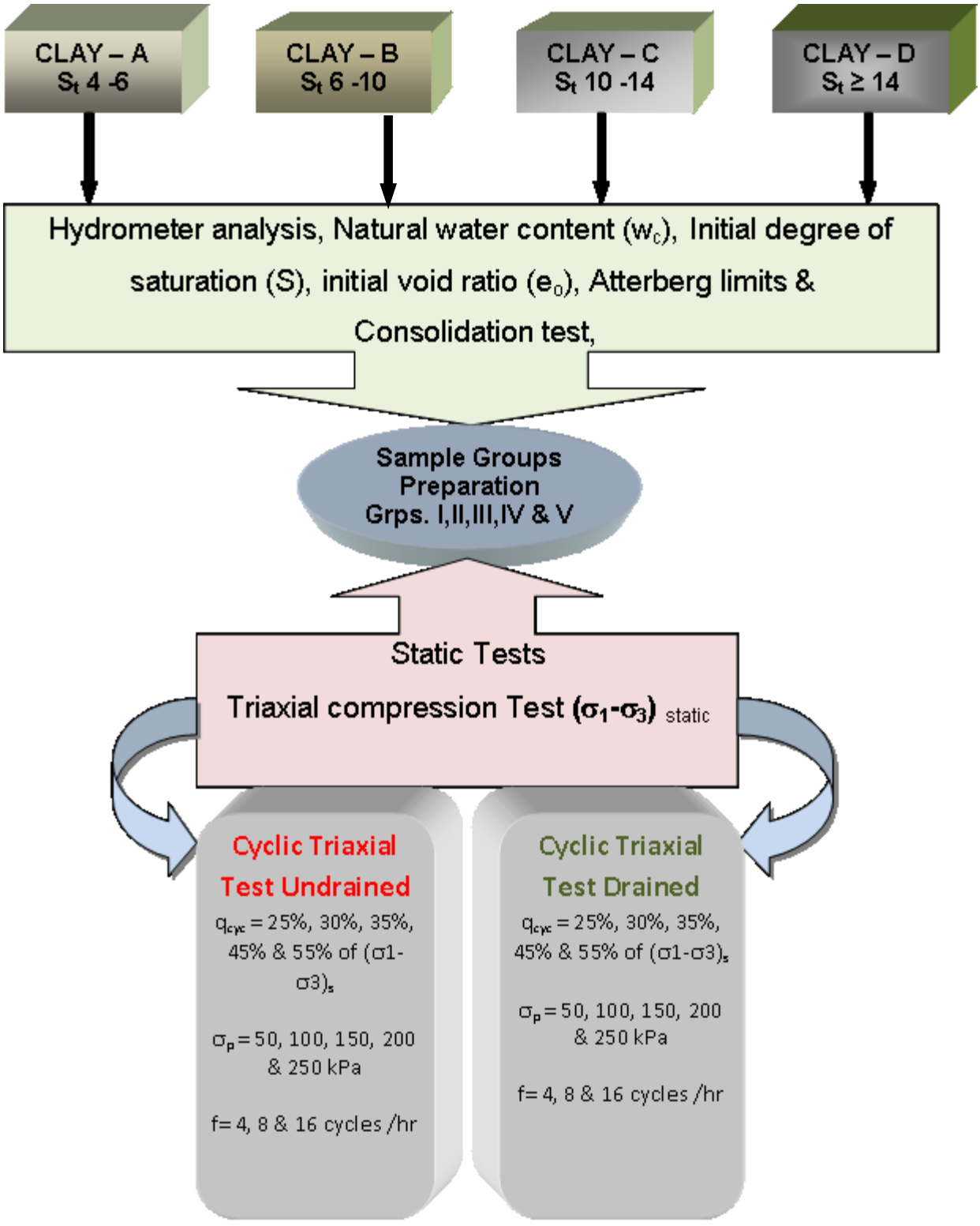

Figure 3.11.1 General experimental plan - layout for the present study

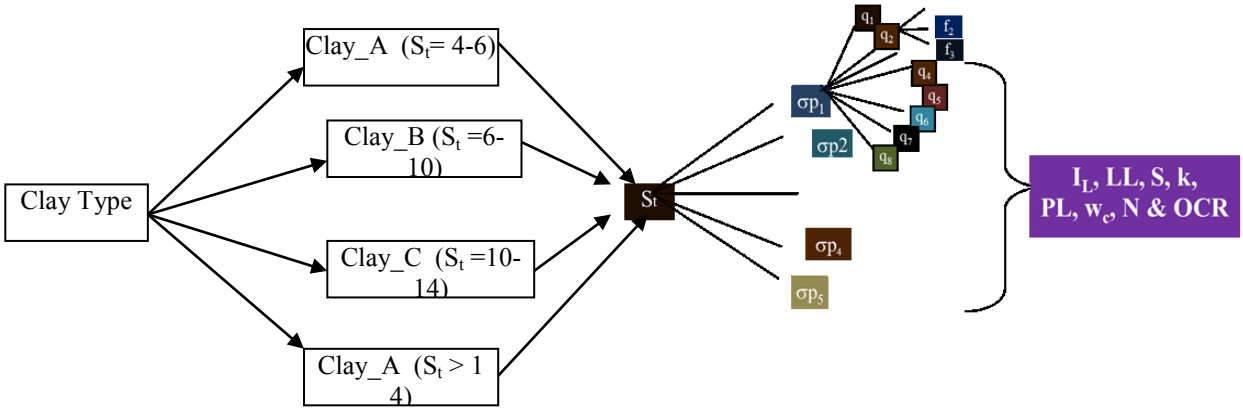

Figure 3.11.2:- Complexity of the experimental work

Chapter 4

Analysis and Theory

This chapter deals with the detailed analysis of the experimental results especially, static and cyclic triaxial tests. The purpose is to analyze the behavior of sensitive clay and to indicate the important factors and the missing gaps for the experimental and model investigation mentioned in the literature. Also, to formulate such a strategy which is capable of addressing also those missing gaps and provide the practical solutions to geotechnical engineers dealing with the complexity of designing new or examining existing foundations on sensitive clay.

The key elements responsible for the complex behavior of sensitive clay are identified and prioritized especially, when subjected to cyclic loading. Since, experimental work took care of the chemical and environmental parameters therefore the analysis is focused to those physical and mechanical parameters, which govern the behavior of sensitive clay when subjected to static or cyclic loading. Physical parameters include; natural water content (w), liquid limit (LL), plastic limit (PL), plasticity index (I_P), liquidity index (I_L), sensitivity (S_t), constant of variation in sensitivity (k) and initial degree of saturation (S). Whereas, mechanical parameters include; cyclic deviator stress (q_{cyc}), pore water pressure (u), axial strain (ε), over consolidation ratio (OCR), preconsolidation pressure (σ_p), confining pressure (σ_3), and number of cycles (N). In the graphical analysis to show the effect of mechanical parameters the number cyclic loading (N) is taken as abscissa i.e., along X-axis and the other parameters along Y-axis. Number of cycles, N helps in indicating cycle by cycle effect of other mechanical parameters. The analysis assisted in identifying those parameters which establish the link between the two governing categories of parameters i.e. physical and mechanical.

A hypothetical model, which explains the behavior of sensitive clay and how its shear strength reduces when subjected to disturbing /remolding action of cyclic loading has been introduced. The hypothetical model is used to adapt the Modified Cam Clay Model for predicting shear strength of sensitive clay subjected to cyclic loading under varying field conditions. The most important of all that the analysis and theory assisted in redefining the safe zone limits, which covers all the shortcomings in the study of Hanna and Javed, 2008. The redefined "safe zone" along with theoretical guide line is a tool, capable of addressing most of those missing gaps mentioned in literature and provides the practical solution to geotechnical engineers dealing with the complexity of designing new or examining existing foundations on sensitive clay.

4.1 Static Triaxial Tests

Conventional static triaxial compression tests were conducted on the selected clay samples. Figures 4.1.1 – 4.1.4 show the plotted data for stress versus peak axial strain and pore water pressure versus peak axial strain. Figure 4.1.5 and 4.1.6 show the typical stress-strain and pore water pressure versus strain curves for some of the selected samples

From the Figures 4.1.1 – 4.1.4 it is clear that strains at the peak shear stress for the most the samples were in the range of 0.3% to 3%, which is consistent as far as the of these clays, are concerned. These figures also show that, the samples from shallow depths have higher axial strain at failure as compared to those from greater depths. The possible reasons for this could be that, the samples at greater depths were more cemented and brittle than those taken from shallow depths. Also, the other possible reason might be that the samples taken from upper soil were loose and having random crack of microscopic proportion, hence, produced less pronounced peak stress requiring higher strain for failure.

The typical curves shown in Figures 4.1.5 and 4.1.6 also pin point an interesting fact that the sample at shallow depths behaved more or less like over consolidated clays (OCC) while, those at higher depths like normally consolidated clays (NCC). The obvious peaks in stress strain curves for test ID 6 A-I, sample ID S-13293-G BH and test ID 15 B-I, sample ID 13221 taken from depth 3.5m as compared to normally consolidated samples test ID 21 C-II, sample ID 13253 ZNA and test ID 2 A-III, sample ID 13293-G(2) further supports this fact.

The peak static strength shown in Figures 4.1.1 and 4.1.2 indicate that the samples belonging to Group-I were stronger than those of group II and III. The graphical analysis shows that the shear strengths for undisturbed samples were higher than remolded or reconstituted samples of groups II and III. There could be a number of reasons for this; as mentioned in the introduction about the card house structure of sensitive clays, the undisturbed samples initially show a high strength at lower strains and then in most of the cases a sudden drop occurred as the card house collapsed. Usually, when an undisturbed sample is brought to the laboratory, in spite of best efforts, somehow the sample loses or gains moisture content in addition to degree of disturbances a sample suffered in transporting process. These factors make the sensitive clay sample more unpredictable as compared to other non- sensitive or less sensitive clays. The most delicate part is keeping an undisturbed sample 100% free form addition or subtraction of moisture content. The samples of Group III whose natural water content was already close to liquid limit behave as a sample of soil bearing intrinsic shear strength. On the other hand, loss in moisture content while remolding and compacting could lead to the development of matric suction showing higher strength as a partially saturated sample. The Test 25C-I of Group-I has almost the same shear strength as of and 16C-III of Group –III. The possible reason for this gain of strength is due to the loss of moisture content during remolding. In general the Group-III

samples have least shear strength among the three groups. The other possible reason that test 25C-I is done on a sample obtained from shallow depth, which was already at the border line of partially saturation. Hence, the sample became brittle and end up in failure in the very early stages of the test.

Similarly by comparing Groups II and III (Figures 4.1.1 - 4.1.6), it is clear that effect of increased moisture content in the reconstituted (water content equal or greater than liquid limit) had made those samples weaker than the remolded samples for the same clay type belonging to Group II, for the same deviator stress and confining pressure combinations. The same trend can be observed in pore water pressures (see figures 4.1.3, 4.1.4 & 4.1.6). The Group III samples produced higher pore water pressures as compared to Group-II for the same or close match of deviator stress and confining pressure combinations. Hence, the samples bearing the intrinsic shear strength (Group-III) represents the critical level of deviator stress for the sensitive clay.

Static triaxial tests done for group IV (samples attaining equilibrium in Group-I cyclic triaxial test and V (samples attaining equilibrium in Group-II cyclic Triaxial test) are shown in Figures 4.12.3 and 4.12.4. The analysis Results for those test where also amazing, like; 1) Obvious reduction in static strength due to disturbance caused by initial cyclic test. 2). Over-consolidated samples behave like normally consolidated samples when subjected to same or higher deviator stress as was in cyclic test. The possible reason might be that after suffering N no. of cycles, samples stress history was changed so it behaved like a NCC sample 3). Also, an interesting fact was revealed that the sensitivity number reduces for the same soil type with an increase in sample taking depth. In other words, same soil showing different sensitivity number is dependent on the stress history and number of vibration which that layer of soil suffered before the sample was taken. This fact is supported by the results of static triaxial tests on the samples

of Group IV and V which, attained equilibrium or quasi elastic resilient state without being failed in the initial cyclic triaxial tests.

4.2 Cyclic Triaxial Tests

Only a few tests were done as consolidated undrained (CU), mostly unconsolidated undrained (UU) triaxial compression tests were done in view of variations in both physical and mechanical categories of parameters. A summary of cyclic triaxial test results is given in Figures 4.2.1 – 4.2.4. Figures 4.2.5 – 4.2.10 (Test ID A57 / Sample ID S-13252_ZF) show the typical stress versus time, pore water pressure versus time, stress versus strain and pore pressure versus strain patterns in cyclic tests. It is clear from the figures that both the pore water pressure and the axial strains increase with the increase in the number of applications deviator stress. The increase in pore pressure is the cause of stress path movement towards the static failure envelope (Figure 4.2.10). The samples which attained quasi elastic resilient state at the end of cyclic test without failing have cyclic strains less than 5%. Test ID – D110, Group II sample ID S-12647-11G attained quasi elastic resilient state at a minimum strain of 0.36%. Test ID – A62, Group III sample ID S-13213-G_PE attained quasi elastic resilient state at a maximum strain value among the survived samples of 6.5%. The maximum value of the cyclic deviator stress under which any sample survived was 55% for drained test, Test ID – A55, Group II, sample ID S-13252_ZF belonging to clay Type-A. On the other hand four samples with IDs A62, A65, C97 & D108, Groups III, II, II & I, sample IDs 13213-G_PE, 13293-G_BH, 13252_ZNA & 13252_CLT respectively got equilibrium at a minimum cyclic deviator stress ratio of 20%. Samples from shallow depths showed less pore water pressure values for approximately same strains as compared to the reconstituted samples of Groups II & III or those obtained from greater depths. The possible reason for this is again the OCR trend of shallow samples like the case of static

tests. The overall scenario shown in Figures 4.2.1 – 4.2.4 tells that there are many parameters in the back ground which could not be shown in these figures played decisive role in the survival or failure of the samples being tested. In some cases, apparently weaker samples (having higher sensitivity number) survived at same deviator stress at which the stronger samples (low sensitivity number) could not able to stand. For instance, Test ID – C33, Group II, sample ID S-13352_GE2 failed at cyclic deviator stress ratio of 35%, while sample test ID – D110, Group II, sample ID S12647-11G survived. A careful review shows that under certain conditions confining pressure was the decisive parameter. Sample of clay Type-C almost under same conditions as of sample of Clay Type-D, the only difference was that Type-C tested under a confining pressure of 100 kPa, while the sample for clay Type-D was tested under a confining stress of 200 kPa. Similarly in many tests where the sample was inclined towards overconsolidation a decrease in pore pressure in the initial loading cycles delay the migration of stress path towards failure. Similarly, application of low cyclic stress level could result in dilation and negligible stress conditions for the tested samples. Hence, many factors like; confining stress, deviator stress ratio, in situ stress states, disturbed/undisturbed or structured/ de-structured state of samples number and frequency of load applications, water content, degree of saturation, sensitivity number etc., etc., become responsible directly or indirectly in attaining equilibrium or failure for the clay samples tested for a triaxial compression test. Under certain conditions as mentioned in above example of clay, Types C & D a single parameter becomes dominant and play the decisive role.

The awareness of the complexity in the behavior of sensitive clay created by the current section demands a clear identification and prioritization of the role of all those physical and mechanical parameters which govern the behavior of sensitive clay under cyclic loading.

Keeping in view the importance of these parameters, the succeeding sections of the present chapter analyzes one by one the situations under which these parameters take over the control of the behavior of sensitive clay and become reason for attaining equilibrium or failure for the samples tested in triaxial compression tests.

4.3 Drained and Undrained Triaxial Compression Tests

Three drained tests were carried out on the selected samples of clay Types A and C. The purpose of these tests was to clarify the fact that the drained cyclic shear strength of a clay sample is always greater than undrained shear strength for a given stress condition. In triaxial testing, especially for clays due to poor hydraulic conductivity, to obtain 100% drained sample need more time requiring and ideally impossible. Hence, the drained strength is estimated with the help of undrained triaxial tests. In case of undrained triaxial test, the undrained shear strength behavior of sensitive clay differs significantly if test at in-situ stresses, or if test at stresses higher than the preconsolidation pressure (σ_p). Chapter 3, Figure 3.6.2 is based on the conventional consolidation test results. Although a significant part of the curve is under normally consolidated region, but the importance of over consolidated region cannot be overlooked, which usually causes a negative pore water pressure. The effective stress which governs the undrained shear strength in a sensitive clay foundation is a vertical effective stress in the soil at the time of construction, and the highest vertical stress previously experienced by the soil. The lowest undrained shear strength occurs when the current vertical effective stress equals the previous maximum value, which is a state of normally consolidated clay. Hence, the triaxial undrained tests done on samples having OCR close to 1, give critical values for shear strength as compared to the drained shear strength values obtained from drained cyclic triaxial test. Figure 4.3.1 shows stress strain chart for drained and undrained triaxial compression tests done on clay Type-C.

Drained tests exhibited shear failure at a higher deviator stress with an accumulated strain range of 6.23% - 6.71%, while, survived samples' accumulated strain range is 1.44% - 2.88%, at comparatively low cyclic deviator stress. On the other hand, undrained tests showed large accumulated strains for same deviator stress level for drained tests. A similar trend was found in clay Types A, B & D. The comparison of accumulated strains for the drained tests and undrained tests clearly indicates that the sample under undrained conditions failed much earlier and at a relatively lower cyclic deviator stress (q_{cyc}) than drained tests.

The increase in pore pressure is associated with the strength reduction in cyclic loading and can be interpreted as showing that the structure of clay is changed significantly by the action of the applied cyclic loading. In other words, the reduction in shear stress is directly proportional to an increase in pore water pressure during cyclic loading which in turn is directly proportional to the number of cyclic loadings. Hence, the undrained cyclic loading of sensitive clay is more likely to cause effective stress failures due to a continued increase in excessive pore water pressure as compared to drained conditions.

Based on the analysis given above, it can be reported that the undrained condition is more critical in terms of reductions in shear stress which as a result directly proportional to the number of cyclic loading (N) which is the major factor in increasing the pore water pressure. Consequently, the succeeding sections in the current chapter mainly focus on undrained triaxial tests' results.

4.4 Effect of Undisturbed and Remolded Samples

Figure 4.4.1 and 4.4.2 shows chart for, stress versus strains for undisturbed samples of Group-I and remolded or reconstituted samples of Group II & III for clay A and C. As mentioned above in case of static triaxal test, that the samples belonging to Group-I were stronger than those of

group II and III. This holds true as far as static strength is concerned, but the results for cyclic triaxial tests give another view also. In case of undisturbed sample, the rigidity of the clay skeleton restrained the buildup of large pore pressure generation in the beginning of the test, then, as time passed, the cyclic load disturbed the clay skeleton and in some cases the undisturbed samples did not show big difference in cyclic shear strength ratio as compared to their remolded or reconstituted samples. Another thing is that there is no such thing as truly undisturbed sample. The process of sampling, trimming and mounting the sample could have significant influence on the structure of soil. Hence, the shear strength for undisturbed samples are less than the original in situ field strength, a fact mentioned by Horslev, 1949, Scmertmann, 1955, Ladd and Lambe, 1963 and Skempton and Sowa, 1963.

Figures 4.2.1 to 4.2.4 clearly show that the samples of Group-III which were reconstituted at water content higher than liquid limit failed much earlier for the same deviator stress ratio due the development of intrinsic cyclic shear strength.

4.5 Effect of over-consolidation ratio

Figure 4.5.1 shows the variation of cyclic stress ratio with respect to number of loading cycles for various over-consolidation ratios in the case of clay Type-C. The figure indicates that the over-consolidation ratio (OCR) increases the number of loading cycles required to initiate initial liquefaction. Also, the cyclic stress ratio and that the cyclic shear strength increases with the increase in OCR.

Since the development of pore water pressure is considered as a main indicator of clay strength during cyclic loading, graphs for pore pressure versus number of loading cycles has been drawn for both normally consolidated clay (NCC) and over consolidated clay (OCC). Figures 4.5.2 and 4.5.3 show the typical development of pore pressure within NCC and OCC

respectively. The comparison of the two figures clearly indicates that the rate of pore pressure buildup within NCC is more than that of OCC. Figure 4.5.3 also shows a slight dilating trend in case of OCC. In OCC, at the beginning of the cyclic loading, decrease in pore pressure occurred due to the dilatancy behavior, while subsequently due to increase in number of cycles the effect of previous greater effective consolidation pressure diminished and the excess pore water pressure also start increasing.

To support the concept further a graph number of cycles, N versus degradation index, I_D (strain ratio at cycle 1 to N) is drawn as shown in figure 4.5.4. It is clear from the figure that the degradation index is high for low OCRs. The clay with high OCR has high strength and resistance against early softening. The same conclusion was drawn by Zhou and Gong (2000), and Vucetic and Dobry (1988). Since, OCR is directly proportional to preconsolidation pressure, σ_p the graphical analysis in the succeeding section shown in Figure 4.8.5 also prove the importance of OCR. Hence, OCR or OCR in terms of preconsolidation pressure, σ_p is identified as an important factor in controlling the behavior of sensitive clays especially under cyclic loading.

4.6 Effect of frequency

The effect of variation in frequency on cyclic shear strength ratio of clay Type-C for undisturbed samples and reconstituted or remolded samples of Group II & III are shown in Figures 4.6.1 and 4.6.2. Keeping in view the compressive load on the foundation due to public coming and going for the high rise building and shopping malls, a slow rate of loading were used in the present experimental investigations. Most of the tests were done with the frequency of 24 cycles per hour. To examine the effect of variation in frequency, a few selected samples were tested at the frequencies equal to 20 cycles and 12 cycles per hour. The samples tested at frequency of 24

cycles per hour reach failure earlier as compared to those samples subjected to frequencies 20 cycles per hour and 12 cycles per hour. Figures 4.6.1 and 4.6.2 clearly indicate that slow loading tests require longer time to cause failure than the rapid loading test. Furthermore, by comparing Figures 4.6.1 and 4.6.2, the reduction in shear strength in reconstituted samples (samples reconstituted at a moisture content equal to or greater than liquid limit) is clearly indicated. It is interesting to note that the lowest frequency curve of reconstituted sample is steeper than that of undisturbed sample. In other words, the reconstituted samples bearing intrinsic properties are more venerable to degradation at slow rate of cyclic loading as compared to undisturbed samples of that particular sensitive clay. Also, by having a close look at Figures 4.6.1 and 4.6.2, it can be seen that the effect of frequency is reducing with the passage of time or with the increase in number of cycles. This fact is also defended by Procter and Khaffaf, 1984.

In case of drained test slow load applications give extra strength to the sample due to the availability of time. In case of undrained tests, the main issue regarding loading rates appears to be stress and pore water redistribution during shear. The limitation in case of faster loading is that the test cannot be idealized. Since, pore water pressures are not allowed to equilibrate throughout the specimen, and the pore water pressure being measured is likely not that induced on some potential plane of failure. This is one of the main reasons that the present study is not conducted for high frequencies in order to reveal the true behavior of sensitive clay under cyclic loading.

4.7 Effect of confining pressure

Figures 4.7.1 and 4.7.2 show the effect of increase or decrease in confining pressure on the cyclic shear strength and pore water pressure of the clay Type-C. The selected clay remolded samples of clay Type – C (Groups II & III) were isotropically consolidated under a confining stress of

150 kPa, 200 kPa and 250 kPa and then, subjected to cyclic loading with a frequency of 24 cycles per hour. The figures show the variation of cyclic stress ratio with number of loading cycles for the two confining stresses, i.e., 100 kPa, and 150 kPa. The reason for the limited data used is because of the selective remolded, normally consolidated samples of Group-II. To achieve the realistic role of confining stress, both cyclic deviator stress and pore pressures are normalized with respect to confining pressure σ_3. It can be noted from the Figure 4.7.1, that the number of load cycles required to achieve a particular cyclic strength ratio with respect to confining pressure increases with a decrease in confining stresses. A best possible explanation is given by corresponding Figure 4.7.2, showing increase in normalized pore water pressure ratio under high confining stresses, initiate a higher normalized pore water pressure ratios.

4.8 Effect of Sensitivity Number and Liquidity Index (I_L)

Figure 4.8.1 shows the relationship between cyclic stress ratio and the number of loading cycles for the undisturbed samples of clay types A, B, C & D. The figure shows that the cyclic shear strength is highest for clay Type – A having the lowest range of sensitivity number. On the other hand, clay Type – D with high sensitivity number has lowest cyclic shear strength and seems to be liquefied at a less number of load cycles. Figure 4.8.2 gives relationship between cyclic stress ratio and the number of loading cycles for the undisturbed samples of clay types A, C & D. The comparison between the two figures further support the preceding argument about remolded samples being more venerable to failure after getting restructured form their in situ state. The effect of sensitivity could not be completely explained unless the role of liquidity index is to be indicated in the complex equation of parameters mentioned in case of sensitive clays. The liquidity index reflects the combined effect of water content (w), liquid limit (LL), plastic limit (PL), plasticity index (I_P), sensitivity number (S_t) and constant of variation in sensitivity (k) as

given by Javed, (2002). The analysis for the current study's experimental data would be incomplete without showing the relationship between sensitivity number (S_t) and liquidity index (I_L) on the same pattern as done by Wood, 1990. Figure 4.8.3 is based on the experimental data of the current study as well as the one used by Wood, 1990. Based on Figure 4.8.3, the data is re-plotted by sorting the k values of 1, 2, 3 and 4 as shown in Figure 4.8.4. In few cases, the values for k exceeded more than 4 which were ignored. The thick lines show the best-fit line for the values of k = 1, 2, 3 & 4. These best-fit curves establish a log linear relationship between sensitivity and liquidity index as follows;

$I_L = a \ln(S_t) + b$…….4.1

Where, a and b are the constants and can easily be determined by using regression analysis.

By reviewing Figure 4.8.4 critically, it is clear that the data points for k values equal to 2 or 3 mostly lie on the best fit curves given by equation 4.1. This indicates that equation 4.1 holds good for sensitive clays with sensitivity number greater than 4. It is also to be noted that for a sensitive clay there must be secondary controller to control the variation of sensitivity specially when the soil sample are taken from different depths and showing same sensitivity values. This problem can be solved by introducing preconsolidation (σ_p) pressure as secondary controller. The importance of this parameter is already established in section 4.5. Experimental data shown in Figure 4.8.3 is reanalyzed by grouping the whole data into different pre consolidation ranges, keeping in view, to have enough data points to set the relationship between undrained shear strength and the liquidity index with respect to constant of variation in sensitivity (k). For this the whole data is divided into five preconsolidation ranges; 0-100 kPa, 100-150 kPa, 150-200 kPa, 200-250 kPa and 250-300 kPa. Figure 4.8.5 shows the results of this analysis. The primary controller constant of variation in sensitivity, k =2 is kept constant and segregating the rest of the

data for the above mentioned preconsolidation σ_p ranges. The figure clearly shows a decrease in the shear strength with increase an increase in liquidity index. Also, the figure indicates that the undrained shear strength is directly related to preconsolidation pressure. This fact is well established in analyzing the effect of OCR on the cyclic shear strength of the sensitive clays (see section 4.5OCR). Figures 4.8.1 – 4.8.5 clearly indicate the importance of sensitivity number and liquidity index along with the role preconsolidation pressure $\sigma_{p.}$ The overall summarized comment for the analysis done in the current section is that, the preconsolidation pressures, σ_p is proved to be one of the key parameters in controlling the behavior of sensitive clays, furthermore, this parameter is a mean of establishing the link between the two main categories of parameters i.e., physical and mechanical.

4.9 Effect of initial degree of saturation

Figures 4.9.1 to 4.9.4 show a graphical attempt to analyze the test results keeping in view the effect of degree of saturation on the cyclic shear strength of the sensitive clays in the current study. The values for initial degree of saturation are taken along X-axis and cyclic stress ratio along the Y-axis. Each of these charts contains contain both the failed samples and those which survived or attained equilibrium or quasi elastic resilient state in the initial cyclic loading test. A hit and trial effort has been done to establish lines of demarcation between the failed and survived samples. In each case, different best fit line with different slopes was obtained. Based on the individual graph for the clay, a best fit curve is selected, shown in Figure 4.9.5.

Figure 4.9.1 shows the plot for the experimental data for the clay Type – A the least sensitive clay among the four types. Most of the test data fall in the range of 89% to 94% degree of saturation out of which samples that were subjected to 35% or less cyclic stress ratio survived or attained equilibrium. It is clear from the figure that a few samples which were subjected to

cyclic stress ratio even greater than 45% survived. Most of the samples subjected to stress ratio greater than 50% failed. By comparing Figures 4.9.1 – 4.9.5, it is clear that those samples with lower degree of saturation (S) survived at higher cyclic stress ratio and vice versa for samples with higher degree of saturation. This fact also proves that a remolded or reconstituted clay at higher moisture content (= LL or greater) or at higher degree of saturation, S is more susceptible to failure as compared to the remolded clay with less value of S

Figure 4.9.2 shows the plot for the experimental data for the clay Type – B with a sensitivity number ranging 6- 10. Test data shows two groups of ranges of S, one in the range of 87% to 92% and the other in the range of 95% to 98%. In contrast to Type-A, three Type-B samples survived between the range of 87% to 90% initial degree of saturation and close to cyclic deviator stress of 50%. The reason for this is that the samples of type B are within the narrow range of the degree of saturation or these sample might be representing the clay sensitivity number at the border of type A and B. By comparing figure 4.9.2 and 4.9.5, it is clear that these sample lie close to the average line of demarcation between failure and stable zones. The second group of samples for the type-B with S ranging from 95% to 98% although, subjected to a cyclic stress ratio lower than 45% even got failed due to higher values of S.

Figure 4.9.3 shows the plot for the experimental data for the clay Type – C with a sensitivity number ranging 10- 16. Like Type-A, the most of the test data fall in the range of 89% to 94% degree of saturation out of which samples that were subjected to 35% or less cyclic stress ratio survived or attained equilibrium. It is clear from the figure that few samples which were subjected to cyclic stress ratio between 45% to 40% also survived having S values less than 92%. The figure shows that there were some samples failed even though they were subjected to cyclic deviator stress less than 40%, the reason was that, S values were greater than 98%. By

comparing Figures 4.9.3 and 4.9.5, it is clear that those samples with lower degree of saturation (S) survived at higher cyclic stress ratio and vice versa for samples with higher degree of saturation.

Figure 4.9.4 shows the plot for the experimental data for the clay Type – D, bearing the maximum sensitivity number among the four types A, B, C & D. Most of the test data for this clay falls in the range of 92% to 100% degree of saturation out of which samples that were subjected to 33% or less cyclic stress ratio survived or attained equilibrium. It is clear from the figure that the samples fall in the range of S 91% to 95% failed at higher cyclic stress ratio as compared to the samples which failed even at cyclic stress ratio of 40% with S values greater than 97%. Although type-D samples missed an important range of 87% to 91% of S, even then, by comparing figures 4.9.4 and 4.9.5 it is clear that those samples with lower degree of saturation (S) failed at a higher cyclic stress ratio as compared to those which failed a lower cyclic stress ratio and having higher values of degree of saturation.

Figure 4.9.5 shows the overall scenario of the relationship between degree of saturation (S) and cyclic stress ratio (q_{cyc}/q_s). It is clear from the figure that a few samples which were subjected to cyclic stress ratio greater than 50% survived due to having lower values of S. Most of the samples subjected to stress ratio less than 50% failed due to higher values of S. Overall summarized effect given in Figure 4.9.5 concludes that the sensitive clay with lower degree of saturation (S) is more resistant to deformation or failure as compared to if the same clay has a higher initial degree of saturation (S).

The analysis of the experimental data done in Figures 4.9.1 – 4.9.5 establishes the importance of the initial degree of saturation in case of sensitive clays especially, when these clays subjected to cyclic loadings. The fact, the samples tested under same total stress conditions

but with higher initial degree of saturation results into failure, while the sample with comparatively lower values of initial degree of saturation survived and attained quasi elastic resilient state gives rise to the relationship among matric suction, initial degree of saturation cyclic shear strength and intrinsic cyclic shear strength. It is an established fact that the matric suction is directly related to shear strength and inversely related to the initial degree of saturation. Furthermore, the way the pore water pressure develops especially, with load cycling, has key role in making a soil sample stable or unstable. This pore water pressure is also dependent on the initial degree of saturation. Hence, the relationship between strength and initial degree of saturation arises from the dependency of pore pressure on the initial degree of saturation.

It is worth mentioning here that the undisturbed samples obtained from field are sometimes not completely saturated. Hence, initial degree of saturation, S is taken as an important parameter for closely relating to those of actual field conditions. Another statement, based on this analysis could be made as; that by taking into account the actual degree of saturation, S in the analysis of the behavior of sensitive clays, it might be to some extent covers the environmental category of the parameters, which is assumed to be balanced out by careful handling, sampling and testing.

4.10 Effect of Cyclic Deviator Stress

The effect of cyclic loading or the cyclic application of a given level of deviator stress is like a disturbing /remolding agent in case of sensitive clay. The cyclic application of deviator stress disturbs the structure of sensitive clay along with facilitating the available water to dissolve down the salts results in leeching, causing reduction in shear strength of the clay. The

undisturbed clay sample gets disturbed, results in collapsing of sensitive card house structure. This remolding action of the deviator stress in the presence or absence of other parameters may result in reaching a sample to its remolded shear strength (Group –II samples) or sometimes even below then that in the presence of high natural water contents (intrinsic shear strength – Group – III samples). Figure 4.10.1 and 4.10.2 show the cyclic mobility or movement of effective stress path controlled by cyclic deviator stress and number of cycles, N. The effect of an increase in load cycles causes an increase in the pore water pressure, which in turn moves the effective stress path towards the failure plane.

Some of the test samples are subjected to multiple levels of deviator stress in order to reveal the role of cyclic deviator in case of sensitive clay. Figure 4.10.3 and 4.10.4 show that higher pore water pressure is generated at higher cyclic stress ratio. Figure 4.10.4 clearly indicates that pore water pressure exhibits only a very slight increase for a lower cyclic deviator stress level, while it increases steeply at higher cyclic deviator levels.

The analysis shown in Figures 4.10.5 – 4.10.9 is done, keeping in view, the effect of cyclic deviator stress and also if the level of this applied stress is increased First of all each clay type data is plotted. The values of number of load cycle applied are taken along X-axis and cyclic stress ratio along the Y-axis. Each of these charts contains contain both the failed samples and those which survived or attained equilibrium or quasi elastic resilient state in the initial cyclic loading test. The best fit curves for the failed and survived samples for each of clay type (A, B, C & D) then determined. Each chart came up with different lines with different values of constants. Finally, based on all the curves' in figures 4.10.5, 4.10.6, 4.10.7 & 4.10.8 a best appropriate curve is obtained to establish the line of demarcation between stable and unstable zones for the selected sensitive clays in the current study.

Figure 4.10.5 shows the plot for the experimental data for the clay Type – A the least sensitive clay among the four types. Most of the test samples failed fall in the range of 50% to 70% cyclic stress ratio. Three samples failed within the range of 40% to 45%. Three samples attained equilibrium or quasi elastic resilient state under a range cyclic stress ratio of 45% to 55%. Most of the samples survived, were under 35% of cyclic deviator stress ratio. Figure shows the best fit curves for the failed and stable samples. The figure clearly indicates that the higher the cyclic deviator stress the more is the chances of failure of the sample. The transition zone between the failed and equilibrium envelope has approximately a thickness of 20% to 25% in terms of cyclic stress ratio and to be on safer side, can also be consider as unstable zone

Figure 4.10.6 shows the plot for the experimental data for the clay Type – B with a sensitivity number ranging 6- 10. Most of the test samples failed fall in the range of 45% to 60% cyclic stress ratio. Three samples failed within the range of 40% to 50%. Three samples attained equilibrium or quasi elastic resilient state under a range cyclic stress ratio of 45% to 50%. Three samples survived, were under 35% of cyclic deviator stress ratio. Figure shows the best fit curves for the failed and stable samples. Like clay Type-A the graphical analysis shown in the figure clearly indicates that the higher the cyclic deviator stress the more is the chances of failure for the sample.. The transition zone between the failed and equilibrium envelope has approximately a thickness of 20% in terms of cyclic stress ratio and to be on safer side, can also be consider as unstable zone

Figure 4.10.7 shows the plot for the experimental data for the clay Type – C with a sensitivity number ranging 10- 16. Most of the test samples failed fall in the range of 40% to 65% cyclic stress ratio. A few samples failed even in the range of 35% to 45%. A few samples attained equilibrium or quasi elastic resilient state under a range cyclic stress ratio of 35% to

45%. Most of the sample survived, were under 33% of cyclic deviator stress ratio. The figure shows the best fit curves for the failed and stable samples. Like the other two clays (A & B), the graphical analysis shown in the figure clearly indicates that the higher the cyclic deviator stress the more is the chances of failure for the sample. The transition zone between the failed and equilibrium envelope has approximately a thickness of 20% in terms of cyclic stress ratio and to be on safer side, can also be consider as unstable zone

Figure 4.10.8 shows the plot for the experimental data for the clay Type – D bearing the maximum sensitivity number among the four types A, B, C & D. Most of the test samples failed fall in the range of 40% to 60% cyclic stress ratio. Three samples failed within the range of 40% to 45%. Two samples attained equilibrium or quasi elastic resilient state under a range cyclic stress ratio of 33% to 35%. Most of the sample survived, were in the range of 20% to 30% of cyclic deviator stress ratio. The figure shows the best fit curves for the failed and stable samples. Like the other clays (A, B & C) the graphical analysis shown in the figure clearly indicates that the higher the cyclic deviator stress the more is the chances of failure for the sample. The transition zone between the failed and equilibrium envelope has approximately a thickness of 20% to 25% in terms of cyclic stress ratio and to be on safer side, can also be consider as unstable zone.

Figure 4.10.9 shows the overall plot for the experimental data for the four types A, B, C & D. Most of the test samples failed fall in the range of 40% to 60% and the survived, were in the range of 20% to 35% of cyclic deviator stress ratio. The figure 4.10.9 clearly indicates that different clays with varying sensitivity have different best curves for the failed and survived samples. The careful review of the figure reveals that each curve is offering a type of save zone introduced by Hanna and Javed (2008). Hence, clays having low sensitivity number has wide

range of safe zone as compared to those with lower sensitivity number. For a sensitive clay region having clays of varying sensitivity the critical limits for the safe zone would be established based on the clay bearing lowest shearing stress or cyclic stress ratio.

4.11 Effect of number of cycles

Figure 4.10.9 and almost all the preceding sections' graphical analysis means nothing if the number of load cycles, N is taken out from the scenario. The distinctive feature of sensitive clay i.e., its card house like structure changes due the disturbance cause by the cyclic loading. The cyclic loading acts a remolding/disturbing agent, which helps the available water in the soil to dissolve away the salts, which results in the change of soil structure and compaction. Hence, the number of load cycles, N is a key parameter which can increase and decrease the influence of other governing physical or mechanical parameters in keeping a sensitive clay sample in stable (safe zone) or unstable (failure zone) during a cyclic triaxial testing.

The main signals for a sample failure like; increase in pore pressure along with axial strain completely dependent on the number of load applications, Hence, the importance of number of cyclic load, N could not be ignored. Effects of all other parameters especially mechanical can be easily translated in terms of number of cyclic loading. For example, a careful review of the figures in the preceding sections show that the undisturbed samples of Group – I can bear more load cycles, N than their corresponding samples belonging to Groups II & III. This fact is well supported by the graphical analysis of the current experimental study. Hence, all those samples which survived or attained equilibrium lying within the transition zones should be considered unsafe if any factor like increase in the level of deviator stress or decrease in confining stresses, degree of saturation etc., etc., combines with continue increase in loading cycle, N. In words, the survived samples in shown in all the figures can be considered stable as

long as there is no change in the given conditions of physical and mechanical parameters in the presence of continuous application of cycling of load, N. Most of the graphical analysis in the present study and also in literature takes into account the number of cycles as key factor in describing the effect of other governing parameters.

In most of the cases (see Figure 4.10.9) where the samples reached equilibrium, after neglecting the initial cycles (15 -20) the reduction in shear strength per cycle becomes constant along with constant pore water pressure. This constant value gives rise to a hypothetical model (mentioned in the succeeding sections) by assuming that the undisturbed samples are at 100% same structure as were in situ state.

4.12 Theoretical Application of Experimental Data

The present experimental results and the analysis presented above, have been used to develop design theories, as follows;

- ***A hypothetical model, which explains the behavior of sensitive clay and how its shear strength reduces when subjected to disturbing / remolding action of cyclic loading.***
- ***Using or adapting a Modified Cam Clay Model or any other clay model in order to predict the behavior of sensitive clay subjected to cyclic loading under varying field conditions.***
- ***Effect of degree of saturation in case of fully saturated samples and matric suction in case of partially saturated samples on the shear strength of the clay.***
- ***Redefining and modifying the safe zone concept given by Hanna and Javed, 2008.***

4.12.1 Hypothetical Model

For the four different sensitive clays A, B, C and D having sensitivity numbers S_{tA}, S_{tB}, S_{tC} and S_{tD} then under ideal conditions;

1. *Ideally a 100% undisturbed sample of a sensitive clay does not display its ultimate sensitivity number (S_t) unless and otherwise disturbed to an extent where its original undrained shear strength (C_{uo}) reduces to a value of undrained remolded shear strength (C_{ur}) without any loss of moisture content. This material parameter of a sensitive clay can be defined as a degree of remolding (r). A schematic presentation for this hypothesis is shown in Figure 4.12.1.*
2. *The shear strength (C_{ur}) of an isotropically consolidated remolded clay sample does not reduce to a value equal to intrinsic shear strength (C_{ur}*) unless or otherwise its natural moisture content (w_c) approaches to liquid limit or greater.*

The sensitivity number (S_t) of the clay can be defined by a known relationship as;

$$S_t = \frac{C_{uo}}{C_{ur}} \quad \text{.....4.2}$$

Where; C_{uo} = Original undrained shear strength of an undisturbed sample, C_{ur} = Shear strength of a remolded sample.

Assuming an ideal situation of having perfectly undisturbed samples of clays of varying sensitivity and stress history (see tables in chapter -3). Group-I & II give most of the physical parameters required for the analysis. Samples of Group-I are to determine undrained shear strength (C_{uo}) of undisturbed samples for each of the selected clays. Group-II samples, the failed samples of Group-I were remolded thoroughly with precautions of avoiding loss of moisture content and reconsolidated close to initial conditions and tested for determining the remolded shear strength (C_{ur}). The ratio of Group-I static shear strength (C_{uo}) to the corresponding Group-

II samples gave the final sensitivity number (S_t) for the selected clays. Group-III samples were reconstituted at water content range equal to LL – 1.5LL, to incorporate intrinsic properties to the mechanical parameters. The intrinsic shear strength (C_{ur}*) obtained from Group-III. Group IV and V were used to determine the reduction in static shear strength after N cycles for samples which attained equilibrium in their initial cyclic triaxial test (see Figures 4.12.1.2. to 4.12.1.6) Moreover, for undisturbed samples number of cycles N = N_{st} needed to reduce the undrained shear (C_u) to remolded shear strength (C_{ur}) will be determined. Also, the amount of water content needed reduce the remolded shear strength to intrinsic shear strength (C_{ur}*) will be determined.

Figure 4.12.1 shows a schematic diagram for hypothesis No.1. This hypothetical model seems to be fully supported by one of the previous studies done by Theirs and Seed (1969) as shown in Figure 4.12.1-1. The figure clearly indicates the sharp decrease in shear strength following the cyclic loading. Also, the analysis of the current experimental work shown in Figures 4.12.1-2 to 4.12.1-6 agrees to hypothetical model shown in Figure 4.12.1.

The remolding parameter r defined in hypothesis No.1 can be a function of cyclic strain (ε_c). Then the cyclic strain can be given as;

$\varepsilon_c = F(r, \tau_c)$ 4.3

And the increase of r with respect to number of cycles can be given as;

$$\frac{dr}{dN} = Q(r, \tau_c) \text{.....4.4}$$

Where; τ_c = cyclic shear stress and N= cyclic load number. The parameter r has to be related to some observable scalar variable i.e. the value for which increases if and only if additional cycles of loading are applied. The literature review makes the choice easy that the positive pore water pressure (u) is the most effective parameter generated with increase in number of cycles. The remolding parameter r plays a dual role of remolding agent as well as strain hardening parameter,

till the clay attains it complete sensitivity. After the clay strength reduces to remolded strength, the parameter r acts as softening agent till the clay sample fails or reach to a quasi elastic resilient stage. Hence, the equations 4.3 and 4.4 can be rewritten in terms of positive pore water pressure as;

$\varepsilon_c = F(u, \tau_c)$.....4.5

$$\frac{du}{dN} = Q(u, \tau_c)$$.....4.6

The functions F (u, τ_c) and Q (u, τ_c) can easily be determined from experimental data.

4.12.2 Adapting the "Modified Cam Clay Model" for Analyzing Behavior of Sensitive Clay Subjected to Cyclic Loading

To adapt or to simply use any existing model in order to comprehend the behavior of sensitive clay is not easy as compared to insensitive clays. The problem becomes manifold when cyclic loading comes into play. From the literature review, it is clear that no single model can comprehend the versatility of the governing parameters for this clay. In the light of above mentioned hypothesis, an effort has been done to incorporate parameter "r" i.e., degree of remolding to the Modified Cam Clay Model for analyzing the behavior of the sensitive clay subjected to cyclic loading. The model adapted to accommodate cycle by cycle variation in cyclic shear strength for the initial stages of an undisturbed clay sample along with the variation in governing parameters (mechanical and physical). Given below, are the summarized salient features of the Modified Cam Clay Model along with the changes in variants and constants in order to adapt the model for cyclic loading.

In critical state mechanics, the state of a soil sample is characterized by three parameters:

- Effective mean stress, p
- Deviatoric shear stress, q and

- Specific volume, υ.

  Under general stress conditions, the mean stress can be calculated in terms of principal stresses p, σ1, σ2 and σ3 as;

  $p = \frac{1}{3}(\sigma_1 + \sigma_2 + \sigma_3)$.....4.7

  Or for conventional triaxial tests as;

  $p = \frac{1}{3}(\sigma_1 + 2\sigma_3)$.....4.8

While; shear stress is defined as;

$q = \frac{1}{\sqrt{2}}\sqrt{(\sigma_1 - \sigma_2)^2 + (\sigma_2 - \sigma_3)^2 + (\sigma_3 - \sigma_1)^2}$ ……..4.9

Or for triaxial tests as;

$q = (\sigma_1 - \sigma_3)$.....4.10

The stress ratio η is defined as;

$\eta = q/p$ ……4.11

The model assumes that, when a soft soil sample is slowly compressed under isotropic stress conditions then $\sigma_1=\sigma_2=\sigma_3=p$. Also, perfectly drained hydrostatic compression moves along a trajectory in υ-ln p plane which consists of two straight lines (Figure 4.12.2). The equation for swelling line (SL) and virgin consolidation line (VCL) are given as:

$\nu + \kappa \ln p = \nu_s$ (Swelling line, SL) 4.12

$\nu + \lambda \ln p = \nu_1$ (Virgin consolidation line, VCL).....4.13

Where: υ = specific volume, κ = gradient of swelling lines, υ_s = volume for each swelling line (SL), λ= gradient of VCL, υ_1= virgin volume at unit pressure,

The behavior of the sample under increasingly triaxial shear is assumed to be elastic, until a 'yield value' of q is reached, called a stable state boundary surface (SSBS) which is given by

$$q^2 - M^2 p^2 \left(\frac{p_o}{p} - 1\right) = 0 \quad \text{.....4.14}$$

Where; M is a clay parameter, and p_o is the drained virgin pressure or pre-consolidation pressure (see Figure 4.12.3). For critical or failure state the following equation is used in the Modified Cam Clay Model:

$$p_f = \frac{1}{2^{\Lambda}} p_u = \left(\frac{1}{2} p_o\right)^{\Lambda} (p_c)^{1-\Lambda} \quad \text{.....4.15}$$

Where; p_f is the consolidation pressure at failure, p_u is the undrained pressure, p_o the preconsolidation pressure, and p_c the consolidation pressure at the start of the static test. Eekelen and Potts (1978), proposed an attraction factor 'a' and replaced p and p_u by (p+ a) and (p_u+ a), and gave the following equation for critical state as:

$$p_f + a = \left(1 - \frac{1}{2\Lambda}\right)^{\Lambda} (p_u + a) = \left(1 - \frac{1}{2\Lambda_o}\right)^{\Lambda} \left[(p_o)^{\Lambda} (p_c)^{1-\Lambda} + a\right] \quad \text{.....4.16}$$

This gives lower values of p and q at failure than Equation 4.15. Similarly, the relationship between the strain-hardening parameter (H) and the plastic shear strain (ε^{p1}) is modified for attraction factor 'a' is given as;

$$\varepsilon^{p1} \sqrt{3} = \xi \frac{H}{1 - S} \quad \text{.....4.17}$$

Where; ξ is constant and H for general static loading is given as;

$$H = \frac{M(p+a)}{(2+M/3)\cos\vartheta + (M/\sqrt{3})\sin\vartheta} \quad \text{.....4.18}$$

The angle ϑ is the Lode angle at failure, which is -30^o for triaxial compression, $+30^o$ for triaxial extension, and 0^o for simple shear. In the three dimensional principal stress space the surface H =1 is a hexagonal cone (see Figure 4.12.3), the locus of the points which satisfy the 'Mohr-Coulomb criterion. For maximum shear stress (τ_f) the relationship is given as:

$$\frac{\tau_f}{s+a} = \frac{M}{(2+M/3)} \equiv \sin\phi \quad \text{.....4.19}$$

Where; $\tau_f = ½ (\sigma_1 - \sigma_3)$ is the maximum shear stress, and $s = ½(\sigma_{1+}\sigma_3)$ is the mean of the largest and the smallest principal stress. The hexagonal cone H=1 is called the Mohr-Coulomb or MC cone. Cone and cap intersect along the hexagon with $p=p_f$ given by Equation 4.16, for a particular value of specific volume (υ). For static strength (C_f) the model gives the following equation:

$$C_f = (b + p_u) = b(p_0^{\wedge} + p_c^{1-\wedge} + a) \quad \text{.....4.20}$$

Where;

$$b = \left[1 - \frac{1}{2\Lambda}\right]^{\Lambda} \frac{M}{(2+M/3)\cos\vartheta + (M/\sqrt{3})\sin\vartheta} \quad \text{.....4.21}$$

The parameter r = u as defined above can be incorporated at this stage as;

$$p_c = p_c - r = p_c - u \quad \text{.....4.22}$$

Then the cyclic strength (C_{fc}) after a given number of cycles is given by;

$$C_{fc} = b\left[p_u\left(1 - \frac{u}{p_c}\right)^{\left(\frac{\kappa}{\lambda}\right)} + a\right] \quad \text{.....4.23}$$

Where; $\kappa/\lambda = 1 - \Lambda$

To check the validity of the approach, undrained triaxial test C20, sample Id 13252_ZNA has been used. Figure 4.12.4 shows the difference between the F.O.S (C_u/C_a) obtained by this approach and the one adopted by Hanna and Javed, 2008. In the Figure ultimate shear strength is termed as C_u and allowable shear strength is termed as C_a. The Modified Cam Clay Model used here predicts cycle by cycle change in strength ratio; therefore the analysis is limited to one selected test only has different value for each load cycle and should be calculated accordingly. A possible guess would be to assume that the Λ is somehow changes with the accumulation in cyclic strain ($\in_c$). A similar parameter used by (Pande and Zienkiewicz, 1982) to describe the nesting surfaces of cyclic loading as a function of accumulated deviatoric plastic strain is given as;

$$\Lambda = \left[\frac{\Lambda_o + \Lambda_u \chi \in_c}{1 + \chi \in_c}\right] \ldots\ldots\ldots\ldots\ldots\ldots\ldots\ldots\ldots\ldots\ldots\ldots\ldots\ldots\ldots\ldots 4.24$$

Where; Λ_o is the initial value of Λ at $\in_c = 0$, χ is a constant parameter and Λ_u is a constant based on the stress history. For $\in_c = \infty$, $\Lambda = \Lambda_u$. Therefore, Equation 4.23 can be further modified to accommodate the variation in Λ as;

$$C_{fc} = b\left[p_u\left(1 - \frac{u}{p_c}\right)^{1-\left(\frac{\Lambda_o + \Lambda_u \chi \epsilon_c}{1+\chi\epsilon_c}\right)} + a\right] \ldots\ldots\ldots\ldots\ldots\ldots\ldots\ldots\ldots 4.25$$

The test results C20 are plotted for this variation in Λ. Figure4.12.5 gives the cycle by cycle variation in Λ. Although, there is not much difference in for constant Λ and variable Λ, but it is recommended to use the shear strength ratios based on the variable Λ especially when dealing with sensitive clays. For detail calculation and analysis please see attached Appendix-I.

Now suppose that a clay specimen subjected to a typical behavior of consolidating and swelling in p-q plane as shown in Figure 4.12.6. The sample is isotropically normally

consolidated to a mean effective stress of p' = $p'_c = \alpha_o$ and is subsequently allowed to swell elastically by reducing the mean effective pressure to a value p' = α_1. Then according to the definition of OCR;

$$OCR = \frac{\alpha_o}{\alpha_1} \quad \ldots\ldots 4.26$$

But for elastic loading in Figure 4.12.6, $p'_y < p'_c$, then;

$$\frac{dp'_c}{p'_c} = r_\theta \frac{dp'_y}{p'_y} \quad \ldots\ldots 4.27$$

Where $dp'_y < 0$ and for $dp'_y \geq 0$

$$\frac{dp'_c}{p'_c} = 0 \quad \ldots\ldots 4.28$$

The parameter r_θ mentioned as ϑ (since ϑ is already used in the above equations as lodge angle so different name is used here) can be determined by knowing the number of cycles and corresponding deviator stress ratio using the method given by Carter et al. (1982). For swelling Equation 4.27 predicts that the value of p'_c is reduced to;

$$p'_c = \alpha_o \left(\frac{\alpha_1}{\alpha_0}\right)^{r_\theta} \quad \ldots\ldots 4.29$$

The loading part of the next load cycle reconsolidates the sample, now if this loading is continued indefinitely, the material will deform plastically and thereafter p'_c will be equal to p'. Hence, each cyclic load contributes in the reduction of OCR as; (a fact already has been proved on preceding sections slowly the OCC starts behaving like NCC under continuous application of load cycles, N)

$$OCR = \left(\frac{\alpha_o}{\alpha_1}\right)^{1-r_\theta} \quad \ldots\ldots 4.30$$

It means that the increase in value of r_θ will decrease the number of cycles to failure. In every cycle, there is yielding and associated permanent strains. For an undrained triaxial test at constant volume, there is always an increase in elastic volume, which means decrease in mean effective stress, i.e. increase in pore water pressure. As the loading continues the sample reach either to liquefaction or attain quasi elastic resilient state. The effect of this behavior will be more obvious in the cyclic loading test on samples of Group-I (see Tables 5 and 6).

Incorporating affect of OCR in the cyclic shear strength, Equation 4.25 can be written as;

$$C_{fc} = b\left[p_u\left(1 - \frac{u}{\propto_o \left(\frac{\propto_1}{\propto_0}\right)^{r_\theta}}\right)^{1-\left(\frac{\Lambda_o + \Lambda_u \chi \epsilon_c}{1+\chi\epsilon_c}\right)} + a\right] \ldots\ldots\ldots\ldots\ldots\ldots\ldots\ldots\ldots\ldots 4.31$$

The experimental work for the present research is designed in such a way that the undrained shear strength C_{ur} is measured immediately after the $N = N_{st}$ cycle as mentioned above. For analysis both cyclic deviator stress (q_{cyc}) and C_{ur} will then normalized by the original shear strength (C_{uo}) of the sample.

4.12.3 Effect of frequency

The effect of frequency is clearly indicated in section that, the cyclic shear strength reduces quickly at slower rate of loading. Although, the fact is true but by having a close look at Figures 4.6.1 and 4.6.2, it can be seen that the effect of frequency is reducing with the passage of time or with the increase in number of cycles. This fact is also defended by Procter and Khaffaf (1984). Sangrey et al. (1978) also mentioned that the measured pore pressures at higher frequencies may

not reflect the actual values, especially during the initial cycles, since sufficient time is not allowed for equalization. As the number of cycles increases, the rate of pore water pressure buildup decreases significantly, and it believed that at this stage the pore pressures measured are sufficiently equalized. Similarly, Matsui et al (1980) and Ogawa et al (1977) indicated that the pore water pressures monitored after cyclic loading do not show a significant increase in cyclic tests conducted at similar frequencies. Yasuhara et al (1982) also reported that there is no significant effect of frequency on cyclic undrained strength. Yoshimine et al. (1999) performed cyclic ring shear tests on 16 different soils. They reported that, cyclic strengths 20% to 100% larger than the slow residual strengths, for tests conducted at cyclic load frequencies of 0.5 Hz, 1.0 Hz, and with actual earthquake time histories. Thammathiwat and Chim-oye, (2004): reported that the effect of loading frequency on the cyclic strength, by the number of loading cycles causing 5% double amplitude strain of cyclic strength increased with increase in loading frequency for a given stress ratio. A general trend is that the slow loading tests require longer time to cause failure than the rapid loading test.

Based on this above mentioned scenario the current study has avoided to propose or formulate any parameter showing frequency affect in the cyclic shear strength equation of modified cam clay model. According to author's view it is more practical to find out the worst frequency of loading situation / pattern in a given period of time (once in a 10 years, or 30, or 50 or 100 years) depending on the importance of the project

4.12.4 Modeling the Role of Physical Parameters

From the category of physical parameters, natural water content and liquidity index are considered as dominant parameters as far as the shear strength of sensitive clay is concerned. The analysis of experimental data made it is clear that preconsolidation pressure plays an

important role in establishing the link between mechanical and physical parameters' categories (see Figure 4.8.5). Figure 4.12.7 (US Navy corps handbook NAVFAC DM-7.1) gives the relationship between preconsolidation stress and liquidity index as a function of clay sensitivity number (S_t). On the other hand presence of water content has a direct effect on the shear strength of the clay with respect to matric suction. As mentioned before, specifying any one or two parameters is not enough in dealing with sensitive clay. The in literature the studies based on the undisturbed partially saturated samples of the sensitive clay generally ignore the matric suction part of the shear strength. While, the studies on the reconstituted samples of sensitive clay with water content 1~1.5 times of liquid limit usually ignore the effect on intrinsic aspects of the clay. An effort has been done in the present study to incorporate the effects of these issues in modeling the behavior of sensitive clay.

4.12.5 Effect of Degree of Saturation

In general, to determine the shear strength of an unsaturated soil, soil-water characteristic curve (Figure 4.12.8) is used either directly or indirectly along with the saturated shear strength parameters, c' and ϕ', to predict the shear strength function for an unsaturated soil (Vanapalli et al. 1996, Fredlund et al. (1996), Oberg and Sallfors (1997), Khallili and Khabbaz (1998) and Bao et al. (1998)). The soil- water characteristic curve defines the relationship between the soil suction and either the degree of saturation, *S*, or gravimetric water content, *w*, or the volumetric water content, θ. The study done by Miller (2000) shows that the normalized shear strength is sensitive to drainage conditions and degree of saturation. The experimental results of Miller's study suggest that the cyclic shear strength may decrease by approximately 80% as the initial degree of saturation is increased from 90% to 100%.

Therefore, the soil-water characteristic curve provides a conceptual and interpretative tool by which the behavior of unsaturated soils can be understood. As the soil moves from a saturated state to drier conditions, the distribution of the soil, water, and air phases change as the stress state changes. The typical soil- water characteristic curve, with various zones of desaturations is shown in Figure 4.12.8.

A number of equations proposed for determining shear strength of unsaturated soils. Equation used by Vanapalli et al. (1996) gives reasonable results as suggested by Vanapalli et al. (1996) and Fredlund et al. (1996). The equation is given below:

$$\mathrm{C} = \mathrm{c}' + (\sigma_n - u_a)\tan\varphi' + (u_a - u_w)\left[\left(\frac{\theta_w - \theta_r}{\theta_s - \theta_r}\right)\tan\varphi'\right] \ldots\ldots\ldots\ldots\ldots\ldots\ldots 4.32$$

Where;

C = shear strength of unsaturated soil,

c' = effective cohesion,

ϕ' = angle of frictional resistance,

σ_n = normal stress,

u_a = pore-air pressure,

u_w = pore-water pressure,

$(\sigma_n - u_a)$ = net normal stress,

$(u_a - u_w)$ = matric suction,

θ_w = volumetric water content,

θ_s = saturated volumetric water content, and

θ_r = residual volumetric water content.

But based on Equation 4.31 and 4.32, the cyclic strength including matric suction (C_{mc}) can be written as;

$$C_{mc} = b\left[p_u\left(1 - \frac{u^+}{\propto_o\left(\frac{\propto_1}{\propto_0}\right)^{r_\theta}}\right)^{1-\left(\frac{\Lambda_o+\Lambda_u\chi\epsilon_c}{1+\chi\epsilon_c}\right)} + a\right] + (u_a - u_w) \ldots\ldots\ldots\ldots\ldots\ldots\ldots\ldots 4.33$$

The effect of water content equal to liquid limit or more brings the intrinsic aspect of sensitive clay, which is just opposite to the matric suction. Liu and Carter (2002) gave the relationship for the isotropic virgin compression line for the reconstituted soil, i.e., ICL*, (see Figure 4.1.9) as;

$$e^* = e^*_{IC} - \lambda^* lnp' \ldots\ldots\ldots\ldots\ldots\ldots\ldots\ldots\ldots\ldots\ldots\ldots\ldots\ldots\ldots\ldots\ldots\ldots\ldots\ldots 4.34$$

Where; e* is the void ratio for the reconstituted clay sample. All the rest of the parameters (M*, λ*,κ*, ν*& Λ*) are same as defined above except with the difference that they are denoted with the sign of asterisk (*). Therefore, based on Equation 4.31, the intrinsic cyclic strength (C_{fc}*) can be written as;

$$C^*_{fc} = b^*\left[p_u\left(1 - \frac{u^+}{\propto_o\left(\frac{\propto_1}{\propto_0}\right)^{r^*_\theta}}\right)^{1-\left(\frac{\Lambda^*_o+\Lambda^*_u\chi^*\epsilon^*_c}{1+\chi^*}\right)} + a^*\right] \ldots\ldots\ldots\ldots\ldots\ldots\ldots\ldots 4.35$$

The use of Modified Cam Caly Model is very helpful in estimating the design shear strength under varying conditions of physical and mechanical parameters. Hence, the ,lowest or the most critical value of shear strength can be selected and used to determine the factor of safety based on the importance and type of project in sensitive clay regions

4.13 Safe Zone

As already mentioned, that one of the main objectives of the current research is to establish a safe zone which has combined effect of both physical and mechanical parameters. The graphical analysis shown in Figures 4.9.1 to 4.9.8 helped in establishing an average line of demarcation

between the failed samples and those which attain a stable position or quasi elastic resilient state based on one of the major governing physical parameters i.e., the degree of saturation. The degree of saturation represents the effect of other physical parameters like water content and liquidity index. The mathematical equation for the line of demarcation between stable and failure zones established in case degree of saturation (figures 4.9.1 to 4.9.8) gives following empirical relationship as;

$$\frac{q_{cyc}}{q_s} = -a_1\, S + b_1 \ldots\ldots\ldots\ldots\ldots\ldots\ldots\ldots\ldots\ldots\ldots\ldots\ldots\ldots\ldots\ldots\ldots\ldots 4.36$$

Where, a_1 and b_1 are constants. This expression is in good agreement with the study of Miller et al. (2000) which is only based on single type of clay and 12 test samples. The relationship given in equation 4.36 clearly indicates that there is a strong relationship between cyclic shear strength and initial degree of saturation.

The graphical analysis shown in Figures 4.10.5 to 4.10.14 helped in establishing an average line of demarcation between the failed samples and those which attain a stable position or quasi elastic resilient state. The key parameter in this case is the number of loading cycles, N (see section 4.11). The best fit curve which, establish the line of demarcation between stable and failure zones can be expressed in general form as;

$$\frac{q_{cyc}}{q_s} = -a_2\, lnN + b_2 \ldots\ldots\ldots\ldots\ldots\ldots\ldots\ldots\ldots\ldots\ldots\ldots\ldots\ldots\ldots\ldots 4.37$$

Where, a_2 and b_2 are constants.

Based on equations 4.36 & 4.37 a design safe zone can be established by selecting the lowest values of cyclic stress ratio, hence, the resultant curve will reflect the combined effect of both physical and mechanical parameters. In other words, by taking degree of saturation, S as a representative of the physical parameters and number of cyclic loading, N for the mechanical

parameters a combined effect safe zone can be defined. Figures 4.13.1 shows the combined effect safe zone for the experimental data of the cyclic triaxial tests. Since, the combined effect safe zone includes the data for the Group I. II and III, therefore, most of the Group-I tests are lying outside the range of the safe zone.

It is interesting to mention the use of Modified Cam Clay Model mentioned in section 4.12.2 at this point. By comparing curves of Figure 4.12.4 and 4.13.1, it is clear that the zones under those curves are the safe zones. Although, the curve in Figure 4.12.4 based only on a single Test, C20 but, it is safe to use it in the projects of extreme importance. Hence, by using of the equations 4.23, 4.25, 4.31, 4.33 and 4.35 the minimum or the most critical value of the shear strength can be selected to design the combined effect safe zone. Finally, based on the analysis of experimental data, proposed hypothetical model, use of Modified Cam Clay Model and the combined effect safe zone a summarized form of guide line is proposed in Figure 4.13.2 to design new or examine existing foundation in sensitive clay regions.

4.14 Discussion

This study is based on a sophisticated experimental investigation and detailed analysis of the experimental data. The static and cyclic triaxial compression tests conducted on the clays with varying sensitivity number, along with step by step analysis of the governing physical and mechanical parameters, assisted in exploring the complexity involved in prioritizing the role of governing parameters on the behavior of sensitive clays subjected to static or cyclic loading.

The two main categories; physical and mechanical are considered to be the controlling parameters for the behavior of the sensitive clay under different loading conditions. Physical category includes parameters like; natural water content (w), liquid limit (LL), plastic limit (PL), plasticity index (I_P), liquidity index (I_L), sensitivity (S_t), constant of variation in sensitivity (k)

and initial degree of saturation (S). Whereas, mechanical category includes parameters like; cyclic deviator stress (q_{cyc}), pore water pressure (u), axial strain (ε), over consolidation ratio (OCR), preconsolidation pressure (σ_p), confining pressure (σ_3), and number of cycles (N).

Test analysis of the test results indicate the importance of conducting tests on both undisturbed and remolded samples, the samples of Group-I (undisturbed) are considered stronger than those of Group II and III (remolded samples). This holds true as far as static strength is concerned, but the results for cyclic triaxial tests have given another view also, i.e., in case of undisturbed sample, the rigidity of the clay skeleton restrained the buildup of large pore pressure generation in the beginning of the test, then, as time passed by the cyclic load disturbed the clay skeleton that is why some undisturbed samples did not show big difference in cyclic shear strength ratio as compared to their remolded or reconstituted samples. The analysis of the data also shows that the initial strength of undisturbed samples cannot be considered as a reliable factor. Hence, for design purposes, it is better to rely on the remolded shear strength. The comparison of shear between remolded samples of Group-II with those reconstituted sample of Group-III helped in predicting shear strength of sensitive when subjected to excessive groundwater fluctuations.

The analysis indicates the undrained triaxial test is more critical than the drained. As the shear stress is directly proportional to an increase in pore water pressure during cyclic loading which in turn is directly proportional to the number of cyclic loadings. Since, the undrained cyclic loading of sensitive clay is more likely to cause effective stress failures due to a continued increase in excessive pore water pressure as compared to drained conditions.

The results support the concept of threshold or critical cyclic shear stress ratio below which no excess pore pressure will develop. When the cyclic stress ratio is higher than the critical stress ratio, the variations of pore pressure and axial strain are different from those when the cyclic stress ratio is lower than the critical stress ratio. The increase in normalized pore water pressure ratio, under high confining stresses, initiate a higher normalized pore water pressure ratios. Also, the axial strain and pore water pressure both increase with increasing number of cyclic loading. Hence, causes stress path to move towards failure envelope. For a given condition, the threshold cyclic shear strength is different for the clays bearing different sensitivity number. A sample of sensitive clay subjected to cyclic loading attains and will keep on retaining equilibrium or quasi elastic resilient state as long as the magnitude of cyclic deviator stress is below a certain threshold level for a given degree of saturation and stress conditions

The analysis of the test data also make it clear that the decrease in the rate of loading leads to an increase in accumulated pore pressures with respect to the number of cycles. Also, the effect of frequency is more dominant during the initial cycles, which, diminishes progressively as the number of cycles, N increases.

The results show that the static and cyclic shear strength is highest for the Group-I (undisturbed samples) amongst the three groups I (Undisturbed samples), II (sample reconstituted or remolded at same moisture content as their undisturbed parent samples Group-I) & III (samples reconstituted at a moisture content equal to or greater than liquid limit). The static and cyclic shear strength is least for the samples reconstituted at a moisture content equal to or greater than liquid limit. In other words, the samples belonging to Group-III bearing intrinsic parameters are the weakest samples among the Group I, II & III. Also, the physical and index property test results for the sensitive clays show that the sensitivity varies with the change in the

natural water content and the depth from where these samples were taken. In other words, sensitivity varies with the liquidity index and pre-consolidation pressure in these sensitive clays. Also, the variation in sensitivity constant, k = 2 to 3 holds good for liquid limit versus sensitivity (S_t) graphical analysis for the selected ranges of preconsolidation pressure.

The study shows that the rate of pore pressure build up within normally consolidated sample is higher than that within over-consolidated sample of the same clay type. The test results indicate that the higher the over-consolidation ratio (OCR) is, the more number of loading cycles are needed to initiate initial liquefaction for a particular cyclic stress ratio and that the cyclic shear strength increases with the increase in OCR. Also, the pre-consolidation pressure σ_p in terms of OCR is identified as an important factor in controlling the behavior of sensitive clays especially under cyclic loading. The results of the standard consolidation test for clay samples indicate that most of the samples belonging to depths greater than 4 m behaved like normally consolidated clays (NCC). While, the samples belonging to shallow depths i.e., less than 3.5 m showed over consolidation clay's behavior.

The analysis for establishing line of demarcation between failed and survived samples based on the degree of saturation clearly indicate that the undrained test results give a lower limit for the shear strength for the clay samples having degree of saturation greater than 98% or fully saturated i.e., 100%. The test results give an idea that an undrained fully saturated test represents the critical situation for sensitive clay subjected to cyclic loading due to complete absence of matric suction. Moreover, the scenario becomes worst in case of a sample reconstituted at moisture content equal to or greater than the liquid limit. In other words samples bearing intrinsic shear strength (C_u*) under the undrained conditions represents the most critical situation. This

represents the field conditions where excessive rainfall along with cyclic load applications cause rapid degradation of the foundation soil resulting into liquefaction and catastrophic failure.

The analysis identify the degree of saturation as a parameter which reflects the combined effect of other physical parameters like; water content (w), liquid limit (LL), plastic limit (PL), plasticity index (I_P), liquidity index (I_L) and constant of variation in sensitivity (k). The fact, that the samples tested under same total stress conditions but with higher initial degree of saturation results into failure, while the sample with comparatively lower values of initial degree of saturation survived and attained quasi elastic resilient state gives rise to the relationship among matric suction, initial degree of saturation cyclic shear strength and intrinsic cyclic shear strength

The analysis of data of group IV and V samples assisted in identifying the number of cycles needed to reduce the static shear strength of an undisturbed clay sample to its remolded strength. The analysis show that the sensitivity number for an undisturbed sensitive clay sample does not apply to it unless and otherwise it is disturbed to an extent where its undranied (undisturbed) shear strength reduces to a value equal to the undrained (disturbed) remolded shear strength (c_{ur}). This analysis assisted in proposing a hypothetical model, which is useful in depicting the shear strength of sensitive clay foundations subjected to cyclic loading. The higher the sensitivity number faster the clay loses its shear strength under cyclic loading, through this hypothetical model a new parameter termed as degree of remolding, r is defined.

Based on the theory of the hypothetical model a successful attempt has been made to adapt the Modified Cam Clay Model for analyzing the behavior of the sensitive clay subjected to cyclic loading. The adapted Modified Cam Clay Model can be used to determine the step by step reduction in the cyclic shear strength subjected to a given set of governing parameters. The model is useful in predicting the minimum or the most critical value of shear strength based on

the importance of the project. Moreover, by using the ratio of ultimate shear strength to allowable shear strength a reliable factor of safety can be selected for designing foundations on sensitive clays.

The relationship given in equation 4.36 clearly indicates that there is a strong relationship between cyclic shear strength and initial degree of saturation. The degree of saturation also identified as parameter, which can translate the effects of parameters belonging to the physical category. On the other equation 4.37 clearly indicates that there is a strong relationship between cyclic shear strength and number of cyclic load, N. The combination of "N" number of cycles (X –axis) and cyclic deviator stress or deviator stress ratio (Y-axis) can easily translate the effect of parameters belonging to the mechanical category. The analysis has shown that the combined effect of both the categories physical and mechanical has a better definition of safe zone than the one given by Hanna & Javed, 2008. The new safe zone is named as combined effect safe zone is considered to be safer and more reliable in designing cyclic shear stress ratios for the foundation design in regions of sensitive clays.

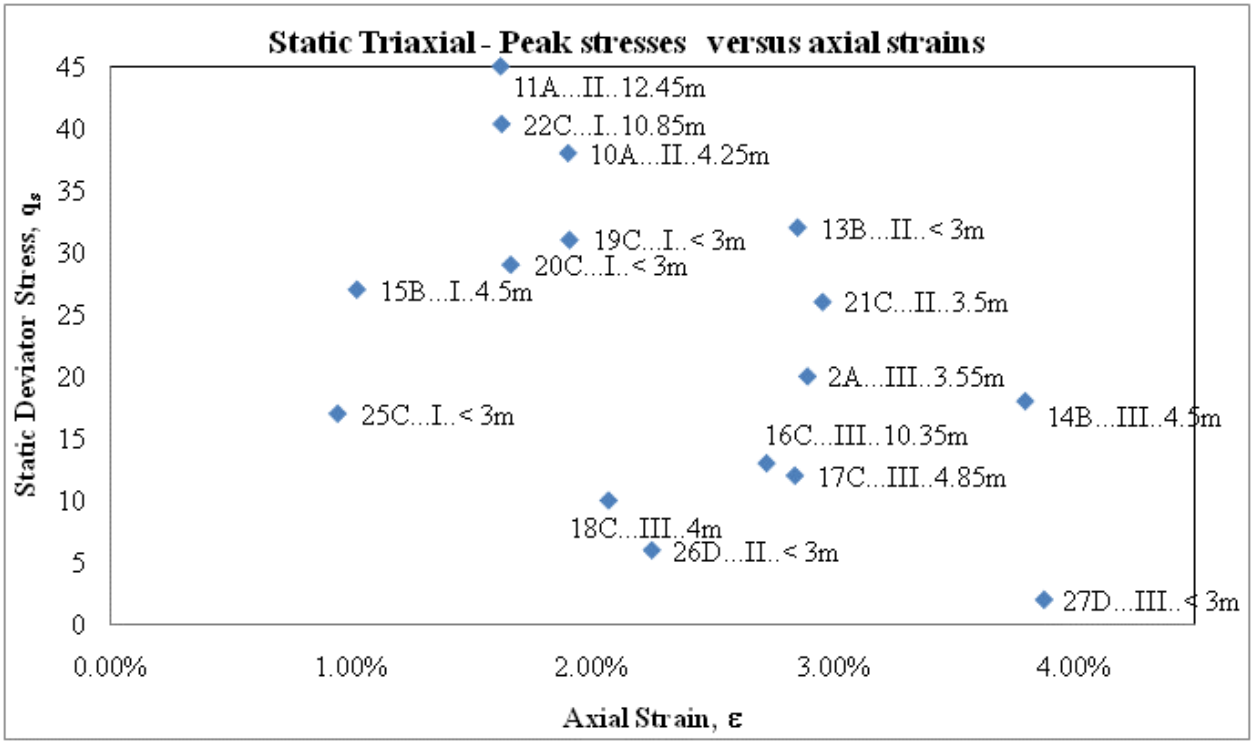

Figure 4.1.1: Static Triaxial Test X-Y scattered chart peak stresses versus strains

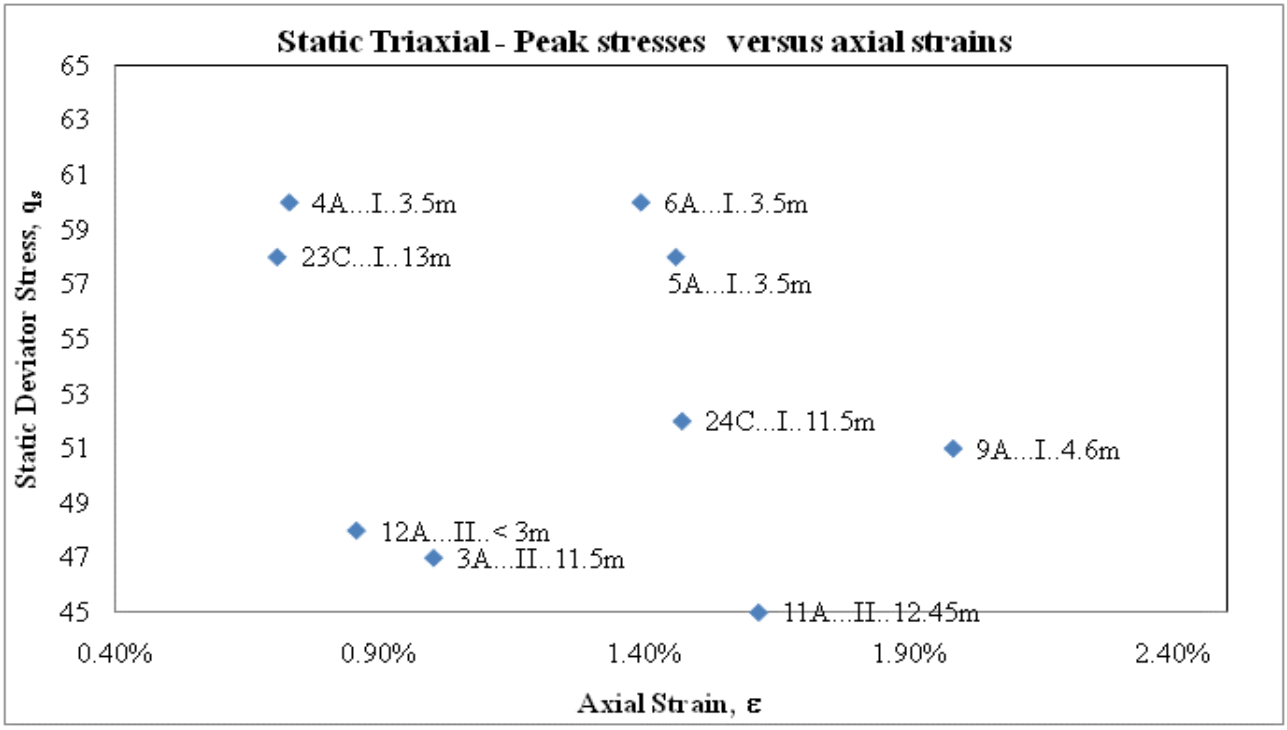

Figure 4.1.2: Static triaxial test X-Y scattered chart peak stresses versus strains

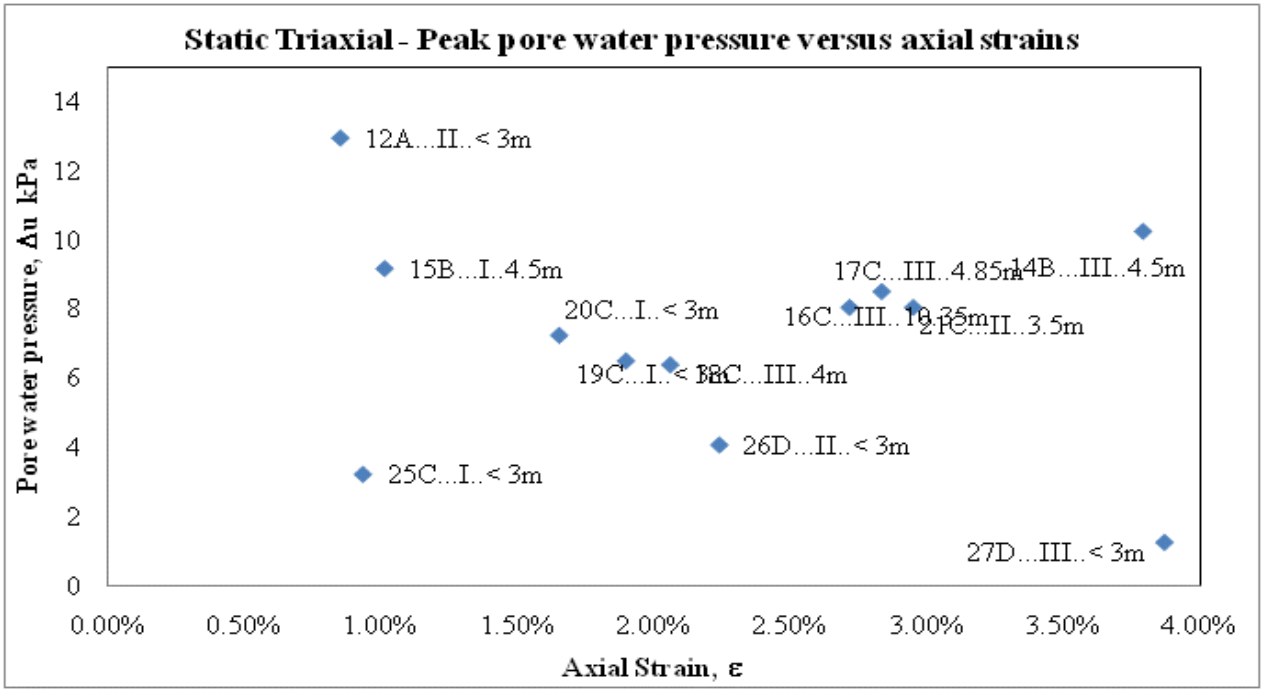

Figure 4.1.3:**Static triaxial test X-Y scattered chart peak pore water pressure versus strains**

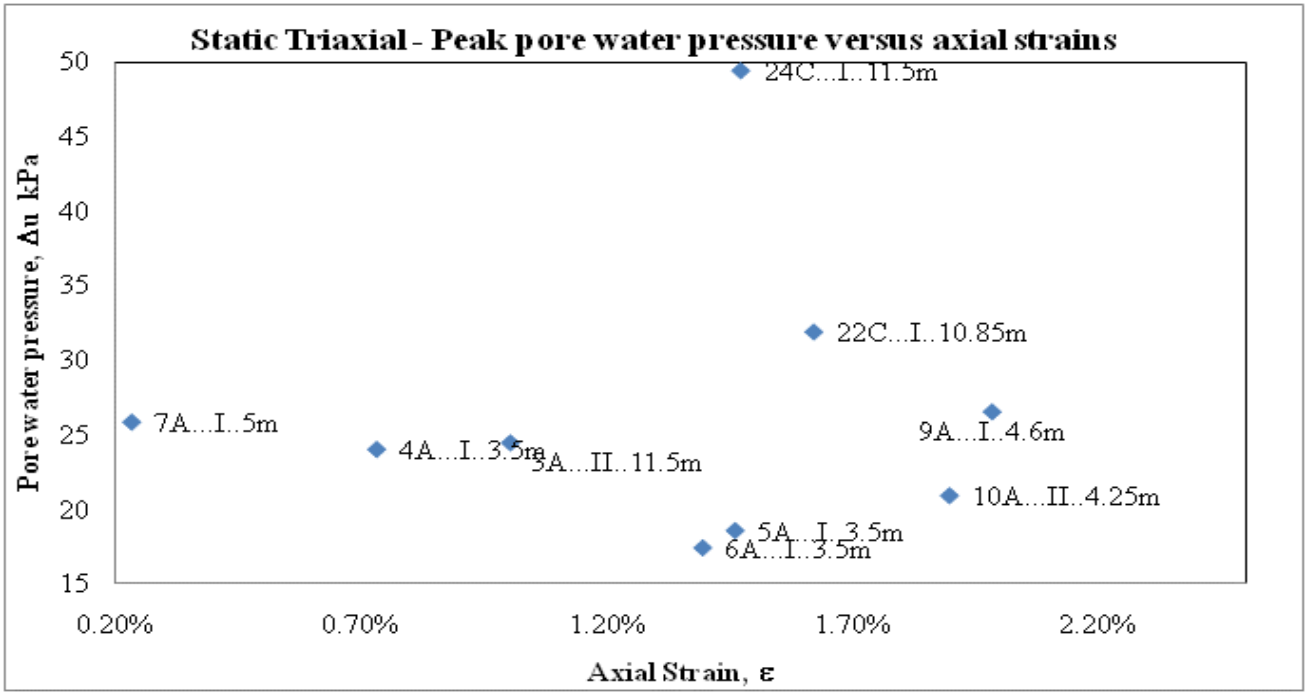

Figure 4.1.4 Static triaxial test X-Y scattered chart peak pore water pressure versus strains

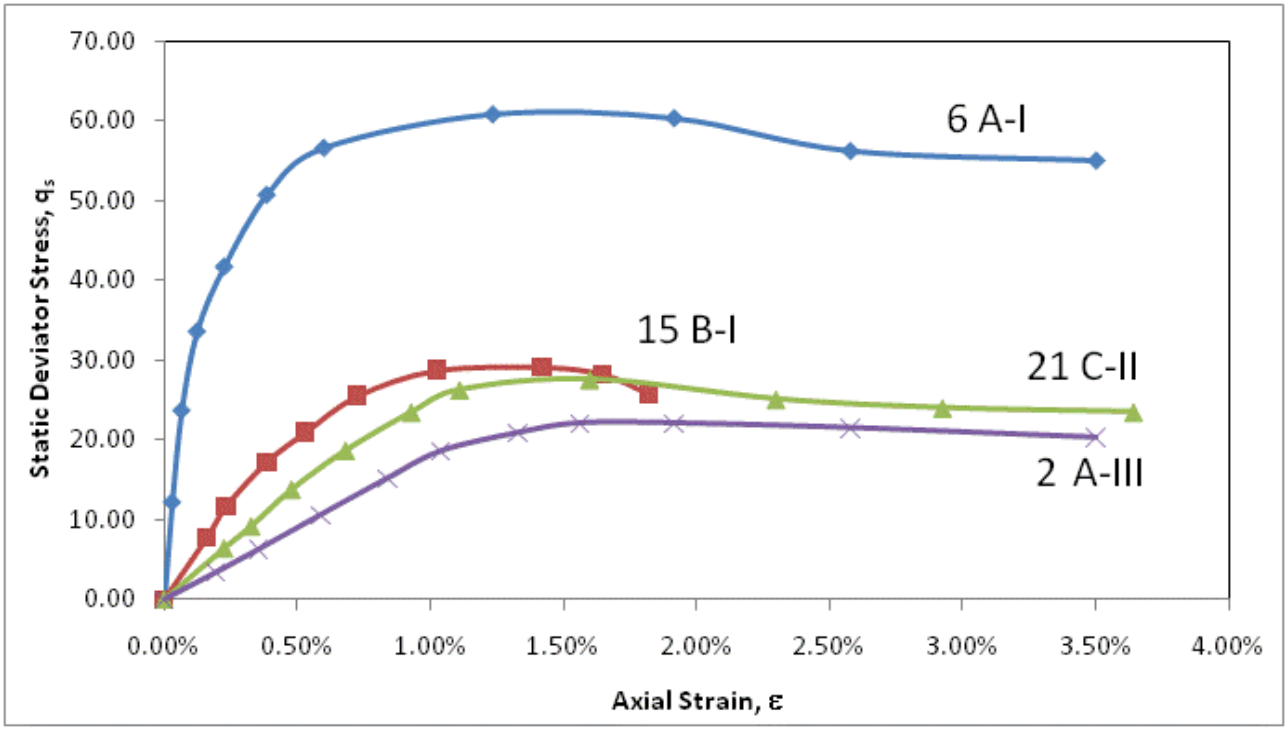

Figure 4.1.5 Static triaxial test typical stress-strain curves

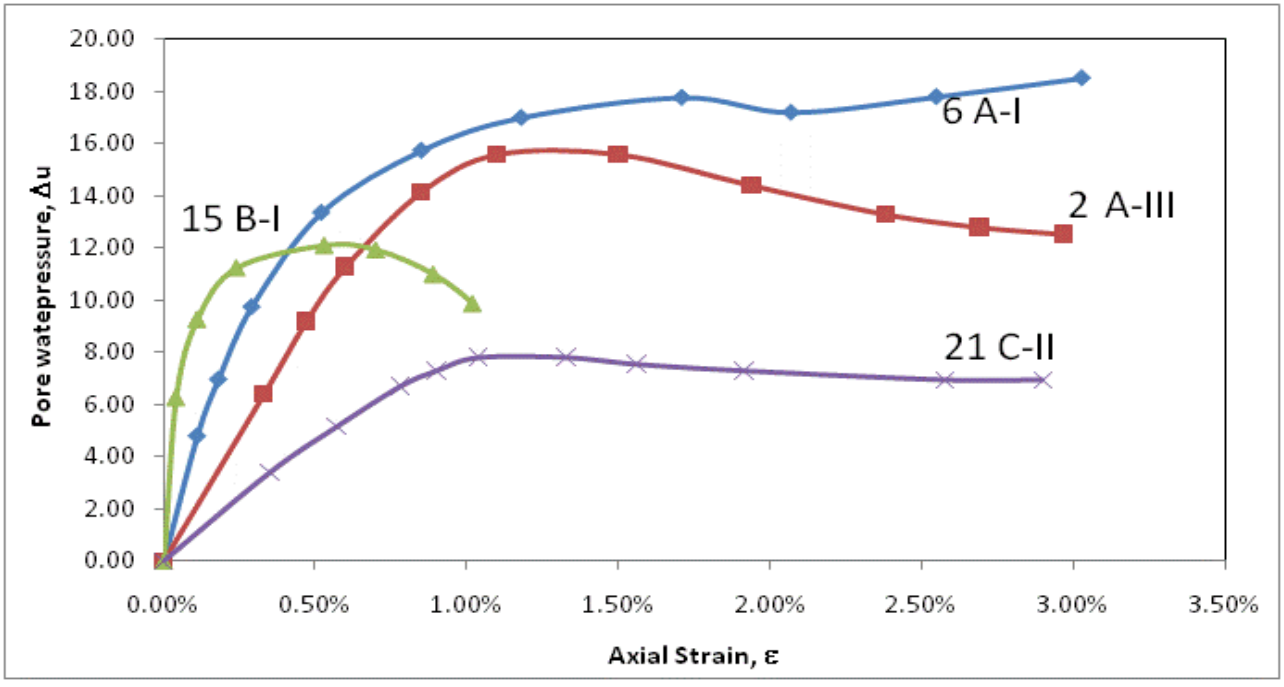

Figure 4.1.6 Static triaxial test typical stress-strain curves

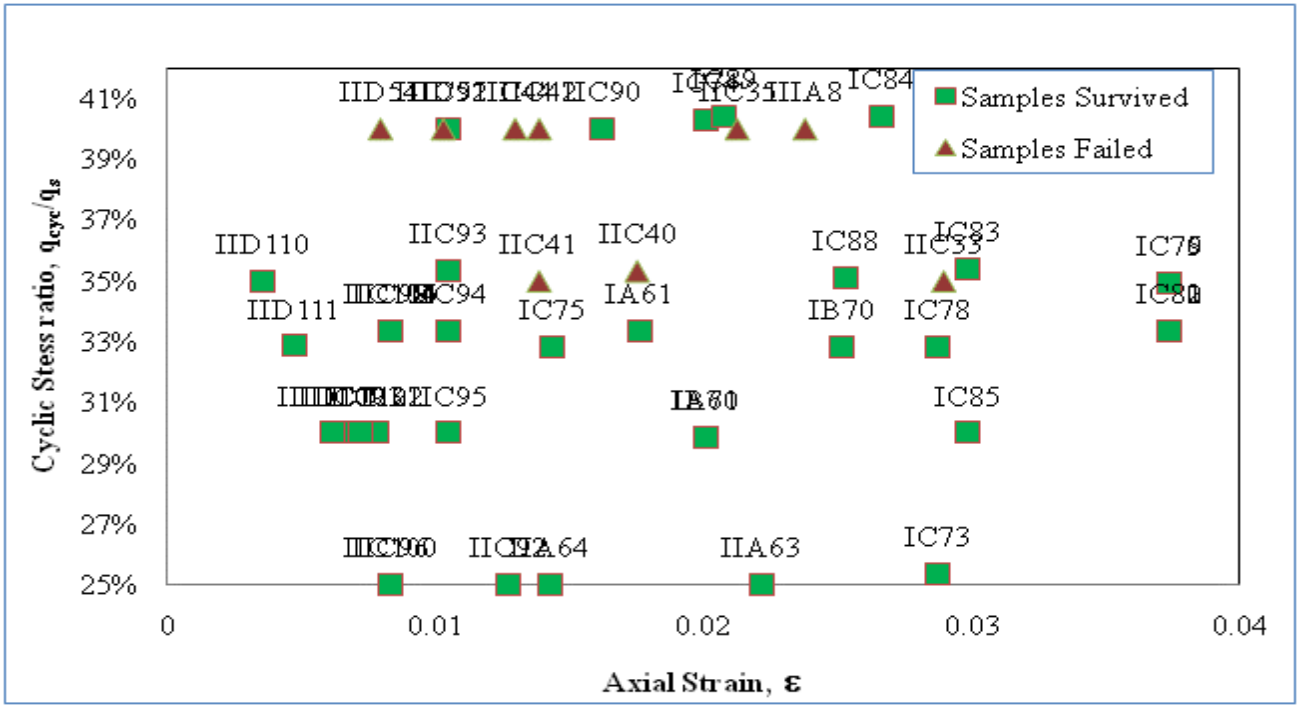

Figure 4.2.1 Cyclic triaxial tests X-Y scattered chart cyclic stress ratio versus axial strains

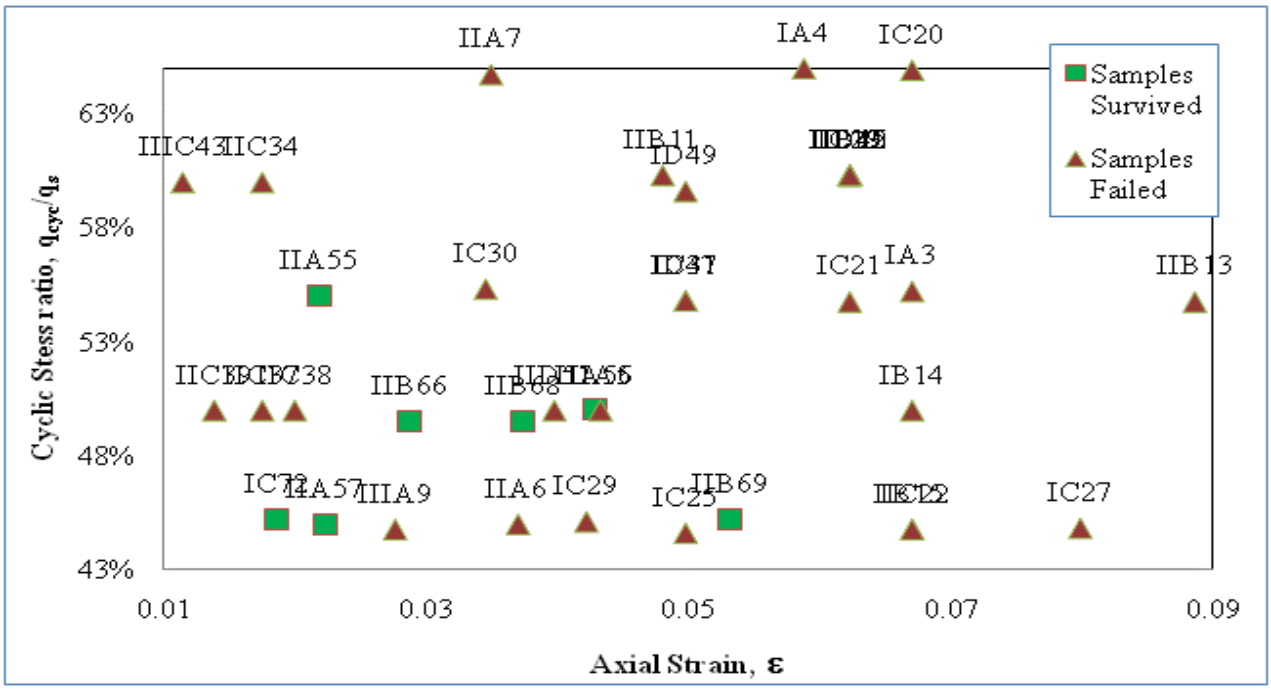

Figure 4.2.2 Cyclic triaxial tests X-Y scattered chart cyclic stress ratio versus axial strains

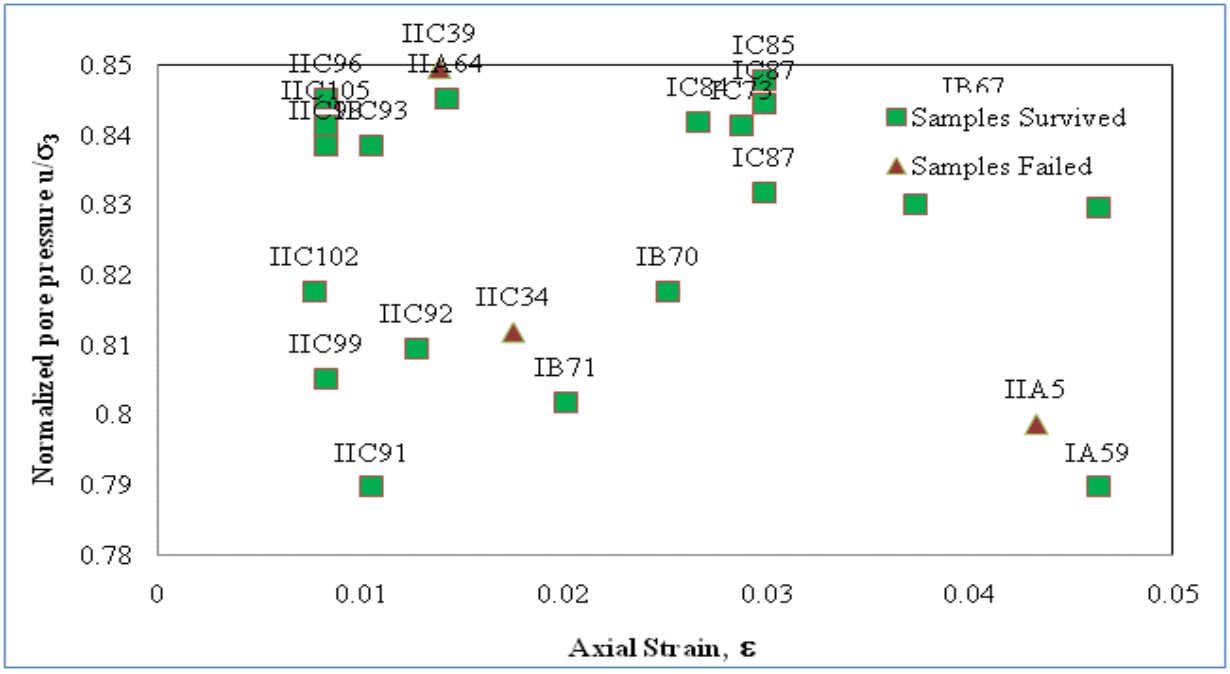

Figure 4.2.3 Cyclic triaxial tests X-Y scattered chart normalized pore water pressure versus axial strains

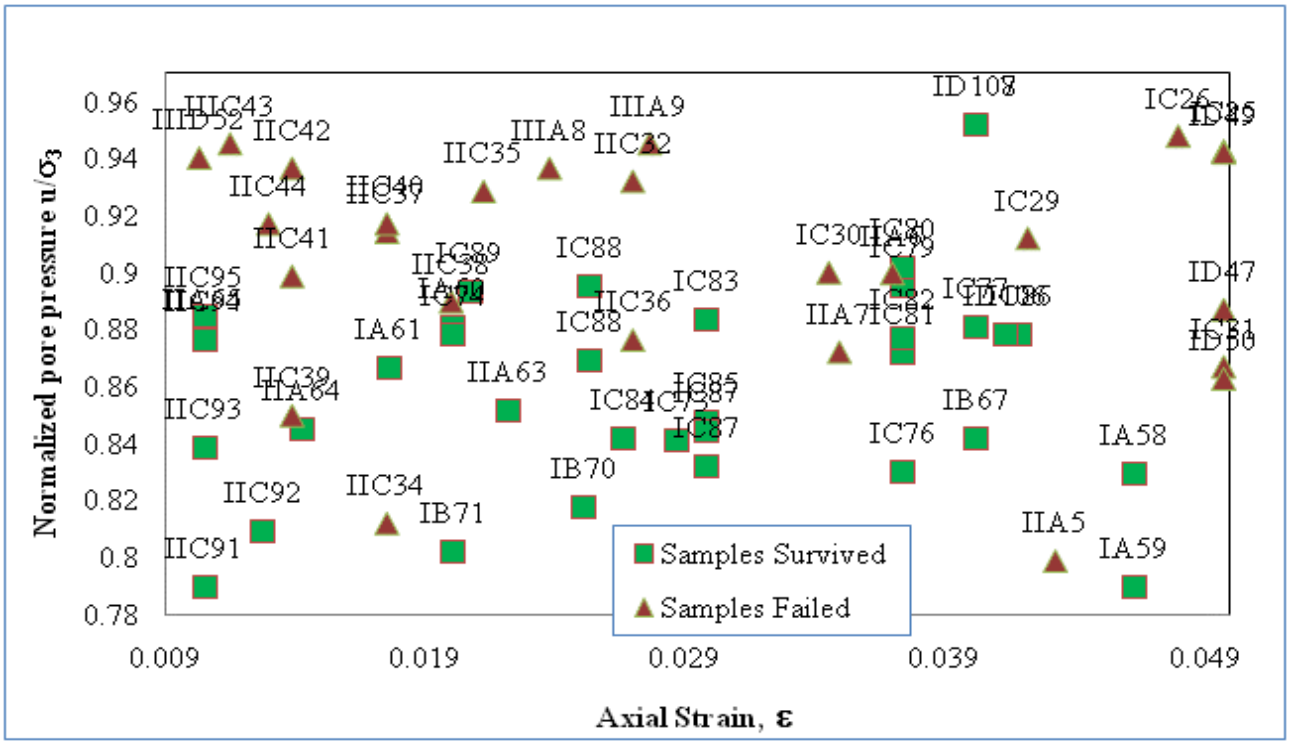

Figure 4.2.4 Cyclic triaxial tests X-Y scattered chart normalized pore water pressure versus axial strains

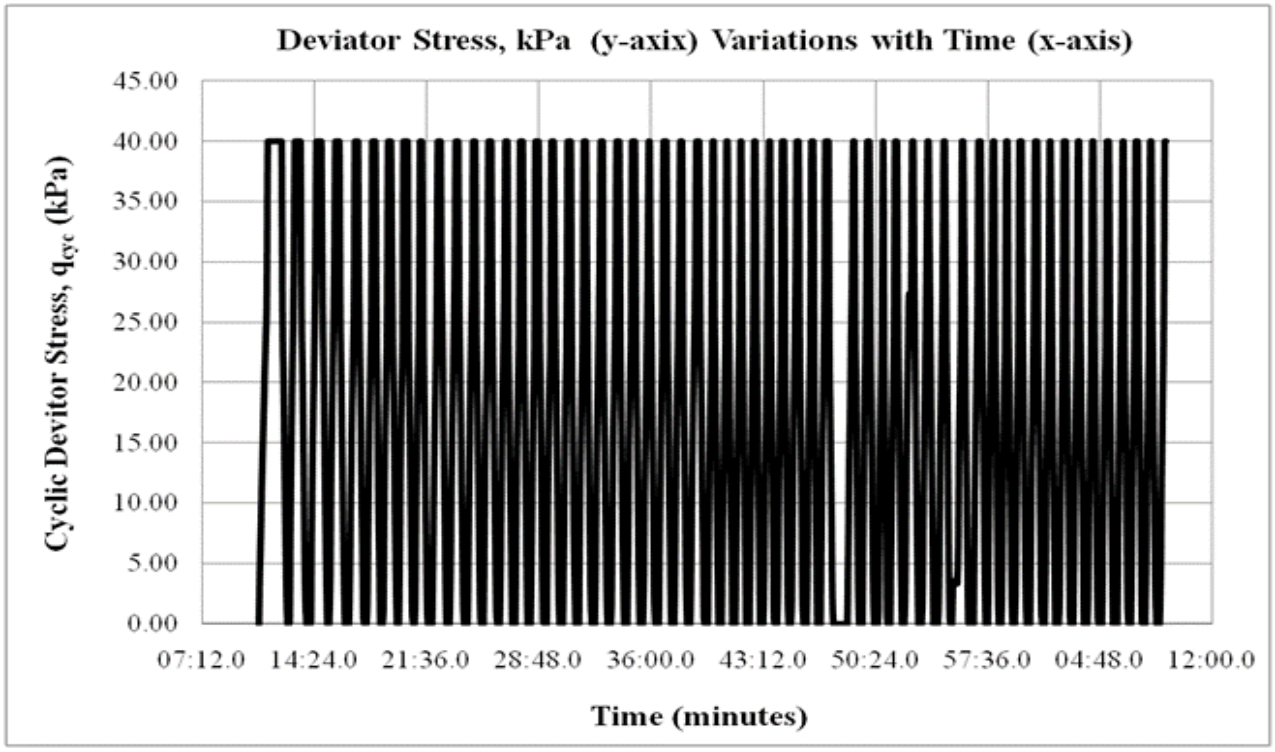

Figure 4.2.5 Cyclic deviator stress versus time (Test ID – A 57, sample ID S-13252_ZF)

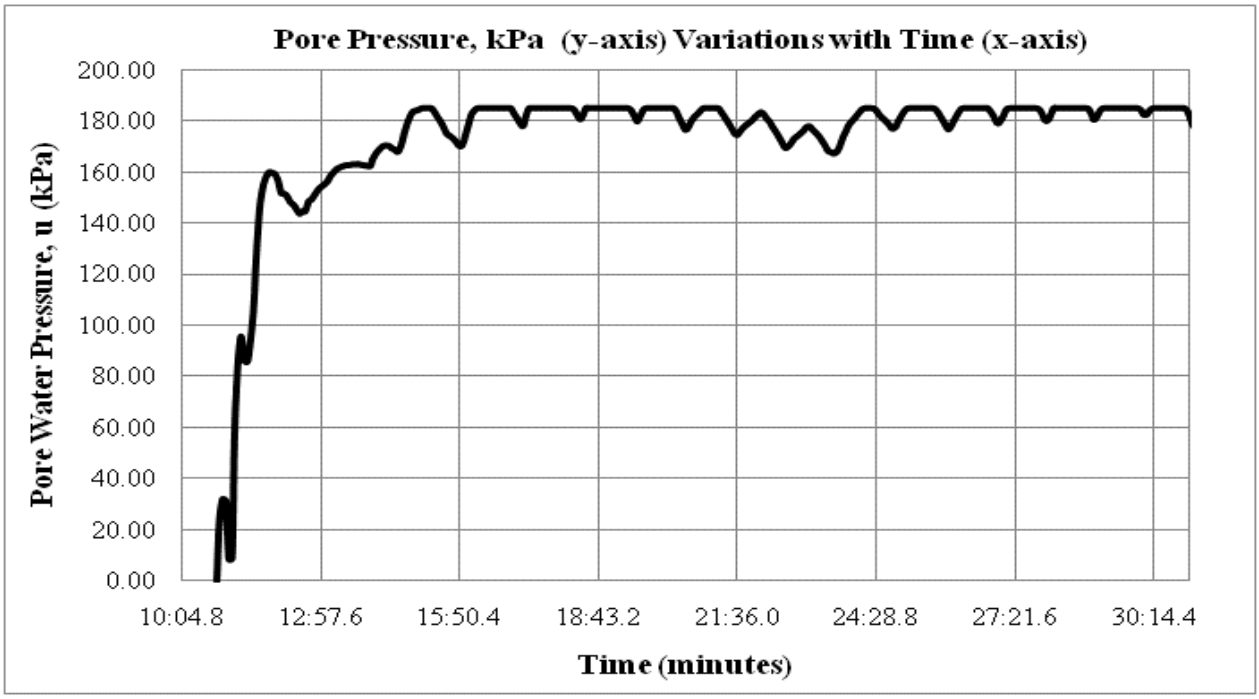

Figure 4.2.6 Pore pressure versus time (Test ID – A 57, sample ID S-13252_ZF)

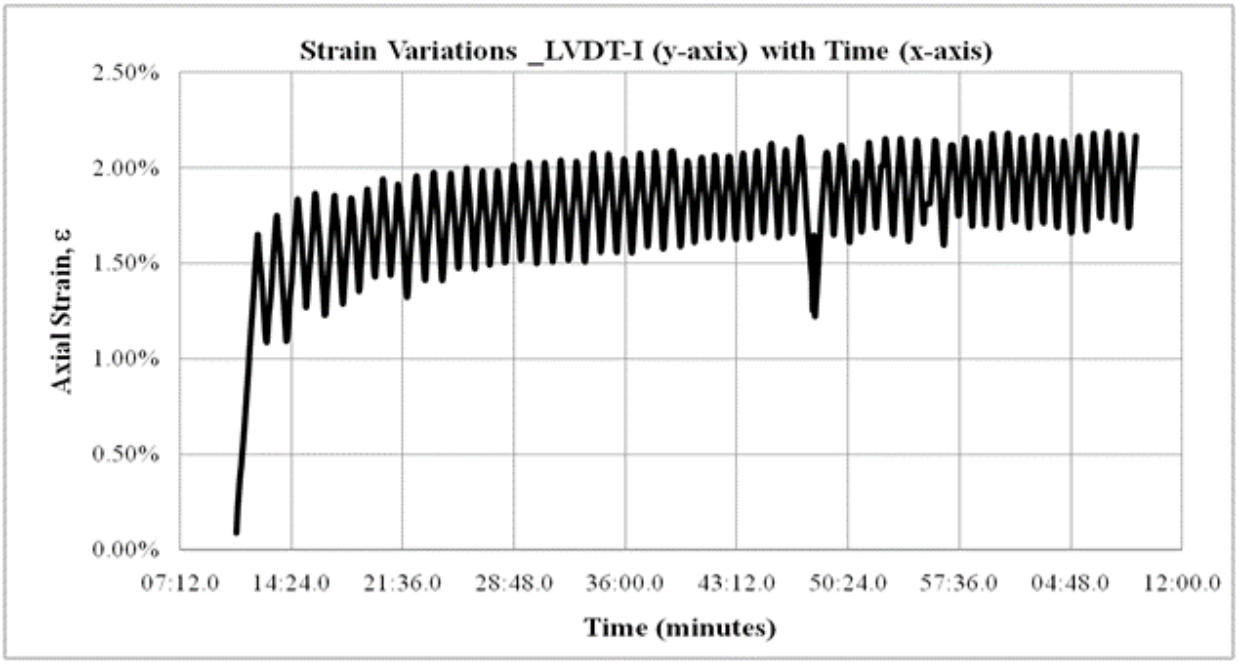

Figure 4.2.7 Axial strain versus time (Test ID – A 57, sample ID S-13252_ZF)

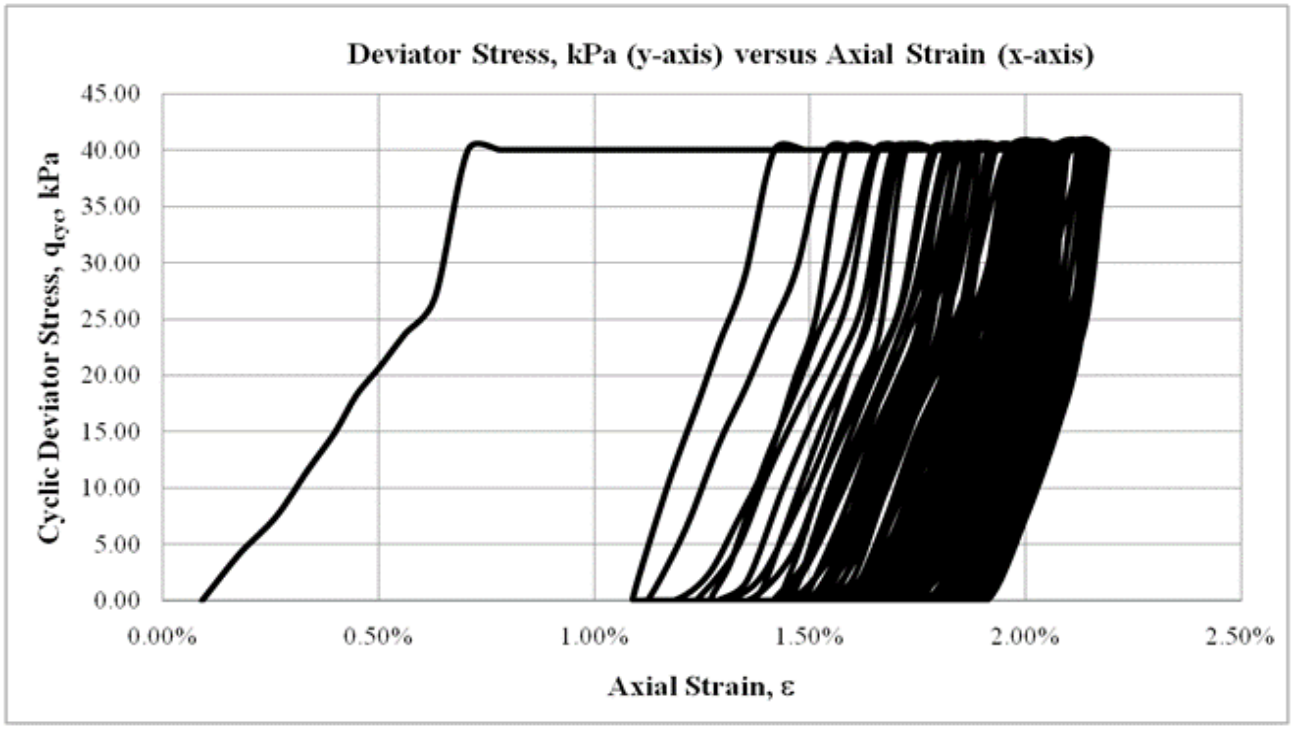

Figure 4.2.8 Cyclic deviator stress versus axial strain (Test ID – A 57, sample ID S-13252_ZF)

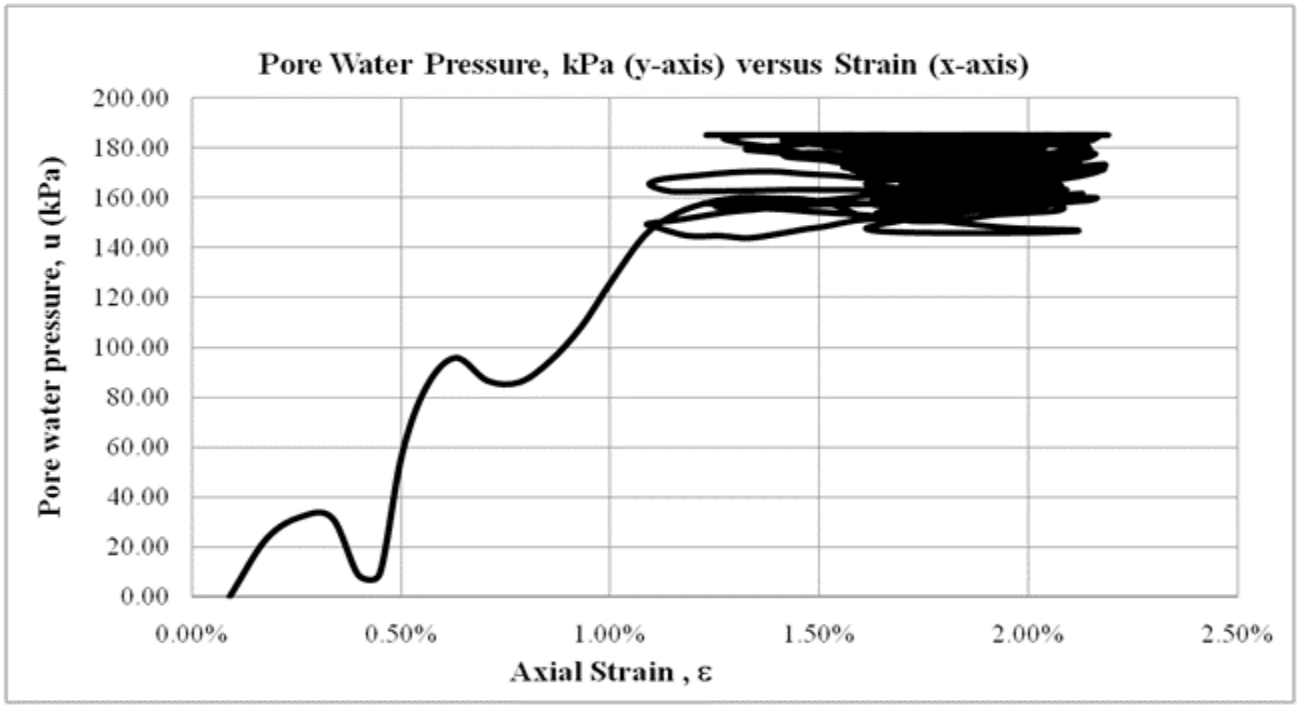

Figure 4.2.9 Pore pressure vs axial strain(Test ID – A 57, sample ID S-13252_ZF)

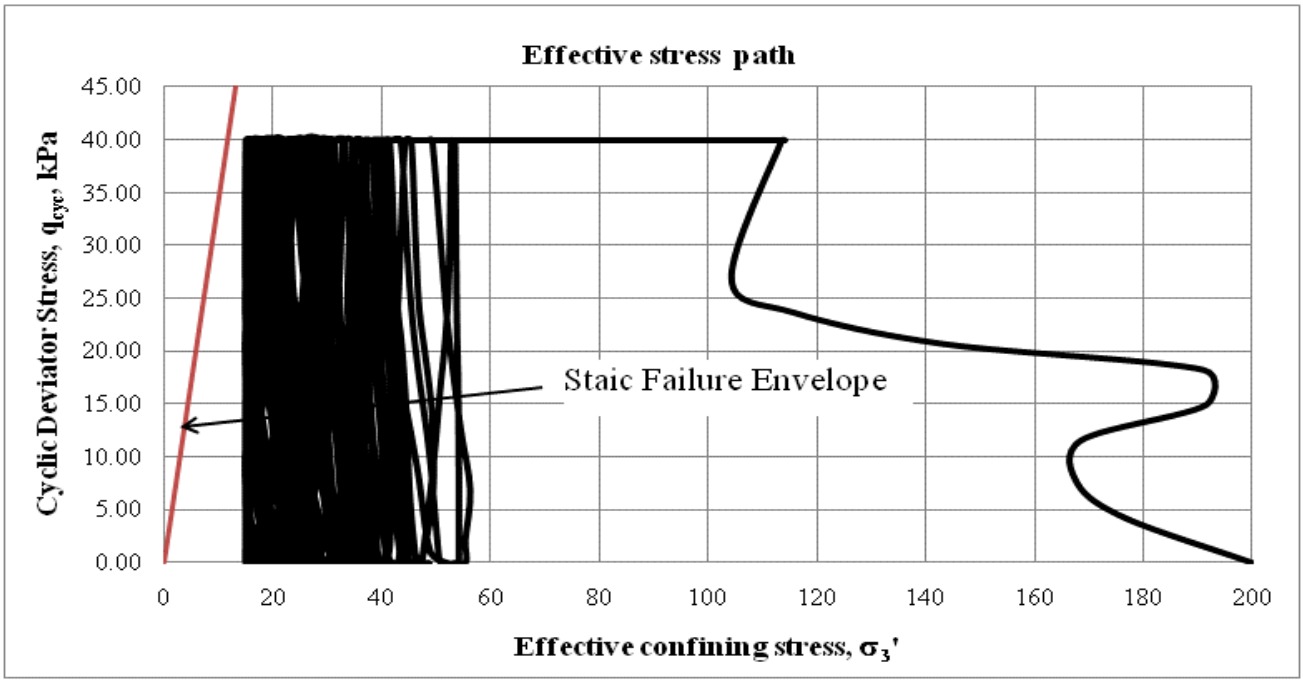

Figure 4.2.10 Effective stress path (Test ID – A 57, sample ID S-13252_ZF)

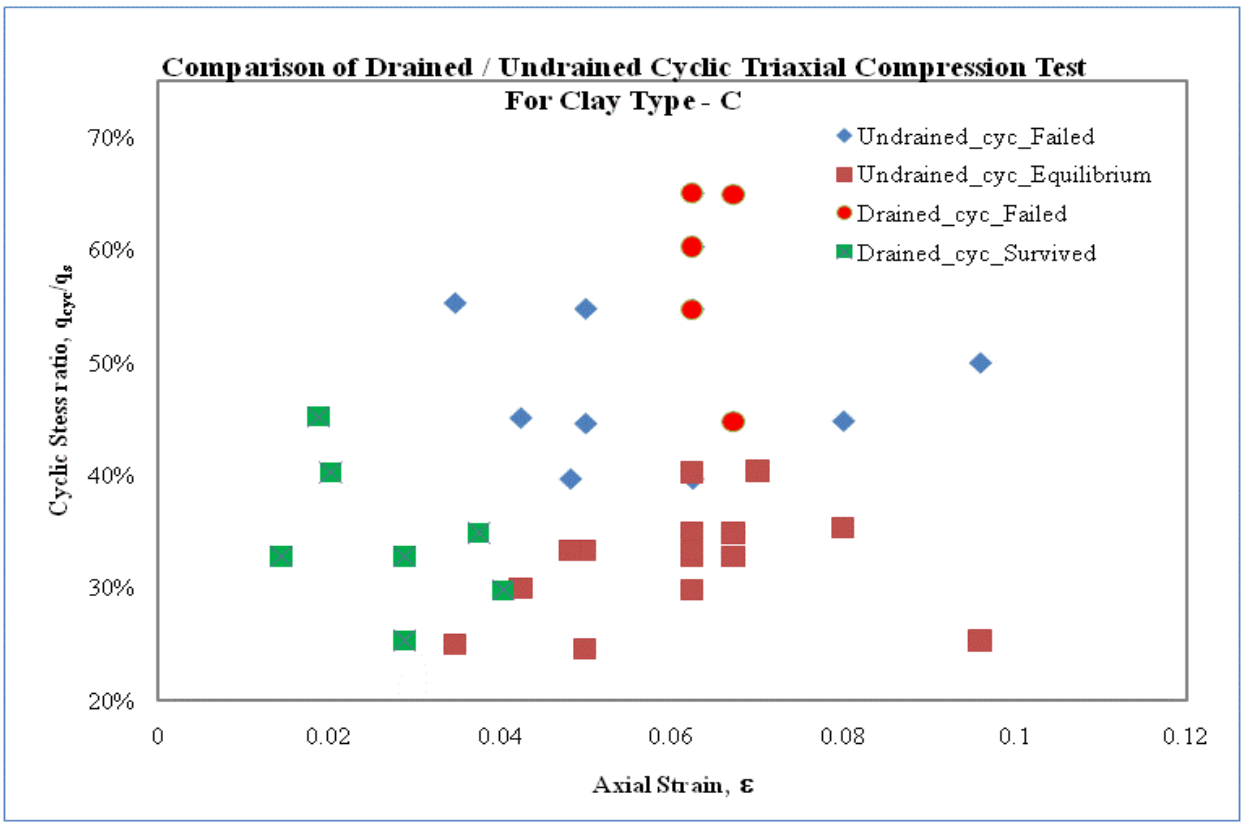

Figure 4.3.1 Comparison of drained/undrained cyclic triaxal compression test Clay Type-C

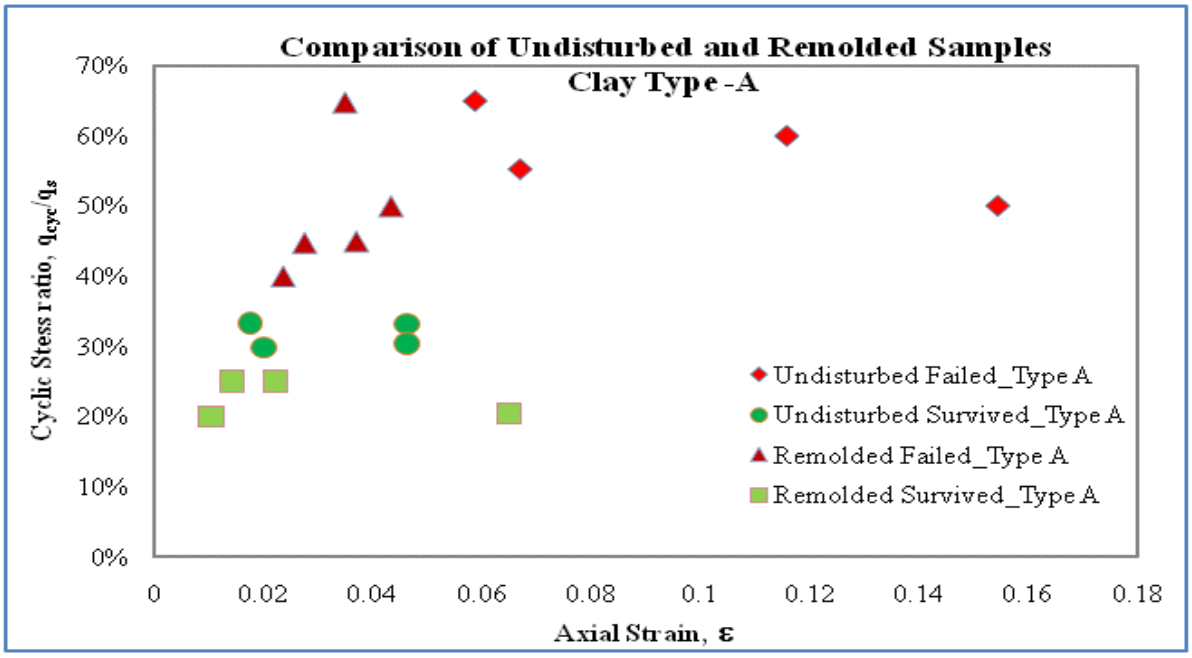

Figure 4.4.1 Comparison of undisturbed and remolded samples Clay Type-A

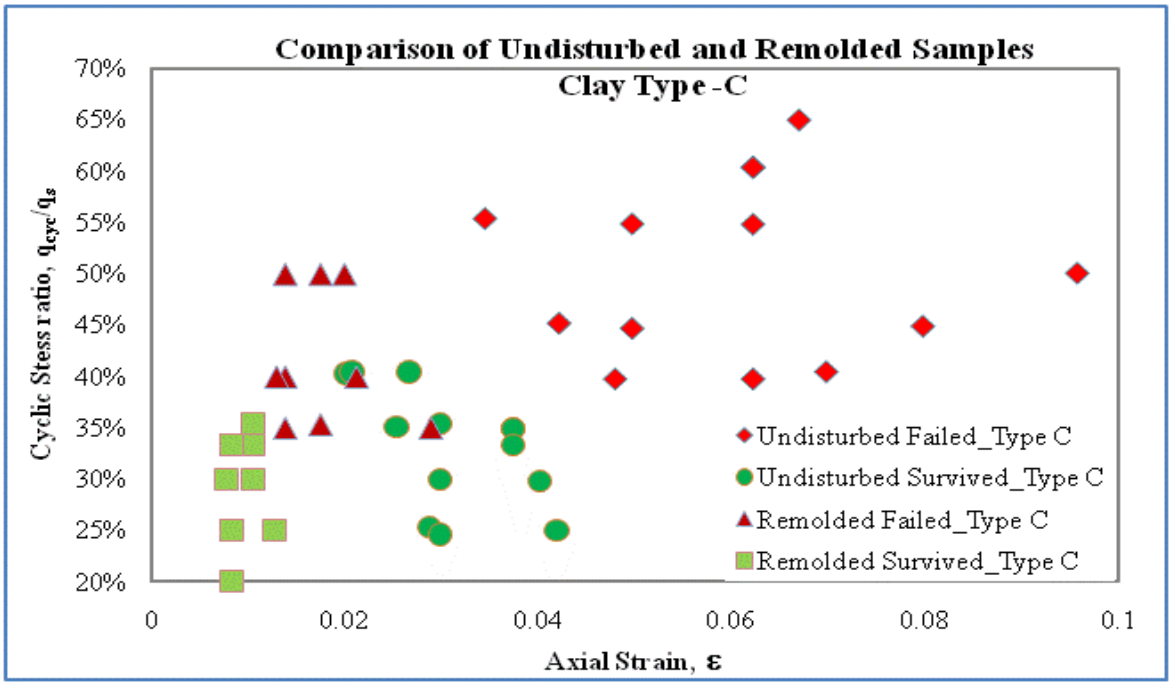

Figure 4.4.2 Comparison of undisturbed and remolded samples Clay Type-C

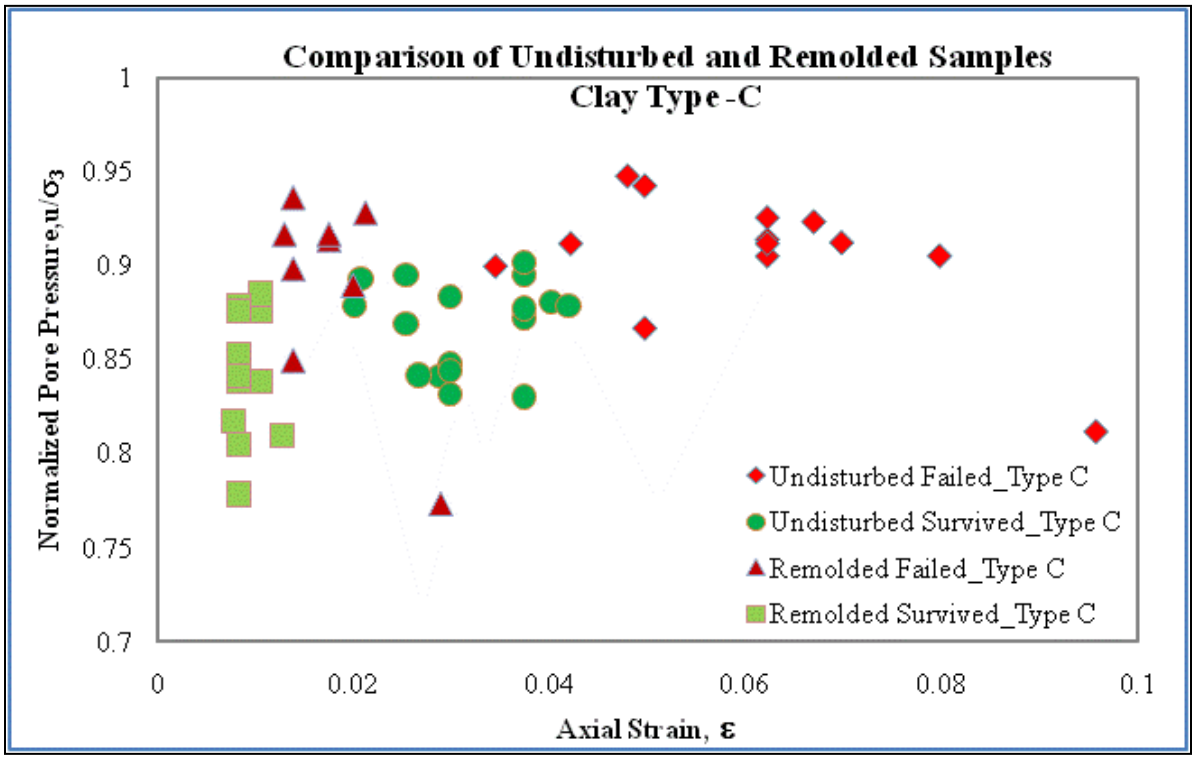

Figure 4.4.3 Comparison of undisturbed and remolded samples Clay Type-C

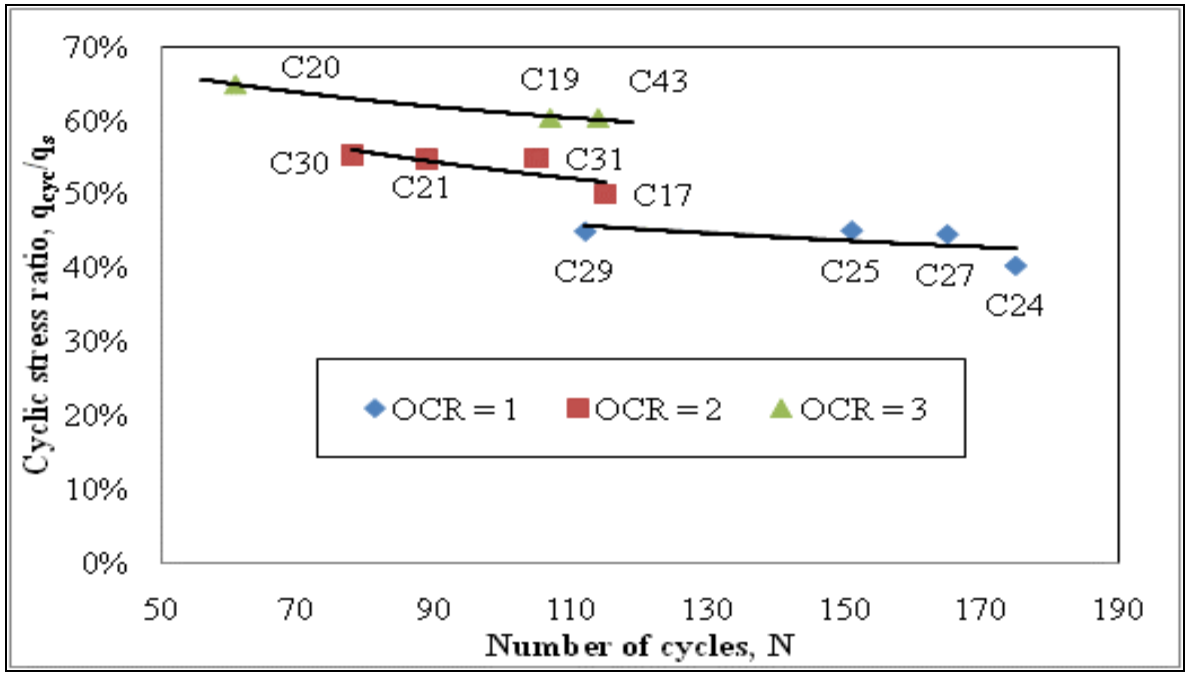

Figure 4.5.1 Effect of OCR, Cyclic stress ratio versus Number of cycles Clay Type – C

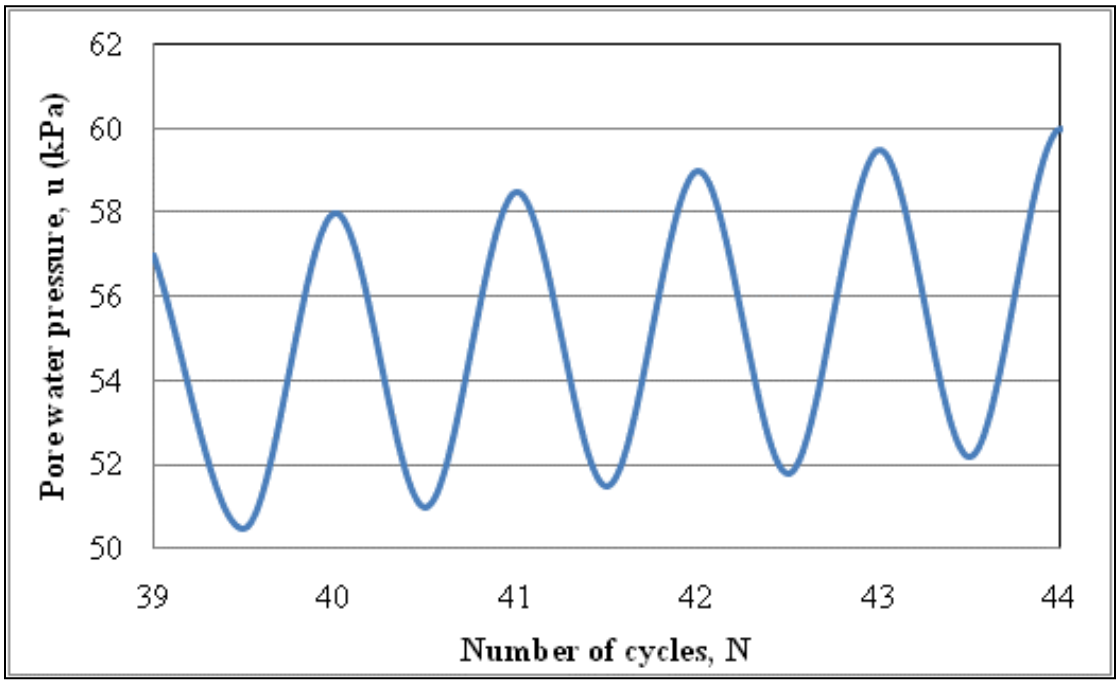

Figure 4.5.2 l Pore water pressure pattern for remolded normally consolidated clay

Test ID C42 Group –II Sample ID S13048-G_BH-02

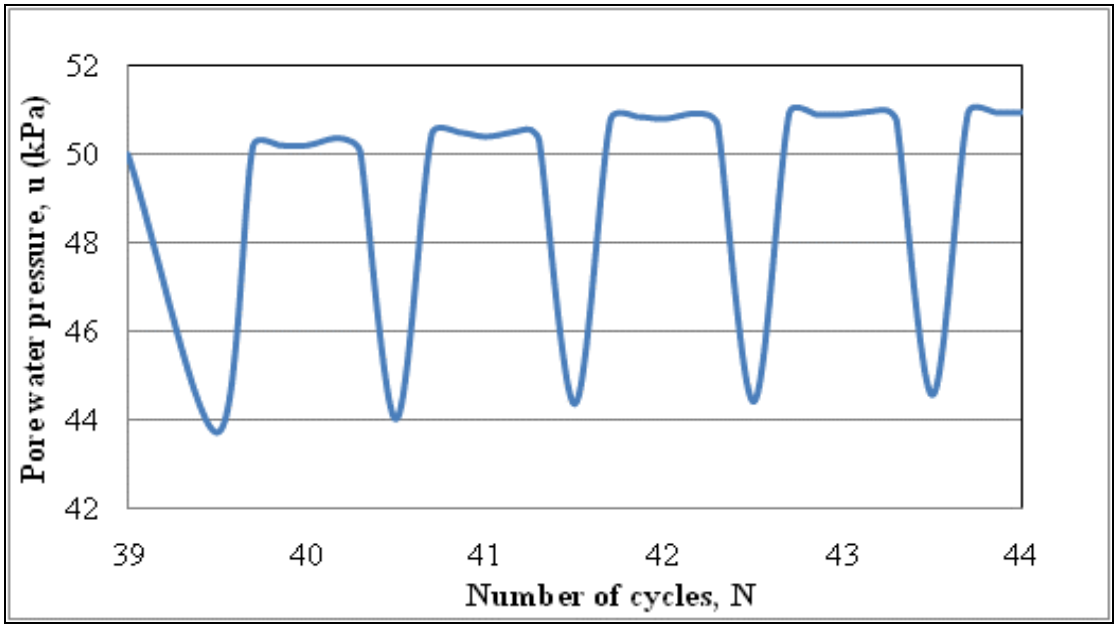

Figure 4.5.3 Pore water pressure pattern for an undisturbed over consolidated clay

Test ID C 31 Group –I Sample ID S13048-G_BH-02-TS

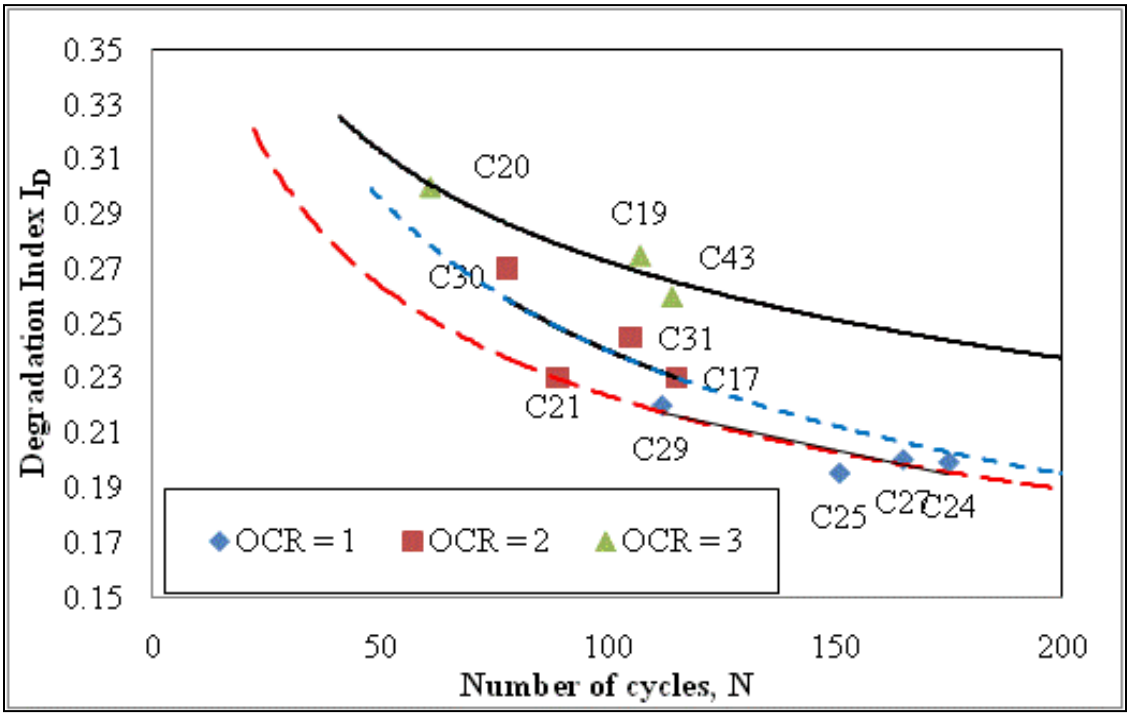

Figure 4.5.4 Degradation Index variation due to OCR – Clay Type – C

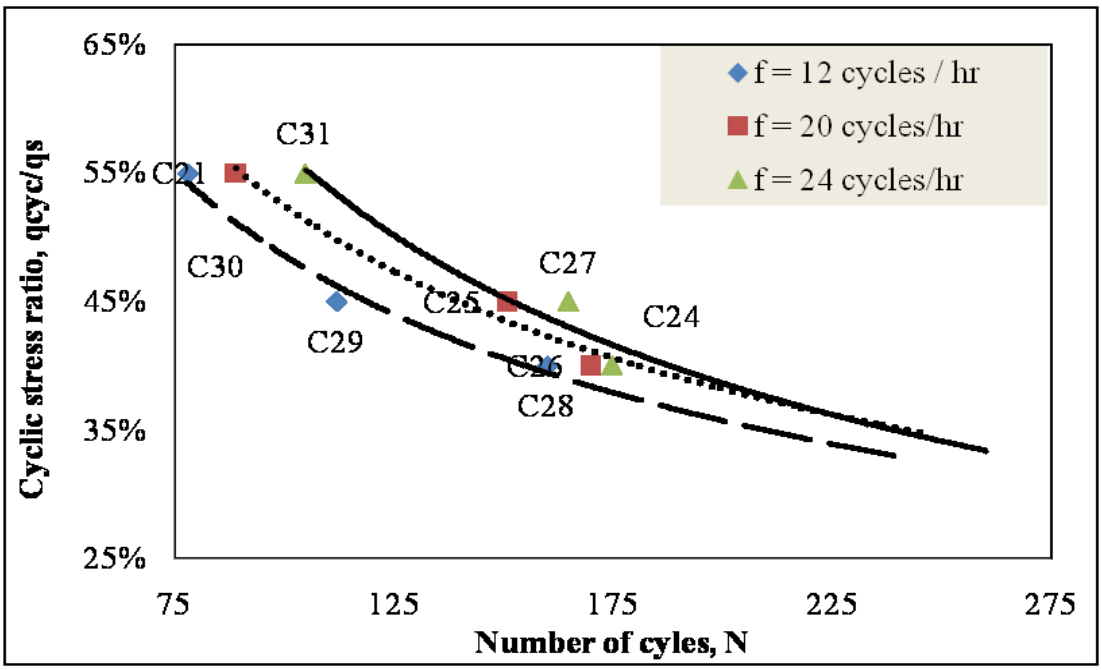

Figure 4.6.1 Effect of loading frequencies on undisturbed samples Clay Type – C

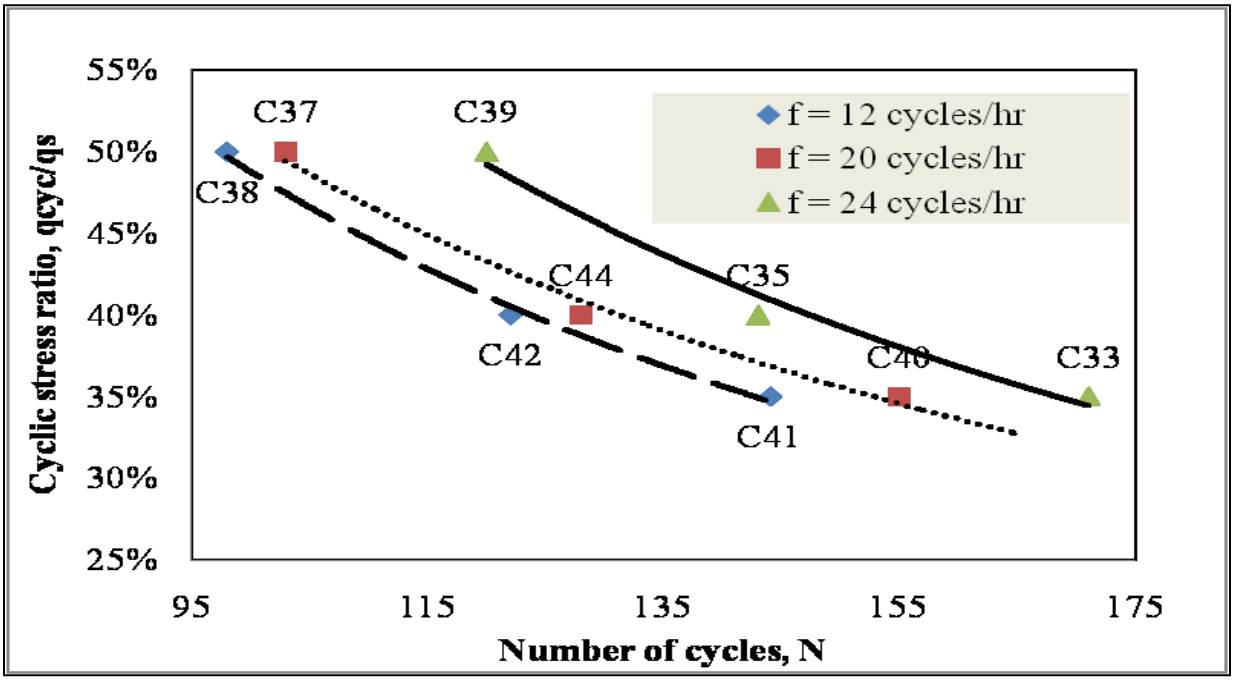

Figure 4.6.2 Effect of loading frequencies on remoulded samples Clay Type – C

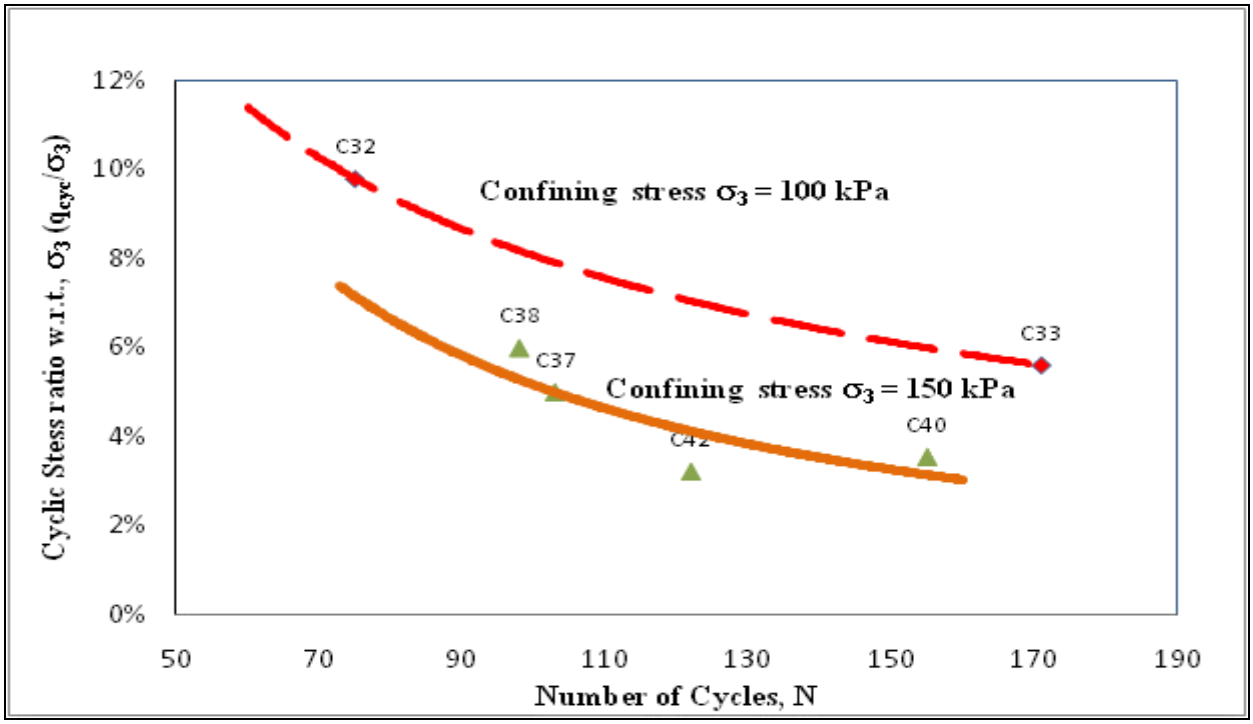

Figure 4.7.1 Effect of confining pressure on cyclic deviator stress ratio w.r.t σ_3, Clay C

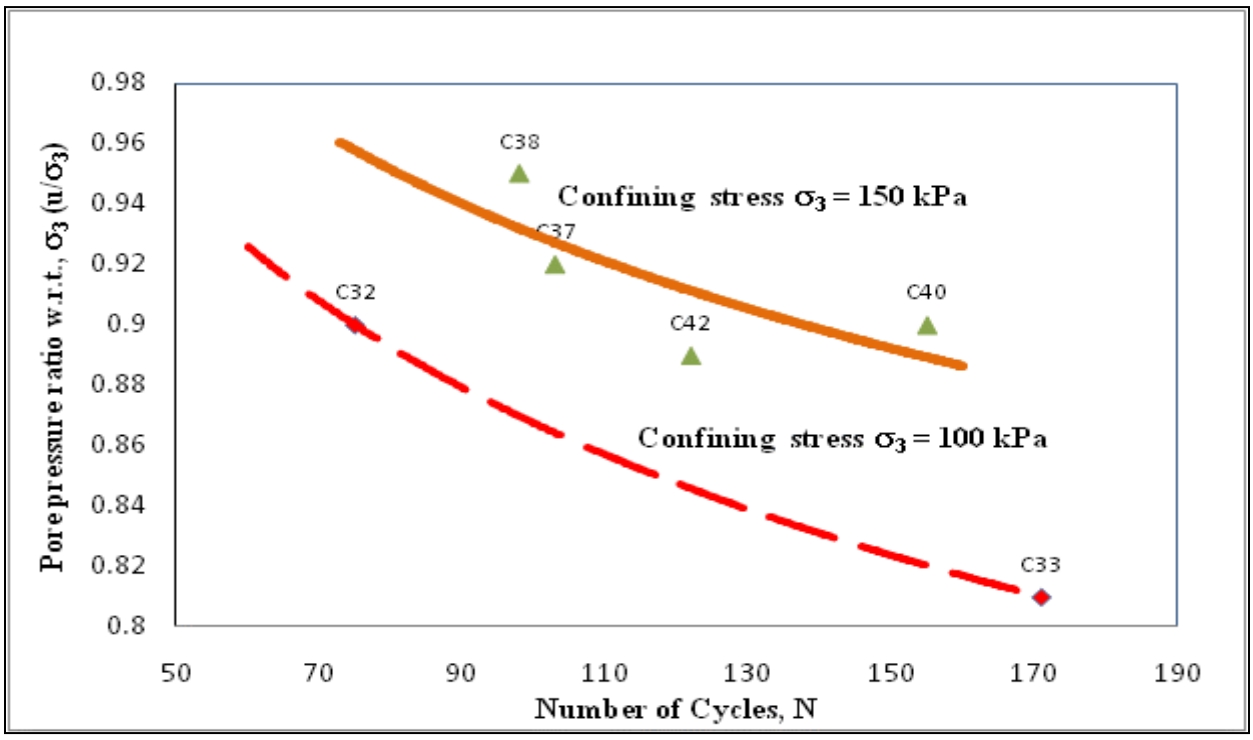

Figure 4.7.2 Effect of confining pressure on pore pressure ratio w.r.t σ_3, Clay Type – C

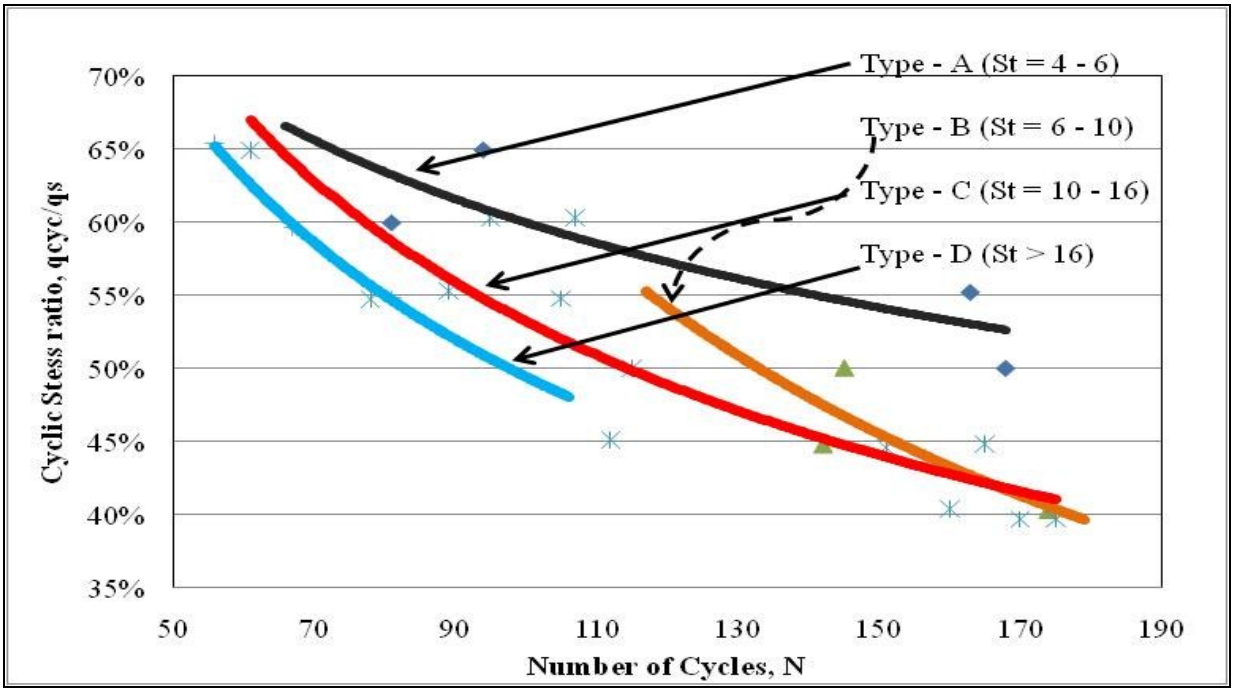

Figure 4.8.1 Effect of Sensitivity Number, Cyclic stress ratio versus Number of cycles

Group – I (undisturbed samples) Clay Types A, B, C & D

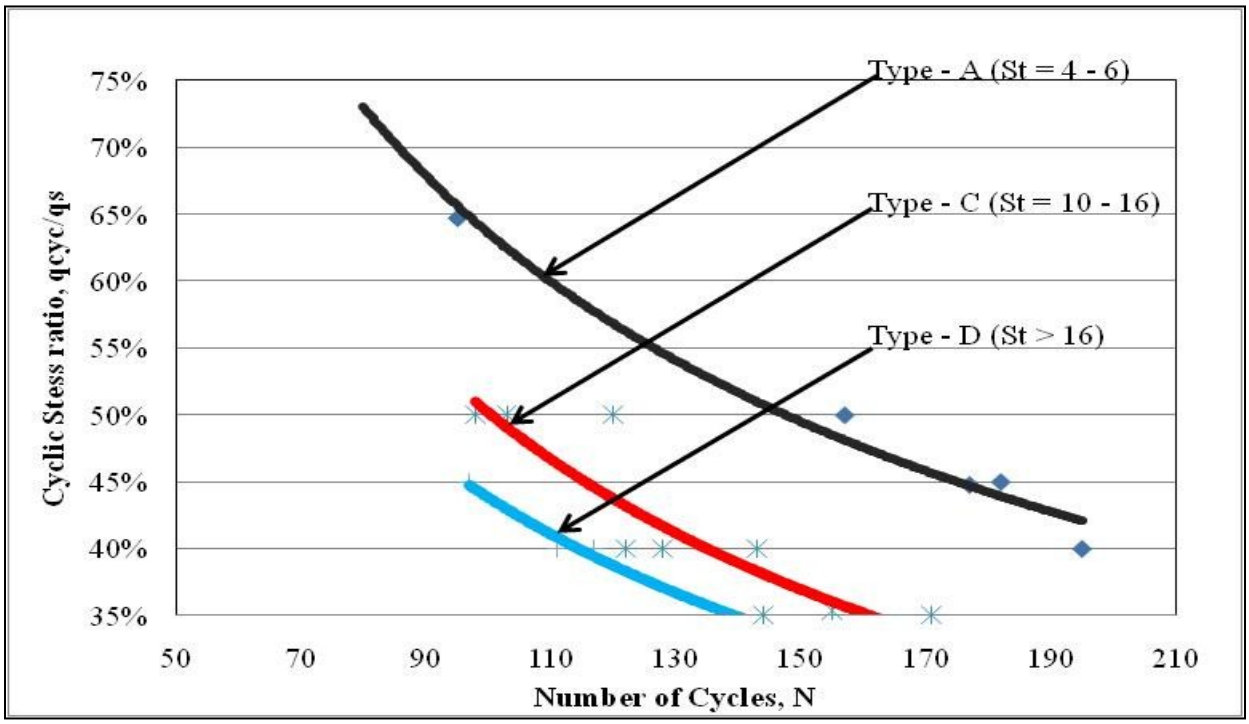

Figure 4.8.2 Effect of Sensitivity Number, Cyclic stress ratio versus Number of cycles

Group – II & III (Remolded samples) Clay Types A, C & D

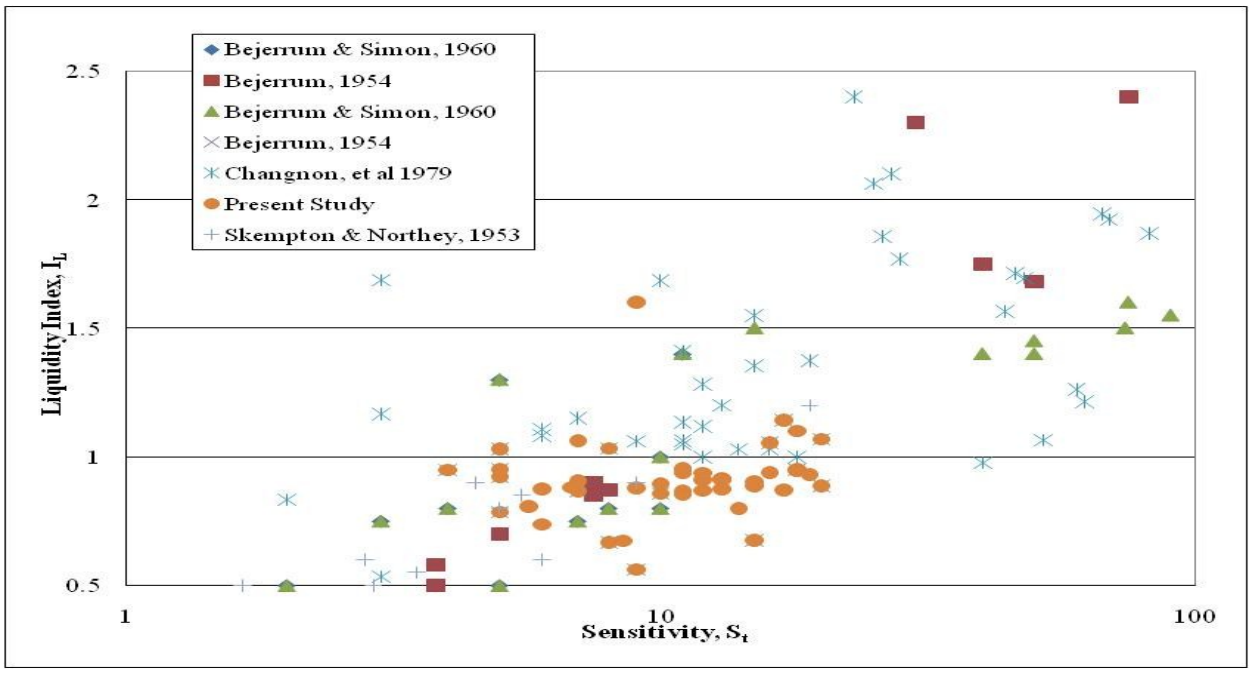

Figure 4.8.3 Liquidity Index, I_L versus Sensitivity Number S_t

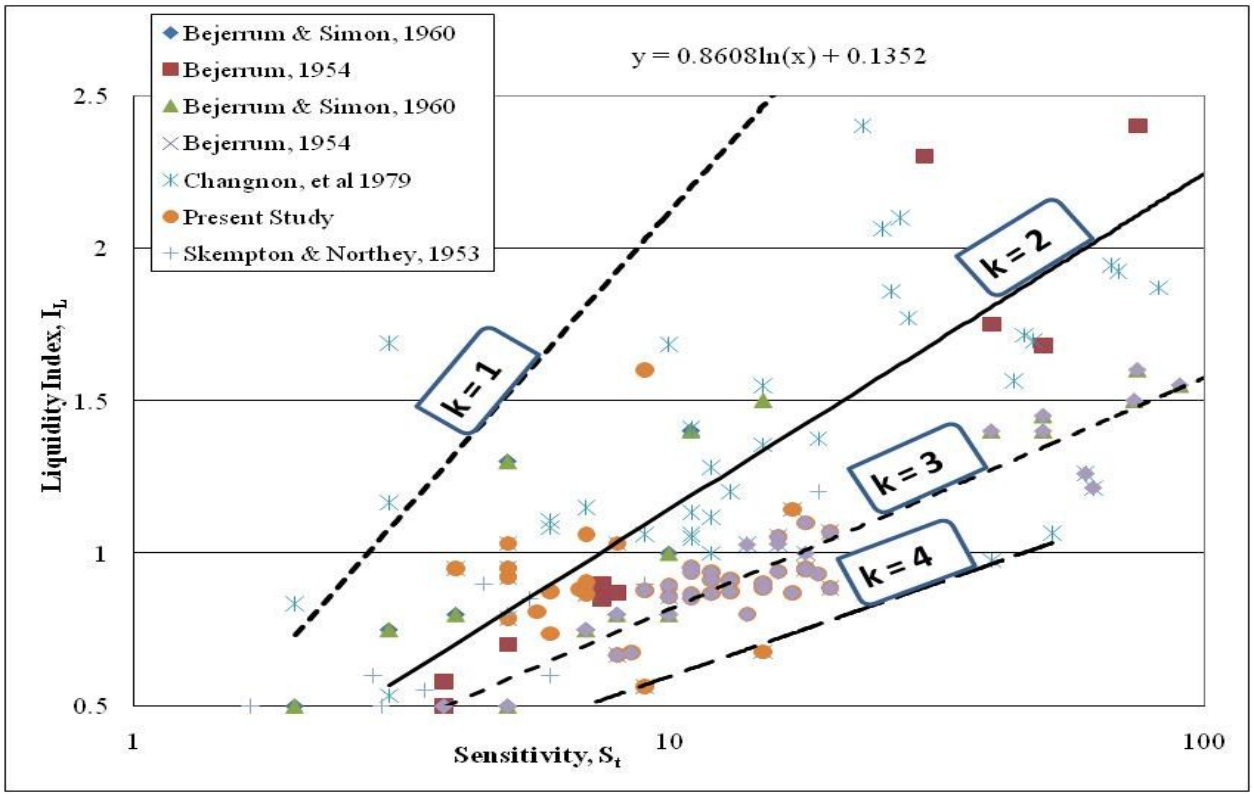

Figure 4.8.4 Variation in sensitivity constant, k Liquidity Index, I_L versus Sensitivity Number S_t

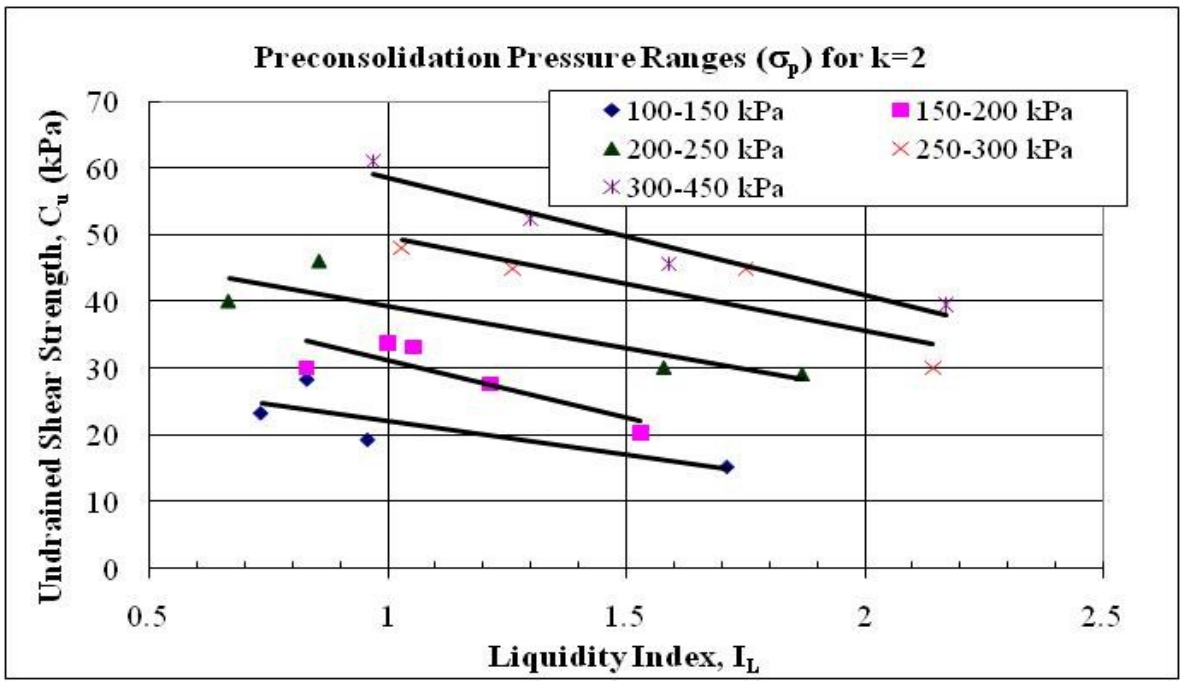

Figure 4.8.5 Effect of Sensitivity constant k, Undrained shear strength versus Liquidity Index

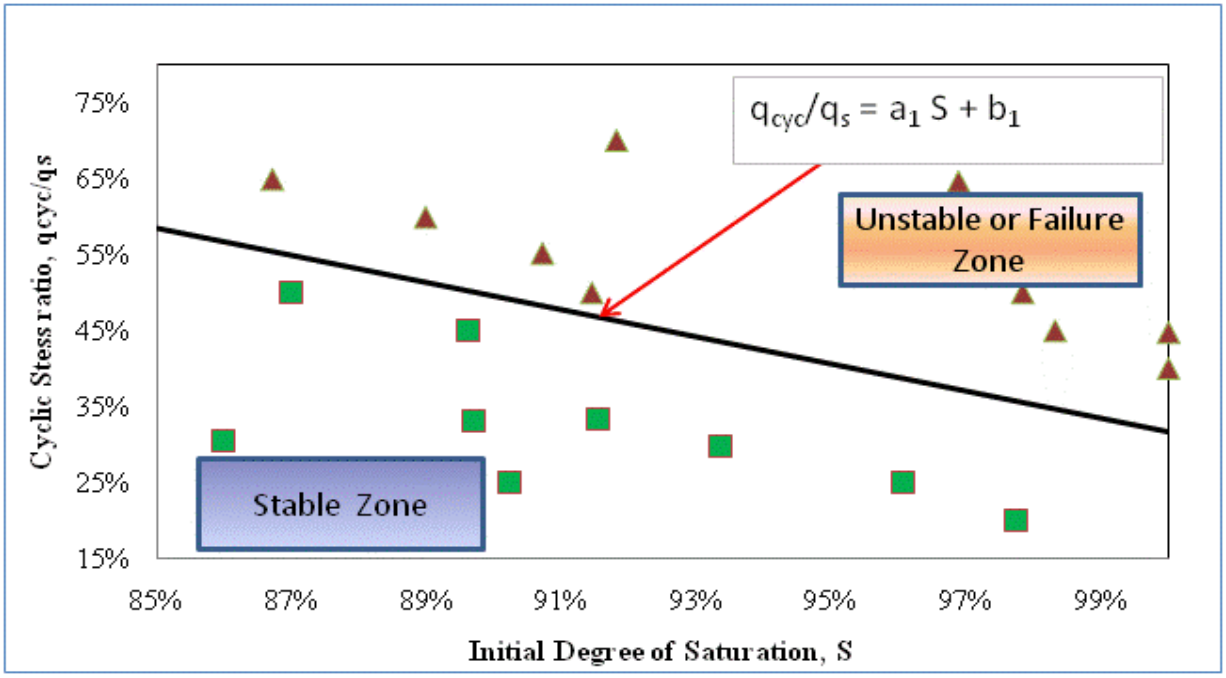

Figure 4.9.1 Relationship between Cyclic Stress Ratio, Degree of Saturation and Failure Clay Type - A

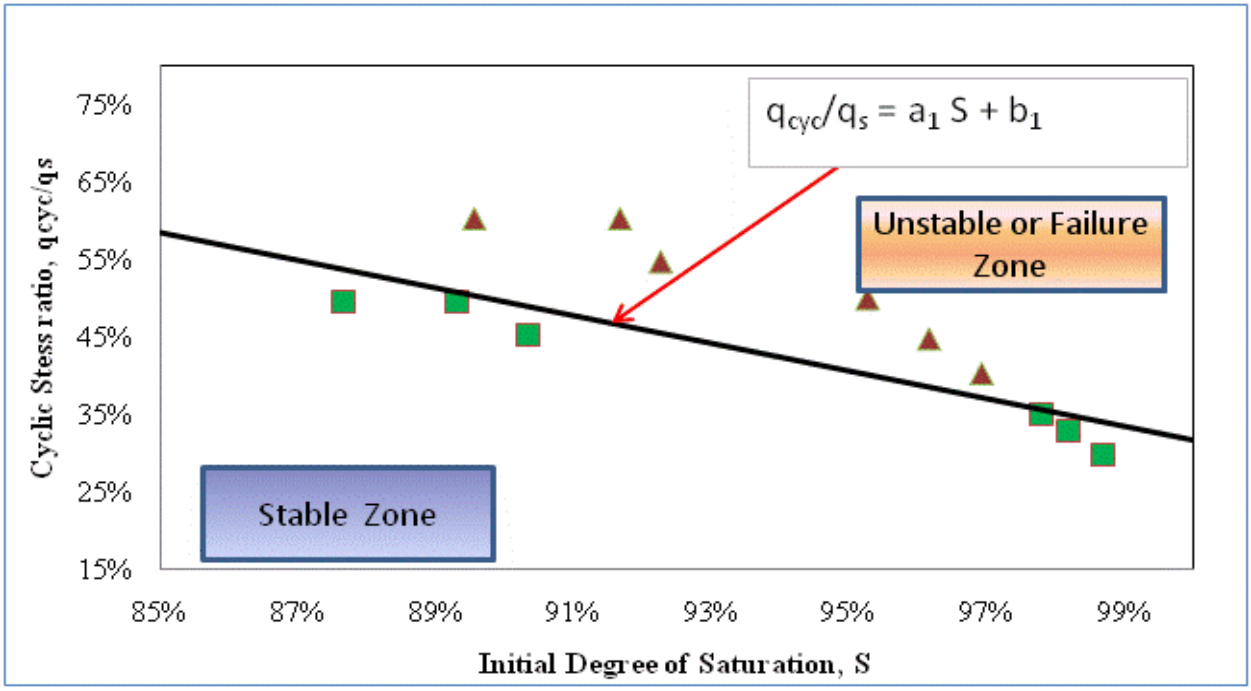

Figure 4.9.2 Relationship between Cyclic Stress Ratio, Degree of Saturation and Failure

Clay Type – B

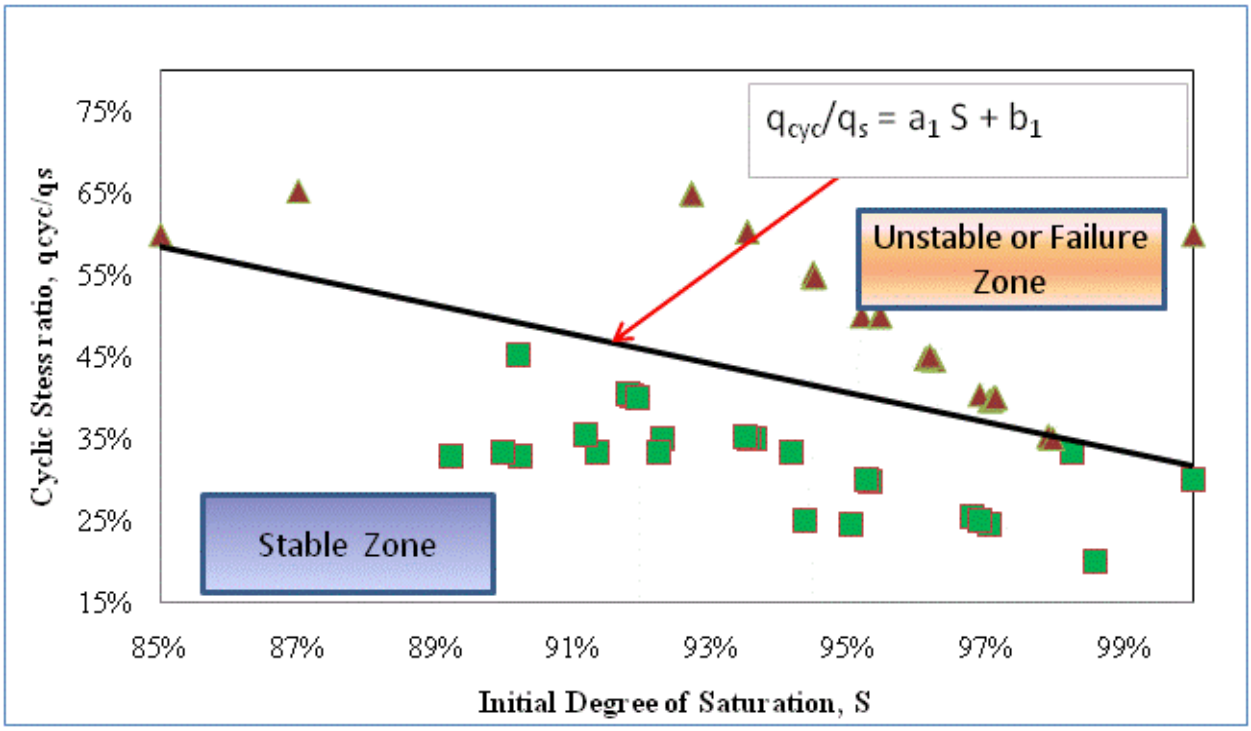

Figure 4.9.3 Relationship between Cyclic Stress Ratio, Degree of Saturation and Failure

Clay Type – C

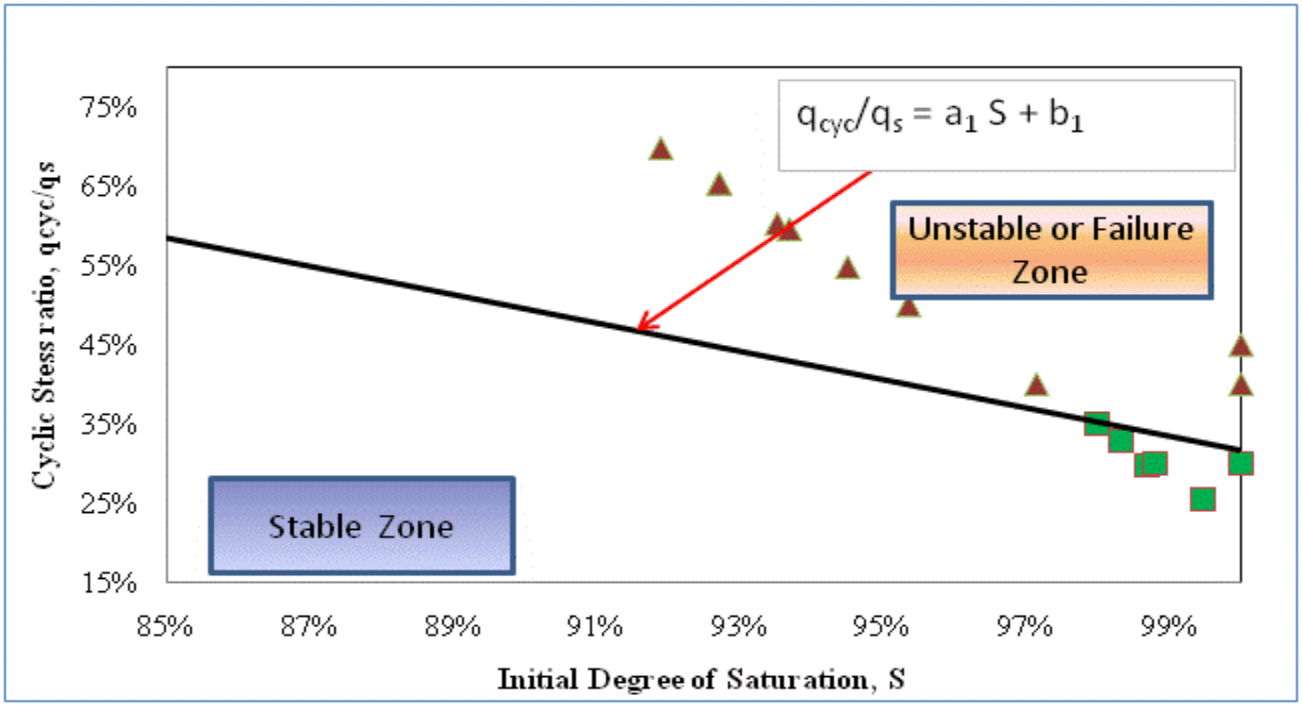

Figure 4.9.4 Relationship between Cyclic Stress Ratio, Degree of Saturation and Failure

Clay Type – D

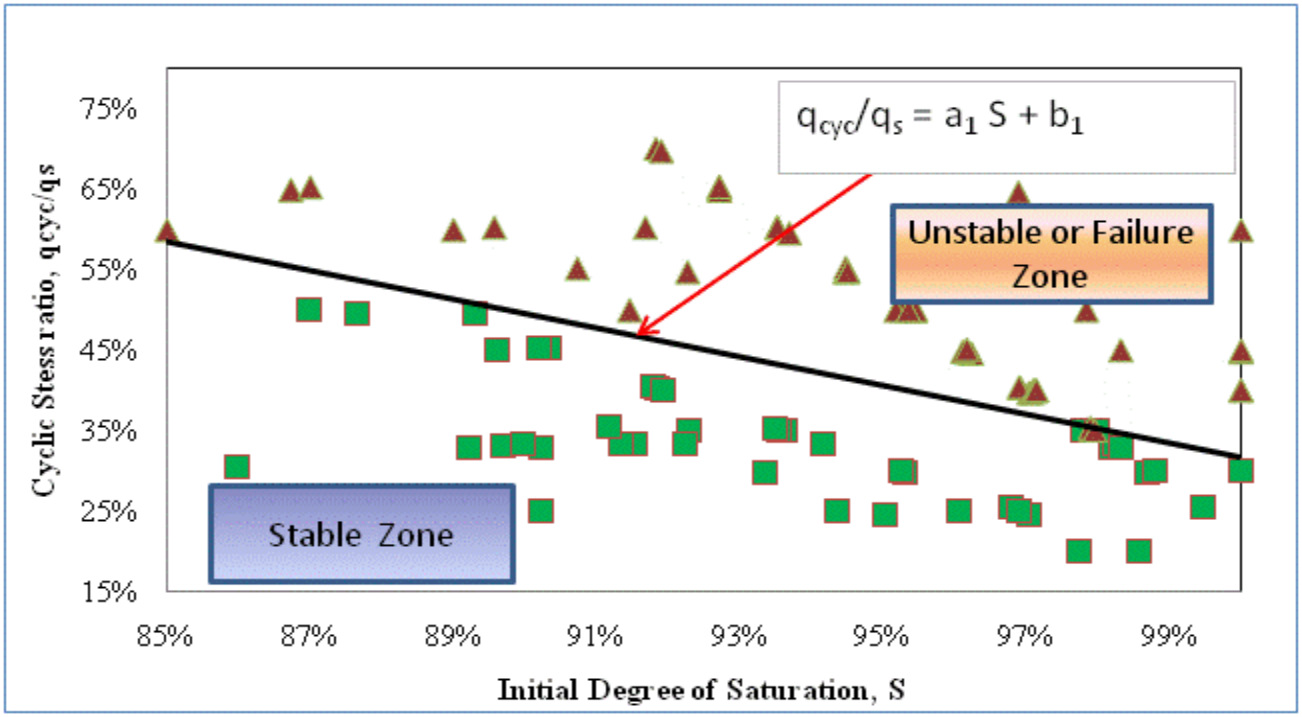

Figure 4.9.5 Relationship between Cyclic Stress Ratio, Degree of Saturation and Failure

Clay Overall

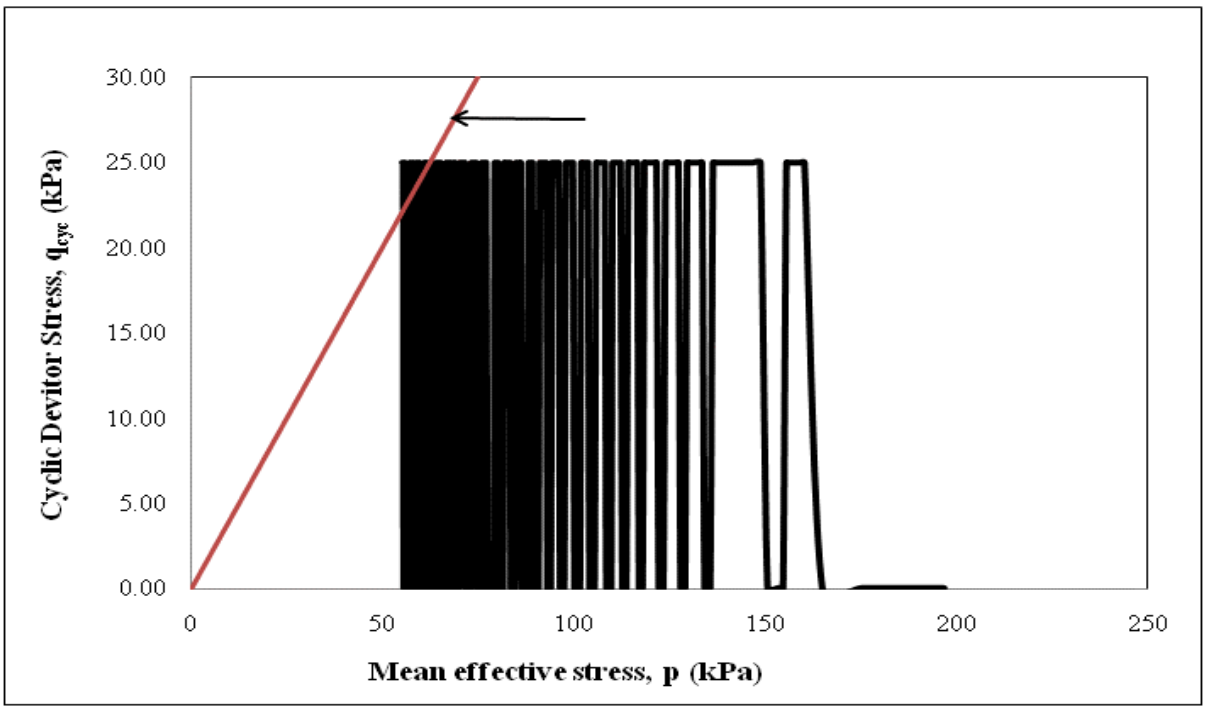

Figure 4.10.1: Deviator Stress Versus Effective Stress Test ID A8, Group – III Sample ID S_13293-G_BH-02_TS Clay Type – A

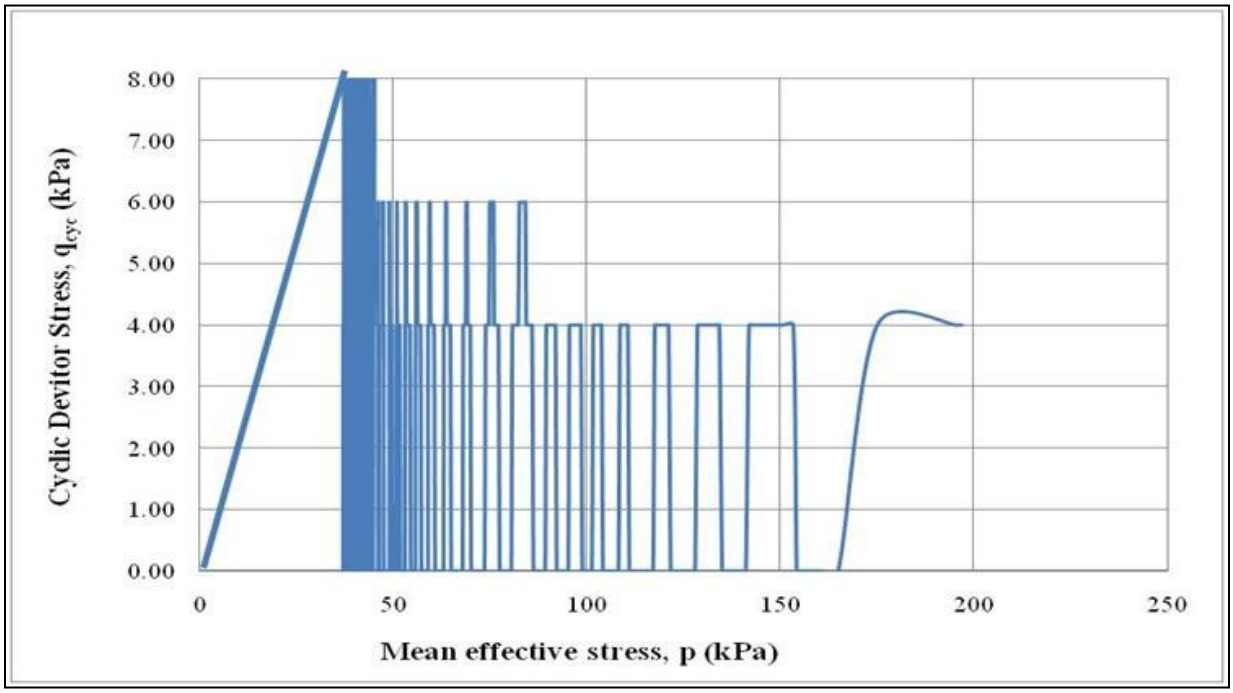

Figure 4.10.2: Stress Path multiple levels for deviator stress versus effective stress Clay Type-C Sample ID 13352_GE

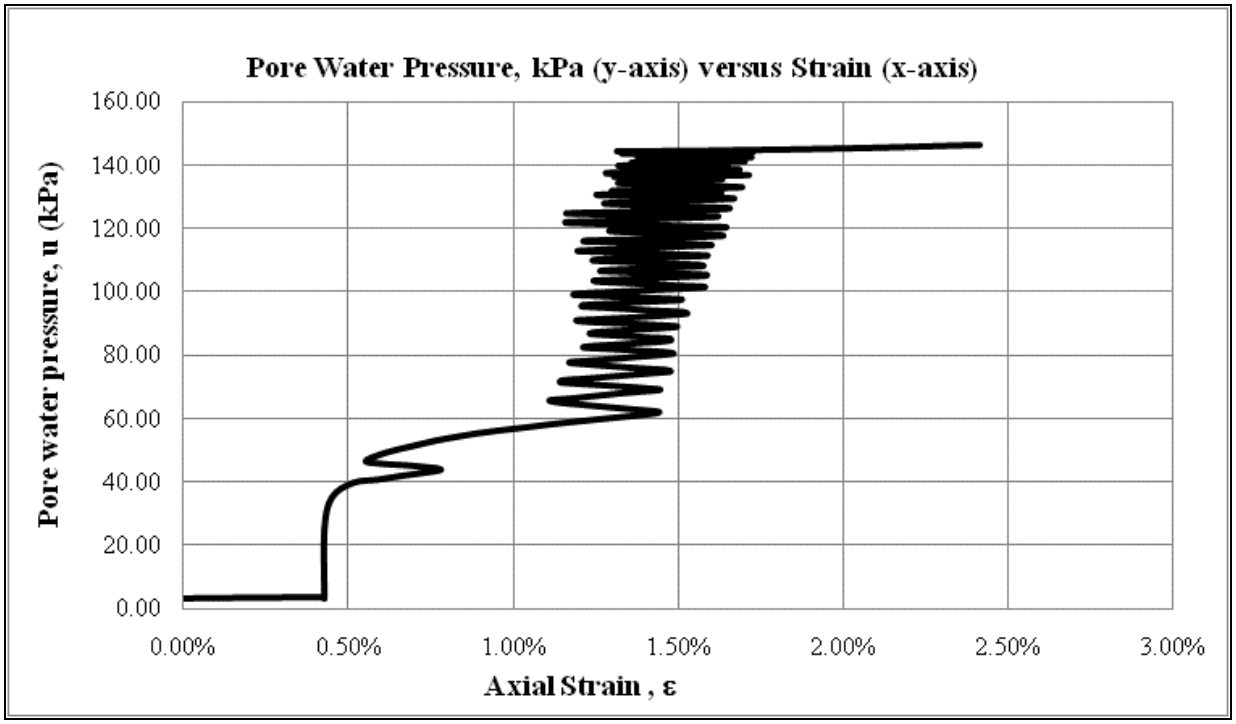

Figure 4.10.3: Pore Water Pressure versus Axial Strain Test ID A8, Group – III Sample ID S_13293-G_BH-02_TS

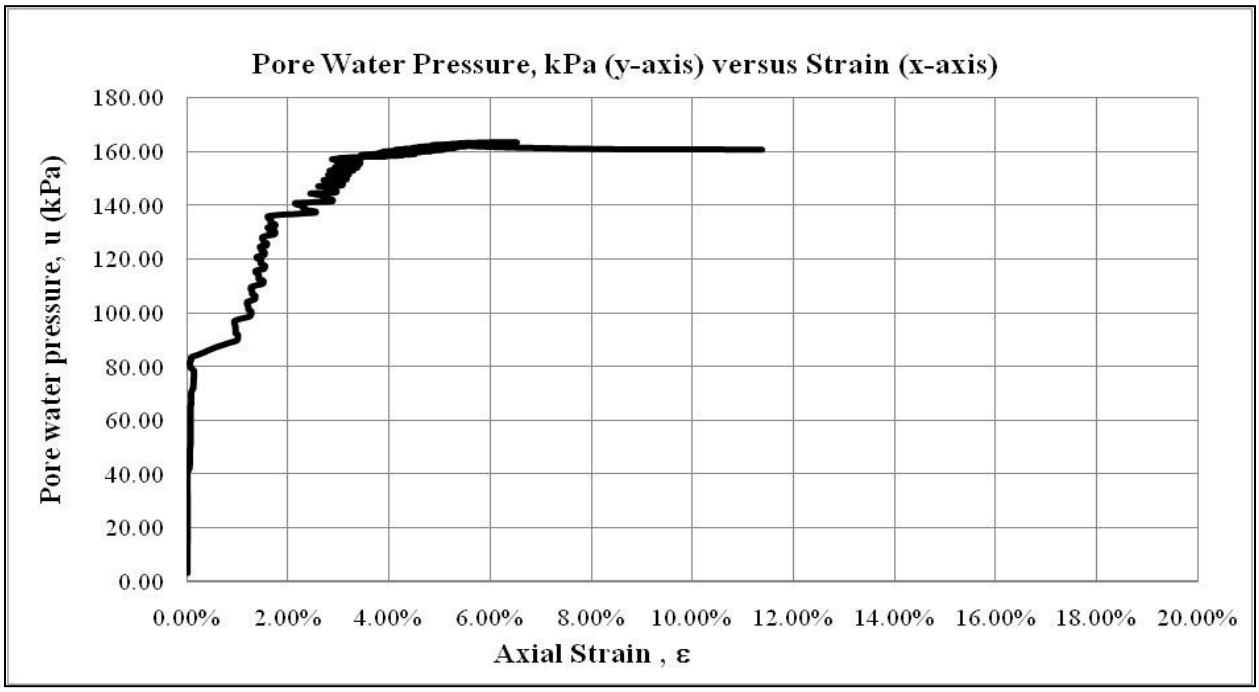

Figure 4.10.4 Pore Water Pressure versus Axial Strain (Clay Type-C Sample ID 13352_GE

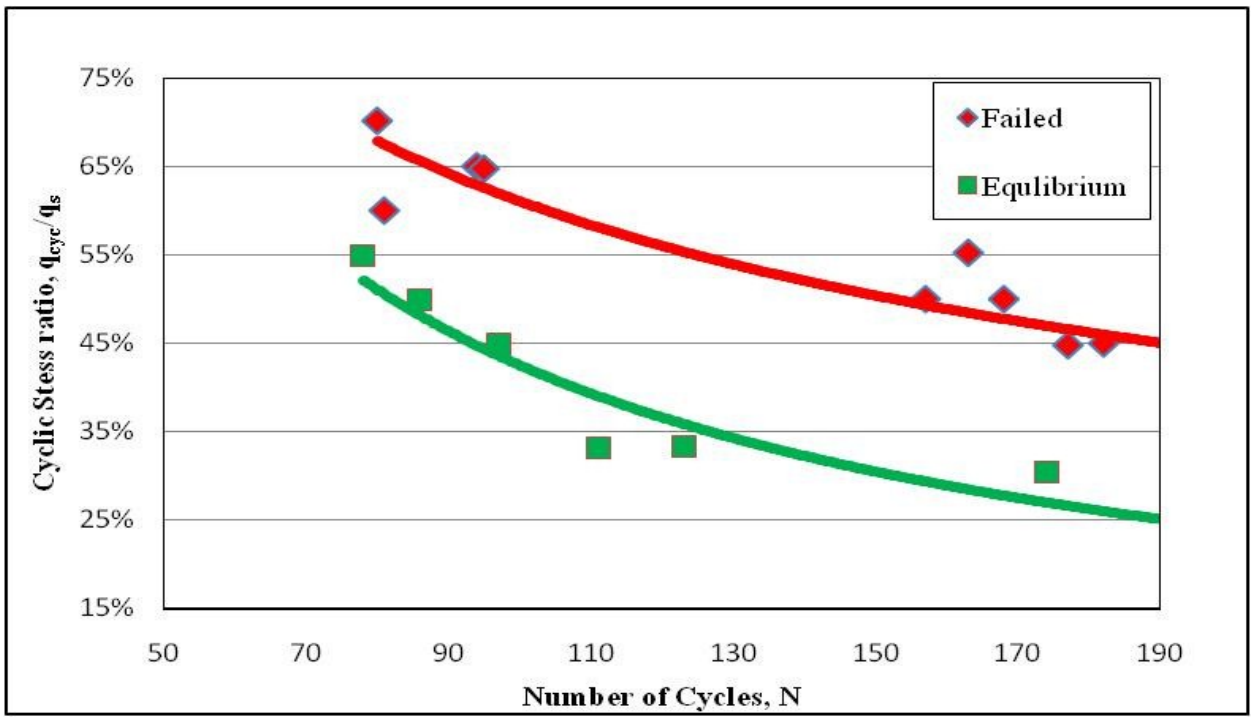

Figure 4.10.5 Best fit Curves for Establishing Failure, Transition and Equilibrium envelopes Clay Type – A

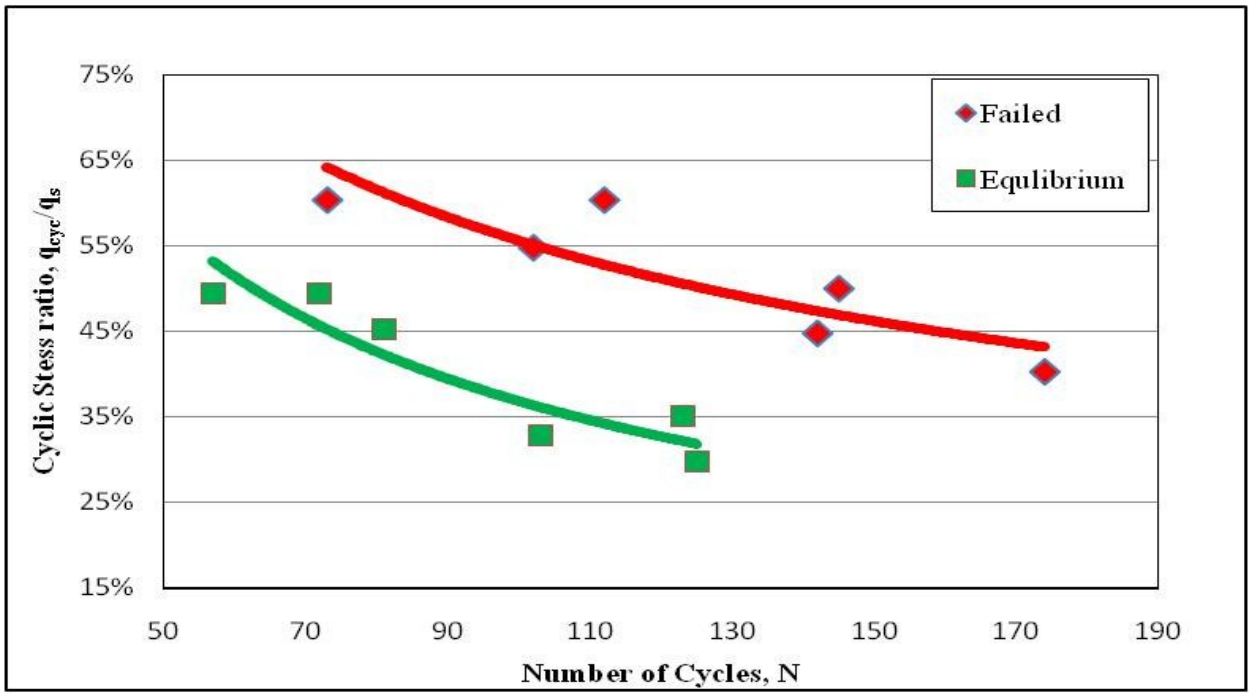

Figure 4.10.6 Best fit Curves for Establishing Failure, Transition and Equilibrium envelopes Clay Type – B

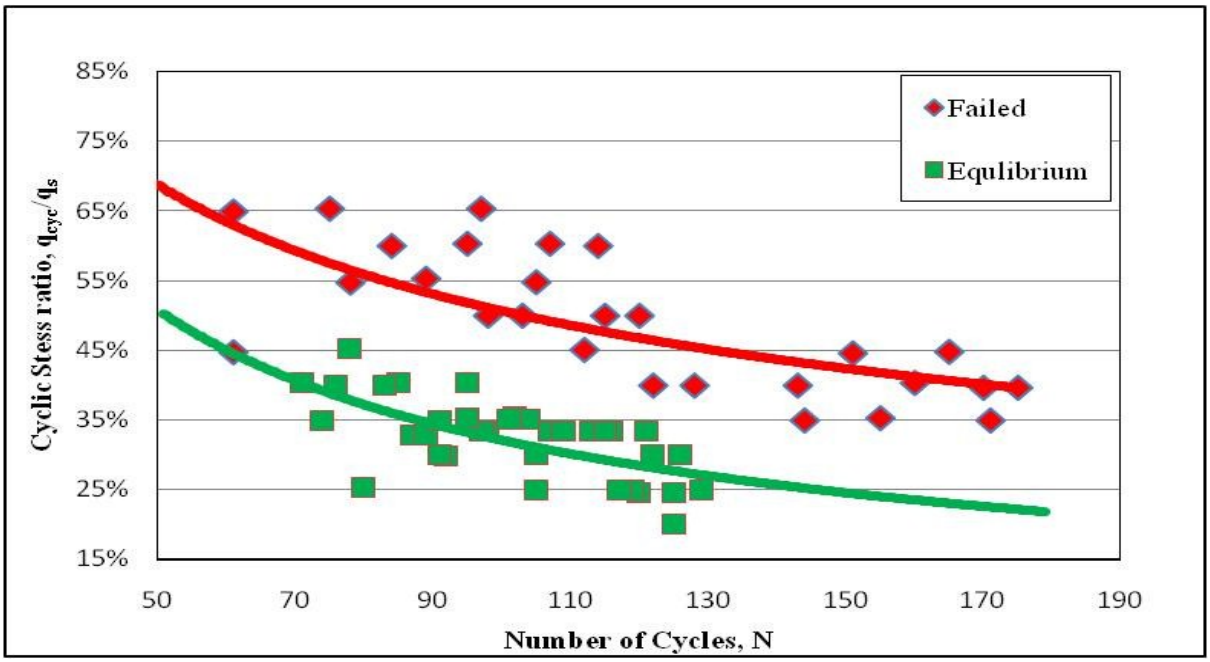

Figure 4.10.7 Best fit Curves for Establishing Failure, Transition and Equilibrium envelopes Clay Type – C

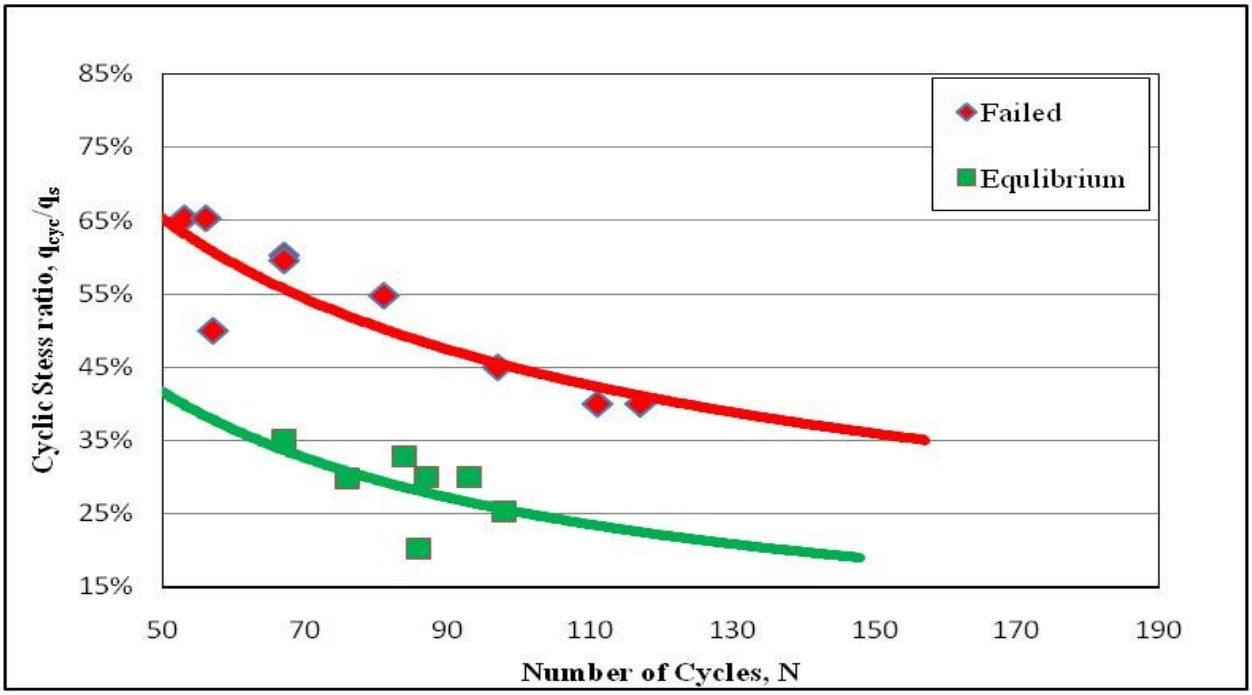

Figure 4.10.8 Best fit Curves for Establishing Failure, Transition and Equilibrium envelopes Clay Type – D

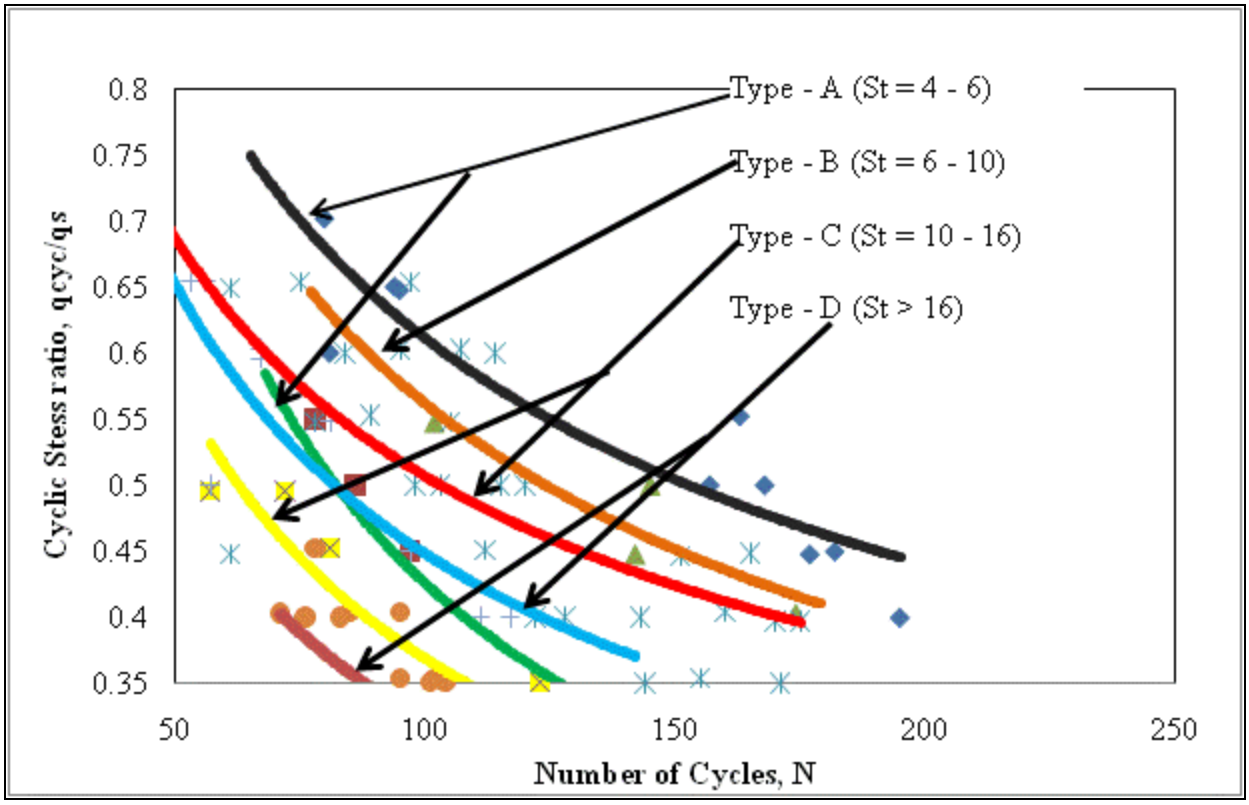

Figure 4.10.9 Best fit Curves for Establishing Failure, Transition and Equilibrium envelopes Clay Types A, B, C & D

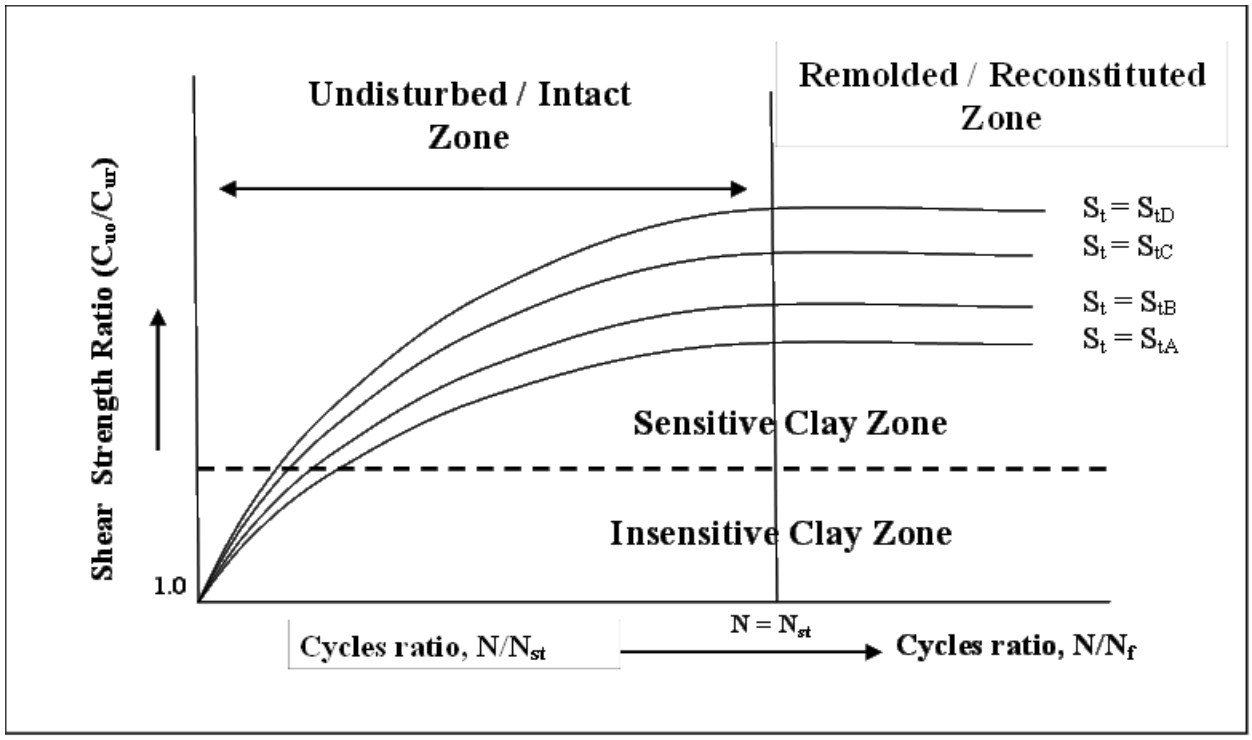

Figure 4.12.1: A schematic diagram for the proposed hypothetical model

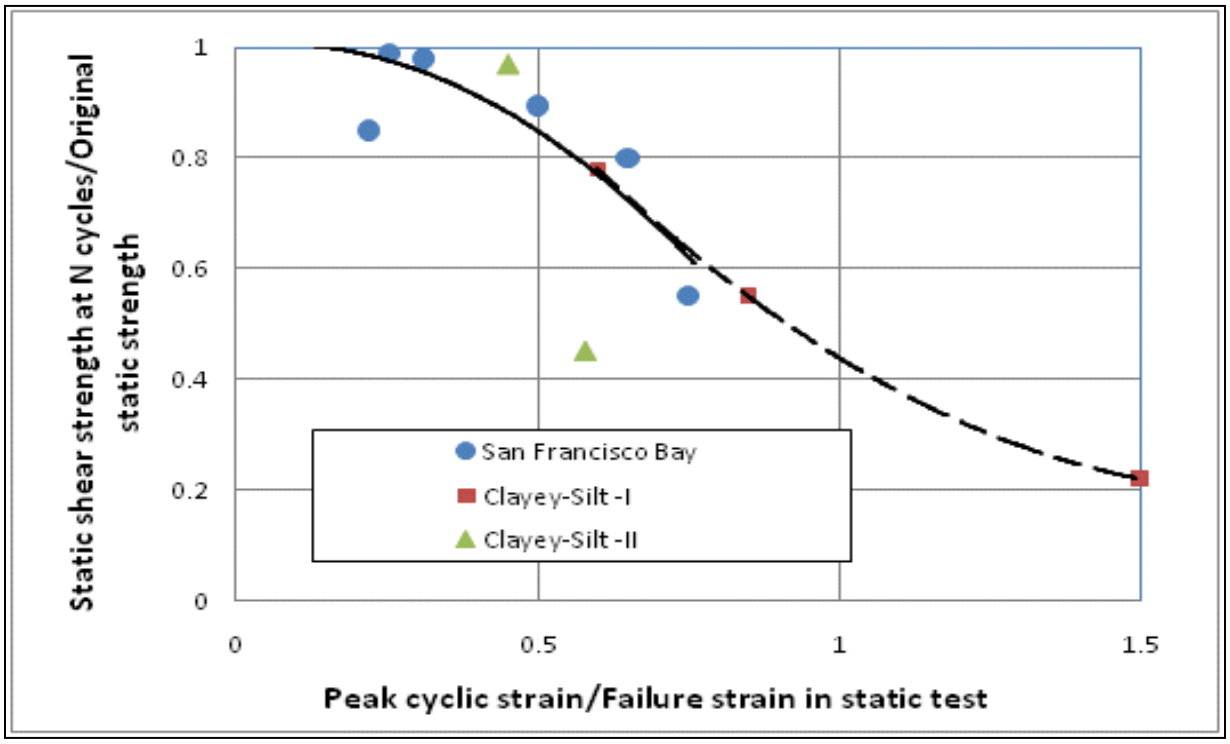

Figure 4.12.1.1: Variation of static strength after cyclic loading

(Data from; Theris and Seed, 1969)

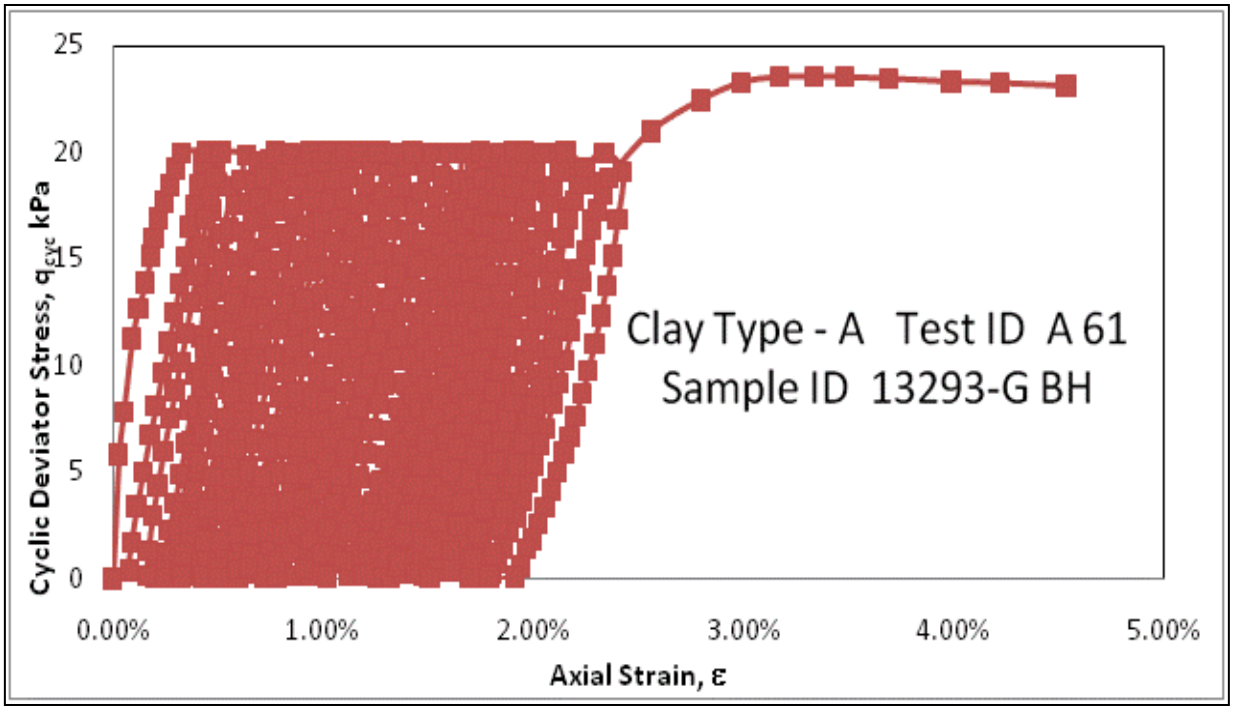

Figure 4.12.1.2:Typical hysterical loops, cyclic deviator stress versus axial strains Clay A

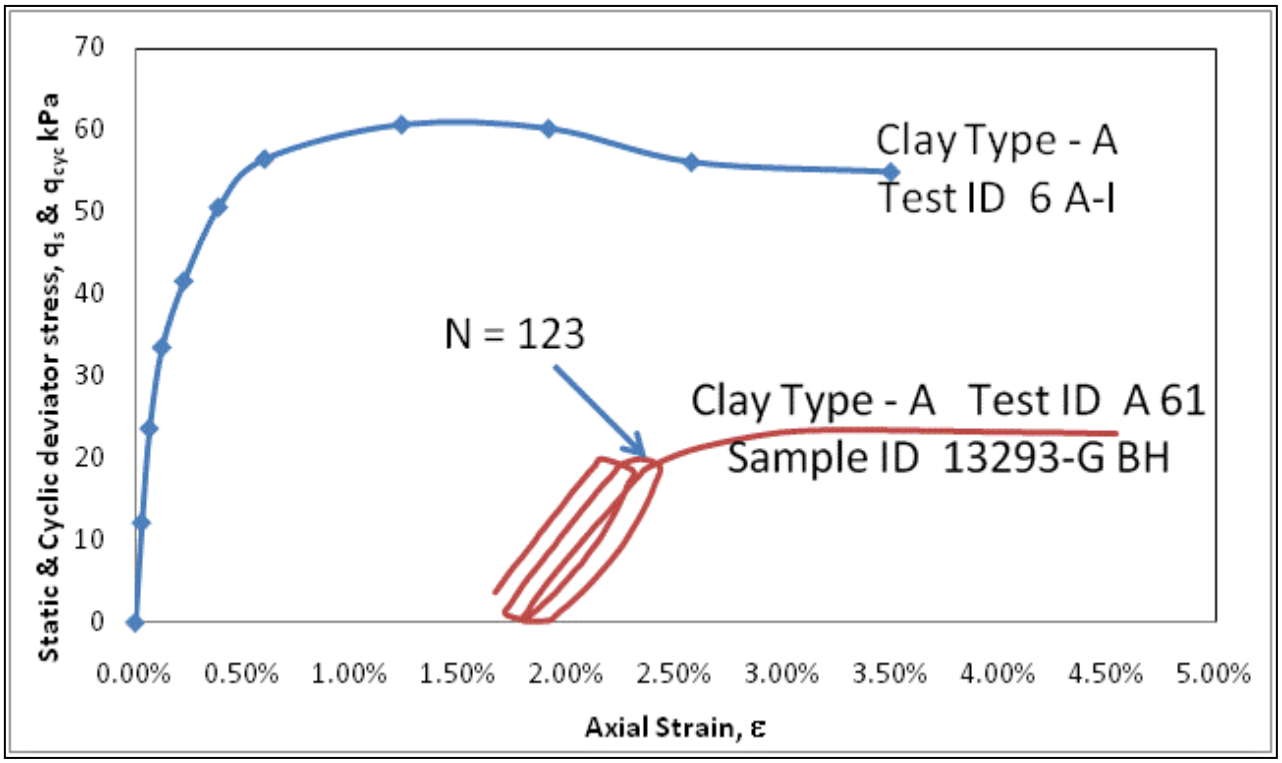

Figure 4.12.1.3: Reduction in shear strength due to cyclic loading Clay Type – A

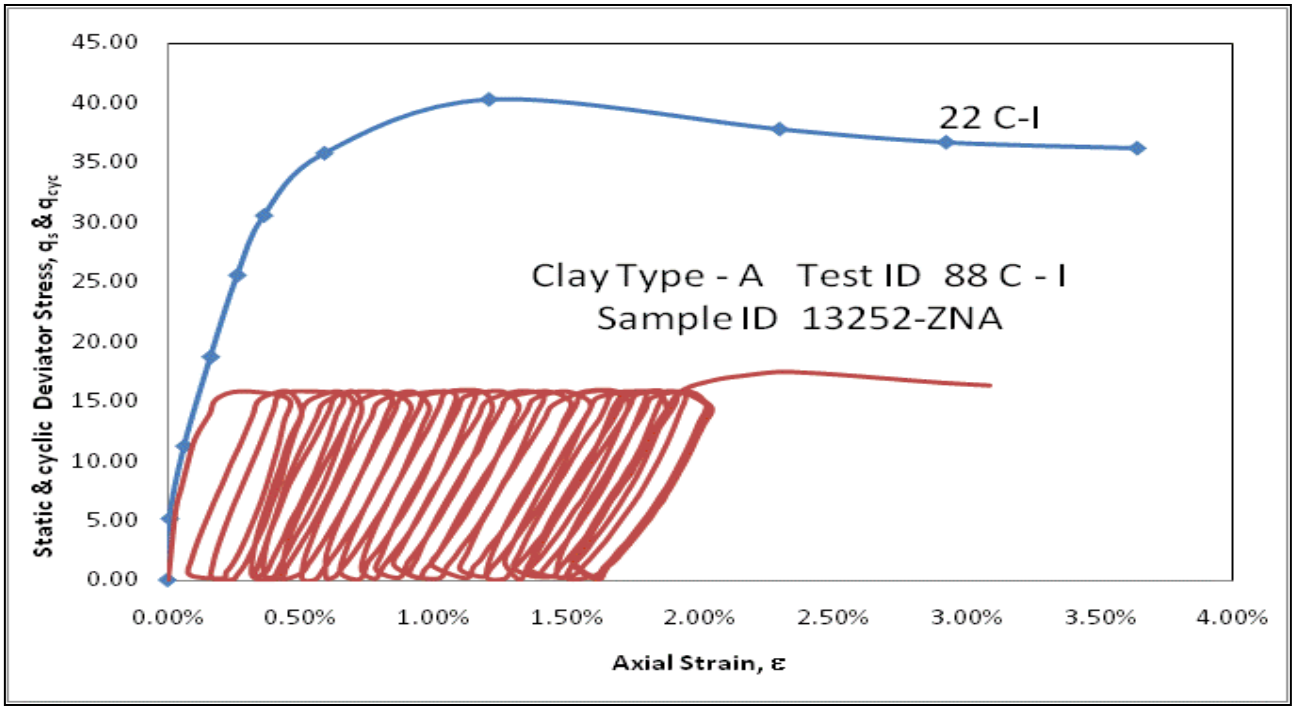

Figure 4.12.1.4: Reduction in shear strength due to cyclic loading Clay Type – C

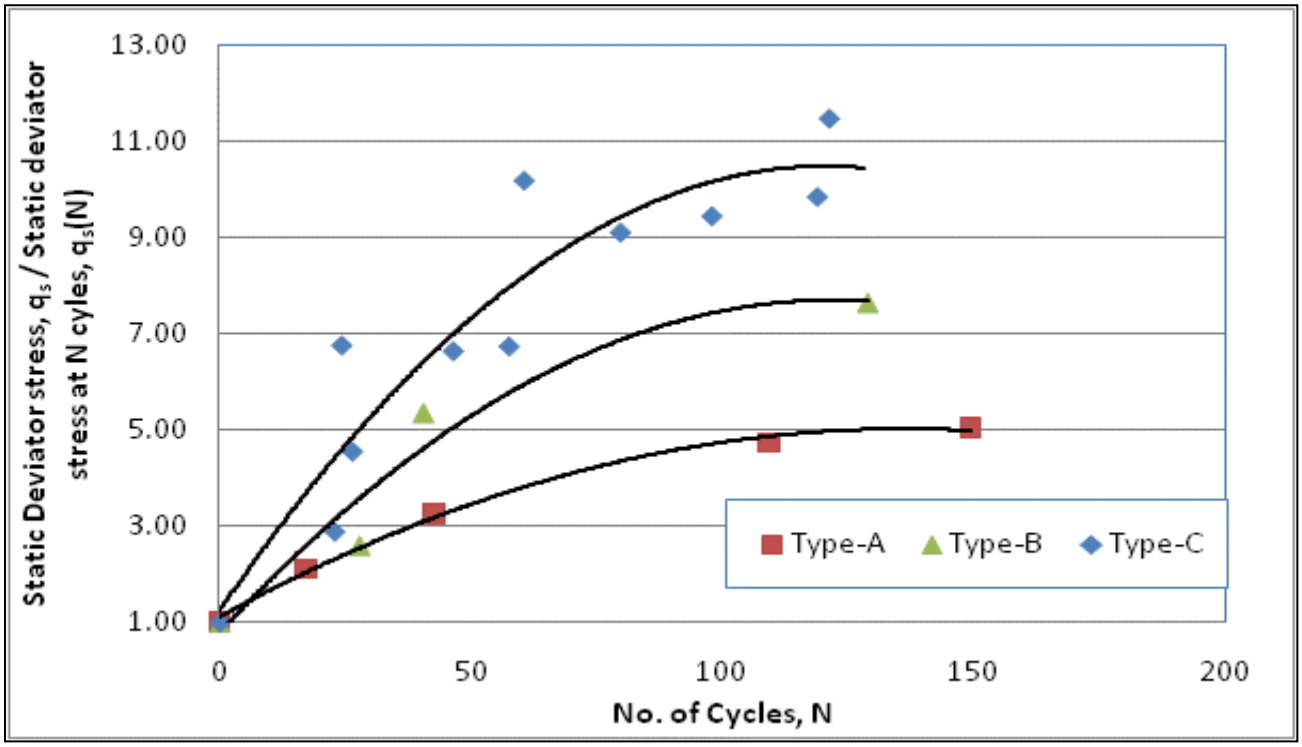

Figure 4.12.1.5: Effect of number of Cycles on static shear strength ratio

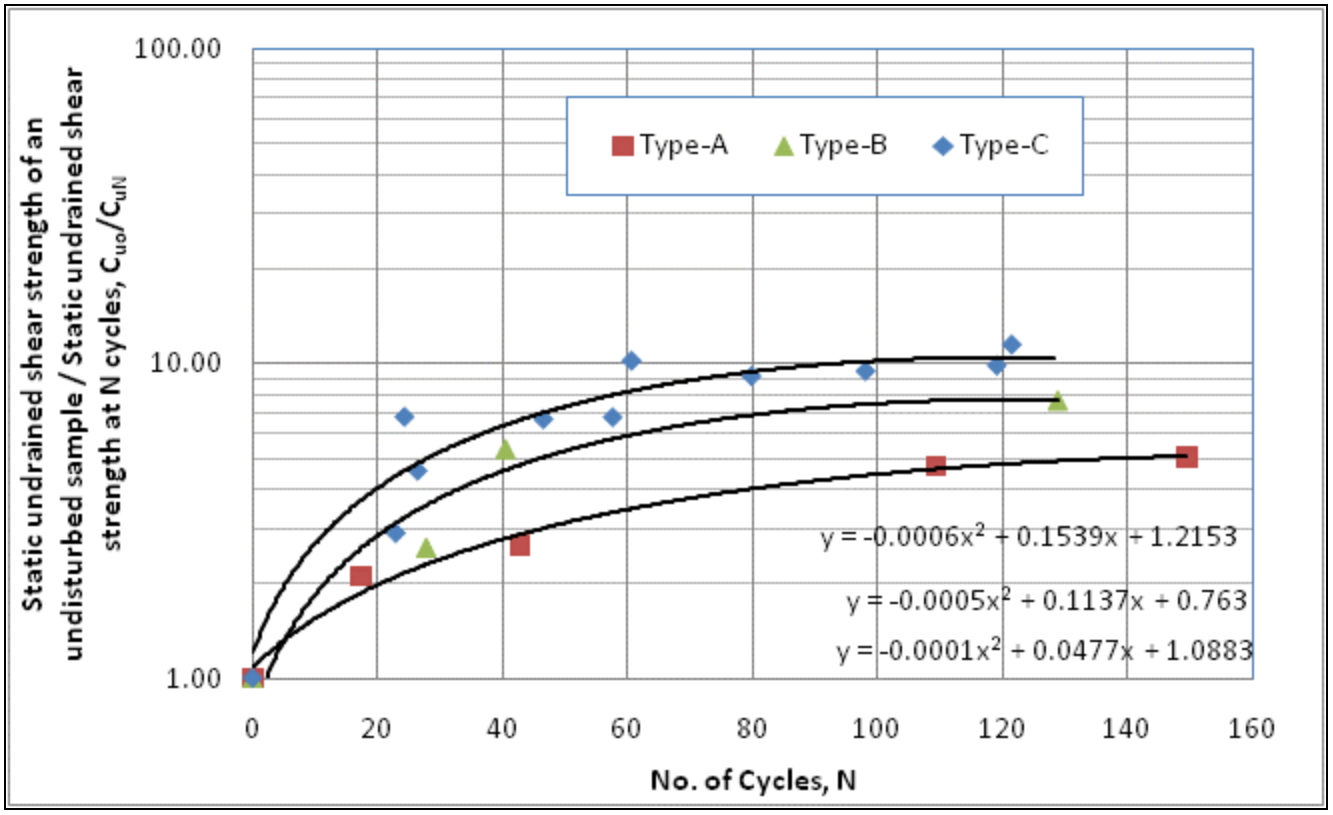

Figure 4.12.1.6: Effect of number of Cycles on static shear strength ratio (log scale)

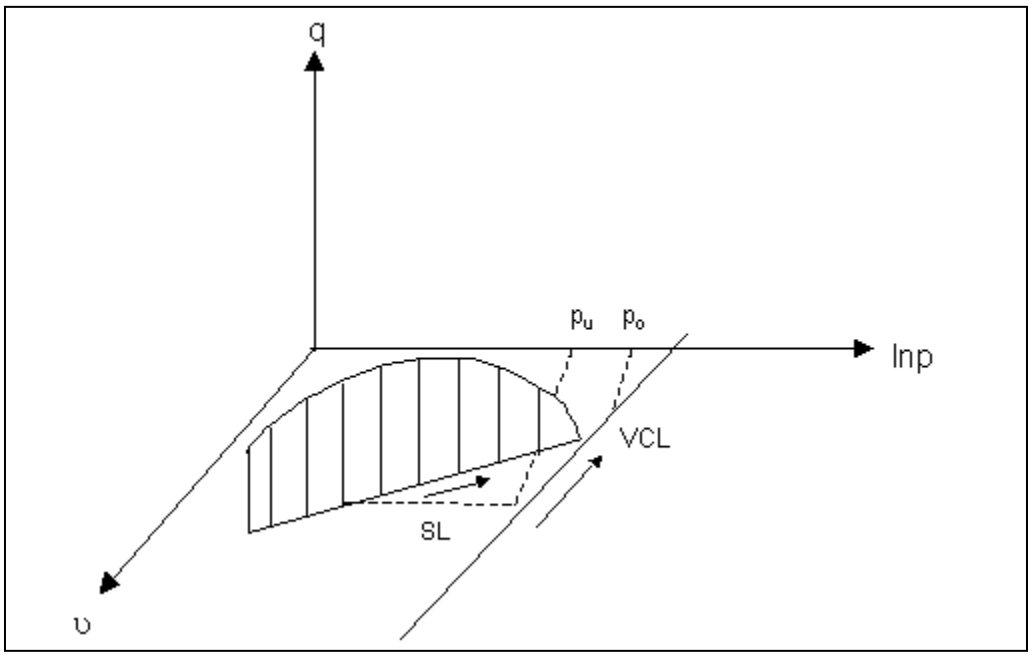

Figure 4.12.2: Consolidation and Yield of Modified Cam Clay Eekelen and Potts, (1978)

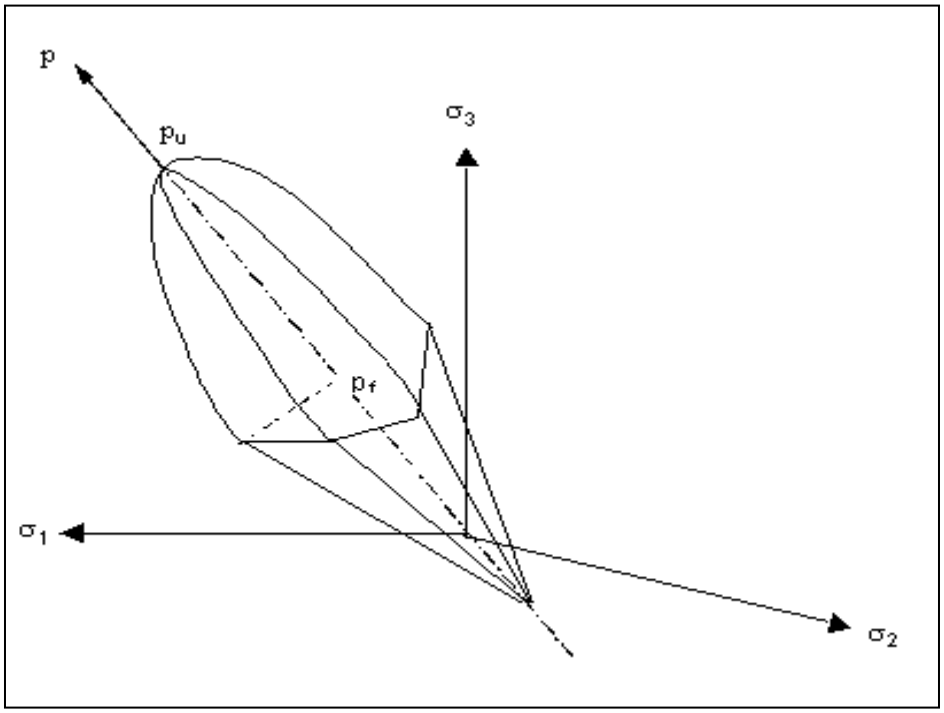

Figure 4.12.3 Stable state boundary surface (SSBS) in three dimensions for one particular value of specific volume (υ). After Eekelen and Potts, (1978)

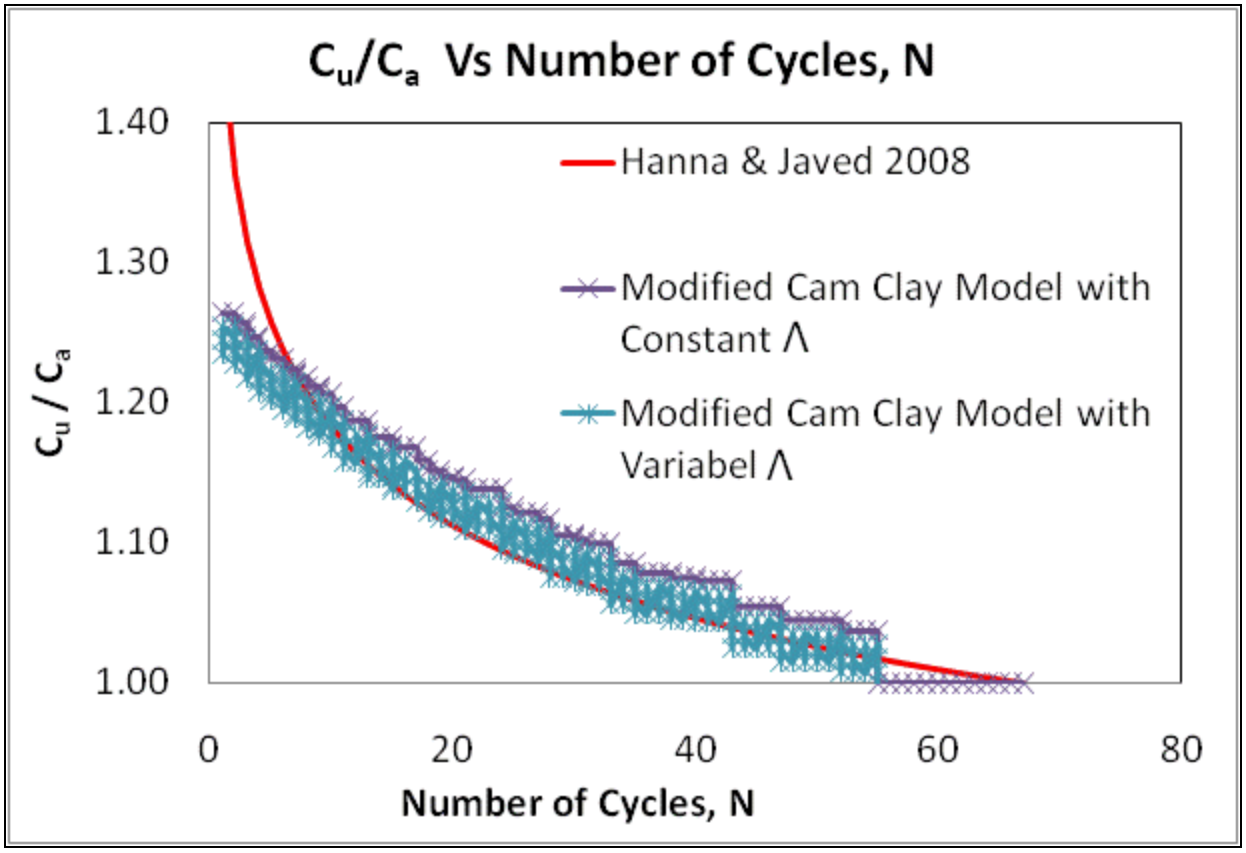

Figure 4.12.4: Shear strength ratio versus number of cycles, N

(Test C20, sample ID 13252_ZNA)

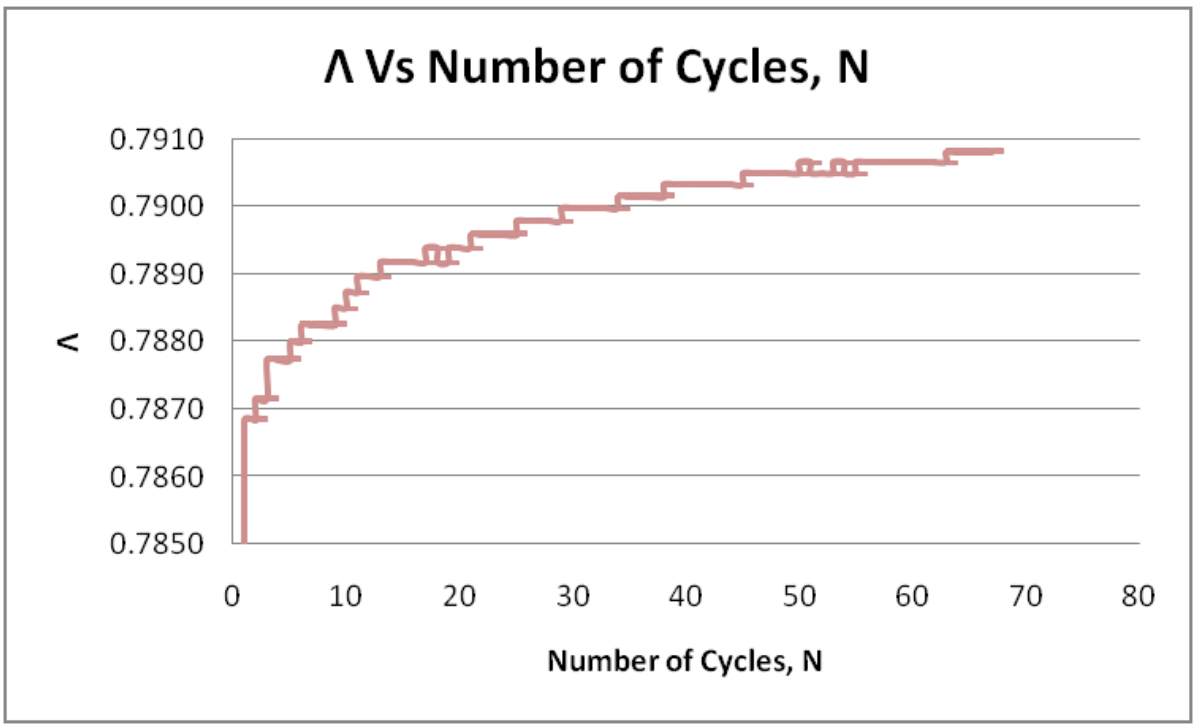

Figure 4.12.5: Variation in parameter (Λ) with the number of cycles, N

(Test C20, sample ID 13252_ZNA)

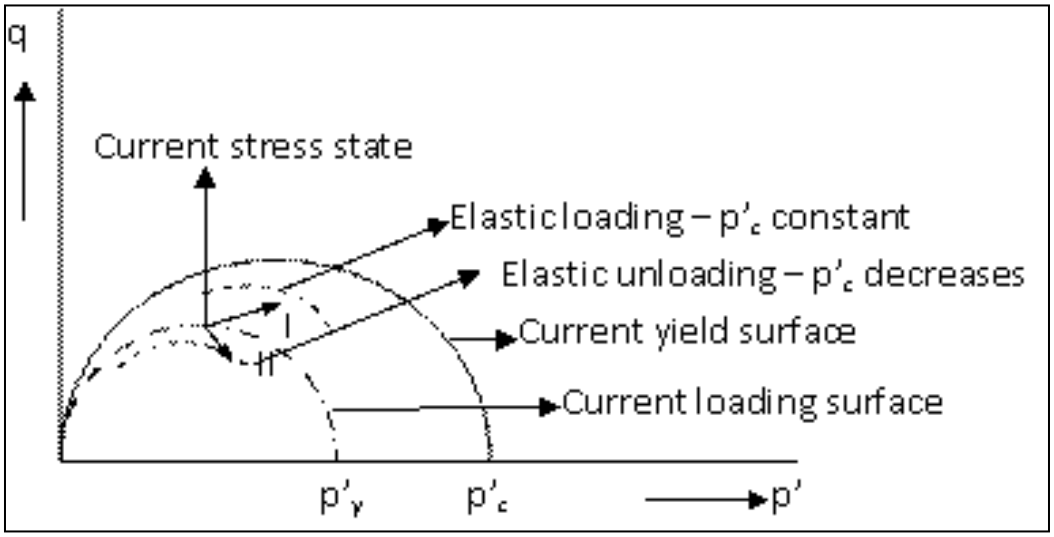

Figure 4.12.6: A typical behavior of consolidating and swelling for p'-q plane

Eekelen and Potts, (1978)

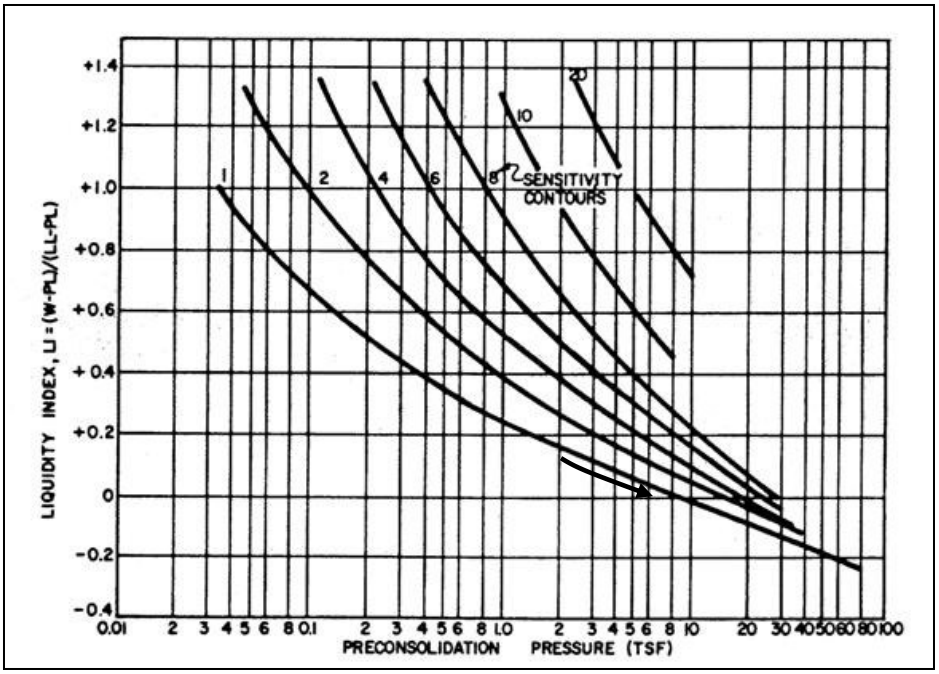

Figure 4.12.7: **Preconsolidation σ'_p Stress as a function of Liquidity Index I_L and clay sensitivity (After NAVFAC DM 7.1)**

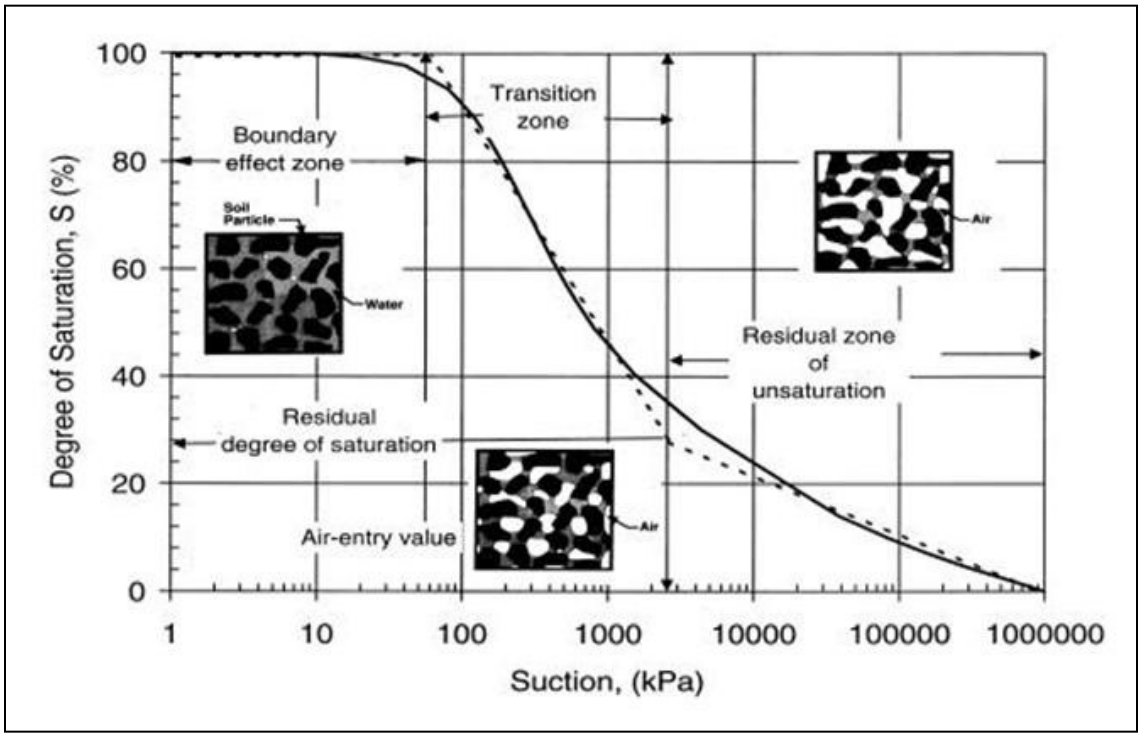

Figure 4.12.8 : Typical soil- water characteristic curve showing zones of desaturation. (Fredlund D.G. and Xing A. 1994)

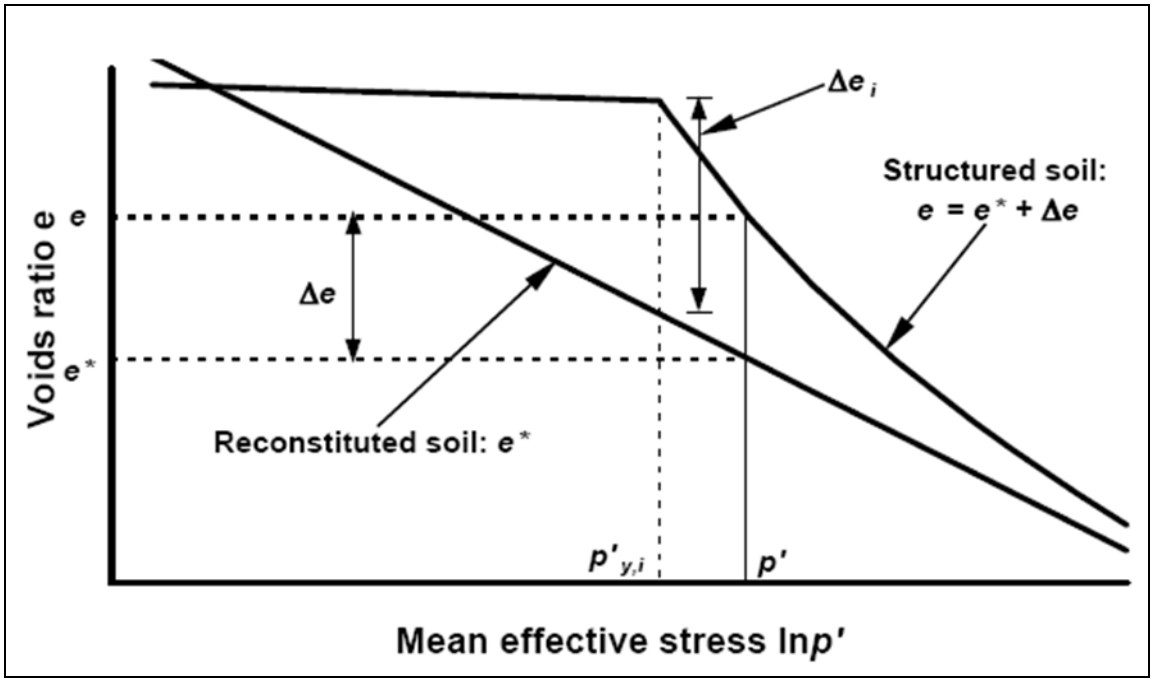

Figure 4.12.9 A typical e-lnp curve for the undisturbed and reconstituted samples (After Liu and Carter, 2002)

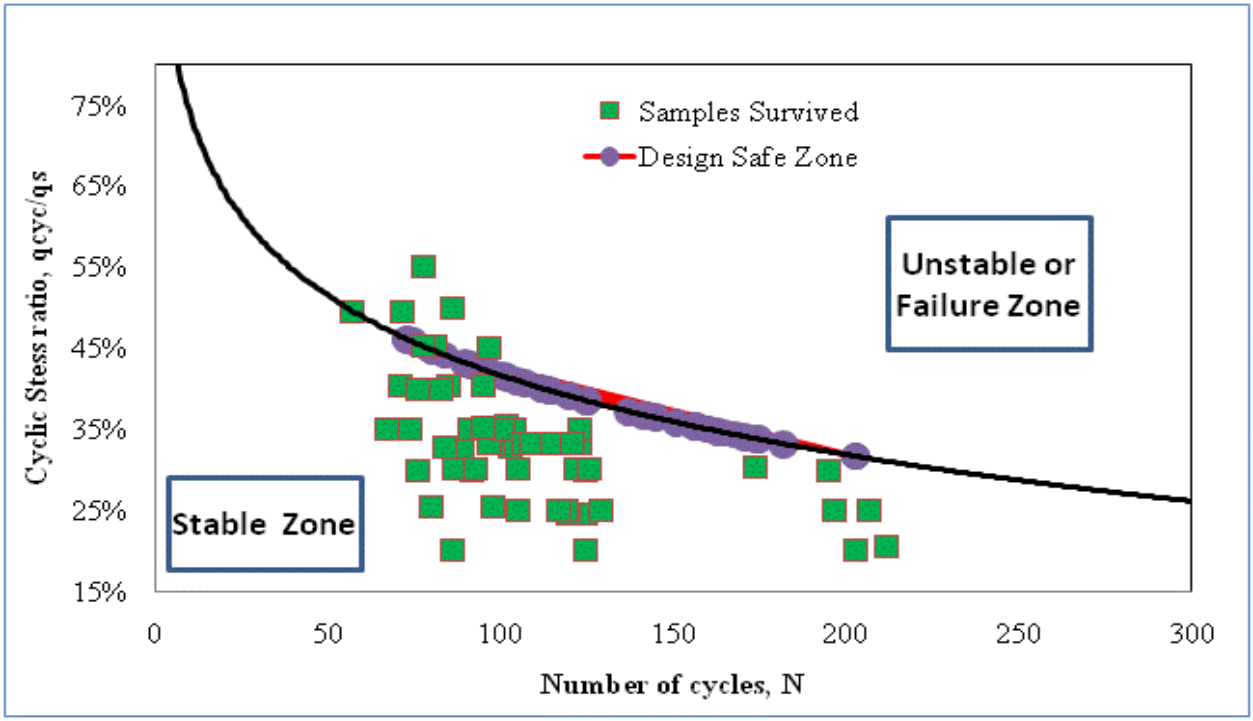

Figure 4.13.1 Designed Safe Zone based on combined effect of physical and mechanical parameters

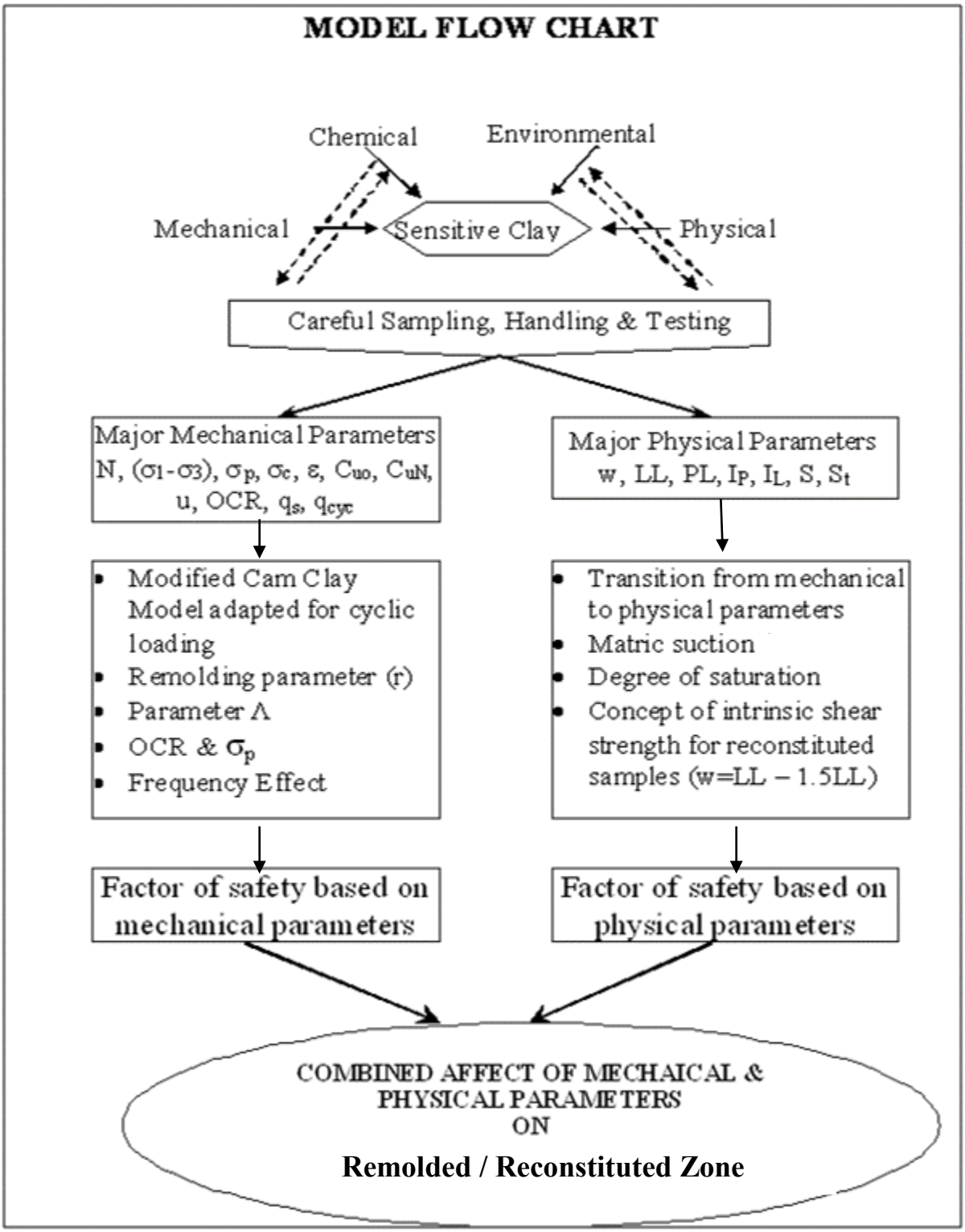

Figure 4.13.2: Flow chart for the proposed guide line to deal with new or examining existing foundations on sensitive clay

Chapter 5

Conclusions and Recommendations

The present research is based on a well-planned and organized experimental program to examine the complexity of the behavior of sensitive clay subjected to cyclic loading. A detailed literature review has identified the study gaps, and accordingly, in formulating well defined objectives for this research. Furthermore, step by step analysis of the experimental data, keeping in view, the complexity involved in dealing with variety of physical and mechanical parameters enhanced the credibility of this study. Based on the results of this study, the following sections of research contribution, limitations, conclusions and recommendations are presented.

5.1 Research Contribution

Chapter One and Two were devoted to an in-depth review of the seminal and contemporary literature on the factors governing the behavior of a sensitive clay and how these characters interrelate with each other when it comes to critical undrained cyclic loading conditions. With the comprehensive overview of the previous studies along with the background of sensitive clay and the different sources contribute in causing disturbances leading to cyclic of loading or repeated load applications (Chapter-1), these chapters functioned to direct the research towards an in-depth experimental exploration of comparatively unexplored issues related to the behavior of sensitive clay subjected to cyclic loading. This thing pops up directly to the question of the present research's contribution to the field the of geotechnical engineering. Some of the main contributions of the current research in the field of geotechnical engineering are as follows;

- Differentiating and prioritizing the role of physical and mechanical parameters in governing the behavior of sensitive clay subjected to cyclic loading.

- The development of a hypothetical model, which explains the behavior of sensitive clay and how its shear strength reduces when subjected to disturbing / remolding action of cyclic loading.
- Developing a Modified Cam Clay Model, which is capable to predict the behavior of sensitive clay subjected to cyclic loading.
- Identify the role of the degree of saturation and the matric suction in case of partially saturated samples on the cyclic shear strength of clay.
- Establishing the safe zone concept for the cases of undrained and drained, which provide a useful technique for designer to determine the condition of the foundation under a given field conditions.

5.2 Limitations of Research

Some of the limitations of this study stem from the method used to obtain undisturbed samples. Furthermore, the difficulties associated in sampling, it can be reported herein that the samples taken for the selected types of clay A, B, C and D were not exactly from the same depths, moreover, the quantity of samples collected for all the selected types were not same. For e.g., only the clay Types A and C had a represent able quantity of required samples. The samples for Types B and D were less and most of them somehow got disturbed. The other important issue is waxing the samples timely and properly which may lead to losing the moisture content, showing a lower value of initial degree of saturation than the actual. As, pertains to methodological approach, the research based on typical classical experimental work.

5.3 Conclusion

Based on the experimental and theoretical investigation performed on the shear strength of sensitive clay, the following can be concluded.

- The behavior of sensitive clay is governed by the four major categories of parameters namely; physical, mechanical, environmental and chemical. For a given region, the effect of environmental and chemical categories will remain unchanged. This research was focused on the role of the physical and mechanical parameters, which govern the behavior of sensitive clay subjected to static and cyclic loading.
- The Physical category includes; natural water content (w), liquid limit (LL), plastic limit (PL), plasticity index (I_P), liquidity index (I_L), sensitivity (S_t), constant of variation in sensitivity (k) and initial degree of saturation (S). Whereas, mechanical category includes; cyclic deviator stress (q_{cyc}), pore water pressure (u), axial strain (ε), over consolidation ratio (OCR), preconsolidation pressure (σ_p), confining pressure (σ_3), and number of cycles (N).
- For a given condition, the threshold cyclic shear strength depends on the sensitivity number. A sample of sensitive clay subjected to cyclic loading attains and will keep on retaining equilibrium or quasi elastic resilient state as long as the magnitude of cyclic deviator stress is below the threshold level for a given degree of saturation and stress conditions
- The effect of frequency is more dominant during the initial cycles, which, diminishes progressively as the number of cycles, N increases. Furthermore, a

decrease in the rate of loading leads to an increase in the accumulated pore pressures with respect to the number of cycles.

- The intrinsic shear strength should be considered as the critical value for estimating the strength parameters for design of the foundation.
- Sensitivity number varies with the liquidity index and pre-consolidation pressures. For design purpose, the value of sensitivity constant, k should be taken between 2 to 3 as it provides good relationship for liquid limit versus sensitivity (S_t) number for the selected ranges of preconsolidation pressure. Also, the preconsolidation pressure σ_p in terms of OCR is an important factor in predicting the shear strength of sensitive clays especially under cyclic loading.
- The undrained fully saturated test represents the critical situation for sensitive clay subjected to cyclic loading due to complete absence of matric suction.
- The degree of saturation is a parameter represents the combined effect of the other physical parameters such as; water content (w), liquid limit (LL), plastic limit (PL), plasticity index (I_P), liquidity index (I_L) and constant of variation in sensitivity (k).
- The proposed hypothetical model together with the Modified Cam Clay Model can be used to determine the step by step reduction in the cyclic shear strength subjected to a given set of governing parameters.
- The safe zones presented in this thesis are based on the combined effect of all the major physical and mechanical parameters which govern the behavior of sensitive clay subjected to static or cyclic loading.

- The identified safe zones together with the theoretical model developed herein constitute a valuable tool for design foundation on sensitive clay subjected to cyclic loading. Also can be used to examine the condition of an existing foundation.

5.4 Recommendation for the future work

- Triaxial static and cyclic compression test should be attempted on partially saturated samples, having degree of saturation ranging 50% to 90%. Such an experimental work will help in establishing line of demarcation between samples, which gain strength due to matric suction and the samples which become more vulnerable to failure due to the absence of water molecules. Hence, concept of threshold value of degree of saturation can be introduced
- Using the safe zone technique and probability analysis such as "Confidence Limits", a comparison among the various cost effective techniques for laying new or strengthening existing foundations on sensitive clay should be attempted.

REFERENCES

Ansal, M. and Erken, A. 1989. Undrained Behavior of Clay under Cyclic Shear Stresses. ASCE, Journal of Geotechnical Engineering, 115 (7), pp 968-981.

Bjerrum, L., 1954. Geotechnical Properties of Norwegian Marine Clays. Geotechnique, 4 (2), pp. 49-69.

Berre, T. (1981). Triaxial testing at NGI. Geotechnical Testing Journal, Vol. 5, 1982, No. 1/2, pp. 3-17.

Chagnon, J.Y., Lebuis, J., Allard, J.D. and Robert, J.M. 1979. Sensitive Clays, Unstable Slopes, Corrective works and Slides in the Quebec and Shawinigan Area. Geological Association of Canada.

Das, Braja, M., Fundamentals of Soil Dynamics, Elver Science Publishers Co., Inc, New York, NY, 1983

Das, Braja, M. (2001). Priciples of Geotecnical Engineering" Fifth Edition,

Eden, WJ, 1971. Sampler Trials in Overconsolidated Sensitive Clay Research Council of Canada, Ont.

Eekelen, H.A.M., and Potts, D.M., 1978. The behavior of Drammen Clay under cyclic loading. Geotechnique 28 (2), pp. 173-196.

Erken, A., and Ulker, C., 2006 Effect of cyclic loading on monotonic shear strength of fine-grained soils. Engineering Geology Volume 89, Issues 3-4, 6. Accepted 25 October 2006., Pages 243-257

Finn, W. D. Liam, Aspects of Constant Volume Cyclic Simple Shear, Advances in the Art of Testing Soils Under Cyclic Conditions, American Society of Civil Engineers, New York, NY, 1985

Fredlund D.G. and Xing A. 1994. Equations for the soil characteristics curve. Canada Geotechnical Journal J. 31. 521-532

Hanna, A.M., and Javid, K. 2008. Foundations on Sensitive Clay Subjected to Cyclic Loading. ASCE, Journal of Geotechnical and Geo-environmental Engineering, 134 (7)

Houstan, W.N., and Hermann, H.G., 1980. Undrained Cyclic Strength of Marine Soils. Journal of Geotechnical Engineering. 106, No. GT6, pp. 691-711.

Hyodo, M., Yamamoto, Y., and Sugiyama, M., 1994. Undrained cyclic shear behavior of normally consolidated clay subjected to initial static shear stress. Soil and Foundations 34 (4), pp. 1-11.

Iwasaki, T., Tatsuoka, F., and Takagi, Y. 1978. Shear modulus of sands under cyclic torsional shear loading," Soils and Found. 18 (1), pp. 39-50

J, Zhou., and X, Gong., 2001. Strain degradation of saturated clay under cyclic loading. Canadian Geotechnical Journal, Volume 38, Number 1, February 2001 , pp. 208-212(5)

Lacasse, S. and T. Berre (1988). Triaxial testing methods for soils. State-of-the-art paper. ASTM, Special Technical Publication, 977, pp. 264-289.

Lefebvre, G., and LeBoeuf, D., 1987. Rate Effects and Cyclic Loading of Sensitive Clays. Journal of Geotechnical Engineering, 113 (5), pp. 476-489.

Lefebvre, G., and Pfendler, P., 1996. Strain Rate and Pre-Shear Effects in Cyclic Resistance of Soft Clay. ASCE, Journal of Geotechnical Engineering, 122 (1), pp. 21-26.

(Lefebvre and Poulin 1979). CHAPTER 3 sherbrooke sampler…….

Leroueil, S., Tavenas, F., and Le Bihan, J.P. 1983. Propriétés caractéristiques des argiles de l'est du Canada. Canadian Geotechnical Journal, 20(4): 681–705.

Li, Tao., and Meissner Helmut., 2002. Two-Surface Plasticity Model for Cyclic Undrained Behavior of Clays. . Geotech. and Geoenvir. Engrg., Volume 128, Issue 7, pp. 613-626 (July 2002)

Liang, R.Y., and Ma, F., 1991. Anisotropic plasticity Model for Undrained Cyclic Behavior of Clays. Journal of Geotechnical Engineering, 118 (2), pp. 229-243.

Liu, Martin D and Carter, John P., 2002. A Structured Cam Clay Model. Center of Geotechnical Research, Report No R814.

Matsui, T. Ohara, H., and Itlo, T. 1980. Cyclic stress-strain history and shear characteristics of clays. ASCE, Journal Geotechnical Engineering, 106 (10) pp. 1101-1120.

McK Yes,E., Sethi, A. And Yong, R.N. 1973. Amorphous Coatings on Particles of Sensitive Clay Soils.Clay and Clay Minerals, Vol. 22, pp. 427 – 433.

Miller. G.A., The, S.Y., Li, D., and Zaman, M.M., 2000. Cyclic Shear Strength of Soft Railroad Subgrade. ASCE, Journal of Geotechnical and Geoenvironmental Engineering, 126 (2), pp. 139-147.

Min, CHEN Yun., Mei-xiu, JI., and Bo, H., 2004. Effect of Cyclic Loading Frequency on Undrained Behaviors of Undisturbed Marine Clay. Journal-China Ocean Engineering 2004.

Oak, Fusao,. Takeshi Kodaka, Takeshi., and [1], Kim, Yong-Seong., 2003. A cyclic viscoelastic-viscoplastic constitutive model for clay and liquefaction analysis of multi-layered

ground. [1]Department of Civil and Earth Resources Engineering, Graduate School of Engineering, Kyoto University, Yoshida Hon-machi, Sakyo-ku, Kyoto 606-8501, Japan.

Prakash, Shamsher, Soil Dynamics, McGraw-Hill, Inc., 1981

Procter, D.C., and Khaffaf, J.H., 1984. Weakening of Undrained Saturated Clays Under Cyclic Loading. Journal of Geotechnical Engineering, Vol. 110, No. 10, pp. 1431-1445.

Reilly, M.P.O and Brown, S.F. 1991. Cyclic Loading of Soils: "From Theory to Design"

Sangrey, D. A., Henckel, D.J., and Esring, M.L., 1969. The Effective Stress Response of a Saturated Clay Soil to Repeated Loading. Canadian Geotechnical Journal, 6 (3), pp. 241-251.

Seed, H.B., and Idriss, I.M., 1981. Ground Motions and Soil Liquefaction During Earthquakes, Earthquake Engineering Research Institute, Oakland, California, Monograph Series, pp. 134.

Silvestri V, 1994. Water Content Relationships of a Sensitive Clay Subjected to Cycles of Capillary Pressures, Volume Geotechnical Testing Journal, Vol. 17, Issue 1 (March 1994).

Silvestri V, 1981. Behavior of an Overconsolidated Sensitive Clay in Drained K^0-Triaxial Tests, Assistant Professor, Department of Civil Engineering, Ecole Polytechnique, P. Q. Published: Jan 1981

Skempton, A.W., 1957. A contribution to the settlement Analysis of Foundations on Clay. Geotechnique, 7 (1), pp. 168.

Wood, D.M., 1990. Soil Behavior and Critical State Soil Mechanics. Cambridge University Press.

Scholey GK, Frost JD, Lo Presti DCF, Jamiolkowski M, A Review of Instrumentation for Measuring Small Strains During Triaxial Testing of Soil Specimens, ASTM Geotechnical Testing Journal, Vol 18, No. 2, pp. 137- 156, 1995.

Thammathiwat, A., and Chim-oye, W., 2004. Behavior of Strength and Pore Pressure of Soft Bangkok Clay under Cyclic Loading. Journal of Science and Technology, Vol. 9, No. 4, October-December 2004

Theris, G.R., and Seed, H.B., 1969. "Strength and Stress – Strain Characteristics of Clays Subjected to Seismic Loading Conditions." Vibration Effects of Earthqaukes on Soils and Foundations, Special Technical Publication 450, ASTM, 1969. Pp. 3-56.

Terzaghi Karl, Brazelton Ralph and Mesri Gholamreza (1944/1947) Published third edition 1995. " Soil Mechanics in Engineering Practice"

Vinod K. Garga, Mahbubul A. Khan and Sai K. Vanapalli (2005)Stress-path dependent behavior of a weathered clay crust Department of Civil Engineering, University of Ottawa, 161 Louis Pasteur, Ottawa, Ontario, K1N 6N5, Canada

Yu, H. S. (1997). A unified state parameter model for clay and sand. Department of Civil Engineering and Surveying. University of Newcastle, N.S.W. 2308, Australia.

APPENDIX –I
Cyclic loading Model for Sensitive Clay
Use of Modified Cam Clay Model

Cyclic Triaxial Compression Test
Test Id C20 Sample Id 13252_ZNA-

N	ϵ_A	Δu	Hanna & Javed, 2008 Λ F.O.S I	Constt Λ F.O.S II	Variable Λ F.O.S III	Constt Λ b	Variable Λ b	Λ
1	0.00	0.00	1.45	1.26	1.30	0.630	0.641	0.0450
2	0.21	0.40	1.36	1.26	1.30	0.630	0.640	0.7868
3	0.21	11.74	1.31	1.26	1.29	0.630	0.640	0.7871
4	0.22	28.29	1.28	1.25	1.28	0.630	0.639	0.7877
5	0.22	43.46	1.26	1.24	1.26	0.630	0.639	0.7877
6	0.23	51.05	1.24	1.23	1.26	0.630	0.639	0.7880
7	0.23	60.70	1.22	1.23	1.25	0.630	0.639	0.7882
8	0.23	68.97	1.21	1.22	1.24	0.630	0.639	0.7882
9	0.23	77.25	1.19	1.21	1.23	0.630	0.639	0.7882
10	0.24	83.45	1.18	1.21	1.23	0.630	0.639	0.7885
11	0.24	93.79	1.17	1.20	1.22	0.630	0.638	0.7887
12	0.25	104.14	1.16	1.19	1.21	0.630	0.638	0.7890
13	0.25	104.14	1.16	1.19	1.21	0.630	0.638	0.7890
14	0.25	115.17	1.15	1.18	1.19	0.630	0.638	0.7892
15	0.25	115.17	1.14	1.18	1.19	0.630	0.638	0.7892
16	0.25	122.06	1.13	1.17	1.18	0.630	0.638	0.7892
17	0.25	122.06	1.13	1.17	1.18	0.630	0.638	0.7892
18	0.26	129.65	1.12	1.16	1.17	0.630	0.638	0.7894
19	0.25	135.16	1.12	1.15	1.17	0.630	0.638	0.7892
20	0.26	138.61	1.11	1.15	1.16	0.630	0.638	0.7894
21	0.26	139.99	1.11	1.15	1.16	0.630	0.638	0.7894
22	0.26	144.82	1.10	1.14	1.15	0.630	0.638	0.7896
23	0.26	144.82	1.10	1.14	1.15	0.630	0.638	0.7896
24	0.26	144.82	1.09	1.14	1.15	0.630	0.638	0.7896
25	0.26	153.09	1.09	1.13	1.14	0.630	0.638	0.7896
26	0.27	155.16	1.09	1.12	1.13	0.630	0.638	0.7898
27	0.27	155.16	1.08	1.12	1.13	0.630	0.638	0.7898
28	0.27	157.92	1.08	1.12	1.13	0.630	0.638	0.7898
29	0.27	164.12	1.08	1.11	1.11	0.630	0.638	0.7898
30	0.27	164.12	1.07	1.11	1.11	0.630	0.638	0.7900
31	0.27	165.50	1.07	1.10	1.11	0.630	0.638	0.7900
32	0.27	166.88	1.07	1.10	1.11	0.630	0.638	0.7900
33	0.27	166.88	1.06	1.10	1.11	0.630	0.638	0.7900
34	0.27	173.09	1.06	1.09	1.09	0.630	0.638	0.7900
35	0.28	173.09	1.06	1.09	1.09	0.630	0.637	0.7901
36	0.28	175.85	1.06	1.08	1.09	0.630	0.637	0.7901
37	0.28	175.85	1.05	1.08	1.09	0.630	0.637	0.7901
38	0.28	175.85	1.05	1.08	1.09	0.630	0.637	0.7901
39	0.28	177.22	1.05	1.08	1.08	0.630	0.637	0.7903
40	0.28	177.22	1.05	1.08	1.08	0.630	0.637	0.7903
41	0.28	177.91	1.04	1.07	1.08	0.630	0.637	0.7903
42	0.28	177.91	1.04	1.07	1.08	0.630	0.637	0.7903
43	0.28	177.91	1.04	1.07	1.08	0.630	0.637	0.7903
44	0.28	184.12	1.04	1.05	1.06	0.630	0.637	0.7903
45	0.28	184.12	1.04	1.05	1.06	0.630	0.637	0.7903
46	0.29	184.12	1.03	1.05	1.06	0.630	0.637	0.7905
47	0.29	184.12	1.03	1.05	1.06	0.630	0.637	0.7905
48	0.29	186.88	1.03	1.05	1.05	0.630	0.637	0.7905
49	0.29	186.88	1.03	1.05	1.05	0.630	0.637	0.7905
50	0.29	186.88	1.03	1.05	1.05	0.630	0.637	0.7905
51	0.29	186.88	1.02	1.05	1.05	0.630	0.637	0.7907
52	0.29	186.88	1.02	1.05	1.05	0.630	0.637	0.7905
53	0.29	188.95	1.02	1.04	1.04	0.630	0.637	0.7905
54	0.29	188.95	1.02	1.04	1.04	0.630	0.637	0.7907
55	0.29	188.95	1.02	1.04	1.04	0.630	0.637	0.7905
56	0.29	196.53	1.02	1.00	1.00	0.630	0.637	0.7907
57	0.29	196.53	1.01	1.00	1.00	0.630	0.637	0.7907
58	0.29	196.53	1.01	1.00	1.00	0.630	0.637	0.7907
59	0.29	196.53	1.01	1.00	1.00	0.630	0.637	0.7907
60	0.29	196.53	1.01	1.00	1.00	0.630	0.637	0.7907
61	0.29	196.53	1.01	1.00	1.00	0.630	0.637	0.7907
62	0.29	196.53	1.01	1.00	1.00	0.630	0.637	0.7907
63	0.29	196.53	1.01	1.00	1.00	0.630	0.637	0.7907
64	0.30	196.53	1.00	1.00	1.00	0.630	0.637	0.7908
65	0.30	196.53	1.00	1.00	1.00	0.630	0.637	0.7908
66	0.30	196.53	1.00	1.00	1.00	0.630	0.637	0.7908
67	0.30	196.53	1.00	1.00	1.00	0.630	0.637	0.7908

LOADING-ZERO DEVIATOR STRESS

N	ϵ_A	Δu	Hanna & Javed, 2008 Λ F.O.S I	Constt Λ F.O.S II	Variable Λ F.O.S III	Constt Λ b	Variable Λ b	Λ
1	0.19	0.30	1.45	1.26	1.30	0.630	0.641	0.7858
2	0.23	0.40	1.36	1.26	1.29	0.630	0.639	0.7882
3	0.25	17.26	1.31	1.25	1.28	0.630	0.638	0.7890
4	0.25	31.05	1.28	1.25	1.27	0.630	0.638	0.7892
5	0.26	44.15	1.26	1.24	1.26	0.630	0.638	0.7894
6	0.26	51.05	1.24	1.23	1.25	0.630	0.638	0.7896
7	0.27	64.84	1.22	1.22	1.24	0.630	0.638	0.7898
8	0.27	68.97	1.21	1.22	1.24	0.630	0.638	0.7900
9	0.27	77.25	1.19	1.21	1.23	0.630	0.638	0.7900
10	0.27	83.45	1.18	1.21	1.23	0.630	0.638	0.7900
11	0.28	93.79	1.17	1.20	1.21	0.630	0.637	0.7901
12	0.28	104.14	1.16	1.19	1.20	0.630	0.637	0.7901
13	0.29	104.14	1.16	1.19	1.20	0.630	0.637	0.7907
14	0.29	115.17	1.15	1.18	1.19	0.630	0.637	0.7907
15	0.29	115.17	1.14	1.18	1.19	0.630	0.637	0.7907
16	0.29	122.06	1.13	1.17	1.18	0.630	0.637	0.7907
17	0.29	129.65	1.13	1.16	1.17	0.630	0.637	0.7905
18	0.30	135.16	1.12	1.15	1.16	0.630	0.637	0.7908
19	0.30	135.16	1.12	1.15	1.16	0.630	0.637	0.7908
20	0.30	138.61	1.11	1.15	1.16	0.630	0.637	0.7908
21	0.30	139.99	1.11	1.15	1.16	0.630	0.637	0.7910
22	0.30	144.82	1.10	1.14	1.15	0.630	0.637	0.7910
23	0.30	144.82	1.10	1.14	1.15	0.630	0.637	0.7910
24	0.30	144.82	1.09	1.14	1.15	0.630	0.637	0.7910
25	0.30	153.09	1.09	1.13	1.13	0.630	0.637	0.7910
26	0.31	155.16	1.09	1.12	1.13	0.630	0.637	0.7911
27	0.31	155.16	1.08	1.12	1.13	0.630	0.637	0.7912
28	0.31	157.92	1.08	1.12	1.13	0.630	0.637	0.7912
29	0.31	164.12	1.08	1.11	1.11	0.630	0.637	0.7912
30	0.31	164.12	1.07	1.11	1.11	0.630	0.637	0.7912
31	0.31	165.50	1.07	1.10	1.11	0.630	0.637	0.7912
32	0.32	166.88	1.07	1.10	1.11	0.630	0.636	0.7914
33	0.32	166.88	1.06	1.10	1.11	0.630	0.636	0.7914
34	0.32	173.09	1.06	1.09	1.09	0.630	0.636	0.7914
35	0.32	173.09	1.06	1.09	1.09	0.630	0.636	0.7914
36	0.32	175.85	1.06	1.08	1.08	0.630	0.636	0.7915
37	0.32	175.85	1.05	1.08	1.08	0.630	0.636	0.7915
38	0.32	175.85	1.05	1.08	1.08	0.630	0.636	0.7915
39	0.32	177.22	1.05	1.08	1.08	0.630	0.636	0.7915
40	0.32	177.22	1.05	1.08	1.08	0.630	0.636	0.7915
41	0.33	177.91	1.04	1.07	1.08	0.630	0.636	0.7916
42	0.33	177.91	1.04	1.07	1.08	0.630	0.636	0.7916
43	0.33	177.91	1.04	1.07	1.08	0.630	0.636	0.7916
44	0.33	184.12	1.04	1.05	1.06	0.630	0.636	0.7916
45	0.33	184.12	1.04	1.05	1.06	0.630	0.636	0.7916
46	0.33	184.12	1.03	1.05	1.06	0.630	0.636	0.7916
47	0.33	184.12	1.03	1.05	1.06	0.630	0.636	0.7918
48	0.33	186.88	1.03	1.05	1.05	0.630	0.636	0.7918
49	0.33	186.88	1.03	1.05	1.05	0.630	0.636	0.7918
50	0.33	186.88	1.03	1.05	1.05	0.630	0.636	0.7918
51	0.33	186.88	1.02	1.05	1.05	0.630	0.636	0.7918
52	0.33	186.88	1.02	1.05	1.05	0.630	0.636	0.7918
53	0.33	188.95	1.02	1.04	1.04	0.630	0.636	0.7918
54	0.33	188.95	1.02	1.04	1.04	0.630	0.636	0.7918
55	0.34	188.95	1.02	1.04	1.04	0.630	0.636	0.7919
56	0.34	196.53	1.02	1.00	1.00	0.630	0.636	0.7919
57	0.34	196.53	1.01	1.00	1.00	0.630	0.636	0.7919
58	0.33	196.53	1.01	1.00	1.00	0.630	0.636	0.7918
59	0.34	196.53	1.01	1.00	1.00	0.630	0.636	0.7919
60	0.34	196.53	1.01	1.00	1.00	0.630	0.636	0.7919
61	0.35	196.53	1.01	1.00	1.00	0.630	0.636	0.7921
62	0.34	196.53	1.01	1.00	1.00	0.630	0.636	0.7919
63	0.34	196.53	1.01	1.00	1.00	0.630	0.636	0.7920
64	0.34	196.53	1.00	1.00	1.00	0.630	0.636	0.7920
65	0.34	196.53	1.00	1.00	1.00	0.630	0.636	0.7920
66	0.34	196.53	1.00	1.00	1.00	0.630	0.636	0.7920
67	0.34	196.53	1.00	1.00	1.00	0.630	0.636	0.7920

LOADING- DEVIATOR STRESS = 20 kPa

N	ϵ_A	Δu	Hanna & Javed, 2008 Λ F.O.S I	Constt Λ F.O.S II	Variable Λ F.O.S III	Constt Λ b	Variable Λ b	Λ
1	0.25	0.30	1.45	1.26	1.29	0.630	0.638	0.7892
2	0.29	0.40	1.36	1.26	1.29	0.630	0.637	0.7907
3	0.30	17.26	1.31	1.25	1.28	0.630	0.637	0.7910
4	0.31	31.05	1.28	1.25	1.27	0.630	0.637	0.7911
5	0.31	51.05	1.26	1.23	1.25	0.630	0.637	0.7912
6	0.32	51.05	1.24	1.23	1.25	0.630	0.636	0.7914
7	0.32	64.84	1.22	1.22	1.24	0.630	0.636	0.7915
8	0.33	77.25	1.21	1.21	1.23	0.630	0.636	0.7916
9	0.33	79.31	1.19	1.21	1.23	0.630	0.636	0.7916
10	0.33	93.79	1.18	1.20	1.21	0.630	0.636	0.7916
11	0.33	93.79	1.17	1.20	1.21	0.630	0.636	0.7918
12	0.34	104.14	1.16	1.19	1.20	0.630	0.636	0.7919
13	0.34	111.03	1.16	1.18	1.19	0.630	0.636	0.7920
14	0.35	115.17	1.15	1.18	1.19	0.630	0.636	0.7921
15	0.35	120.69	1.14	1.17	1.18	0.630	0.636	0.7921
16	0.35	122.06	1.13	1.17	1.18	0.630	0.636	0.7921
17	0.35	129.65	1.13	1.16	1.17	0.630	0.636	0.7922
18	0.35	135.16	1.12	1.15	1.16	0.630	0.636	0.7922
19	0.35	135.16	1.12	1.15	1.16	0.630	0.636	0.7922
20	0.35	138.61	1.11	1.15	1.16	0.630	0.636	0.7922
21	0.36	139.99	1.11	1.15	1.15	0.630	0.636	0.7923
22	0.36	144.82	1.10	1.14	1.15	0.630	0.636	0.7923
23	0.36	144.82	1.10	1.14	1.15	0.630	0.636	0.7925
24	0.36	153.09	1.09	1.13	1.13	0.630	0.636	0.7925
25	0.36	153.09	1.09	1.13	1.13	0.630	0.636	0.7925
26	0.37	155.16	1.09	1.12	1.13	0.630	0.636	0.7926
27	0.37	155.16	1.08	1.12	1.13	0.630	0.636	0.7926
28	0.37	157.92	1.08	1.12	1.12	0.630	0.636	0.7927
29	0.37	164.12	1.08	1.11	1.11	0.630	0.636	0.7927
30	0.37	164.12	1.07	1.11	1.11	0.630	0.636	0.7927
31	0.37	165.50	1.07	1.10	1.11	0.630	0.636	0.7927
32	0.37	166.88	1.07	1.10	1.11	0.630	0.636	0.7927
33	0.37	166.88	1.06	1.10	1.11	0.630	0.636	0.7927
34	0.37	173.09	1.06	1.09	1.09	0.630	0.636	0.7927
35	0.38	173.09	1.06	1.09	1.09	0.630	0.635	0.7927
36	0.38	175.85	1.06	1.08	1.08	0.630	0.635	0.7927
37	0.38	175.85	1.05	1.08	1.08	0.630	0.635	0.7927
38	0.38	175.85	1.05	1.08	1.08	0.630	0.635	0.7928
39	0.38	177.22	1.05	1.08	1.08	0.630	0.635	0.7927
40	0.38	177.91	1.05	1.07	1.08	0.630	0.635	0.7928
41	0.39	177.91	1.04	1.07	1.08	0.630	0.635	0.7929
42	0.38	177.91	1.04	1.07	1.08	0.630	0.635	0.7928
43	0.39	177.91	1.04	1.07	1.08	0.630	0.635	0.7929
44	0.39	184.12	1.04	1.05	1.06	0.630	0.635	0.7929
45	0.39	184.12	1.04	1.05	1.06	0.630	0.635	0.7929
46	0.39	184.12	1.03	1.05	1.06	0.630	0.635	0.7929
47	0.39	184.12	1.03	1.05	1.06	0.630	0.635	0.7929
48	0.39	186.88	1.03	1.05	1.05	0.630	0.635	0.7929
49	0.38	186.88	1.03	1.05	1.05	0.630	0.635	0.7927
50	0.39	186.88	1.03	1.05	1.05	0.630	0.635	0.7930
51	0.39	186.88	1.02	1.05	1.05	0.630	0.635	0.7929
52	0.39	186.88	1.02	1.05	1.05	0.630	0.635	0.7930
53	0.39	188.95	1.02	1.04	1.04	0.630	0.635	0.7930
54	0.39	188.95	1.02	1.04	1.04	0.630	0.635	0.7930
55	0.39	188.95	1.02	1.04	1.04	0.630	0.635	0.7930
56	0.40	196.53	1.02	1.00	1.00	0.630	0.635	0.7931
57	0.40	196.53	1.01	1.00	1.00	0.630	0.635	0.7931
58	0.40	196.53	1.01	1.00	1.00	0.630	0.635	0.7931
59	0.40	196.53	1.01	1.00	1.00	0.630	0.635	0.7931
60	0.40	196.53	1.01	1.00	1.00	0.630	0.635	0.7932
61	0.40	196.53	1.01	1.00	1.00	0.630	0.635	0.7932
62	0.40	196.53	1.01	1.00	1.00	0.630	0.635	0.7932
63	0.40	196.53	1.01	1.00	1.00	0.630	0.635	0.7932
64	0.40	196.53	1.00	1.00	1.00	0.630	0.635	0.7932
65	0.40	196.53	1.00	1.00	1.00	0.630	0.635	0.7932
66	0.40	196.53	1.00	1.00	1.00	0.630	0.635	0.7932
67	0.40	196.53	1.00	1.00	1.00	0.630	0.635	0.7932

LOADING- DEVIATOR STRESS = 40 kPa

N	ϵ_A	Δu	Hanna & Javed, 2008 Λ F.O.S I	Constt Λ F.O.S II	Variable Λ F.O.S III	Constt Λ b	Variable Λ b	Λ
1	0.33	0.30	1.45	1.26	1.28	0.630	0.636	0.7918
2	0.34	11.74	1.36	1.26	1.28	0.630	0.636	0.7920
3	0.35	28.29	1.31	1.25	1.26	0.630	0.636	0.7922
4	0.36	42.77	1.28	1.24	1.25	0.630	0.636	0.7923
5	0.36	51.05	1.26	1.23	1.25	0.630	0.636	0.7925
6	0.37	60.70	1.24	1.23	1.24	0.630	0.636	0.7926
7	0.37	67.59	1.22	1.22	1.23	0.630	0.636	0.7926
8	0.37	77.25	1.21	1.21	1.23	0.630	0.636	0.7927
9	0.38	79.31	1.19	1.21	1.22	0.630	0.635	0.7927
10	0.38	93.79	1.18	1.20	1.21	0.630	0.635	0.7928
11	0.38	104.14	1.17	1.19	1.20	0.630	0.635	0.7928
12	0.39	104.14	1.16	1.19	1.20	0.630	0.635	0.7929
13	0.39	111.03	1.16	1.18	1.19	0.630	0.635	0.7929
14	0.39	115.17	1.15	1.18	1.19	0.630	0.635	0.7929
15	0.39	120.69	1.14	1.17	1.18	0.630	0.635	0.7930
16	0.39	122.06	1.13	1.17	1.18	0.630	0.635	0.7930
17	0.40	129.65	1.13	1.16	1.17	0.630	0.635	0.7931
18	0.40	135.16	1.12	1.15	1.16	0.630	0.635	0.7931
19	0.40	138.61	1.12	1.15	1.16	0.630	0.635	0.7932
20	0.40	138.61	1.11	1.15	1.16	0.630	0.635	0.7932
21	0.40	139.99	1.11	1.15	1.15	0.630	0.635	0.7932
22	0.40	144.82	1.10	1.14	1.15	0.630	0.635	0.7932
23	0.41	144.82	1.10	1.14	1.15	0.630	0.635	0.7933
24	0.41	153.09	1.09	1.13	1.13	0.630	0.635	0.7934
25	0.41	155.16	1.09	1.12	1.13	0.630	0.635	0.7934
26	0.41	155.16	1.09	1.12	1.13	0.630	0.635	0.7934
27	0.41	157.92	1.08	1.12	1.12	0.630	0.635	0.7934
28	0.42	164.12	1.08	1.11	1.11	0.630	0.635	0.7934
29	0.42	164.12	1.08	1.11	1.11	0.630	0.635	0.7934
30	0.42	165.50	1.07	1.10	1.11	0.630	0.635	0.7934
31	0.42	166.88	1.07	1.10	1.10	0.630	0.635	0.7934
32	0.42	166.88	1.07	1.10	1.10	0.630	0.635	0.7935
33	0.42	173.09	1.06	1.09	1.09	0.630	0.635	0.7935
34	0.42	173.09	1.06	1.09	1.09	0.630	0.635	0.7935
35	0.42	175.85	1.06	1.08	1.08	0.630	0.635	0.7935
36	0.42	175.85	1.06	1.08	1.08	0.630	0.635	0.7935
37	0.42	175.85	1.05	1.08	1.08	0.630	0.635	0.7935
38	0.42	177.22	1.05	1.08	1.08	0.630	0.635	0.7935
39	0.43	177.22	1.05	1.08	1.08	0.630	0.635	0.7936
40	0.43	177.91	1.05	1.07	1.08	0.630	0.635	0.7936
41	0.43	177.91	1.04	1.07	1.08	0.630	0.635	0.7936
42	0.43	177.91	1.04	1.07	1.08	0.630	0.635	0.7936
43	0.43	177.91	1.04	1.07	1.08	0.630	0.635	0.7936
44	0.43	184.12	1.04	1.05	1.06	0.630	0.635	0.7937
45	0.43	184.12	1.04	1.05	1.06	0.630	0.635	0.7937
46	0.43	184.12	1.03	1.05	1.06	0.630	0.635	0.7937
47	0.43	184.12	1.03	1.05	1.06	0.630	0.635	0.7937
48	0.44	186.88	1.03	1.05	1.05	0.630	0.635	0.7937
49	0.43	186.88	1.03	1.05	1.05	0.630	0.635	0.7937
50	0.43	186.88	1.03	1.05	1.05	0.630	0.635	0.7937
51	0.44	186.88	1.02	1.05	1.05	0.630	0.635	0.7937
52	0.44	188.95	1.02	1.04	1.04	0.630	0.635	0.7937
53	0.44	188.95	1.02	1.04	1.04	0.630	0.635	0.7937
54	0.44	188.95	1.02	1.04	1.04	0.630	0.635	0.7937
55	0.44	188.95	1.02	1.04	1.04	0.630	0.635	0.7937
56	0.44	196.53	1.02	1.00	1.00	0.630	0.635	0.7938
57	0.44	196.53	1.01	1.00	1.00	0.630	0.635	0.7938
58	0.44	196.53	1.01	1.00	1.00	0.630	0.635	0.7938
59	0.44	196.53	1.01	1.00	1.00	0.630	0.635	0.7938
60	0.44	196.53	1.01	1.00	1.00	0.630	0.635	0.7938
61	0.45	196.53	1.01	1.00	1.00	0.630	0.635	0.7939
62	0.45	196.53	1.01	1.00	1.00	0.630	0.635	0.7939
63	0.45	196.53	1.01	1.00	1.00	0.630	0.635	0.7939
64	0.45	196.53	1.00	1.00	1.00	0.630	0.635	0.7939
65	0.45	196.53	1.00	1.00	1.00	0.630	0.635	0.7939
66	0.45	196.53	1.00	1.00	1.00	0.630	0.635	0.7939
67	0.45	196.53	1.00	1.00	1.00	0.630	0.635	0.7939

LOADING- DEVIATOR STRESS = 65 kPa

N	ϵ_A	Δu	Hanna & Javed, 2008 Λ F.O.S I	Constt Λ F.O.S II	Variable Λ F.O.S III	Constt Λ b	Variable Λ b	Λ
1	0.205	0.40	1.45	1.26	1.30	0.630	0.640	0.7868
2	0.21	11.74	1.36	1.26	1.29	0.630	0.640	0.7871
3	0.22	28.29	1.31	1.25	1.28	0.630	0.639	0.7877
4	0.22	43.46	1.28	1.24	1.26	0.630	0.639	0.7877
5	0.225	51.05	1.26	1.23	1.26	0.630	0.639	0.7880
6	0.23	60.70	1.24	1.23	1.25	0.630	0.639	0.7882
7	0.23	68.97	1.22	1.22	1.24	0.630	0.639	0.7882
8	0.23	77.25	1.21	1.21	1.23	0.630	0.639	0.7882
9	0.235	83.45	1.19	1.21	1.23	0.630	0.639	0.7885
10	0.24	93.79	1.18	1.20	1.22	0.630	0.638	0.7887
11	0.245	104.14	1.17	1.19	1.21	0.630	0.638	0.7890
12	0.245	104.14	1.16	1.19	1.21	0.630	0.638	0.7890
13	0.25	115.17	1.16	1.18	1.19	0.630	0.638	0.7892
14	0.25	115.17	1.15	1.18	1.19	0.630	0.638	0.7892
15	0.25	122.06	1.14	1.17	1.18	0.630	0.638	0.7892
16	0.25	122.06	1.13	1.17	1.18	0.630	0.638	0.7892
17	0.255	129.65	1.13	1.16	1.17	0.630	0.638	0.7894
18	0.25	135.16	1.12	1.15	1.17	0.630	0.638	0.7892
19	0.255	138.61	1.12	1.15	1.16	0.630	0.638	0.7894
20	0.255	139.99	1.11	1.15	1.16	0.630	0.638	0.7894
21	0.26	144.82	1.11	1.14	1.15	0.630	0.638	0.7896
22	0.26	144.82	1.10	1.14	1.15	0.630	0.638	0.7896
23	0.26	144.82	1.10	1.14	1.15	0.630	0.638	0.7896
24	0.26	153.09	1.09	1.13	1.14	0.630	0.638	0.7896
25	0.265	155.16	1.09	1.12	1.13	0.630	0.638	0.7898
26	0.265	155.16	1.09	1.12	1.13	0.630	0.638	0.7898
27	0.265	157.92	1.08	1.12	1.13	0.630	0.638	0.7898
28	0.265	164.12	1.08	1.11	1.11	0.630	0.638	0.7898
29	0.27	164.12	1.08	1.11	1.11	0.630	0.638	0.7900
30	0.27	165.50	1.07	1.10	1.11	0.630	0.638	0.7900
31	0.27	166.88	1.07	1.10	1.11	0.630	0.638	0.7900
32	0.27	166.88	1.07	1.10	1.11	0.630	0.638	0.7900
33	0.27	173.09	1.06	1.09	1.09	0.630	0.638	0.7900
34	0.275	173.09	1.06	1.09	1.09	0.630	0.637	0.7901
35	0.275	175.85	1.06	1.08	1.09	0.630	0.637	0.7901
36	0.275	175.85	1.06	1.08	1.09	0.630	0.637	0.7901
37	0.275	175.85	1.05	1.08	1.09	0.630	0.637	0.7901
38	0.28	177.22	1.05	1.08	1.08	0.630	0.637	0.7903
39	0.28	177.22	1.05	1.08	1.08	0.630	0.637	0.7903
40	0.28	177.91	1.05	1.07	1.08	0.630	0.637	0.7903
41	0.28	177.91	1.04	1.07	1.08	0.630	0.637	0.7903
42	0.28	177.91	1.04	1.07	1.08	0.630	0.637	0.7903
43	0.28	184.12	1.04	1.05	1.06	0.630	0.637	0.7903
44	0.28	184.12	1.04	1.05	1.06	0.630	0.637	0.7903
45	0.285	184.12	1.04	1.05	1.06	0.630	0.637	0.7905
46	0.285	184.12	1.03	1.05	1.06	0.630	0.637	0.7905
47	0.285	186.88	1.03	1.05	1.05	0.630	0.637	0.7905
48	0.285	186.88	1.03	1.05	1.05	0.630	0.637	0.7905
49	0.285	186.88	1.03	1.05	1.05	0.630	0.637	0.7905
50	0.29	186.88	1.03	1.05	1.05	0.630	0.637	0.7907
51	0.285	186.88	1.02	1.05	1.05	0.630	0.637	0.7905
52	0.285	188.95	1.02	1.04	1.04	0.630	0.637	0.7905
53	0.29	188.95	1.02	1.04	1.04	0.630	0.637	0.7907
54	0.285	188.95	1.02	1.04	1.04	0.630	0.637	0.7905
55	0.29	196.53	1.02	1.00	1.00	0.630	0.637	0.7907
56	0.29	196.53	1.02	1.00	1.00	0.630	0.637	0.7907
57	0.29	196.53	1.01	1.00	1.00	0.630	0.637	0.7907
58	0.29	196.53	1.01	1.00	1.00	0.630	0.637	0.7907
59	0.29	196.53	1.01	1.00	1.00	0.630	0.637	0.7907
60	0.29	196.53	1.01	1.00	1.00	0.630	0.637	0.7907
61	0.29	196.53	1.01	1.00	1.00	0.630	0.637	0.7907
62	0.29	196.53	1.01	1.00	1.00	0.630	0.637	0.7907
63	0.295	196.53	1.01	1.00	1.00	0.630	0.637	0.7908
64	0.295	196.53	1.00	1.00	1.00	0.630	0.637	0.7908
65	0.295	196.53	1.00	1.00	1.00	0.630	0.637	0.7908
66	0.295	196.53	1.00	1.00	1.00	0.630	0.637	0.7908

UNLOADING-ZERO DEVIATOR STRESS

N	ϵ_A	Δu	Hanna & Javed, 2008 Λ F.O.S I	Constt Λ F.O.S II	Variable Λ F.O.S III	Constt Λ b	Variable Λ b	Λ
1	0.275	0.40	1.45	1.26	1.29	0.630	0.637	0.7901
2	0.275	11.74	1.36	1.26	1.28	0.630	0.637	0.7901
3	0.28	28.29	1.31	1.25	1.27	0.630	0.637	0.7903
4	0.285	43.46	1.28	1.24	1.26	0.630	0.637	0.7905
5	0.29	51.05	1.26	1.23	1.25	0.630	0.637	0.7907
6	0.29	60.70	1.24	1.23	1.24	0.630	0.637	0.7907
7	0.29	68.97	1.22	1.22	1.24	0.630	0.637	0.7907
8	0.3	77.25	1.21	1.21	1.23	0.630	0.637	0.7910
9	0.3	83.45	1.19	1.21	1.22	0.630	0.637	0.7910
10	0.3	93.79	1.18	1.20	1.21	0.630	0.637	0.7910
11	0.305	104.14	1.17	1.19	1.20	0.630	0.637	0.7911
12	0.305	104.14	1.16	1.19	1.20	0.630	0.637	0.7911
13	0.31	115.17	1.16	1.18	1.19	0.630	0.637	0.7912
14	0.315	115.17	1.15	1.18	1.19	0.630	0.636	0.7914
15	0.315	122.06	1.14	1.17	1.18	0.630	0.636	0.7914
16	0.315	122.06	1.13	1.17	1.18	0.630	0.636	0.7914
17	0.32	129.65	1.13	1.16	1.17	0.630	0.636	0.7915
18	0.32	135.16	1.12	1.15	1.16	0.630	0.636	0.7915
19	0.32	138.61	1.12	1.15	1.16	0.630	0.636	0.7915
20	0.32	138.61	1.11	1.15	1.16	0.630	0.636	0.7915
21	0.32	144.82	1.11	1.14	1.15	0.630	0.636	0.7915
22	0.32	144.82	1.10	1.14	1.15	0.630	0.636	0.7915
23	0.325	144.82	1.10	1.14	1.15	0.630	0.636	0.7916
24	0.325	153.09	1.09	1.13	1.13	0.630	0.636	0.7916
25	0.33	155.16	1.09	1.12	1.13	0.630	0.636	0.7918
26	0.33	155.16	1.09	1.12	1.13	0.630	0.636	0.7918
27	0.33	157.92	1.08	1.12	1.12	0.630	0.636	0.7918
28	0.33	164.12	1.08	1.11	1.11	0.630	0.636	0.7918
29	0.335	164.12	1.08	1.11	1.11	0.630	0.636	0.7919
30	0.335	165.50	1.07	1.10	1.11	0.630	0.636	0.7919
31	0.335	166.88	1.07	1.10	1.11	0.630	0.636	0.7919
32	0.335	166.88	1.07	1.10	1.11	0.630	0.636	0.7919
33	0.34	173.09	1.06	1.09	1.09	0.630	0.636	0.7920
34	0.34	173.09	1.06	1.09	1.09	0.630	0.636	0.7920
35	0.34	175.85	1.06	1.08	1.08	0.630	0.636	0.7920
36	0.34	175.85	1.06	1.08	1.08	0.630	0.636	0.7920
37	0.34	175.85	1.05	1.08	1.08	0.630	0.636	0.7920
38	0.34	177.22	1.05	1.08	1.08	0.630	0.636	0.7920
39	0.34	177.22	1.05	1.08	1.08	0.630	0.636	0.7920
40	0.34	177.91	1.05	1.07	1.08	0.630	0.636	0.7920
41	0.34	177.91	1.04	1.07	1.08	0.630	0.636	0.7920
42	0.345	177.91	1.04	1.07	1.08	0.630	0.636	0.7921
43	0.345	184.12	1.04	1.05	1.06	0.630	0.636	0.7921
44	0.345	184.12	1.04	1.05	1.06	0.630	0.636	0.7921
45	0.345	184.12	1.04	1.05	1.06	0.630	0.636	0.7921
46	0.345	184.12	1.03	1.05	1.06	0.630	0.636	0.7921
47	0.33	186.88	1.03	1.05	1.05	0.630	0.636	0.7918
48	0.35	186.88	1.03	1.05	1.05	0.630	0.636	0.7922
49	0.35	186.88	1.03	1.05	1.05	0.630	0.636	0.7922
50	0.35	186.88	1.03	1.05	1.05	0.630	0.636	0.7922
51	0.35	186.88	1.02	1.05	1.05	0.630	0.636	0.7922
52	0.35	188.95	1.02	1.04	1.04	0.630	0.636	0.7922
53	0.35	188.95	1.02	1.04	1.04	0.630	0.636	0.7922
54	0.355	188.95	1.02	1.04	1.04	0.630	0.636	0.7923
55	0.355	196.53	1.02	1.00	1.00	0.630	0.636	0.7923
56	0.335	196.53	1.02	1.00	1.00	0.630	0.636	0.7919
57	0.355	196.53	1.01	1.00	1.00	0.630	0.636	0.7923
58	0.355	196.53	1.01	1.00	1.00	0.630	0.636	0.7923
59	0.355	196.53	1.01	1.00	1.00	0.630	0.636	0.7923
60	0.355	196.53	1.01	1.00	1.00	0.630	0.636	0.7923
61	0.36	196.53	1.01	1.00	1.00	0.630	0.636	0.7925
62	0.36	196.53	1.01	1.00	1.00	0.630	0.636	0.7925
63	0.36	196.53	1.01	1.00	1.00	0.630	0.636	0.7925
64	0.36	196.53	1.00	1.00	1.00	0.630	0.636	0.7925
65	0.36	196.53	1.00	1.00	1.00	0.630	0.636	0.7925
66	0.36	196.53	1.00	1.00	1.00	0.630	0.636	0.7925

UNLOADING- DEVIATOR STRESS = 20 kPa

N	ϵ_A	Δu	Hanna & Javed, 2008 Λ F.O.S I	Constt Λ F.O.S II	Variable Λ F.O.S III	Constt Λ b	Variable Λ b	Λ
1	0.31	0.40	1.45	1.26	1.29	0.630	0.637	0.7912
2	0.32	11.74	1.36	1.26	1.28	0.630	0.636	0.7915
3	0.33	28.29	1.31	1.25	1.27	0.630	0.636	0.7918
4	0.33	42.77	1.28	1.24	1.26	0.630	0.636	0.7918
5	0.335	51.05	1.26	1.23	1.25	0.630	0.636	0.7919
6	0.34	60.70	1.24	1.23	1.24	0.630	0.636	0.7920
7	0.34	67.59	1.22	1.22	1.24	0.630	0.636	0.7920
8	0.345	77.25	1.21	1.21	1.23	0.630	0.636	0.7921
9	0.35	83.45	1.19	1.21	1.22	0.630	0.636	0.7922
10	0.35	93.79	1.18	1.20	1.21	0.630	0.636	0.7922
11	0.35	104.14	1.17	1.19	1.20	0.630	0.636	0.7922
12	0.355	104.14	1.16	1.19	1.20	0.630	0.636	0.7923
13	0.36	115.17	1.16	1.18	1.19	0.630	0.636	0.7925
14	0.36	115.17	1.15	1.18	1.19	0.630	0.636	0.7925
15	0.365	120.69	1.14	1.17	1.18	0.630	0.636	0.7926
16	0.365	122.06	1.13	1.17	1.18	0.630	0.636	0.7926
17	0.365	129.65	1.13	1.16	1.17	0.630	0.636	0.7926
18	0.365	135.16	1.12	1.15	1.16	0.630	0.636	0.7926
19	0.37	138.61	1.12	1.15	1.16	0.630	0.636	0.7927
20	0.37	138.61	1.11	1.15	1.16	0.630	0.636	0.7927
21	0.37	144.82	1.11	1.14	1.15	0.630	0.636	0.7927
22	0.37	144.82	1.10	1.14	1.15	0.630	0.636	0.7927
23	0.37	144.82	1.10	1.14	1.15	0.630	0.636	0.7927
24	0.38	153.09	1.09	1.13	1.13	0.630	0.635	0.7928
25	0.38	155.16	1.09	1.12	1.13	0.630	0.635	0.7928
26	0.38	155.16	1.09	1.12	1.13	0.630	0.635	0.7928
27	0.375	157.92	1.08	1.12	1.12	0.630	0.635	0.7927
28	0.38	164.12	1.08	1.11	1.11	0.630	0.635	0.7928
29	0.38	164.12	1.08	1.11	1.11	0.630	0.635	0.7928
30	0.385	164.47	1.07	1.10	1.11	0.630	0.635	0.7929
31	0.385	166.88	1.07	1.10	1.11	0.630	0.635	0.7929
32	0.385	166.88	1.07	1.10	1.11	0.630	0.635	0.7929
33	0.385	173.09	1.06	1.09	1.09	0.630	0.635	0.7929
34	0.39	173.09	1.06	1.09	1.09	0.630	0.635	0.7930
35	0.39	175.85	1.06	1.08	1.08	0.630	0.635	0.7930
36	0.39	175.85	1.06	1.08	1.08	0.630	0.635	0.7930
37	0.39	175.85	1.05	1.08	1.08	0.630	0.635	0.7930
38	0.39	177.22	1.05	1.08	1.08	0.630	0.635	0.7930
39	0.39	177.22	1.05	1.08	1.08	0.630	0.635	0.7930
40	0.395	177.91	1.05	1.07	1.08	0.630	0.635	0.7931
41	0.395	177.91	1.04	1.07	1.08	0.630	0.635	0.7931
42	0.395	177.91	1.04	1.07	1.08	0.630	0.635	0.7931
43	0.395	184.12	1.04	1.05	1.06	0.630	0.635	0.7931
44	0.395	184.12	1.04	1.05	1.06	0.630	0.635	0.7931
45	0.395	184.12	1.04	1.05	1.06	0.630	0.635	0.7931
46	0.395	184.12	1.03	1.05	1.06	0.630	0.635	0.7931
47	0.4	186.88	1.03	1.05	1.05	0.630	0.635	0.7932
48	0.4	186.88	1.03	1.05	1.05	0.630	0.635	0.7932
49	0.4	186.88	1.03	1.05	1.05	0.630	0.635	0.7932
50	0.4	186.88	1.03	1.05	1.05	0.630	0.635	0.7932
51	0.4	186.88	1.02	1.05	1.05	0.630	0.635	0.7932
52	0.4	188.95	1.02	1.04	1.04	0.630	0.635	0.7932
53	0.405	188.95	1.02	1.04	1.04	0.630	0.635	0.7933
54	0.405	188.95	1.02	1.04	1.04	0.630	0.635	0.7933
55	0.405	196.53	1.02	1.00	1.00	0.630	0.635	0.7933
56	0.405	196.53	1.02	1.00	1.00	0.630	0.635	0.7933
57	0.405	196.53	1.01	1.00	1.00	0.630	0.635	0.7933
58	0.405	196.53	1.01	1.00	1.00	0.630	0.635	0.7933
59	0.405	196.53	1.01	1.00	1.00	0.630	0.635	0.7933
60	0.41	196.53	1.01	1.00	1.00	0.630	0.635	0.7934
61	0.41	196.53	1.01	1.00	1.00	0.630	0.635	0.7934
62	0.41	196.53	1.01	1.00	1.00	0.630	0.635	0.7934
63	0.41	196.53	1.01	1.00	1.00	0.630	0.635	0.7934
64	0.41	196.53	1.00	1.00	1.00	0.630	0.635	0.7934
65	0.41	196.53	1.00	1.00	1.00	0.630	0.635	0.7934
66	0.41	196.53	1.00	1.00	1.00	0.630	0.635	0.7934

UNLOADING- DEVIATOR STRESS = 40 kPa

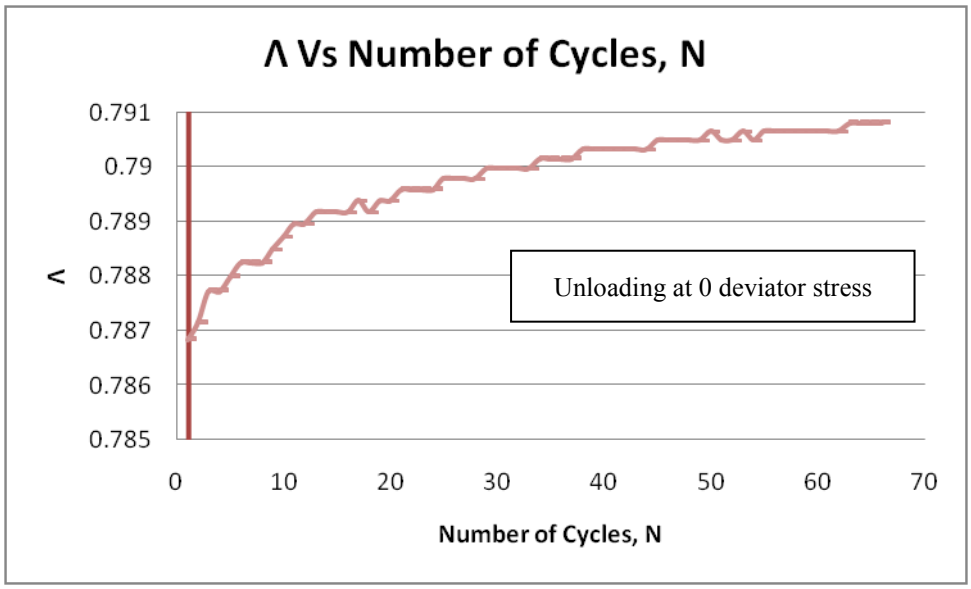
Λ Vs Number of Cycles, N
0.791
0.79
0.789
0.788
0.787
0.786
0.785
Λ
0
10
20
30
40
50
60
70
Number of Cycles, N
Unloading at 0 deviator stress

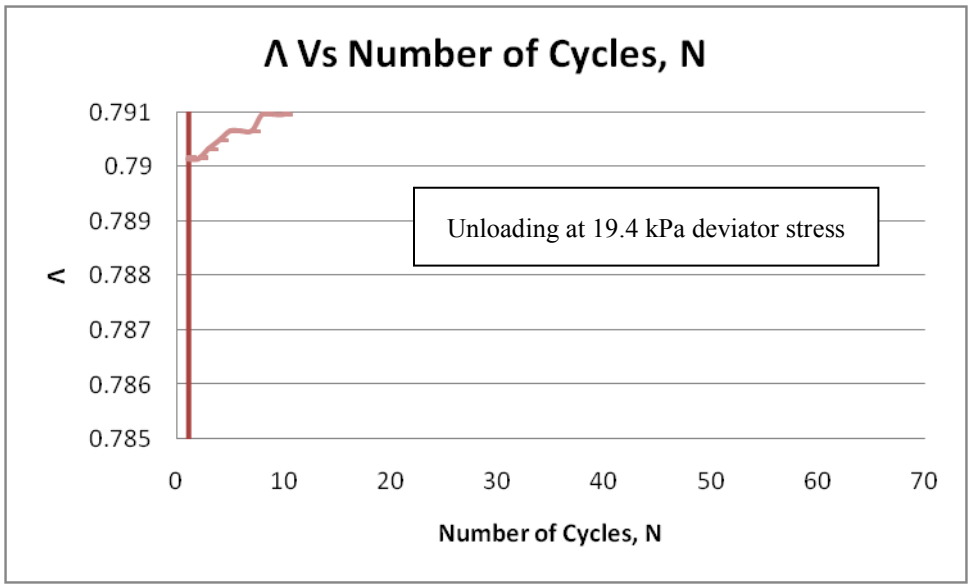
Λ Vs Number of Cycles, N
0.791
0.79
0.789
0.788
0.787
0.786
0.785
Λ
0
10
20
30
40
50
60
70
Number of Cycles, N
Unloading at 19.4 kPa deviator stress

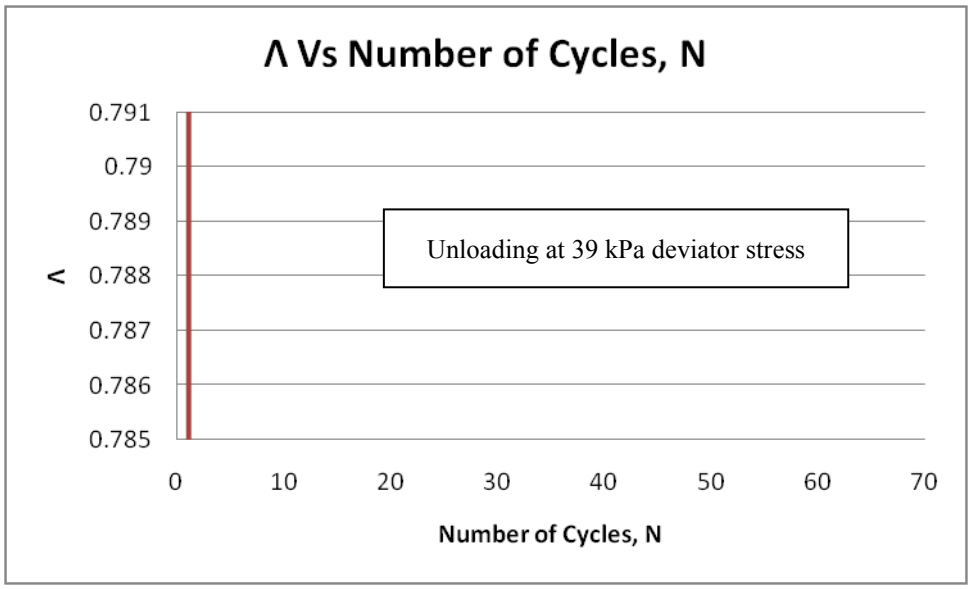
Λ Vs Number of Cycles, N
0.791
0.79
0.789
0.788
0.787
0.786
0.785
Λ
Unloading at 39 kPa deviator stress
0
10
20
30
40
50
60
70
Number of Cycles, N

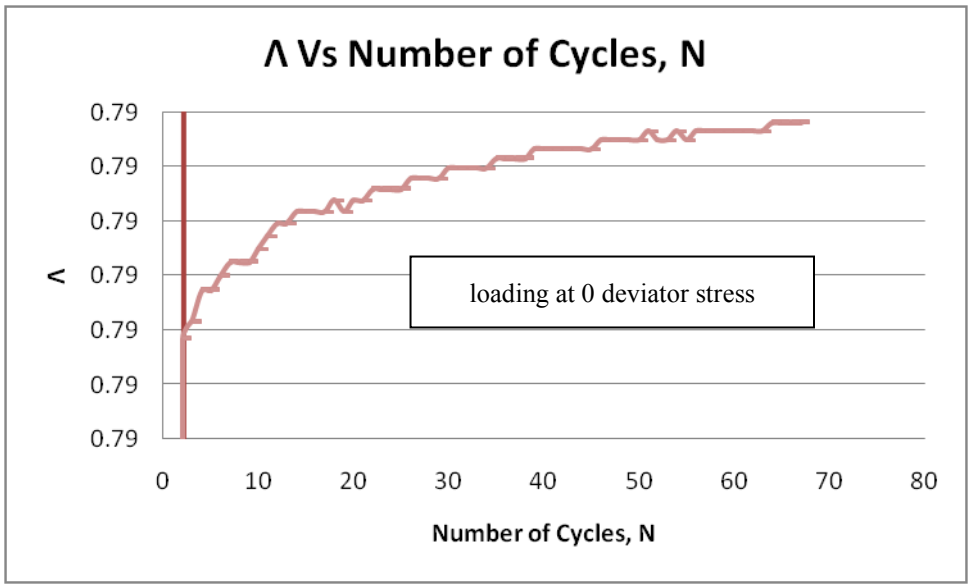
Λ Vs Number of Cycles, N
0.79
0.79
0.79
0.79
0.79
0.79
Λ
loading at 0 deviator stress
0
10
20
30
40
50
60
70
80
Number of Cycles, N

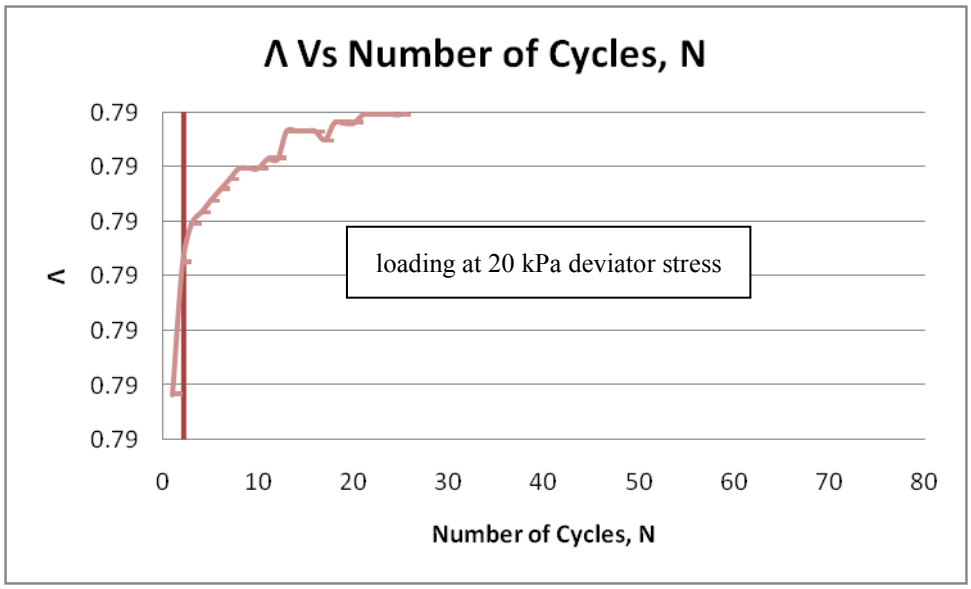
Λ Vs Number of Cycles, N
0.79
0.79
0.79
0.79
0.79
0.79
Λ
loading at 20 kPa deviator stress
0
10
20
30
40
50
60
70
80
Number of Cycles, N

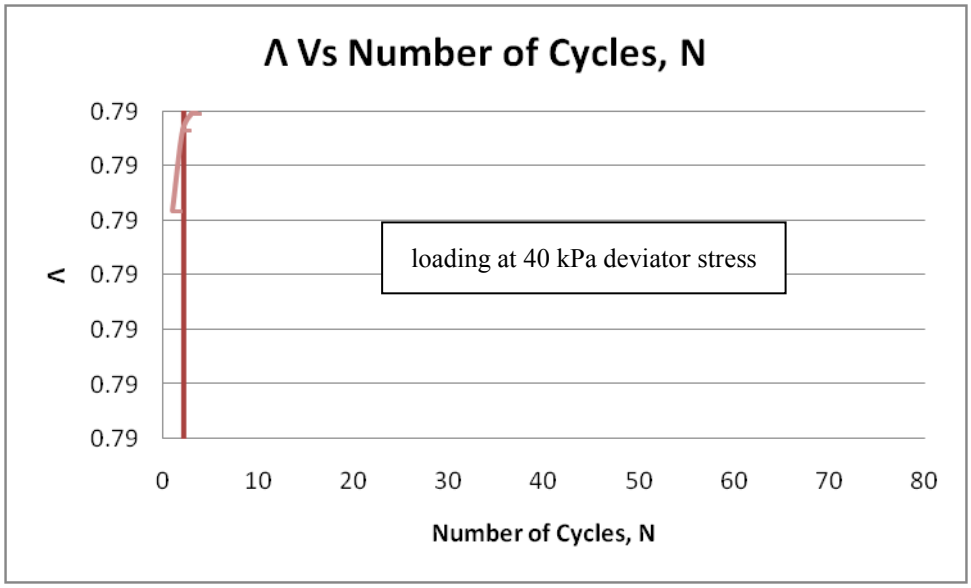
Λ Vs Number of Cycles, N
0.79
0.79
0.79
0.79
0.79
0.79
Λ
loading at 40 kPa deviator stress
0
10
20
30
40
50
60
70
80
Number of Cycles, N

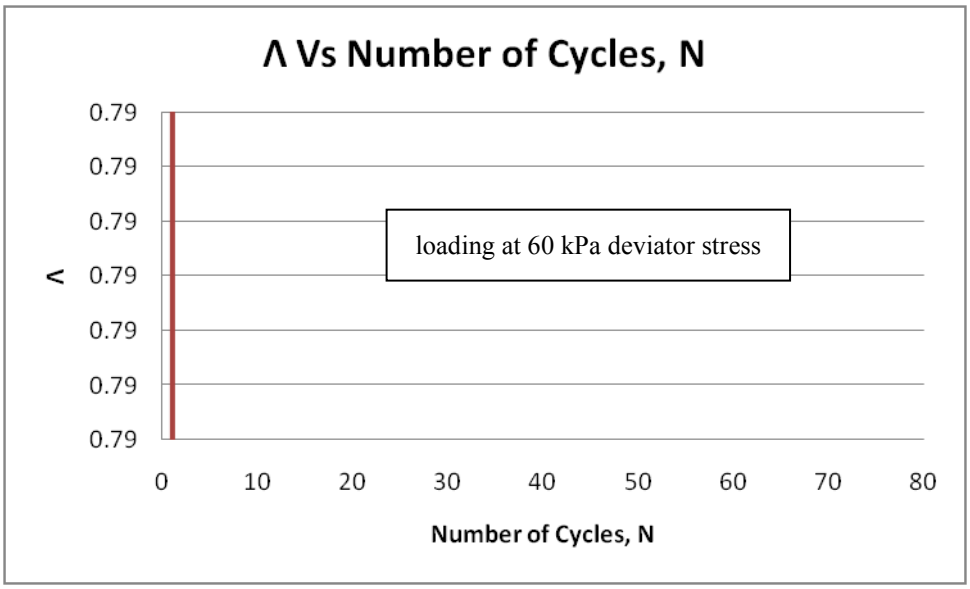
Λ Vs Number of Cycles, N
0.79
0.79
0.79
Λ
0.79
0.79
0.79
loading at 60 kPa deviator stress
0
10
20
30
40
50
60
70
80
Number of Cycles, N

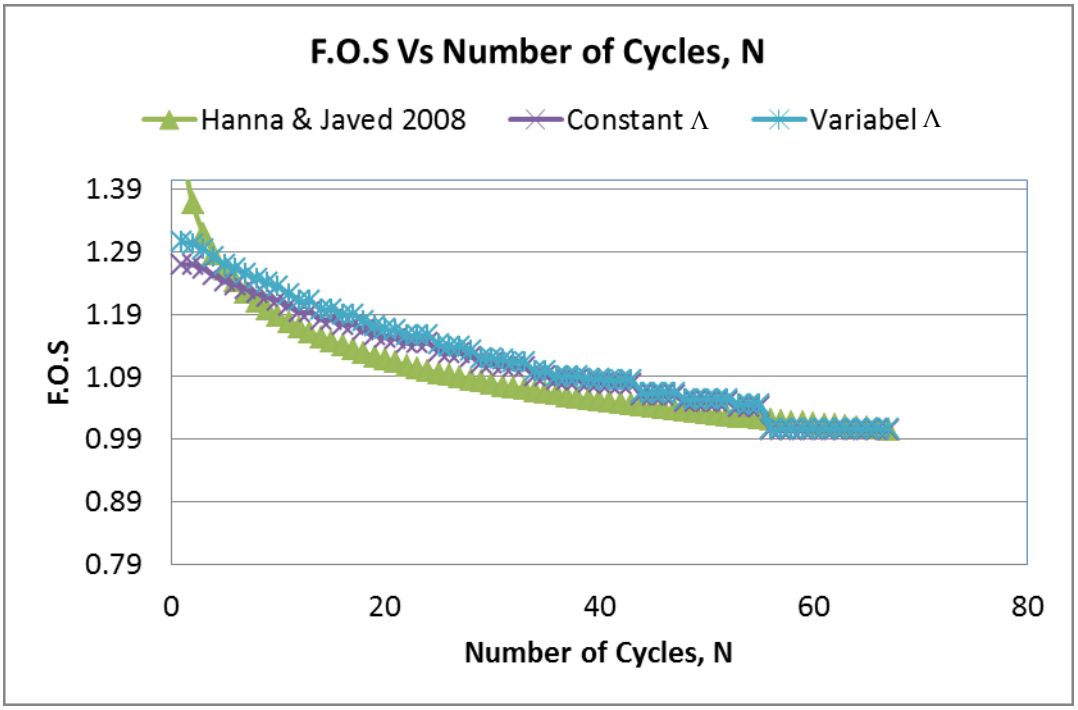
F.O.S Vs Number of Cycles, N
Hanna & Javed 2008
Constant Λ
Variabel Λ
1.39
1.29
1.19
1.09
0.99
0.89
0.79
F.O.S
0
20
40
60
80
Number of Cycles, N